Betel (*Piper betle* L.) Leaf Ethanolic Extract Dechlorophyllized by Sedimentation: Uses in Conjunction with Cold Plasma and for Preparation of Active Packaging to Extend the Shelf-Life of Nile Tilapia Slices

Mohamed Abdelmonem Tagrida

A Thesis Submitted in Partial Fulfillment of the Requirements for the Degree of Doctor of Philosophy in Food Science and Technology

Prince of Songkla University

2022

Thesis Title	Betel (*Piper betle* L.) Leaf Ethanolic Extract Dechlorophyllized by Sedimentation: Uses in Conjunction with Cold Plasma and for Preparation of Active Packaging to Extend the Shelf-Life of Nile Tilapia Slices
Author	Mr. Mohamed Abdelmonem Tagrida
Major Program	Food Science and Technology
Academic Year	2022

ABSTRACT

Sedimentation process was used to remove chlorophyll from betel and chaphlu leaf ethanolic extracts (BLEE and CLEE, respectively) by mixing the extract with water. The process showed a remarkable reduction in chlorophyll content for both extracts. No differences in chlorophyll contents, total phenolic content (TPC), or antioxidant activities were observed between the dechlorophyllized fractions using different extract/water ratios ($p > 0.05$). Liquid Chromatography-Mass Spectrometry (LC/MS) profiling showed that BLEE dechlorophyllized using the extract/water ratio of 1:1 (BLEE-DC1) had higher phenolic compounds than CLEE dechlorophyllized counterpart (CLEE-DC1). Isovitexin was the most abundant compound identified in the BLEE-DC1, while vitexin 4′-O-galactoside was the most prevalent in CLEE-DC1. BLEE-DC1 was generally more heat stable than CLEE-DC1.

Different solvents were used for the dechlorophyllization of BLEE in comparison with sedimentation process. Sedimentation reduced the chlorophyll content and color of BLEE more efficiently ($p < 0.05$), while antioxidant and antibacterial activities were enhanced ($p < 0.05$). BLEE dechlorophyllized by the sedimentation (BLEE-SED) had lower minimum inhibitory concentration (MIC) and minimum bactericidal concentration (MBC) as compared to other dechlorophyllized extracts. Lower microbiological and chemical changes took place in Nile tilapia slices treated with BLEE-SED at 400 and 600 ppm after 12 days of storage at 4˚C.

BLEE-SED was loaded in liposomes at 1 and 2% (w/v) using two different methods, namely thin film hydration (TF) and ethanol injection (EI) methods.

Liposomes loaded with 1% BLEE prepared by TF method (L/BLEE-T1) had the smallest particle size, paler color and was more stable than the other prepared liposomes ascertained by its lowest zeta potential and polydispersity index ($p < 0.05$). The highest encapsulation efficiency (EE) and lowest releasing efficiency (RE) were also found with L/BLEE-T1. L/BLEE-T1 showed higher antioxidant stability than unencapsulated BLEE prepared at equivalent amount based on EE (U/BLEE-T1) after *in vitro* gastrointestinal tract digestion. L/BLEE-T1 could be therefore an efficient delivery system for improving stability of antioxidant activities of BLEE.

L/BLEE-T1 showed enhanced antibacterial activity as witnessed by lower MIC and MBC ($p < 0.05$). L/BLEE-T1 also caused larger inhibition zones, lower triphenyl-2H tetrazolium chloride (TTC) dehydrogenase activity, and higher release rates of K^+ and Mg^{2+} ions to the tested bacteria ($p < 0.05$). Additionally, scanning electron microscopic (SEM) images showed deformations and perforation on cell walls of the tested bacteria after treatment with L/BLEE-T1. At 400 ppm, L/BLEE-T1 combined with modified atmospheric packaging (MAP) (CO_2: Ar: O_2 = 60: 30: 10) and non-thermal plasma (NTP) (80 KV-RMS for 5 min) exhibited the highest inhibition effect ($p < 0.05$) toward the challenged bacteria over 15 days of storage at 4˚C.

Nile tilapia slices treated with L/BLEE-T1 or U/BLEE-T1 at 400 ppm, packed under MAP (CO_2: Ar: O_2 = 60:30:10) and subjected to NTP for 5 min (L/BLEE 400/MAP-NTP and U/BLEE-400/MAP-NTP, respectively) had the lowest microbial and chemical changes during storage of 12 days at 4˚C ($p < 0.05$). Lipid oxidation was lower in these samples, as indicated by more retained polyunsaturated fatty acids and lower lipid oxidation based on Fourier transform infrared (FT-IR) spectra. Overall likeness scores were similar ($p > 0.05$) between all the samples at day 0 of storage. However, only L/BLEE-400/MAP-NTP and U/BLEE-400/MAP-NTP were still sensorially acceptable after 12 days of storage.

Incorporation of dechlorophyllized BLEE at 1 and 2% enhanced elasticity and heat-seal ability of the gelatin/chitosan blend films, particularly, those plasticized with glycerol (GLY). Ultraviolet and visible light barrier abilities along with water vapor permeability were improved ($p < 0.05$) for films containing 2% BLEE. Swelling and water solubility of the films were lessened with augmenting BLEE

concentrations ($p<0.05$). Antioxidant and antibacterial activities were surged as BLEE levels incorporated increased. Type of plasticizer had no effect on antioxidant and antibacterial activities of films ($p > 0.05$). SEM images showed smooth homogenous surface and cross-section in film sample devoid of BLEE, while those incorporated with BLEE had slightly rough surface and cross-section, but the roughest surface and cross section were found for films incorporated with L/BLEE. FT-IR spectra revealed the difference in peaks and patterns between films without and with BLEE. Addition of BLEE lowered thermal stability of film associated with looser structure of film. Pouches made from gelatin/chitosan blend plasticized with GLY and incorporated with BLEE at 2% (B-GLY) were used to pack shrimp oil. They could prevent lipid oxidation more efficiently than lower density polyethylene (LDPE) pouches as ascertained by less peroxide values, thiobarbituric acid reactive substances, and astaxanthin decomposition. B-GLY could be thus used as active packaging to retard lipid oxidation in shrimp oil.

Gelatin/chitosan solutions incorporated with BLEE at varying concentrations were electro-spun on polylactic acid (PLA) films. Gelatin/chitosan nanofibers (GC/NF) with different morphologies, as indicated by SEM, were formed. PLA films coated with GC/NF added with BLEE showed antioxidant and antibacterial activities. Lowered water vapor permeability and enhanced mechanical properties were achieved for GC/NF coated PLA films ($p<0.05$). Microbial growth and lipid oxidation of Nile tilapia slices packaged in PLA films coated with GC/NF containing 2% BLEE were more retarded than those packaged in low density polyethylene (LDPE) bags over the refrigerated storage of 12 days. Based on microbial limit, the shelf-life was escalated to 9 days, while the control had shelf-life of 3 days. Therefore, such a novel film/bag could be a promising active packaging for perishable fish and fish products.

ACKNOWLEDGEMENT

I would like to express my heartfelt gratitude and reverence to my advisor Prof. Dr. Soottawat Benjakul, director of the International Center of Excellence in Seafood Science and Innovation (ICE-SSI), Faculty of Agro-Industry, Prince of Songkla University, for his guidance, generous monitoring skills, unfailing inspiration, deep patience and immense knowledge. I will always be indebted to your teachings and unwavering support since the day I joined your lab. Many Thanks!

I would like to thank the rest of my thesis committee: Asst. Prof. Dr. Punnanee Sumpavapol, Dr. Thanasak Sae-leaw, and Dr. Krisana Nilsuwan of the Faculty of Agro-Industry, Prince of Songkla University and Assoc. Prof. Dr. Kitiya Vongkamjan Aurand of the Department of Biotechnology, Faculty of Agro-Industry, Kasetsart University.

My respect and love to my beloved father and mother, my dear brother and sister for their love, support and for always believing in me.

I would like to express my gratitude to all the members of the International Center of Excellence in Seafood Science and Innovation (ICE-SSI) for their kindness, unfailing support, guidance and suggestions during the course of my program. Thank you for making the laboratory as home for me.

My sincere appreciation goes to all the faculty members and staff of Agro-Industry for their kind co-operation and collaboration during my study program. And also, for all the professional scientist and technical personnel in the Office of Scientific Instrument and Testing (OSIT) for their assistance and work.

With gratitude, I acknowledge the generous financial support provided by Prince of Songkhla University (PSU), Hat Yai, Thailand, under the Prachayacharn program (Grant no. AGR6402088N).

Thanks to everyone soliciting their good wishes and unconditional support during these 3 years of doctoral journey in Prince of Songkla University, Hat Yai, Thailand.

Mohamed Abdelmonem Tagrida

CONTENTS

CONTENTS (Continued)

CONTENTS (Continued)

CONTENTS (Continued)

CONTENTS (Continued)

CONTENTS (Continued)

CONTENTS (Continued)

CONTENTS (Continued)

LIST OF TABLES

LIST OF TABLES (Continued)

LIST OF TABLES (Continued)

LIST OF FIGURES

LIST OF FIGURES (Continued)

LIST OF FIGURES (Continued)

LIST OF FIGURES (Continued)

LIST OF FIGURES (Continued)

CHAPTER 1

INTRODUCTION AND LITERATURE REVIEW

1.1. Introduction

Seafoods are extremely valued because of their content of proteins, polyunsaturated fatty acids (PUFAs), minerals, and vitamins that are essential for body functions and growth (Tacon, 2020). Such content can aid in improving imbalanced dietary habits by enhancing essential nutritional functions and reducing the risk of lifestyle-related diseases. (Hosomi *et al.*, 2012). Nile tilapia (*Oreochromis niloticus*) is important seafood both nutritionally and economically, contributing markedly to worldwide food security (El Asely *et al.*, 2020). Tilapia is famous for its mild taste, tender texture, and low-fat content, besides being one of the healthiest sources of proteins and omega-3 fatty acids, along with other nutrients such as niacin, choline, vitamin D, vitamin B12, phosphorus, and calcium (Srisapoome and Areechon, 2017). Due to that content, eating tilapia regularly can provide many benefits like improving cardiovascular health, maintaining the nervous system, boosting bone strength, and preventing cancer (Khalili Tilami and Sampels, 2018). Because of being an ideal choice for fish farming and its increasing suitability as a replacement for costly species like salmon, in addition to its valuable nutritional content, tilapia is one of the most consumed seafood nowadays and the global tilapia market is expected to reach 9.2 billion USD by 2027, from 7.9 billion USD in 2020 (Tacon, 2020).

However, this rich content makes tilapia highly prone to spoilage, thus their protection particularly during preparation, storage, and distribution is needed (Cyprian *et al.*, 2021). Fish spoilage is generally attributed to several factors such as autolysis, oxidative stress, and microbial growth, which took place in various stages of fish preparation and would lead eventually to the unaccepted changes in the sensorial and nutritional properties, hence the reduction in their shelf-life and acceptability (Olatunde and Benjakul, 2018). Since the demand for high-quality and safe seafood with extended shelf-life is increased, the implementation of the optimum preservation techniques is required (Ghaly *et al.*, 2010). Usually, chemical additives such as sodium nitrite, sodium benzoates, and sulfur dioxide are used for preservation of different fish products, however accumulation of these additives in these products can be transferred to the consumer causing serious health issues. Therefore, food manufacturers have sought other safe alternatives as a response to the consumers' demands by adopting natural additives (Shahmohammadi *et al.,* 2016).

Due to their abundance and low cost, plants could serve as source of natural compounds such as plant extracts and essential oils known for their possession to several bioactivities including antioxidant and antibacterial activities, that can be used as alternative means for seafood preservation (Al-Maqtari *et al.,* 2021). These bioactivities are mainly attributed to the sub-constituents including phenolic compounds, terpenes, and phenylpropanoids found in either plant extracts or essential oils (Sadgrove *et al.,* 2022). Differences in structures and amounts of these compounds could led to variation in their bioactivities (Benjakul *et al.,* 2014). Betel (*Piper betle* L.) is a leafy plant from the family "*Piperaceae*" grown in the Indian subcontinent and the Southeast Asian countries, where it is used in traditional medicine and in the local cuisines due to its copious content of compounds having many bioactivities including antioxidant, antimicrobial, and anticancer activities (Salehi *et al.,* 2019). Therefore, extract made from betel leaves can be exploited as a preservative for tilapia. Nevertheless, the presence of high chlorophyll content in leaves could hinder its use in food applications since foods with changed color is not sensorially acceptable, hence an appropriate dechlorophyllization technique is crucial for producing an extract with paler color (Olatunde *et al.,* 2021). Sedimentation with distilled water can be a suitable and safe green process to replace the use of hazardous solvents for dechlorophyllization of different plant extracts (Olatunde *et al.,* 2021). Moreover, encapsulation in liposomes which are spherical vesicles composed mostly of natural phospholipids and have amphiphilic properties, can be used to mask the color of the extract as well as to protect the extract from unwanted changes in the environment and for better function (Liu *et al*., 2019).

Non-thermal processes have attracted the attention recently because of the upsurging requests for minimally processed seafoods having premium nutritional values and fresh-like characteristics (Olatunde and Benjakul, 2018). Additionally, such technologies are renowned for their eco-friendly approaches and affordability (Morris *et al.,* 2007). Non-thermal plasma (NTP) has been considered as non-thermal technology applied on different foods to combat quality loss in food industry mainly induced by food microbial contaminants (Afshari and Hosseini, 2014). It can be generated when electrical energy is applied on neutral gas or mixture of gases, leading to ionization of these gases (Mishra *et al.,* 2016). Many reactive species such as reactive oxygen species (ROS), ultraviolet (UV), negative and positive ions will be produced as a result for this gas ionization which can inactivate different microorganisms, thus the shelf-life of different perishable foods exposed to NTP could be extended (Ganesan *et al.,* 2021). Air is commonly the source of the ionized gases, however for the better exploitation of NTP and to avoid any uncontrolled oxidation of foods, the appropriate mixture of gases can be selected, hence the use of modified atmospheric packaging (MAP) (Singh *et al.,* 2011). MAP is a preservation technique involves the refilling of the air in the packaging containers by a mixture of inert gases, with certain composition, thus the loss of the unstable excited reactive species that may lead to the re-proliferation of microorganisms, can be compensated (Olatunde *et al.,* 2020). NTP coupled with MAP are chemical-free and contactless techniques that cause no discoloration, dehydration, or have any drawbacks on the different properties of foods and have been extensively used for fish products preservation (Olatunde *et al.,* 2020). The mechanism of action of the NTP against the microorganisms contaminating the food products involves the damaging of cell wall, alteration of permeability, affecting microbial organelles and metabolism (Mishra *et al.,* 2016). Despite the efficiency of NTP and MAP in retarding microbial growth, unavoidable extent of lipid oxidation can take place because of the actions of the generated free radicals (Ganesan *et al.,* 2021). Therefore, the usage of plant extracts with antioxidant activities in combination with NTP and MAP can lessen the oxidation extent and the entire system can be regarded as hurdles for shelf-life extension of tilapia slices.

Incorporation of plant extracts with bioactivities into biodegradable packaging materials is another way that can be used for better exploitation of these extracts and to avoid any discoloration or undesired changes in the sensorial or chemical natural of the foods that may result from the direct treatment (Chen *et al.,* 2020). Biodegradable films made from various biopolymers such as gelatin, chitosan, etc., and added with active compounds (plant extracts) can provide enhanced mechanical and barrier properties against moisture and gas transmission, hence lipid oxidation, unwanted enzymatic activities, and microbial spoilage can be lowered and shelf-life of packaged foods can be extended (Bourtoom, 2008). Polylactic acid (PLA) a natural polymer resulting from the fermentation of agricultural wastes, can be used to produce more tolerable packaging materials (Pang *et al.,* 2010). To elevate the efficiency of the PLA films and to achieve the concept of active packaging, plant extracts with bioactivities can be incorporated into the film forming solutions then loaded to the PLA films by electrospinning (He *et al.,* 2019). Electrospinning which is based on high electric fields applied to viscoelastic solutions containing bioactive compounds to generate a mat of polymer nanofibers (Radusin *et al.,* 2019). Thus, the high surface area-to-volume ratio of these nanofibers with elevated porosity will guarantee the sustained release of the bioactive compounds into the packaged foods (Wen *et al.,* 2016).

Therefore, the quality and keeping qualities of Nile tilapia in view of oxidative stability, antimicrobial efficacy and sensorial quality could be achieved by the application of natural extract from plant leaves coupled with non-thermal plasma and modified atmosphere packaging or as active packaging containing the extract. Henceforth, the aforementioned approaches could be potential means for better preservation and shelf-life extension of Nile tilapia under refrigerated conditions.

1.2. Literature Review

1.2.1. Nile tilapia (*Oreochromis niloticus*)

Nile tilapia (*Oreochromis niloticus*) has been consumed globally owing to its content of valuable nutrients with high protein content and considerably low fats (El Asely *et al.,* 2020). The production of tilapia was sharply expanded in the past two decades reaching about 13.5% of freshwater fish production worldwide and it has been cultured in more than 130 countries (Abu-Elala *et al.,* 2021). This expansion was due to tilapia ability to be cultured in various aquatic niches, and its potential to replace costly marine fish products, making its farming the backbone of many aquaculture farmers especially in the poor and developing countries (Abu-Elala *et al.,* 2021). However, tilapia is prone to spoilage due to its content particularly during storage or transportation, this will cause not only serious health risks to consumers but also will contribute to heavy economic losses (Bono *et al.*, 2017). Usually, synthetic preservatives were used for preservation and shelf-life extension of tilapia, but due to safety and environmental concerns, calls have been raised to seek safer alternatives (Hassoun and Çoban, 2017).

1.2.2. Spoilage process in fish

The process in which fish products can no longer be consumed because of radical alterations in their fresh state such as the occurrence of unpalatable odor, taste, appearance, and texture is referred to as spoilage (Ghaly *et al.*, 2010). Several intrinsic and extrinsic factors including microbiota of the original fish environment, methods of catching and preparation, as well as how the product is packaged and stored strongly involved in spoilage. Such factors will trigger the activities of autolytic enzymes, lipid oxidation, and spoilage microorganisms to accelerate the spoilage process (Odeyemi *et al.*, 2020). Using suitable pre-treatments, safe preservatives and packaging techniques can prevent or minimize fish spoilage (Gokoglu, 2019).

1.2.2.1. Autolysis

During improper storage of fish different chemical and biological changes take place in fish soon after capturing due to autolytic enzymes, causing degradation to major fish constituents (Sikorski *et al.*, 2020). Several autolytic enzymes including proteolytic enzymes, phosphorylases, lipases, cathepsins and gut enzymes located in the muscle and viscera of fish will be involved in the post-mortem degradation of the fish's flesh leading to flesh softening, belly wall rupturing and blood water drainage which contain both proteins and lipids (Ghaly *et al.*, 2010). This will lead to the reduction of textural quality in fish, indicating a limitation in the fish quality even with considerably low load of spoilage microorganisms, nevertheless the main characteristics of spoilage like the unpalatable taste and off-odor will not yet be sensible (Cheng et al., 2014). Proteins and lipids will further be degraded resulting in formation of peptides and free fatty acids which will eventually lead to the growth of microbial growth (Bono *et al.*, 2017). Other autolytic enzymes such as trimethylamine oxide demethylase will reduce the trimethylamine oxide (TMAO) into dimethylamine (DMA), trimethylamine (TMA) and formaldehyde linked with adverse alteration to flesh texture and generation of fishy odor, in addition to the upsurging of the alkalinity of fish meat increasing the microbial growth (Benjakul *et al.*, 2003).

1.2.2.2. Lipid oxidation

After autolysis in fish, lipid oxidation induced by free radicals is considered the major cause of spoilage in fish, and its effect is more pronounced in fish characterized with the presence of high lipid content (Xu *et al.*, 2015). Typically, lipid oxidation occurs because of the reaction of oxygen, which is activated by the presence of transition metals, with double bonds found in the fatty acids, therefore fish lipids with high amount of polyunsaturated fatty acids (PUFA) are highly prone to oxidation (Johnson and Decker, 2015). The oxidation process involves three main stages: initiation, propagation, and termination (Ghaly *et al.*, 2010). Schematic representation of lipid oxidation pathway is depicted in Fig. 1. In the initiation stage, lipid free radicals are formed as a result of catalysts including heat, metal ions, and irradiation. These radicals will react with atmospheric oxygen to form peroxyl radicals and begin the propagation stage. During propagation, the generated peroxyl radicals will react with more lipid molecules and form hydroperoxides and new free radicals. The accumulation and interaction of these free radicals will lead to the formation of non-radical products that their presence is an indication for the termination stage and completion of the lipid oxidation process (Shahidi and Zhong, 2010).

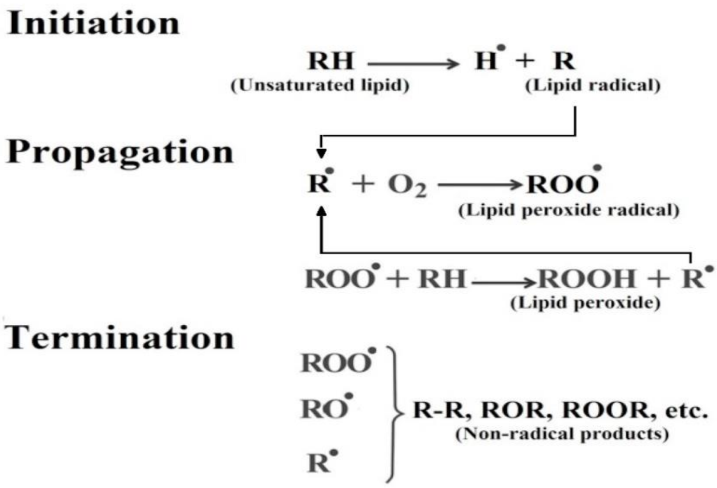

Figure 1. Lipid oxidation pathway

Source: Gavahian *et al.* (2018)

Lipid oxidation can take place enzymatically or non-enzymatically. Generally, lipolysis is the term describing the enzymatic degradation of lipids and it is brought about by different varieties of lipases that could be either endogenous or secreted by microorganisms (Hasan *et al.,* 2009). In lipolysis, the lipases degrade the glycerides to form free fatty acids characterized by their rancidity and to indicate the reduction in the quality of fish (Ghaly *et al.,* 2010). The main lipases involved in lipolysis are phospholipase A2, phospholipase B, and triacyl lipase found in the skin, blood, and organs of fish (Izquierdo and Henderson, 1998). Non-enzymatic lipid oxidation is induced by hematin compounds, which are the compounds that contain iron in the ferric state in their center such as hemoglobin, myoglobin, and cytochrome and are obtained by the oxidation of haem (Tappel *et al.,* 1961). Hydroperoxides are generated because of such oxidation and their content reflect the extent of lipid deterioration, on the other hand, fatty acids formed during non-enzymatic oxidation will interact with proteins in fish muscles causing their denaturation, thus fish spoilage (Gebicki, 1997).

1.2.2.3. Microbial spoilage

The growth of different arrays of microorganisms in fish and production of their proteolytic and lipolytic enzymes to degrade the fish contents, producing by-products and changing fish nature is considered as microbial spoilage (Gram, 2009). The presence of secondary products with their unpleasant off-flavors such as amines, histamine, sulfides, organic acids, aldehydes, and ketones, is an indication of microbial spoilage (Carocho *et al.,* 2015). Different bacteria are responsible for fish spoilage including the psychrophilic bacteria that thrive in chilled conditions (Jin *et al.,* 2022), Gram-positive or negative mesophiles whether aerobic or facultative anaerobic that can grow when the appropriate storage conditions are not followed (Gram and Huss, 1996), and *Enterobacteriaceae* that their presence is linked with the unsanitized preparation environments which can cause food poisoning in addition to the spoilage (Oliveira *et al.,* 2017).

Substances, such as peptides, carbohydrates, and free amino acids in fish products are the main nutrients for spoilage microorganisms, in which they are used for metabolism and bacteria functions (Premkumar and Vasudevan, 2018). Various by-products resulted from the activity of these microorganisms, and the amount and type of these products determine the extent of microbial contamination (Boziaris and Parlapani, 2017). Enzymatic activity of bacteria including *Escherichia spp., Vibrio spp.,* and *Aeromonas spp.,* has been connected with the reduction of trimethylamine oxide (TMAO) used by fish as an osmo-regulate, to trimethylamine (TMA) causing the unaccepted fishy odor (Romano *et al.,* 2015). TMAO is not utilized by spoiling microorganisms as catabolic substrate, but can act as an electron acceptor, thus accelerating microbial growth particularly in the absence of oxygen (Leisner and Gram, 2000). The total quantification of nitrogenous compounds such as NH_3, DMA, and TMA is given by the total volatile nitrogen (TVN) content and its levels in fish indicats the extent of microbial spoilage in fish (Khalafalla *et al.,* 2015). Usually, hypoxanthine is produced with TMA by the decomposition of nucleotides in fish cells and its occurrence can cause the bitter taste in fish undergoing spoilage (Lawal and Adeloju, 2012).

1.2.3. Prevention of spoilage and shelf-life extension using hurdle technologies

The combined use of different sets of techniques for preservation and enhancing the quality of foods as long as possible in certain conditions is termed as hurdle technology (Leistner, 2000). One aspect of hurdles is the use of preservatives for the better keeping of fish products, however most of the preservatives used in this endeavor are from synthetic origin such as formalin, sorbic acid, sulfites, sodium benzoate, butylated hydroxytoluene (BHT), and butylated hydroxyanisole (BHA), infamous widely in the food manufacturing sector for their adverse health effects (Anand and Sati, 2013). Therefore, calls were raised for natural safe alternatives to be used instead of these chemicals. Natural preservatives from different origins were proposed as possible candidates to substitute the commonly used chemicals including plant extracts and essential oils from plant origins, chitosan, chito-oligosaccharides, active peptides, and hydrolysates from animal origins (Olatunde and Benjakul, 2018). Additionally, antibiotics and bacteriocins extracted from different microorganisms can be involved in food preservation (Sahoo *et al.,* 2016).

Another aspect of hurdles is the manipulation of physical parameters controlling the environment at which fish are preserved such as water activity (a_w), pH, and temperature (Ghaly *et al.,* 2010). Non-thermal processes including modified atmospheric packaging (MAP), irradiation, pulsed electric field (PEF), ultraviolet (UV) radiation, high pressure, and non-thermal plasma (NTP) were proposed recently to be used as hurdles after confirming their suitability and efficiency in preventing microbial proliferation and chemical deterioration in different kind of foods (Andoni *et al.*, 2021). Some of the aforementioned hurdles may enhance the properties of the foods they used to protect by improving their bioactivities or sensorial attributes, others may negatively impact the properties of the foods, and this depends on the intensity, time of exposure, or concentration involved in the chosen hurdle (Singh and Shalini, 2016). For example, the excessive use of plant extracts or essential oils with intense color or flavor may affect the sensorial attributes of the product, also some treatments like fermentation for the purpose of inhibiting both spoilage and pathogenic microorganisms may severely change the quality attributes of the treated foods leading to consumer unacceptability (Leistner, 2000). Hence, the optimum range of each hurdle should be used to achieve the maximum effectiveness in microbial inhibition and chemical deterioration prevention, in addition, to avoid any unwanted effects on the sensorial, safety, and nutritional qualities of the treated food.

1.2.3.1. Plant extracts as a natural fish preservative

Plant extracts have been used in many applications including pharmaceutical, nutritional and cosmetic applications, due to their immense content of bioactive compounds (Pabón-Baquero *et al.,* 2018). The trending direction of abandoning chemical preservatives and using preservatives of natural origin, particularly from plant origin, led the food manufacturers including fish and fish products manufacturers to adopt the use of plant extracts as a new favorite candidate (Mostafa *et al.*, 2018). Several bioactive compounds were identified in different plant extracts. Among them are the secondary metabolites known as polyphenols that contain one or more aromatic rings with several hydroxyl groups (Viji *et al.*, 2017). Based on their chemical structures, polyphenols can be divided into different groups including phenolic acids, flavonoids, hydroxycinnamic acids and lignans (Kähkönen *et al.*, 1999). Bioactivities such as antioxidant, antimicrobial, anticancer and anti-inflammatory activities were documented to be found in several plant extracts, and their effect is linked with these polyphenols and varies according to the type, quantity, and modes of action of these bioactive compounds (Redondo-Blanco *et al.*, 2020).

The antimicrobial activity of plant extracts is mostly attributed to the bioactive polyphenols that adsorb to bacterial membrane affecting its integrity and causing its disruption, leading to the uncontrolled permeability and leakage of microbial cell constituents, which are essential for cell metabolism and growth, and ultimately ending with cell death (Mei *et al.*, 2019). Response of different microorganisms towards the actions of polyphenols differ according to the structure of their cell membranes, for example Gram-positive bacteria generally show more resistance than Gram-negative bacteria due to the thick peptidoglycan layer found in the Gram-positive bacteria acting as barrier against the plant polyphenols (Mai-Prochnow *et al.*, 2016). The effect of polyphenols on the different bacteria is depicted in Fig. 2.

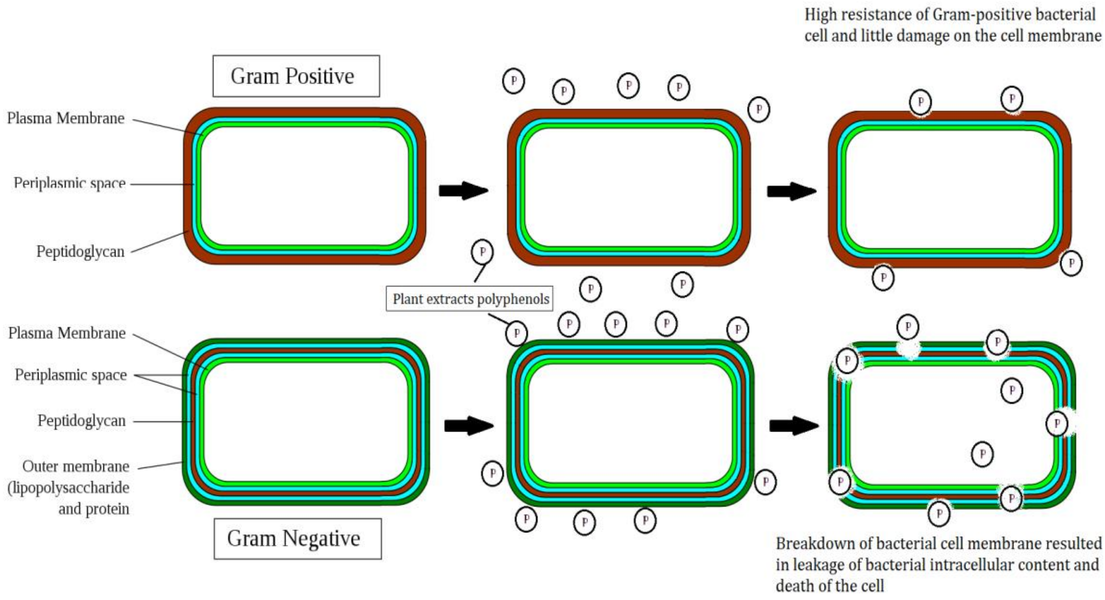

Figure 2. Effect of plant extract polyphenols on different bacteria.
Source: Abdollahzadeh *et al.* (2014)

Fish rich in PUFA are susceptible to lipid oxidation, therefore a plant extract with antioxidant activities will be highly regarded and like the antibacterial activity the amount and types of polyphenols will determine the efficiency of the plant extract to retard lipid oxidation (Medina *et al.*, 2003). Lipid oxidation can be lowered by antioxidants which can inhibit or interrupt the formation of free radicals by different mechanisms including the scavenging of the radicals that induces the peroxidation through either by single electron transfer (SET) pathway or hydrogen atom transfer (HAT) pathway (Fig. 3) (Liang and Kitts, 2014). Other antioxidant mechanism includes chelating with metal ions that catalyze the oxidation, quenching of excessive oxygen that causes lipid oxidation, and shattering the entire chain reaction of lipid oxidation hence, the effectiveness of an antioxidant compound can be governed by its ability to break this chain reaction and the presence of –OH group in the polyphenol structure and its exact position on the ring determine the antioxidant capacity (Santos-Sánchez *et al.*, 2019).

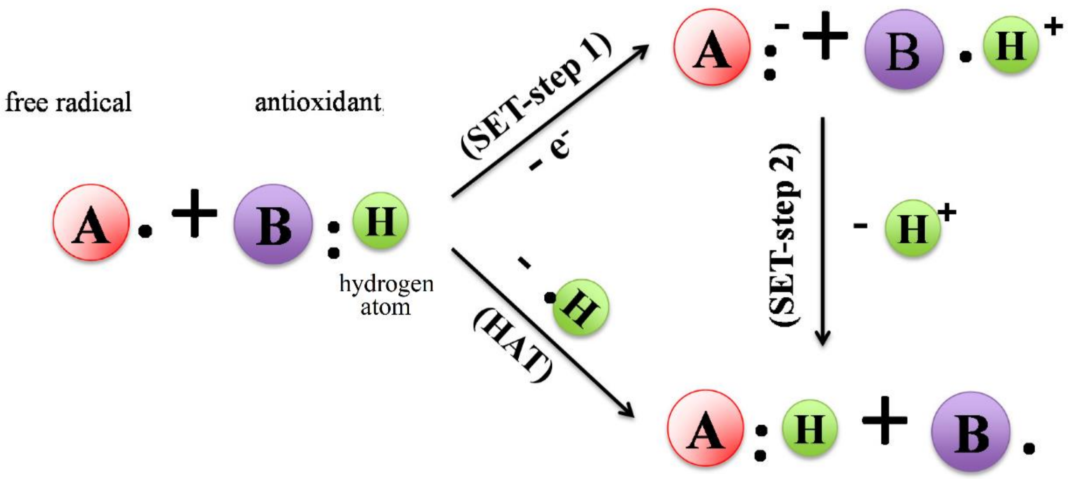

Figure 3. Antioxidants react with free radicals through single electron transfer (SET) or hydrogen atom transfer (HAT) pathways.

Source: Liang and Kitts (2014)

In general, the antioxidant action of polyphenols depends on their phenolic hydroxyl groups which are either electron or hydrogen donors. After interaction with free radicals and losing a hydrogen or electron, depending on the pathway taken, polyphenols don't become radical themselves, but they became stabilized by the quinone structures formed in addition to resonance delocalization caused by remaining electrons within the aromatic ring of the polyphenolic compound (Santos-Sánchez *et al.,* 2019). Hence, lipid oxidation can be avoided by plant-based polyphenols. Application of some plant extracts in fish preservation are summarized in Table 1.

Table 1. Applications of plant extracts for fish preservation

Plant extract	Concentration and storage condition	Treated fish	Results	References
Dried red beetroot peel	100 mg/100 mL at 5˚C	Nile Tilapia fish	- Reduce microbial load - Lower lipid oxidation - Extend shelf-life for 12 days	El-Beltagi *et al.* (2022)
Noni (*Morinda citrifolia* L.) leaf extract	400 mg/kg at 4˚C	Striped catfish slices	- Reduce microbial load - Lower lipid oxidation - Extend shelf-life for 9 days	Olatunde *et al.* (2021a)
Thyme extract	0.5%, v/v at 4˚C	Nile tilapia fillets	- Maintain the quality parameters - extend the shelf life for 18 days	Khalafalla *et al.* (2015)

Table 1 (continued)

Plant extract	Concentration and storage condition	Treated fish	Results	References
lavender and lemon balm extracts	1%, v/v at 4˚C	Anchovy	- Retard microbial growth - Lower lipid oxidation - Extend shelf life for 11 days	Özogul *et al.* (2017)
Wild mint leaf extract	6%, v/v at 4˚C	Rainbow trout	- Delay lipid oxidation - Retard microbial spoilage - Extend shelf life for 18 days	Raeisi *et al.* (2016)
Grape extract	4%, v/v at 4˚C	Common carp	- Lower oxidation and microbial spoilage - Extend shelf life for 15 days	Hasani and Hasani (2014)

1.2.3.1.1. Betel and chaphlu leaves as possible sources of plant extracts

Betel (*Piper betle* L.) and chaphlu (*Piper sarmentosum* Roxb.) are leafy plants from the family "*Piperaceae*", both plants have been cultured predominantly in Southeast Asian countries where they were used in tradition medicine or as food (Salehi *et al.,* 2019). The high content of secondary metabolites, particularly polyphenols and essential oils, made these plants useful in many applications, most importantly as nutraceuticals because of the valuable bioactivities they provide (Nouri *et al.,* 2014). Among the phytochemicals identified and documented in betel leaf extract are chavicol, hydroxychavicol, estragole, eugenol, methyl eugenol, caryophyllene, 1,8-cineol, α-pinene, β-pinene (Salehi *et al.,* 2019). Some of these phytochemicals are known to possess valuable bioactivities and to be involved in many applications such as eugenol which is a fat-soluble antioxidant that can scavenge free radicals in red blood cells, it also was used as flavoring and in medicine as a local antiseptic and anesthetic (Saxena *et al.,* 2014). LC/MS analysis of the betel leaf aqueous extracts identified p-hydroxybenzoic acid, eugenol, and 4-p-coumaroylquinic acid as the most abundant phytochemicals and were reported to show antioxidant and antimicrobial activities (Sazwi *et al.*, 2013).

Chaphlu leaf extract on the other hand, was documented to show antibacterial, antioxidant, and anti-inflammatory activities due to the presence of phytochemicals such as 3-allyl-6-methoxyphenol (Hussain *et al.*, 2012). In addition, chaphlu is recommended as an edible vegetable due to its high content of vitamin C (Salehi *et al.,* 2019). LC/MS analysis of the chaphlu leaf extract identified more than 67 compounds with reported remarkable bioactivities, including 2,4,5-trimethoxy-1-propenylbenzene, cis-caryophyllene, and δ-cadinene (Song *et al.,* 2006). Because of all these identified phytochemicals in both plants, betel or chaphlu leaf extracts could be the source of a potential natural preservative for food applications.

1.2.3.1.2. Dechlorophyllization of plant extracts

Although showing remarkable antimicrobial and antioxidant activities, plant extracts still couldn't fully substitute the synthetic preservatives due to some limitations, among them is that they are required at elevated concentration than their synthetic counterparts (Campos *et al.,* 2012). Regretfully, fish treated with such elevated concentration may not be acceptable from a sensorial point of view (García-Díez *et al.,* 2016). Additionally, the preservative effect of certain plant extract may vary because of many factors including condition and age of the plant, harvesting time, and method of extraction (Weerakkody *et al.,* 2010). But one of the most important factors limiting the use of plant extracts in food applications is color, particularly the green color attributed to the presence of chlorophyll. Fish with changed color will not be acceptable to consumers, moreover, chlorophyll is unstable molecule and its presence in food materials will induces lipid oxidation because of its photo-oxidation properties and the reaction of its magnesium ion with the acids found in foods, thus lowering the keeping qualities of the treated food (Tzima *et al.,* 2020).

Chlorophyll is a magnesium-porphyrin amphiphilic compound, insoluble in water but dissolves in organic solvents, therefore it can be co-extracted with the plant extract especially if solvent extraction process is involved (Olatunde and Benjakul, 2018). Apart from laying an unacceptable color to the treated food, chlorophyll can induce oxidation due to its photosensitizer and pro-oxidant properties (Brown *et al.,* 2019). Therefore, for the plant extract to be suitable as food additive, the chlorophyll must be removed. The traditional methods used for this purpose are either not considered as safe or practice since they were not effective in removing the excess coloring pigments from the extracts (Olatunde *et al.,* 2021). Usually, chlorophyll was removed from the plant extracts with the aid of organic solvents but in addition to be not very effective in the dechlorophyllization and losing some of the bioactivities, the remining organic solvents in the plant extract after dechlorophyllization process may restrict its use in food applications due to its toxicity (Benjakul *et al.,* 2014). Newly proposed techniques such as liquid-liquid partitioning, chloroFiltr cartridges, and countercurrent separation (CCS) were also involved in the removal of chlorophyll from different plant extracts, however, process duration, complexity, affordability, and absence of required instrumentation and maintenance make these techniques less appealing to food (Tzima *et al.,* 2020).

The trend of green processing and the need for practical methods safe and affordable, urged the search for novel methods for dechlorophyllization from the plant extracts that can guarantee their safety with maintaining their bioactivities. A potential green method which is the sedimentation induced by water showed a satisfying outcome in chlorophyll removal (Olatunde *et al.,* 2021). Sedimentation can be defined as the tendency of suspended particles in a fluid to settle down in the bottom. The excess water will push chlorophyll particles to be separated from aqueous phase and settle down mediated by some forces such as gravity, difference in polarity, electromagnetism, and centrifugal acceleration (Carpenter *et al.,* 1986). Because of the increased non-polar nature of chlorophyll molecules, they can be sedimented in the bottom of a container once the medium become more polar when water is added to that container thus, chlorophyll can be removed without the use of any organic solvents i.e., a green process for dechlorophyllization.

1.2.3.1.3. Encapsulation of plant extracts in liposomes

Despite the efforts of minimizing the color of the plant extracts, some color may persist due to solubility differences (Mazandrani *et al.,* 2016). Also, instability of some compounds of the plant extracts in certain mediums may restrict their usage, therefore encapsulation of these plant extracts may provide an efficient means to maintain or even enhance their properties (Karpuz *et al.,* 2020). Encapsulation is a delivery system of entrapping bioactive agents within a carrier matrix to improve its bioavailability and stability by reducing the reactivity between those bioactive agents and the surrounding medium, in addition to improve the half-life, and handling ability of the bioactive agents by the controlled release (Muñoz-Shugulí *et al.,* 2020). Encapsulation of plant extracts can improve their uniformity in the food system and mask any unpleasant flavor associated with them (Mancini *et al.,* 2018). Various kinds of carrier matrixes have been used in many pharmaceutical and nutritional applications, one of the most used carrier matrixes is liposomes (Bruni *et al.*, 2017).

Liposomes are spherical amphiphilic vesicles of hydrophobic tails and hydrophilic heads, composed mostly of natural phospholipids, with regarded characteristics such as biocompatibility, stability, and non-toxicity. Moreover, liposomes can be utilized in the entrapment, delivery, and release of water-soluble, lipid-soluble, and amphiphilic materials, making them suitable delivery systems (Mozafari *et al.,* 2008). Liposomes are formed when the amphiphilic phospholipids aggregate once placed in an aqueous medium to protect their hydrophobic core from the aqueous molecules, while maintaining connection with the aqueous medium via the hydrophilic parts. Application of sufficient energy into these aggregates will force them to rearrange themselves in the organized closed vesicles that will entrap any hydrophilic compounds found in the aqueous medium (Muñoz-Shugulí *et al.*, 2020). Lipophilic compounds can be mixed with the phospholipids of the liposomes; hence the bioactive agents will be entrapped in the wall of liposomes not in the core (Fig. 4) (Mozafari *et al.*, 2008).

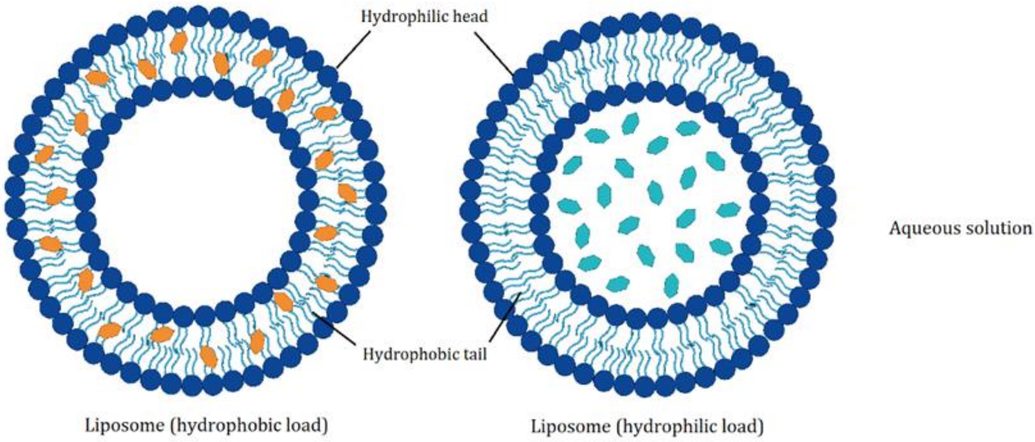

Figure 4. Liposomes loaded with hydrophobic or hydrophilic compounds.
Source: Sannikova (2021)

The type of shell material used in liposomes preparation and presence or absence of stabilizing agents e.g., cholesterol, is crucial for the success of the entrapment system (Mancini *et al.*, 2018). Moreover, the size, morphology, and release of entrapped compounds from the prepared liposomes can determine their homogeneity and efficiency within the food system (Bruni *et al.*, 2017). Methods of liposomes preparation can be classified under three categories those are mechanical methods including thin film hydration method, organic solvent replacement methods such as the reverse-phase evaporation and ethanol injection methods, and size transformation-based methods represented by the freeze-thaw extrusion method, each method will yield liposomes with different size and distinctive shell wall (Mozafari *et al.*, 2008).

Liposomes were employed to encapsulate different bioactive compounds with different nature. For microbial spoilage prevention in dairy products, (da Silva Malheiros *et al.,* 2012) reported the better preservation activity as the bacteriocins were protected and their activity was delayed when loaded into liposomes because of the controlled release, they found that the direct addition of the bacteriocins into the dairy products was lethal to the starter culture, therefore, the liposomes loaded with bacteriocins were more effective against spoilage. Lower lipid oxidation and better keeping qualities were attained after treatment the silver carp fillets with liposomes containing fennel extract during storage at 4˚C, the shelf-life was extended to 15 days compared to fillets treated with the unencapsulated extract (Mazandrani *et al.,* 2016). Tometri *et al.* (2020) found that the liposomal encapsulation process enhanced the bioactivities of hydroalcoholic bay leaf (*Laurus nobilis*) extract and after treating minced meat with1500 ppm of these liposomes it was found that the microbial spoilage and lipid oxidation were delayed. Limonene was encapsulated into liposomes which were then applied as an edible coating for strawberries protection, the wrapped strawberries had the reduction in the respiration rate, pH, and the higher anthocyanin content indicating an extended shelf-life and maintained organoleptic properties (Dhital *et al.,* 2018).

1.2.3.2. Non-thermal processes for spoilage prevention and shelf-life extension

Technologies that are functioning at low temperatures and are based on the use of mechanical, electromagnetic, light, or electric energies for inhibiting microbial spoilage and avoiding any alteration in the food samples are referred to as "non-thermal processing" (Andoni *et al.,* 2021). Technologies belonging to this concept such as pulsed light, high-intensity ultrasound, irradiation, high hydrostatic pressure, ultraviolet light, pulsed electric fields, and non-thermal plasma have been used in different food industries, and as a result of their usage, the keeping qualities and shelf-life of the food products were enhanced (Afshari and Hosseini, 2014). Noninvolvement of heat in these technologies will ensure no adverse changes in the sensory perception and maintaining the nutritive value of the treated foods (Crapo *et al.,* 2004). Using such processes will equilibrate between minimal processing and efficient preservation, additionally they will ensure the balance between the required food safety and consumers acceptability.

1.2.3.2.1. Modified atmosphere packaging (MAP)

Modified atmosphere packaging is a non-thermal preservation technique that involves substituting the air in a packaging container with mixture of gases that have a specific composition (Church and Parsons, 1995). Argon, nitrogen, oxygen, and carbon dioxide are the most used gases in MAP and each gas has its own specific function (Singh *et al.*, 2011). Argon is an inert gas that its addition to the package will ensure no reactivity with food components, it also displace oxygen, needed for aerobic food spoilers and pathogens to grow thus, inhibiting them, additionally, its microbial oxidases inactivation capacity will prevent lipid oxidation (Rocculi *et al.*, 2005).

Nitrogen prevents packaging collapse plus; it has low reactivity with the packaged foods (Masniyom, 2011). Although responsible for oxidation of foods particularly those containing high lipid content, oxygen is needed to inhibit the growth of obligatory anaerobic bacteria. It is also required for packaging certain foods with high water activity (a_w) like fish products (Olatunde *et al.*, 2019). Carbon dioxide in packages will dissociate to carbonic acid leading to increase the storage stability of the packaged food by lowering the pH and inhibiting bacterial growth, in which the acidic medium will affect the permeability of the bacterial membranes leading to leakage of cell components (Mastromatteo *et al.*, 2010). Decreased pH will alter enzymes reactions resulting in alterations in the metabolism of the bacterial cells, which will inevitably lead to the death of bacterial cells, however excess carbon dioxide might bring about the packaging collapse by dissolution (Sivertsvik *et al.*, 2002). The highest effectivity of MAP will not be achieved without ensuring the good hygienic practices during preparation and packaging of the food, additionally low temperature during storage will elevate the life span of the packaged food products such as meat, fish, poultry (Church and Parsons, 1995).

The limitation of MAP may include the change in the functionality and organoleptic properties of the packaged foods. Increased acidity, for example, can induce release of non-heme iron in meat that can act as prooxidant causing oxidation (Olatunde *et al.*, 2019). Previous applications of MAP for fish preservation are summarized in Table 2.

Table 2. Applications of MAP for fish preservation

Fish	Treatment	Results	References
Tilapia fillets	MAP (50%CO_2/50%N_2)	- Reduce microbial load - Lower lipid oxidation - Extend shelf-life for 23 days at 1˚C	Cyprian *et al.* (2013)
Puffer fish	Immersion in weakly acidic electrolysed water (3% HCl) + MAP (60%CO_2/5%O_2/35%N_2)	- Reduce microbial load - Lower lipid oxidation - Extend shelf-life for18 days	Li *et al.* (2020)
Red drum fillets	Vacuum packaged + MAP (50%CO_2/50%N_2)	- Maintain the quality parameters - extend the shelf life for 29 days compared to only vacuum packaged fillets (15 days)	Silbande *et al.* (2018)
Common carp	MAP (20%CO_2 /80%O_2)	- Reduce microbial growth - Increase sensorial acceptability - Extend shelf life for 8 days compared to 3 days for samples packaged in air	Hudecová *et al.* (2010)
Asian Sea Bass Slices	Ethanolic coconut husk extract (ECHE) (200 ppm) + MAP (60% CO_2/30% N_2/10% O_2)	- Reduce microbial growth - Lower PV and TBA values - Extend shelf life for 15 days at 4˚C	Olatunde *et al.* (2019)

1.2.3.2.2. Non-thermal plasma (NTP)

When sufficient energy is applied on a mixture of gases, reactive species will be generated and the system will reach to an ionization state which is referred to plasma, according to the temperature of the energy applied the plasma can be divided into thermal and non-thermal plasma (Misra *et al.*, 2011). Generally, non-thermal plasma (NTP) take place when a gas or mixture of gases is ionized to generate reactive species without the involvement or production of heat, these reactive species, such as reactive oxygen species (ROS), reactive nitrogen species (RNS) and other free radicals, can inhibit microbial growth (Gavahian *et al.*, 2018). Type and composition of gases, intensity of electric current applied, and exposure time decide the antimicrobial effectiveness of NTP (Miyamoto *et al.*, 2016). Normally, atmospheric air is gas used for generation of non-thermal plasma, however due to the uncontrolled production of free radicals that may have drawbacks on the treated samples, the appropriate mixture of gases is preferably required (Misra *et al.*, 2011).

NTP is used for sanitizing surfaces, containers, and can be beneficial to food manufacturers for ensuring food safety, this technology is gaining increased popularity because it does not cause any discoloration, dehydration, or have any adverse effects on the sensory and nutritive characteristics of food products (Sonawane and Patil, 2020). Different sources have been used for NTP generation including corona discharge, dielectric barrier discharge, atmospheric pressure plasma jet, and plasma needle (Rana *et al.*, 2020). Schematic diagram of dielectric barrier discharge cold plasma system is depicted in Fig.5.

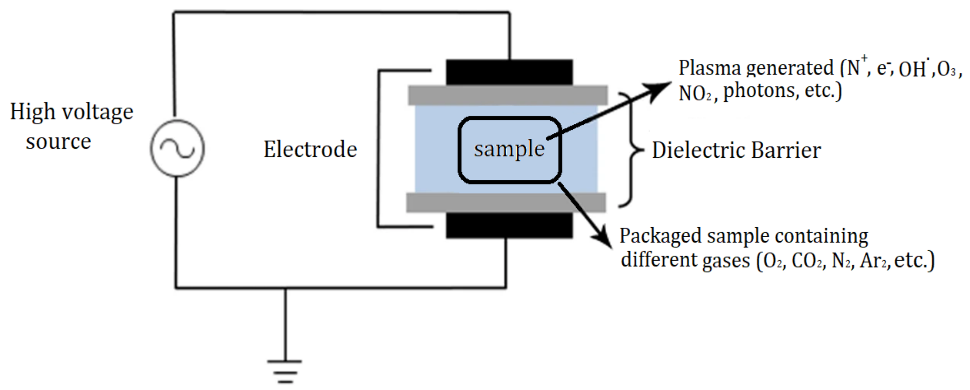

Figure 5. Schematic diagram of dielectric barrier discharge cold plasma system.

Source: modified from Luo *et al.* (2019)

Using inert gases would be beneficial for NTP generation as it will not cause any oxidative degradation for food, however the cost of treatment might increase (Misra *et al.,* 2014). Overall, the different operating and design parameters will result in different types of reactive species which will be associated with different degrees of decontamination (Aboubakr *et al.*, 2015).

The potential antimicrobial mechanism of NTP implicates the interaction of the reactive species generated with the microbial cell membranes, these reactive species can damage the cell constituents including proteins, lipids, and nucleic acids through a chain of oxidation reactions (Afshari and Hosseini, 2014). Oxidation of these constituents causes the severe changes in the microbial cell function and morphology, which can lead to damage and death to the targeted microorganisms (Misra *et al.*, 2016).

The use of NTP in food applications is an increasing trend due to its advantages. NTP combined with liposomes containing coconut husk extract was an effective in extending the shelf-life of Asian sea bass slices stored at 4˚C for 18 days (Olatunde *et al.,* 2020a). Lee *et al.* (2011) found that the treatment with NTP for 2 min using the mixture of gases (He (5 L/min) + O_2 (0.1 L/min)) at 30 kV and 60 Hz retarded the microbial growth on smoked salmon by 1 log CFU/g. A significant decrease in the microbial counts was reported when treating dried filefish fillets with NTP at 50 kV for 3 min (Park and Ha, 2015). Dielectric barrier discharge-NTP at 60 kV and 4 min extended the shelf-life of tilapia fillets stored at 4˚C for 10 days, compared with the control which lasted to only 4 days (Mohamed *et al.,* 2021). Chub mackerel (*Scomber japonicus*) treated with NTP at 60 kV and 60 s had an extended shelf-life of 14 days, scanning electron microscopy showed a delay in the degradation of myofibrillar proteins resulted from the treatment thus, the stability of tissue structures was maintained during the storage (Chen *et al.,* 2019).

Despite the breakthrough achieved by NTP technology in the food safety sector, undesired drawbacks may occur. As a consequence of the presence of free radicals, lipid oxidation might happen particularly in foods containing high lipid content (Ekezie *et al.,* 2017). Additionally, changes in the textural properties, and discoloration of the treated food can take place (Ganesan *et al*., 2021). Moreover, the overall cost of the NTP process and the inability to be used on an industrial scale may limit the employment of NTP in some food applications (Misra *et al.,* 2016).

1.2.3.3. Active packaging for food preservation

As response to the concerns raised about the safety and additive content of packaged food, in addition to the calls for minimizing the usage of commonly used petrochemical plastics. Novel trends have been directed to the production of high-quality and minimally processed foods, devoid of any preservatives, but have an acceptable shelf-life (Kerch, 2015). Of these trends are the packaging systems incorporated with bioactive components that would be released or absorbed by the packaged foods for the purpose of extending their shelf-life or to maintaining or enhancing their properties which are referred to as active packaging (Yildirim *et al.,* 2018). These systems must prevent any unwanted chemical and biological changes thus preserving food quality and ensuring its safety from production stages to final consumption (Kong *et al.,* 2022).

Films, whether edible or biodegradable which are made from various bio-based polymers such as polysaccharides, proteins, lipids, and composite materials, are preferable in active packaging (Sapper *et al.,* 2019). Mechanical and barrier properties of the prepared films are dependent on the nature of biopolymers used, additionally other factors such production process, concentration will surely affect on the produced films (Yousuf *et al.,* 2018). Using one type of polymer may result in a film that lack the desired mechanical and physical properties plus having some defects such as less water and oxygen barrier abilities, therefore composite or mixture of polymers might help in reducing unexpected defects in addition to have better mechanical and physical properties (Thakur *et al.,* 2019).

Composite films made of biopolymers such as gelatin, gluten, starch, chitosan, polylactic acid bee wax, and paraffin wax were used to produce biodegradable films with better mechanical and physical properties (Kerch, 2015). To avoid any stiffness or rigidity of the resulted films, usually plasticizers are involved in the matrix of the films to lower the extensive interactions between the different polymers by placing themselves between these polymers thus, more flexible, and processable film can be acquired (Thakur *et al.,* 2019). The majority of the plasticizers are hydrophilic thus, drawing water molecules and forming a large plasticizer-water hydrodynamic complex. Plasticizers used commonly in the formula of many films are glycerin, sucrose, polyethylene glycol, and corn syrup (Kumar *et al.*, 2019).

Several methods have been employed for preparing biodegradable films including casting method, mostly used in laboratories or pilot scales, and involving the solubilization of the biopolymer mixture in a suitable solvent, casting of that mixture in a mold, and finally drying the casted solution (Munhoz *et al.*, 2018). Extrusion method is used to produce films at commercial scale, this method involves alterations on the biopolymers structure, thus improving the properties of extruded films (Azevedo *et al.*, 2017). Electrospinning has gained the attention to produce different bioactive packaging systems, it is based on a high electric field applied to viscoelastic polymer solutions containing the bioactive compounds to generate a mat of polymer nanofibers incorporated with bioactive compounds (Fig. 6) (Radusin *et al.*, 2019). The high surface area-to-volume ratio of these nanofibers with elevated porosity will guarantee the sustained release of the bioactive compounds (Wen *et al.*, 2016). This technology can be applied as coatings or films to form novel active packaging systems (Torres-Giner *et al.*, 2018).

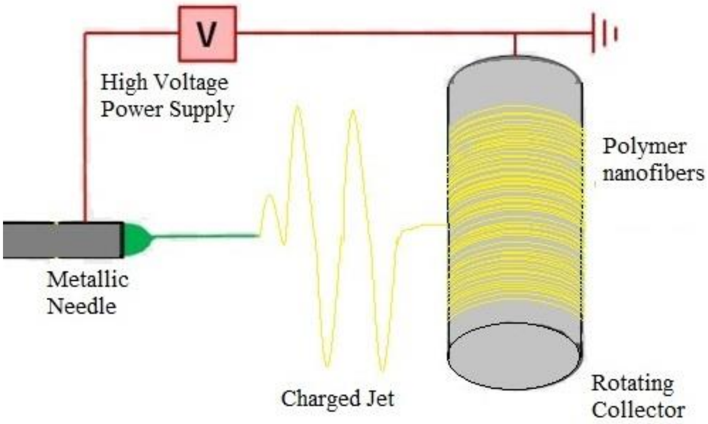

Figure 6. Schematic of electrospinning of polymer nanofibers.
Source: modified from Santangelo (2019).

Lately active packaging has been applied for the preservation of fish and fish products and were reported suitable for maintaining the nutritional and organoleptic properties of these products, some of these applications are summarized in Table 3.

Table 3. Applications of active packaging for fish and fish products preservation

Product	Active package composition	Active compound	Results	References
Hake fillets	Agar (1.5%, w/v), glycerol (1%, w/v), glucose (2%, w/v)	Green tea extract (1%) (50:50) of film solution	- Delay microbial growth - Lower lipid oxidation - Extend shelf life for 7 days	De Lacey *et al.* (2014)
Rainbow trout fillets	Gelatin (8%, w/v), glycerol (0.1 mL/g gelatin) D-sorbitol (0.15g/g glatin)	Laurel leaf essential oil (1%, v/w gelatin)	- Maintain the quality characteristics of fillets under refrigerated storage - Extend shelf life to 22 days compared to 15 days for the control	Alparslan *et al.* (2014)
Fried salmon skin	Layer 1: Gelatin (3.5%, w/v), glycerol (30%, w/w gelatin) Layer 2: Gelatin (3.5%, w/v), glycerol (10%, w/w gelatin), Palm oil mixed with 50% soy lecithin used as surfactant	Epigallocatechin gallate (12%, w/w gelatin)	- Lower PV and TBARS throughout 30 days of storage - Maintain PUFAs in fried salmon skin more effectively	Nilsuwan *et al.* (2021)

Table 3. (continued)

Product	Active package composition	Active compound	Results	References
Rainbow trout fillets	Quince seed mucilage (QSM; 1%, w/v), glycerol (35%, w/w of QSM)	Thyme essential oil (2%, v/v of film solution)	- Prevent lipid oxidation - Reduce microbial spoilage - Extend shelf life for 18 days compared to 7 days for the control	Jouki *et al.* (2014)
Asian seabass	Gelatin (20%, w/v acetic acid (90%)), chitosan (3%,w/v acetic acid(90%)), polylactic acid (PLA) film (5%, w/v chloroform).	Nisin (0.4%, w/v gelatin/chitosan nanofibers solution) loaded via electrospinning (flow rate 0.5mL/hr, 20kV)	- Reduce microbial counts - Lower TVBN values and lipid oxidation - Extend shelf life for 12 days compared to 3 days for the control	Gulzar *et al.* (2022)
Japanese seabass	Poly (vinyl alcohol) (PVA) fibrous films (12%, w/v DW)	Poly (hexamethylene biguanide) hydrochloride (PHMB) (10%, w/v PVA) loaded via electrospinning (flow rate 0.3mL/hr, 23kV)	- Retard microbial growth - Lower lipid oxidation - Better textural properties - extend shelf-life to 8 days based of total viable counts	Zhang *et al.* (2021)

1.3. Objectives of the study

The objectives of this research can be summarized as follows:

1.3.1. To investigate the characteristics and antioxidant activities of the ethanolic extracts of betel (*Piper betle* L.) and chaphlu (*Piper sarmentosum* Roxb.) dechlorophyllized using sedimentation process.

1.3.2. To study the characteristics, antioxidant, and antibacterial activities of betel ethanolic extract dechlorophyllized using different methods and the application for shelf-life extension of Nile tilapia (*Oreochromis niloticus*) slices.

1.3.3. To evaluate the antimicrobial and antioxidative properties of betel ethanolic extract dechlorophyllized by sedimentation and encapsulated in liposome.

1.3.4. To study the synergistic effects of liposomal encapsulated betel leaf ethanolic extract and non-thermal plasma on the prevention of lipid oxidation and shelf-life extension of refrigerated Nile tilapia slices packaged under different atmospheres.

1.3.5. To investigate the antioxidant, antimicrobial, and mechanical properties of gelatin/chitosan blend films incorporated with betel leaf ethanolic extracts.

1.3.6. To study the effects of pouches made from gelatin/chitosan blend films containing betel leaf ethanolic extract or liposomes loaded with the extract on shelf-life and quality attributes of shrimp oil during extending storage.

1.3.7. To evaluate the characteristics and bioactivities of polylactic acid films electrospun by gelatin/chitosan nanofibers containing betel leaf ethanolic extract and the effectiveness of bags made from such films in extending the shelf-life of Nile tilapia slices.

1.4. References

Abdollahzadeh, E., Rezaei, M. and Hosseini, H. 2014. Antibacterial activity of plant essential oils and extracts: The role of thyme essential oil, nisin, and their combination to control *Listeria monocytogenes* inoculated in minced fish meat. Food Control. 35: 177-183.

Aboubakr, H. A., Williams, P., Gangal, U., Youssef, M. M., El-Sohaimy, S. A., Bruggeman, P. J. and Goyal, S. M. 2015. Virucidal effect of cold atmospheric gaseous plasma on feline calicivirus, a surrogate for human norovirus. Applied and Environmental Microbiology. 81: 3612-3622.

Abu-Elala, N. M., Ali, T. E.-S., Ragaa, N. M., Ali, S. E., Abd-Elsalam, R. M., Younis, N. A., Abdel-Moneam, D. A., Hamdien, A. H., Bonato, M. and Dawood, M. A. 2021. Analysis of the Productivity, Immunity, and Health Performance of Nile Tilapia (*Oreochromis niloticus*) Brood stock-fed Dietary Fermented Extracts Sourced from *Saccharomyces cerevisiae* (Hilyses): A Field Trial. Animals. 11: 815.

Afshari, R. and Hosseini, H. 2014. Non-thermal plasma as a new food preservation method, its present and future prospect. Archives of Advances in Biosciences. 5: 4978.

Al-Maqtari, Q. A., Rehman, A., Mahdi, A. A., Al-Ansi, W., Wei, M., Yanyu, Z., Phyo, H. M., Galeboe, O. and Yao, W. 2021. Application of essential oils as preservatives in food systems: challenges and future prospectives–a review. Phytochemistry Reviews. 21: 1209 - 1246.

Alparslan, Y., Baygar, T., Baygar, T., Hasanhocaoglu, H. and Metin, C. 2014. Effects of gelatin-based edible films enriched with laurel essential oil on the quality of rainbow trout (*Oncorhynchus mykiss*) fillets during refrigerated storage. Food Technology and Biotechnology. 52: 325 - 333.

Anand, S. and Sati, N. 2013. Artificial preservatives and their harmful effects: looking toward nature for safer alternatives. International Journal of Pharmaceutical Sciences and Research. 4: 2496.

Andoni, E., Ozuni, E., Bijo, B., Shehu, F., Branciari, R., Miraglia, D. and Ranucci, D. 2021. Efficacy of non-thermal processing methods to prevent fish spoilage. Journal of Aquatic Food Product Technology. 30: 228 - 245.

Azevedo, V. M., Borges, S. V., Marconcini, J. M., Yoshida, M. I., Neto, A. R. S., Pereira, T. C. and Pereira, C. F. G. 2017. Effect of replacement of corn starch by whey protein isolate in biodegradable film blends obtained by extrusion. Carbohydrate Polymers. 157: 971 - 980.

Benjakul, S., Kittiphattanabawon, P., Sumpavapol, P. and Maqsood, S. 2014. Antioxidant activities of lead (*Leucaena leucocephala*) seed as affected by extraction solvent, prior dechlorophyllisation and drying methods. Journal of Food Science and Technology. 51: 3026 - 3037.

Benjakul, S., Visessanguan, W. and Tanaka, M. 2003. Partial purification and characterization of trimethylamine-N-oxide demethylase from lizardfish kidney. Comparative Biochemistry and Physiology Part B: Biochemistry and Molecular Biology. 135: 359 - 371.

Bensid, A., Ucar, Y., Bendeddouche, B. and Özogul, F. 2014. Effect of the icing with thyme, oregano and clove extracts on quality parameters of gutted and beheaded anchovy (*Engraulis encrasicholus*) during chilled storage. Food Chemistry. 145: 681 - 686.

Bono, G., Okpala, C. O. R., Vitale, S., Ferrantelli, V., Noto, A. D., Costa, A., Di Bella, C. and Monaco, D. L. 2017. Effects of different ozonized slurry-ice treatments and superchilling storage (- 1˚C) on microbial spoilage of two important pelagic fish species. Food Science and Nutrition. 5: 1049 - 1056.

Bourtoom, T. 2008. Edible films and coatings: characteristics and properties. International Food Research Journal. 15: 237 - 248.

Boziaris, I. S. and Parlapani, F. F. 2017. Specific spoilage organisms (SSOs) in fish. The Microbiological Quality of Food. Woodhead Publishing Series in Food Science, Technology and Nutrition. 2017: 61 - 98.

Brown, N., John, J. A. and Shahidi, F. 2019. Polyphenol composition and antioxidant potential of mint leaves. Food Production, Processing and Nutrition. 1: 1 - 14.

Bruni, N., Stella, B., Giraudo, L., Della Pepa, C., Gastaldi, D. and Dosio, F. 2017. Nanostructured delivery systems with improved leishmanicidal activity: a critical review. International Journal of Nanomedicine. 12: 5289.

Campos, C. A., Castro, M. P., Aubourg, S. P. and Velázquez, J. B. 2012. Use of natural preservatives in seafood. Novel Technologies in Food Science. 7: 325 - 360.

Carocho, M., Morales, P. and Ferreira, I. C. 2015. Natural food additives: Quo vadis? Trends in Food Science and Technology. 45: 284 - 295.

Carpenter, S. R., Elser, M. M. and Elser, J. J. 1986. Chlorophyll production, degradation, and sedimentation: Implications for paleolimnology 1. Limnology and Oceanography. 31: 112 - 124.

Chen, H., Wang, J., Jiang, G., Guo, H., Liu, X. and Wang, L. 2020. Active packaging films based on chitosan and *Herba lophatheri* extract for the shelf-life extension of fried bighead carp fillets. International Food Research Journal. 27: 720 - 726.

Chen, J., Wang, S. Z., Chen, J. Y., Chen, D. Z., Deng, S. G. and Xu, B. 2019. Effect of cold plasma on maintaining the quality of chub mackerel (*Scomber japonicus*): biochemical and sensory attributes. Journal of the Science of Food and Agriculture. 99: 39 - 46.

Cheng, J. H., Sun, D. W., Han, Z. and Zeng, X. A. 2014. Texture and structure measurements and analyses for evaluation of fish and fillet freshness quality: a review. Comprehensive Reviews in Food Science and Food Safety. 13: 52 - 61.

Church, I. J. and Parsons, A. L. 1995. Modified atmosphere packaging technology: a review. Journal of the Science of Food and Agriculture. 67: 143 - 152.

Crapo, C., Himelbloom, B., Vitt, S. and Pedersen, L. 2004. Ozone efficacy as a bactericide in seafood processing. Journal of Aquatic Food Product Technology. 13: 111 - 123.

Cyprian, O., Lauzon, H. L., Jóhannsson, R., Sveinsdóttir, K., Arason, S. and Martinsdóttir, E. 2013. Shelf life of air and modified atmosphere packaged fresh tilapia (*Oreochromis niloticus*) fillets stored under chilled and superchilled conditions. Food Science and Nutrition. 1: 130 - 140.

Cyprian, O., Oduor-Odote, P., Lauzon, H., Martinsdóttir, E. and Arason, S. 2021. Microbiological quality and shelf life of fresh packaged tilapia fillets stored under different chill temperatures. Journal of Microbiology, Biotechnology and Food Sciences. 2021: 2456 - 2465.

Da Silva Malheiros, P., Sant'anna, V., De Souza Barbosa, M., Brandelli, A. and De Melo Franco, B. D. G. 2012. Effect of liposome-encapsulated nisin and bacteriocin-like substance P34 on *Listeria monocytogenes* growth in Minas frescal cheese. International Journal of Food Microbiology. 156: 272 - 277.

De Lacey, A. L., López-Caballero, M. and Montero, P. 2014. Agar films containing green tea extract and probiotic bacteria for extending fish shelf-life. LWT-Food Science and Technology. 55: 559 - 564.

Dhital, R., Mora, N. B., Watson, D. G., Kohli, P. and Choudhary, R. 2018. Efficacy of limonene nano coatings on post-harvest shelf life of strawberries. LWT-Food Science and Technology. 97: 124 - 134.

Ekezie, F.-G. C., Sun, D.-W. and Cheng, J.-H. 2017. A review on recent advances in cold plasma technology for the food industry: Current applications and future trends. Trends in Food Science and Technology. 69: 46 - 58.

El-Beltagi, H. S., El-Mogy, M. M., Parmar, A., Mansour, A. T., Shalaby, T. A. and Ali, M. R. 2022. Phytochemical characterization and utilization of dried red beetroot (*Beta vulgaris*) peel extract in maintaining the quality of Nile Tilapia fish fillet. Antioxidants. 11: 906.

El Asely, A. M., Reda, R. M., Salah, A. S., Mahmoud, M. A. and Dawood, M. A. 2020. Overall performances of Nile tilapia (*Oreochromis niloticus*) associated with using vegetable oil sources under suboptimal temperature. Aquaculture Nutrition. 26: 1154 - 1163.

Ganesan, A. R., Tiwari, U., Ezhilarasi, P. and Rajauria, G. 2021. Application of cold plasma on food matrices: A review on current and future prospects. Journal of Food Processing and Preservation. 45: e15070.

García-Díez, J., Alheiro, J., Pinto, A., Soares, L., Falco, V., Fraqueza, M. and Patarata, L. 2016. Behaviour of food-borne pathogens on dry cured sausage manufactured with herbs and spices essential oils and their sensorial acceptability. Food Control. 59: 262 - 270.

Gavahian, M., Chu, Y.-H., Khaneghah, A. M., Barba, F. J. and Misra, N. 2018. A critical analysis of the cold plasma induced lipid oxidation in foods. Trends in Food Science and Technology. 77: 32 - 41.

Gebicki, J. 1997. Protein hydroperoxides as new reactive oxygen species. Redox Report. 3: 99 - 110.

Ghaly, A. E., Dave, D., Budge, S. and Brooks, M. 2010. Fish spoilage mechanisms and preservation techniques. American Journal of Applied Sciences. 7: 859.

Gokoglu, N. 2019. Novel natural food preservatives and applications in seafood preservation: A review. Journal of the Science of Food and Agriculture. 99: 2068 - 2077.

Gulzar, S., Tagrida, M., Prodpran, T., and Benjakul, S. 2022. Antimicrobial film based on polylactic acid coated with gelatin/chitosan nanofibers containing nisin extends the shelf life of Asian seabass slices. Food Packaging and Shelf Life. 34: 100941.

Gram, L. 2009. Microbiological spoilage of fish and seafood products. Compendium of the microbiological spoilage of foods and beverages. Food Microbiology and Food Safety. Springer. 87 - 119.

Gram, L. and Huss, H. H. 1996. Microbiological spoilage of fish and fish products. International Journal of Food Microbiology. 33: 121 - 137.

Hasan, F., Shah, A. A. and Hameed, A. 2009. Methods for detection and characterization of lipases: a comprehensive review. Biotechnology Advances. 27: 782 - 798.

Hasani, S. and Hasani, M. 2014. Antimicrobial properties of grape extract on common carp (*Cyprinus carpio*) fillet during storage in 4˚C. International Journal of Fisheries and Aquatic Studies. 1: 130 - 136.

Hassoun, A. and Çoban, Ö. E. 2017. Essential oils for antimicrobial and antioxidant applications in fish and other seafood products. Trends in Food Science and Technology. 68: 26 - 36.

He, L., Lan, W., Ahmed, S., Qin, W. and Liu, Y. 2019. Electrospun polyvinyl alcohol film containing pomegranate peel extract and sodium dehydroacetate for use as food packaging. Food Packaging and Shelf Life. 22: 100390.

Hosomi, R., Yoshida, M. and Fukunaga, K. 2012. Seafood consumption and components for health. Global Journal of Health Science. 4: 72.

Hudecová, K., Buchtová, H. and Steinhauserová, I. 2010. Effects of modified atmosphere packaging on the microbiological properties of fresh common carp (*Cyprinus carpio* L.). Acta Veterinaria Brno. 79: 93 - 100.

Hussain, K., Hashmi, F. K., Latif, A., Ismail, Z. and Sadikun, A. 2012. A review of the literature and latest advances in research of *Piper sarmentosum*. Pharmaceutical Biology. 50: 1045 - 1052.

Izquierdo, M. and Henderson, R. 1998. The determination of lipase and phospholipase activities in gut contents of turbot (*Scophthalmus maximus*) by fluorescence-based assays. Fish Physiology and Biochemistry. 19: 153 - 162.

Jin, S., Wang, Y. and Zhao, X. 2022. Cold-adaptive mechanism of psychrophilic bacteria in food and its application. Microbial Pathogenesis. 169: 105652.

Johnson, D. R. and Decker, E. A. 2015. The role of oxygen in lipid oxidation reactions: a review. Annual Review of Food Science and Technology. 6: 171 - 190.

Jouki, M., Yazdi, F. T., Mortazavi, S. A., Koocheki, A. and Khazaei, N. 2014. Effect of quince seed mucilage edible films incorporated with oregano or thyme essential oil on shelf life extension of refrigerated rainbow trout fillets. International Journal of Food Microbiology. 174: 88 - 97.

Kähkönen, M. P., Hopia, A. I., Vuorela, H. J., Rauha, J.-P., Pihlaja, K., Kujala, T. S. and Heinonen, M. 1999. Antioxidant activity of plant extracts containing phenolic compounds. Journal of Agricultural and Food Chemistry. 47: 3954 - 3962.

Karpuz, M., Gunay, M. S. and Ozer, A. Y. 2020. Liposomes and phytosomes for phytoconstituents. Advances and Avenues in the Development of Novel Carriers for Bioactives and Biological Agents. Elsevier. 2020: 525 - 553.

Kerch, G. 2015. Chitosan films and coatings prevent losses of fresh fruit nutritional quality: A review. Trends in Food Science and Technology. 46: 159 - 166.

Khalafalla, F. A., Ali, F. H. and Hassan, A.-R. H. 2015. Quality improvement and shelf-life extension of refrigerated Nile tilapia (*Oreochromis niloticus*) fillets using natural herbs. Beni-Suef University Journal of Basic and Applied Sciences. 4: 33 - 40.

Khalili tilami, S. and Sampels, S. 2018. Nutritional value of fish: lipids, proteins, vitamins, and minerals. Reviews in Fisheries Science and Aquaculture. 26: 243 - 253.

Kumar, R., Ghoshal, G. and Goyal, M. 2019. Synthesis and functional properties of gelatin/CA–starch composite film: excellent food packaging material. Journal of Food Science and Technology. 56: 1954 - 1965.

Lawal, A. T. and Adeloju, S. B. 2012. Progress and recent advances in fabrication and utilization of hypoxanthine biosensors for meat and fish quality assessment: a review. Talanta. 100: 217 - 228.

Lee, H.-B., Noh, Y.-E., Yang, H.-J. and Min, S.-C. 2011. Inhibition of foodborne pathogens on polystyrene, sausage casings, and smoked salmon using nonthermal plasma treatments. Korean Journal of Food Science and Technology. 43: 513 - 517.

Leisner, J. and Gram, L. 2000. Spoilage of fish. Encyclopedia of Food Microbiology. Academic Press. 2000: 813 - 820.

Leistner, L. 2000. Basic aspects of food preservation by hurdle technology. International Journal of Food Microbiology. 55: 181 - 186.

Li, P., Chen, Z., Tan, M., Mei, J. and Xie, J. 2020. Evaluation of weakly acidic electrolyzed water and modified atmosphere packaging on the shelf life and quality of farmed puffer fish (*Takifugu obscurus*) during cold storage. Journal of Food Safety. 40: e12773.

Liang, N. and Kitts, D. D. 2014. Antioxidant property of coffee components: assessment of methods that define mechanisms of action. Molecules. 19: 19180 - 19208.

Liu, W., Ye, A., Han, F. and Han, J. 2019. Advances and challenges in liposome digestion: Surface interaction, biological fate, and GIT modeling. Advances in Colloid and Interface Science. 263: 52 - 67.

Luo, J., Yan, W., Nasiru, M. M., Zhuang, H., Zhou, G. and Zhang, J. 2019. Evaluation of physicochemical properties and volatile compounds of Chinese dried pork loin curing with plasma-treated water brine. Scientific Reports. 9: 13793.

Mai-Prochnow, A., Clauson, M., Hong, J. and Murphy, A. B. 2016. Gram positive and Gram negative bacteria differ in their sensitivity to cold plasma. Scientific Reports. 6: 38610.

Mancini, S., Nardo, L., Gregori, M., Ribeiro, I., Mantegazza, F., Delerue-Matos, C., Masserini, M. and Grosso, C. 2018. Functionalized liposomes and phytosomes loading *Annona muricata* L. aqueous extract: Potential nanoshuttles for brain-delivery of phenolic compounds. Phytomedicine, 42: 233 - 244.

Masniyom, P. 2011. Deterioration and shelf-life extension of fish and fishery products by modified atmosphere packaging. Songklanakarin Journal of Science and Technology, 33(2): 181 - 192.

Mastromatteo, M., Conte, A. and Del Nobile, M. 2010. Combined use of modified atmosphere packaging and natural compounds for food preservation. Food Engineering Reviews. 2: 28 - 38.

Mazandrani, H. A., Javadian, S. and Bahram, S. 2016. The effect of encapsulated fennel extracts on the quality of silver carp fillets during refrigerated storage. Food Science and Nutrition. 4: 298 - 304.

Medina, I., González, M. J., Pazos, M., Della Medaglia, D., Sacchi, R. and Gallardo, J. M. 2003. Activity of plant extracts for preserving functional food containing n-3-PUFA. European Food Research and Technology. 217: 301 - 307.

Mei, J., Ma, X. and Xie, J. 2019. Review on natural preservatives for extending fish shelf life. Foods. 8: 490.

Mishra, R., Bhatia, S., Pal, R., Visen, A. and Trivedi, H. 2016. Cold plasma: emerging as the new standard in food safety. International Journal of Engineering Research and Technology. 6: 15 - 20.

Misra, N., Schlüter, O. and Cullen, P. J. 2016. Cold plasma in food and agriculture: fundamentals and applications. Academic Press. ISBN: 978-0-12-801365-6: 317 - 325.

Misra, N., Tiwari, B., Raghavarao, K. and Cullen, P. 2011. Nonthermal plasma inactivation of food-borne pathogens. Food Engineering Reviews. 3: 159 - 170.

Misra, N. N., Keener, K. M., Bourke, P., Mosnier, J.-P. and Cullen, P. J. 2014. In-package atmospheric pressure cold plasma treatment of cherry tomatoes. Journal of Bioscience and Bioengineering. 118: 177 - 182.

Miyamoto, K., Ikehara, S., Takei, H., Akimoto, Y., Sakakita, H., Ishikawa, K., Ueda, M., Ikeda, J.-I., Yamagishi, M. and Kim, J. 2016. Red blood cell coagulation induced by low-temperature plasma treatment. Archives of Biochemistry and Biophysics. 605: 95 - 101.

Mohamed, E. E., Younis, E. R. and Mohamed, E. A. 2021. Impact of atmospheric cold plasma (ACP) on maintaining bolti fish (*Tilapia nilotica*) freshness and quality criteria during cold storing. Journal of Food Processing and Preservation. 45: e15442.

Morris, C., Brody, A. L. and Wicker, L. 2007. Non-thermal food processing/preservation technologies: A review with packaging implications. Packaging Technology and Science: An International Journal. 20: 275 - 286.

Mostafa, A. A., Al-Askar, A. A., Almaary, K. S., Dawoud, T. M., Sholkamy, E. N. and Bakri, M. M. 2018. Antimicrobial activity of some plant extracts against bacterial strains causing food poisoning diseases. Saudi Journal of Biological Sciences. 25: 361 - 366.

Mozafari, M. R., Khosravi-darani, K., Borazan, G. G., Cui, J., Pardakhty, A. and Yurdugul, S. 2008. Encapsulation of food ingredients using nanoliposome technology. International Journal of Food Properties. 11: 833 - 844.

Munhoz, D. R., Moreira, F. K., Bresolin, J. D., Bernardo, M. P., De Sousa, C. P. and Mattoso, L. H. 2018. Sustainable production and in vitro biodegradability of edible films from yellow passion fruit coproducts *via* continuous casting. ACS Sustainable Chemistry and Engineering. 6: 9883 - 9892.

Muñoz-Shugulí, C., Vidal, C. P., Cantero-López, P. and Lopez-Polo, J. 2020. Encapsulation of plant extract compounds using cyclodextrin inclusion complexes, liposomes, electrospinning and their combinations for food purposes. Trends in Food Science and Technology. 11(7): 373 - 384.

Nouri, L., Nafchi, A. M. and Karim, A. 2014. Phytochemical, antioxidant, antibacterial, and α-amylase inhibitory properties of different extracts from betel leaves. Industrial Crops and Products. 62: 47 - 52.

Odeyemi, O. A., Alegbeleye, O. O., Strateva, M. and Stratev, D. 2020. Understanding spoilage microbial community and spoilage mechanisms in foods of animal origin. Comprehensive Reviews in Food Science and Food Safety. 19: 311 - 331.

Olatunde, O. O. and Benjakul, S. 2018. Natural preservatives for extending the shelf-life of seafood: a revisit. Comprehensive Reviews in Food Science and Food Safety. 17: 1595 - 1612.

Olatunde, O. O., Benjakul, S. and Vongkamjan, K. 2019. Combined Effect of ethanolic coconut husk extract and modified atmospheric packaging (MAP) in extending the shelf life of Asian sea bass slices. Journal of Aquatic Food Product Technology. 28: 689 - 702.

Olatunde, O. O., Benjakul, S. and Vongkamjan, K. 2020a. Cold plasma combined with liposomal ethanolic coconut husk extract: A potential hurdle technology for shelf-life extension of Asian sea bass slices packaged under modified atmosphere. Innovative Food Science and Emerging Technologies. 65: 102448.

Olatunde, O. O., Benjakul, S. and Vongkamjan, K. 2020b. Shelf-life of refrigerated Asian sea bass slices treated with cold plasma as affected by gas composition in packaging. International Journal of Food Microbiology. 324: 108612.

Olatunde, O. O., Benjakul, S., Huda, N., Zhang, B. and Deng, S. 2021a. Ethanolic noni (*Morinda citrifolia* L.) leaf extract dechlorophyllised using sedimentation process: Antioxidant, antibacterial properties and efficacy in extending the shelf-life of striped catfish slices. International Journal of Food Science and Technology. 56: 2804 - 2819.

Olatunde, O. O., Della Tan, S. L., Shiekh, K. A., Benjakul, S. and Nirmal, N. P. 2021b. Ethanolic guava leaf extracts with different chlorophyll removal processes: Anti-melanosis, antibacterial properties and the impact on qualities of Pacific white shrimp during refrigerated storage. Food Chemistry. 341: 128251.

Oliveira, R. V., Oliveira, M. C. and Pelli, A. 2017. Disease infection by *Enterobacteriaceae* family in fishes: a review. Journal of Microbiology and Experimentation. 4(5): 00128.

Özogul, F., Aksun, E. T., Öztekin, R. and Lorenzo, J. M. 2017. Effect of lavender and lemon balm extracts on fatty acid profile, chemical quality parameters and sensory quality of vacuum packaged anchovy (*Engraulis encrasicolus*) fillets under refrigerated condition. LWT- Food Science and Technology. 84: 529 - 535.

Pabón-Baquero, L. C., Otálvaro-Álvarez, Á. M., Fernández, M. R. R. and Chaparro-González, M. P. 2018. Plant extracts as antioxidant additives for food industry. Antioxidants. 64: 509 - 515.

Pang, X., Zhuang, X., Tang, Z. and Chen, X. 2010. Polylactic acid (PLA): research, development and industrialization. Biotechnology Journal. 5: 1125 - 1136.

Park, S. Y. and Ha, S. D. 2015. Application of cold oxygen plasma for the reduction of *Cladosporium cladosporioides* and *Penicillium citrinum* on the surface of dried file fish (*Stephanolepis cirrhifer*) fillets. International Journal of Food Science and Technology. 50: 966 - 973.

Premkumar, J. and Vasudevan, R. T. 2018. Bioingredients: functional properties and health impacts. Current Opinion in Food Science. 19: 120 - 128.

Radusin, T., Torres-Giner, S., Stupar, A., Ristic, I., Miletic, A., Novakovic, A. and Lagaron, J. M. 2019. Preparation, characterization and antimicrobial properties of electrospun polylactide films containing *Allium ursinum* L. extract. Food Packaging and Shelf Life. 21: 100357.

Raeisi, S., Quek, S. Y., Ojagh, S. M. and Alishahi, A. R. 2016. Effects of cumin (*Cuminum cyminum* L.) seed and wild mint (*Mentha longifolia* L.) leaf extracts on the shelf life and quality of rainbow trout (*Oncorhynchus mykiss*) fillets stored at 4˚C ± 1. Journal of Food Safety. 36: 271 - 281.

Rana, S., Mehta, D., Bansal, V., Shivhare, U. and Yadav, S. K. 2020. Atmospheric cold plasma (ACP) treatment improved in-package shelf-life of strawberry fruit. Journal of Food Science and Technology. 57: 102 - 112.

Redondo-Blanco, S., Fernandez, J., Lopez-Ibanez, S., Miguelez, E. M., Villar, C. J. and Lombo, F. 2020. Plant phytochemicals in food preservation: Antifungal bioactivity: A review. Journal of Food Protection. 83: 163 - 171.

Rocculi, P., Romani, S. and Dalla Rosa, M. 2005. Effect of MAP with argon and nitrous oxide on quality maintenance of minimally processed kiwifruit. Postharvest Biology and Technology. 35: 319 - 328.

Romano, K. A., Vivas, E. I., Amador-Noguez, D. and Rey, F. E. 2015. Intestinal microbiota composition modulates choline bioavailability from diet and accumulation of the proatherogenic metabolite trimethylamine-N-oxide. MBio. 6: e0248.

Sadgrove, N. J., Padilla-González, G. F. and Phumthum, M. 2022. Fundamental chemistry of essential oils and volatile organic compounds, methods of analysis and authentication. Plants. 11: 789.

Sahoo, T. K., Jena, P. K., Patel, A. K. and Seshadri, S. 2016. Bacteriocins and their applications for the treatment of bacterial diseases in aquaculture: a review. Aquaculture Research. 47: 1013 - 1027.

Salehi, B., Zakaria, Z. A., Gyawali, R., Ibrahim, S. A., Rajkovic, J., Shinwari, Z. K., Khan, T., Sharifi-Rad, J., Ozleyen, A. and Turkdonmez, E. 2019. Piper species: A comprehensive review on their phytochemistry, biological activities and applications. Molecules. 24: 1364.

Sannikova, N. E., Timofeev, I. O., Chubarov, A. S., Lebedeva, N. S., Semeikin, A. S., Kirilyuk, I. A., Tsentalovich, Y. P., Fedin, M. V., Bagryanskaya, E. G. and Krumkacheva, O. A. 2020. Application of EPR to porphyrin-protein agents for photodynamic therapy. Journal of Photochemistry and Photobiology B: Biology. 211: 112008.

Santangelo, S. 2019. Electrospun nanomaterials for energy applications: Recent advances. Applied Sciences. 9: 1049.

Santos-Sánchez, N. F., Salas-Coronado, R., Villanueva-Cañongo, C. and Hernández-Carlos, B. 2019. Antioxidant compounds and their antioxidant mechanism. Antioxidants. 10: 1 - 29.

Sapper, M., Bonet, M. and Chiralt, A. 2019. Wettability of starch-gellan coatings on fruits, as affected by the incorporation of essential oil and/or surfactants. LWT-Food Science and Technology. 116: 108574.

Saxena, H. O., Soni, A., Mohammad, N. and Choubey, S. K. 2014. Phytochemical screening and elemental analysis in different plant parts of *Uraria picta* Desv.: A Dashmul species. Journal of Chemical and Pharmaceutical Research. 6: 756 - 760.

Sazwi, N. N., Nalina, T. and Rahim, Z. H. A. 2013. Antioxidant and cytoprotective activities of *Piper betle*, *Areca catechu*, *Uncaria gambir* and betel quid with and without calcium hydroxide. BMC Complementary and Alternative Medicine. 13: 1-12.

Shahidi, F. and Zhong, Y. 2010. Lipid oxidation and improving the oxidative stability. Chemical Society Reviews. 39: 4067 - 4079.

Shahmohammadi, M., Javadi, M. and Nassiri-ASL, M. 2016. An overview on the effects of sodium benzoate as a preservative in food products. Biotechnology and Health Sciences. 3: 7 - 11.

Sikorski, Z. E., Kołakowska, A. and Burt, J. R. 2020. Postharvest biochemical and microbial changes. Seafood: Resources, nutritional composition, and preservation. CRC Press. ISBN: 9781003068419: 1 -20.

Silbande, A., Adenet, S., Chopin, C., Cornet, J., Smith-Ravin, J., Rochefort, K. and Leroi, F. 2018. Effect of vacuum and modified atmosphere packaging on the microbiological, chemical and sensory properties of tropical red drum *(Sciaenops ocellatus)* fillets stored at 4˚C. International Journal of Food Microbiology. 266: 31 - 41.

Singh, P., Wani, A. A., Saengerlaub, S. and Langowski, H.-C. 2011. Understanding critical factors for the quality and shelf-life of MAP fresh meat: a review. Critical Reviews in Food Science and Nutrition. 51: 146 - 177.

Singh, S. and Shalini, R. 2016. Effect of hurdle technology in food preservation: a review. Critical Reviews in Food Science and Nutrition. 56: 641 - 649.

Sivertsvik, M., Rosnes, J. T. and Bergslien, H. 2002. Modified atmosphere packaging. Minimal processing technologies in the food industry. Woodhead Publishing, 2002: 61-86.

Sonawane, S. K. and Patil, S. 2020. Non-thermal plasma: An advanced technology for food industry. Food Science and Technology International. 26: 727 - 740.

Song, Y., Xu, M. and Liang, Y. 2006. Analysis of chemical constituents of essential oil in *Piper sarmentosum* Roxb. by gas chromatography/mass spectrometry. Chinese Journal of Analysis Laboratory. 25: 24.

Srisapoome, P. and Areechon, N. 2017. Efficacy of viable Bacillus pumilus isolated from farmed fish on immune responses and increased disease resistance in Nile tilapia (*Oreochromis niloticus*): Laboratory and on-farm trials. Fish and Shellfish Immunology. 67: 199 - 210.

Tacon, A. G. 2020. Trends in global aquaculture and aquafeed production: 2000 – 2017. Reviews in Fisheries Science and Aquaculture. 28: 43 - 56.

Tappel, A., Brown, W. D., Zalkin, H. and Maier, V. 1961. Unsaturated lipid peroxidation catalyzed by hematin compounds and its inhibition by vitamin E1. Journal of the American Oil Chemists' Society. 38: 5 - 9.

Thakur, R., Pristijono, P., Scarlett, C. J., Bowyer, M., Singh, S. and Vuong, Q. V. 2019. Starch-based films: Major factors affecting their properties. International Journal of Biological Macromolecules. 132: 1079 - 1089.

Tometri, S. S., Ahmady, M., Ariaii, P. and Soltani, M. S. 2020. Extraction and encapsulation of *Laurus nobilis* leaf extract with nano-liposome and its effect on oxidative, microbial, bacterial and sensory properties of minced beef. Journal of Food Measurement and Characterization. 14: 3333 - 3344.

Torres-Giner, S., Busolo, M., Cherpinski, A. and Lagaron, J. 2018. Electrospinning in the packaging industry. Electrospinning: from basic research to commercialization. eISBN: 978-1-78801-294-2: 238 - 260.

Tzima, K., Brunton, N. P. and Rai, D. K. 2020. Evaluation of the impact of chlorophyll removal techniques on polyphenols in rosemary and thyme by-products. Journal of Food Biochemistry. 44: e13148.

Viji, P., Venkateshwarlu, G., Ravishankar, C. and Srinivasa Gopal, T. 2017. Role of plant extracts as natural additives in fish and fish products-A Review. Measurement and Characterization. 41: 438 - 451.

Weerakkody, N. S., Caffin, N., Turner, M. S. and Dykes, G. A. 2010. *In vitro* antimicrobial activity of less-utilized spice and herb extracts against selected food-borne bacteria. Food Control. 21: 1408 - 1414.

Wen, P., Zhu, D.-H., Wu, H., Zong, M.-H., Jing, Y.-R. and Han, S.-Y. 2016. Encapsulation of cinnamon essential oil in electrospun nanofibrous film for active food packaging. Food Control. 59: 366 - 376.

Xu, J. L., Riccioli, C. and Sun, D. W. 2015. An overview on nondestructive spectroscopic techniques for lipid and lipid oxidation analysis in fish and fish products. Comprehensive Reviews in Food Science and Food Safety. 14: 466 - 477.

Yildirim, S., Röcker, B., Pettersen, M. K., Nilsen-nygaard, J., Ayhan, Z., Rutkaite, R., Radusin, T., Suminska, P., Marcos, B. and Coma, V. 2018. Active packaging applications for food. Comprehensive Reviews in Food Science and Food Safety. 17: 165 - 199.

Yousuf, B., Qadri, O. S. and Srivastava, A. K. 2018. Recent developments in shelf-life extension of fresh-cut fruits and vegetables by application of different edible coatings: A review. LWT- Food Science and Technology. 89: 198 - 209.

Zhang, Y., Yang, L., Dong, Q. and Li, L. 2021. Fabrication of antibacterial fibrous films by electrospinning and their application for Japanese sea bass (*Lateolabrax japonicus*) preservation. LWT- Food Science and Technology. 149: 111870.

CHAPTER 2

ETHANOLIC EXTRACT OF BETEL (*PIPER BETLE* L.) AND CHAPHLU (*PIPER SARMENTOSUM* ROXB.) DECHLOROPHYLLIZED USING SEDIMENTATION PROCESS: PRODUCTION, CHARACTERISTICS, AND ANTIOXIDANT ACTIVITIES

2.1. Abstract

Sedimentation process was used to remove chlorophyll from betel leaf ethanolic extracts (BLEE) and chaphlu leaf ethanolic extracts (CLEE). The influence of water quantity on chlorophyll content, total phenolic content (TPC), and antioxidant activity of the extracts was studied. The sedimentation process showed a remarkable reduction in chlorophyll A, chlorophyll B, and total chlorophyll contents of both extracts. Nevertheless, no differences in chlorophyll content, TPC, and antioxidant activities were observed between dechlorophyllized fractions in both extracts ($p > 0.05$). Liquid Chromatography-Mass Spectrometry (LC/MS) profiling showed that the BLEE dechlorophyllized using the extract/water ratio of 1:1 (BLEE-DC1) had higher phenolic compounds than CLEE-DC1. Isovitexin was the most abundant compound identified in the BLEE-DC1 while vitexin 4′-O-galactoside was the most prevalent in CLEE-DC1. When thermal and pH stabilities of the dechlorophyllized extracts were tested, BLEE-DC1 exhibited more heat stability (at 60 – 100˚C for 0 – 60 min) than CLEE-DC1. Both dechlorophyllized extracts showed optimum antioxidant activities at pH 5.0.

2.2. Introduction

Plants have been used as promising sources of food and medicine because of their nutritional and pharmacological properties (Salehi *et al.*, 2019). Plants consist of several valuable compounds, especially the secondary metabolites known as polyphenols (Maqsood *et al.*, 2014). Polyphenolic compounds can be subdivided based on their chemical structures into several groups such as flavonoids, phenolic acids, lignans, coumarins, quinones, tannins, and stilbenes (Gan *et al.*, 2019). Those compounds are documented to have a broad range of beneficial bioactivities including antioxidant, antimicrobial, anticancer, and anti-inflammatory activities, which are governed by the quantity, types, and modes of action of these compounds (Braga *et al.,* 2014; Maqsood *et al.,* 2013; Olatunde *et al.,* 2018). Antioxidant activities of the phenolic compounds vary significantly according to their modes of action, including scavenging of free radicals, transition metal chelation, quenching of reactive oxygen species, and inhibiting oxidative enzymes (Benjakul *et al.,* 2014). Synthetic or chemical preservatives can be substituted by plant extracts for preservation of foods (Hamad *et al.,* 2017). Moreover, plant extracts can be used to develop novel nutraceutical products with protective abilities against the oxidative stress or damage in the body associated with numerous diseases (Martinez *et al.,* 2016).

Betel (*Piper betle* L.) and wild betel (*Piper sarmentosum* Roxb.), known in Thailand as "phlu" and "chaphlu," respectively are the plants from the family "*Piperaceae*" grown predominantly in East Asian countries (Nouri *et al.,* 2014). Leaves from both plants have been used in traditional medicine; betel leaves are chewed to prevent oral malodor, harden the gum, and as a stress reliever, while chaphlu leaves differ in appearance and has less aromatic odor and taste, compared to betel leaves. Chaphlu leaves have been used to treat coughs, asthma, and promote blood circulation. Additionally, they have been used for many local dishes and recipes (Salehi *et al.,* 2019). Leaves of both plants possessed antibacterial, anticancer, anti-inflammatory, antioxidant, and herbicidal activities (Ismail *et al.,* 2018; Leesombun *et al.,* 2016; Madhumita *et al.,* 2019). These valuable activities were attributed to the high nutritive and pharmacological activities, related with their high contents of minerals, vitamins, polyphenols, and essential oils (Madhumita *et al.,* 2019). In general, the concentration, nature and corresponding activity of plant compounds can be varied, depending on environment the plants grew, or processing used (Arabshahi-D *et al.*, 2007). Antioxidant activities and stability of the plant extracts could be affected by diverse factors during preservation or processing (Nicoli *et al.*, 1999).

Chlorophyll is a magnesium-porphyrin compound, consisting of a hydrophilic ring porphyrin (head) centered with magnesium atom and bonded by an ester bond to a long hydrocarbon phytol (tail), which is hydrophobic in nature (Li *et al.,* 2016). Chlorophyll is water insoluble but dissolves in organic solvents (Hosikian *et al.,* 2010). As a consequence, chlorophyll can be co-extracted using the solvent for extraction of polyphenols. Chlorophyll can act as a photosensitizer and pro-oxidant apart from rendering certain bioactivities (Brown *et al.,* 2019). However, chlorophyll shows negative impact in the resulting extract, leading to the limited applications especially in foods, due to its green color (Olatunde *et al.,* 2018). Therefore, the removal of chlorophyll by an efficient non-harmful method from plant extracts rich in phenolic compounds is an essential step to enhance its use in pharmaceutical and food-related industries. Previously, solvents such as chloroform has been used to remove chlorophyll from plant leaves, prior to extraction, to obtain the extract rich in polyphenols (Olatunde *et al.,* 2018). For safety concerns, the residual solvents, which are toxic, is a drawback for further application of the leave extract. Green process, using ethanol extraction, followed by sedimentation induced by water with higher polarity at an appropriate ratio, can be the promising and safe method to replace the use of hazardous solvents for chlorophyll removal.

The study aimed to compare characteristics and antioxidant activities of betel and chaphlu ethanolic leaf extracts dechlorophyllized with the aid of different proportions of water on the efficiency of sedimentation process for chlorophyll removal. Thermal and pH stabilities of dechlorophyllized extracts were also examined.

2.3. Objectives

To investigate the characteristics and antioxidant activities of the ethanolic extracts of betel (*Piper betle* L.) and chaphlu (*Piper sarmentosum* Roxb.) dechlorophyllized using sedimentation process.

2.4. Materials and methods

2.4.1. Chemicals

Ethanol and chloroform were purchased from RCI Labscan (Bangkok, Thailand). 6-hydroxy-2,5,7,8-tetramethylchroman-2-carboxylic acid (Trolox) was procured from Aldrich Chemical Company (Steinheim, Germany), gallic acid, ethylene diamine tetra-acetic acid (EDTA), 2, 2 diphenyl-1-picrylhydrazyl (DPPH), 2,2-azino-bis-(3 ethylbenzothiazoline-6-sulfonic acid) di-ammonium salt (ABTS), 3-(2-pyridyl)-5,6-di-phenyl-1.2.4-triazine-4′,4″-di-sulfonic acid sodium salt (ferrozine), ferric chloride ($FeCl_3.6H_2O$), ferrous sulfate ($FeSO_4$), fluorescein sodium salt, and potassium per-sulfate were purchased from SigmaAldrich, Inc. (St. Louis, MO, USA). Tween 40 and 2,4,6-tri (2-pyridyl)- S-triazine (TPTZ) were obtained from Fluka Chemicals (Buchs, Switzerland). 2,2′-azobis (2-methylpropionamidine) di-hydrochloride was purchased from Acros Organics (NJ, USA). Disodium hydrogen orthophosphate and sodium dihydrogen phosphate were obtained from Thermo Fisher Scientific (NSW, Australia). β-carotene was procured from Lab-Scan (Bangkok, Thailand).

2.4.2. Preparation of betel and chaphlu leaf powder

Betel leaves (*Piper betle* L.) were collected from a local garden in Songkhla province, Thailand between February, and March 2020 and Chaphlu (*Piper sarmentosum* Roxb.) leaves were procured from the local green market, Hat Yai, Songkhla province, Thailand, at the same period. Vines were about 3–5 years old and only mature leaves with no apparent damage were collected and used in this study. Both leaves were prepared separately (Sae-leaw and Benjakul, 2019). Leaves were thoroughly washed with tap water and dried in a hot air oven at 50˚C overnight until moisture content of the leaves was less than 10%. Dried samples were blended, and then sieved using 80 mesh stainless-steel sieve. The obtained powder named as "betel leaf powder" and "chaphlu leaf powder" were kept in zip-lock bags and placed in a desiccator at room temperature until used for extraction.

2.4.3. Preparation of betel leaf ethanolic extracts (BLEE) and chaphlu leaf ethanolic extracts (CLEE)

The method described by Chotphruethipong *et al.* (2017) was adopted for the preparation of betel leaf and chaphlu leaf extracts. Ethanol (70% v/v) was used as an extraction solvent. The solvent was mixed with the leaf powders using a powder/solvent ratio of 1:15 (w/v). The mixtures were continuously stirred for 1 hr and subsequently centrifuged at 5,000 × g for 30 min at 4˚C. The supernatants were filtered through a Whatman filter paper No. 1, and then, the filtrates of each leaf were separated into four portions (200 mL each) and each portion was evaporated separately at 40˚C using an Eyela rotary evaporator (Tokyo Rikakikai, Co. Ltd., Tokyo, Japan). Residual ethanol was eliminated by nitrogen purging.

2.4.4. Dechlorophyllization of ethanolic leaf extracts

Sedimentation process was used to remove chlorophyll from the ethanolic extracts. Each extract, in which ethanol was removed, was added with distilled water to obtain various extract/water ratios, (1:1, 1:2 and 1:3 v/v). All the mixtures were kept for sedimentation for 24 hr at 4˚C. After settling, only the top layer was collected, and the sediments were discarded. The collected fractions (top layer) were subjected to centrifugation at 10,000 × g for 30 min at 4˚C. The precipitates were discarded, and the supernatants were collected and frozen at −20˚C prior to lyophilization using a Scanvac Model Coolsafe 55 freeze dryer (Coolsafe, Lynge, Denmark). Dried extracts were kept in zip-lock bags at −20˚C before analysis. The ethanolic extract (without chlorophyll removal) was also lyophilized and used as the control. The dried extracts without chlorophyll removal were named “BLEE” and “CLEE” for betel leaf and chaphlu leaf ethanolic extracts, respectively. For dechlorophyllized extracts using the extract/water ratios of 1:1, 1:2, and 1:3, they were referred to as BLEE-DC1, BLEE-DC2, BLEE-DC3 for betel leaf extract and CLEE-DC1, CLEE-DC2, CLEE-DC3 for chaphlu leaf extract, respectively.

2.4.5. Analyses

2.4.5.1. Extraction yield

Extraction yield (%) of both extracts was calculated as tailored by Benjakul *et al.* (2014). Yield was defined as the dry weight of extracts relative to the initial dry weight of leaf powders. It was calculated as follows:

$$\text{Extraction yield (\%)} = \frac{W_2}{W_1} \times 100$$

where w_1 is the initial dry weight of leaf powders and w_2 is the dry weight of extract.

2.4.5.2. Chlorophyll content

The chlorophyll content of the extracts without and with dechlorophyllization (2 mg/mL) was estimated spectrophotometrically following the AOAC (2002) method. The absorbance of prepared solutions was read at 663 and 645 nm using a spectrophotometer (UV-1800, Shimadzu, Kyoto, Japan). For the blank, ethanol was used instead of extracts. Chlorophyll A, chlorophyll B and total chlorophyll contents were calculated using the following equations:

$$\text{Chlorophyll A (mg/mL)} = 12.7\ (A_{663}) - 2.69\ (A_{645})$$

$$\text{Chlorophyll B (mg/mL)} = 22.9\ (A_{645}) - 4.68\ (A_{663})$$

$$\text{Total chlorophyll (mg/mL)} = 20.2\ (A_{645}) + 8.02\ (A_{663})$$

where A_{663} is the absorbance at 663 nm and A_{645} is the absorbance at 645 nm.

2.4.5.3. Color

Color of the extracts without and with dechlorophyllization was determined using the colorimeter (ColorFlex, Hunter Lab Reston, VA, USA) according to the method of Olatunde *et al.* (2018). The manufacturer's standard white plate was used for the calibration. Lightness (L^*), redness/greenness (a^*) and yellowness/blueness (b^*) were determined. Hue angle, chroma value, and ΔE^* was calculated as follows:

$$\text{Hue angle } (h°) = 180 + \tan^{-1}\left(\frac{b^*}{a^*}\right)$$

$$\text{Chroma value } (C^*) = (a^{*2} + b^{*2})^{1/2}$$

$$\Delta E^* = (\Delta L^{*2} + \Delta a^{*2} + \Delta b^{*2})^{1/2}$$

where ΔL^* , Δa^* and Δb^* are the differences between the corresponding color parameter of the sample and that of white standard (L^* = 90.77, a^* = -1.27 and b^* = 0.50).

2.4.5.4. Total phenolic content (TPC)

The TPC of the extracts without and with dechlorophyllization was determined spectrophotometrically with Folin-Ciocalteu's reagent (FCR) as tailored by Benjakul *et al.* (2014). Approximately 0.1 mL of the extract at the desired concentration was mixed with 0.75 mL of 10% Folin-Ciocalteu reagent. The mixtures were allowed to stand for 5 min. Thereafter, 0.75 mL of a saturated sodium carbonate solution was added. The mixtures were allowed to stand for 1 h at room temperature. The absorbance of the blue color developed was measured spectrophotometrically at 760 nm using distilled water as a blank. TPC was expressed as mg gallic acid equivalent (GE)/g dry extract.

2.4.5.5. Antioxidant activities

2.4.5.5.1. $ABTS^+$ scavenging activity

ABTS radical scavenging activity (ABTS-RSA) was determined as described by Karnjanapratum and Benjakul (2015). The stock solutions included 7.4 mM ABTS solution and 2.6 mM potassium persulfate solution. The working solution was prepared by mixing the two stock solutions in equal quantities. The mixture was allowed to react for 12 h at room temperature in the dark. The solution obtained was then diluted with 50 mL of methanol (99.9%) until attaining an absorbance of 1.1 ± 0.02 units at 734 nm using a UV-1601 spectrophotometer (Shimadzu, Kyoto, Japan).

Fresh ABTS solution was prepared for each assay. The extract at the desired concentration (150 µL) was mixed with 2850 µL of ABTS solution and the mixture was left at room temperature for 1 h in the dark. The absorbance was then measured at 734 nm using a spectrophotometer. Distilled water was used as blank. A standard curve of Trolox ranging from 50 to 600 µM was prepared. The ABTS-RSA was expressed as µmol Trolox equivalent (TE)/g dry extract.

2.4.5.5.2. DPPH scavenging activity

The method of Benjakul *et al.* (2014) was used to determine DPPH radical scavenging activity (DPPH-RSA). The extract at the desired concentration (0.3 mL) was mixed with 2.7 mL of methanolic solution containing DPPH (0.15 mM). The mixture was shaken vigorously and left to stand for 1 hr in the dark until stable absorption values was obtained at room temperature (25˚C). The DPPH-RSA was measured by monitoring continuously the decrease in absorbance at 517 nm. DPPH-RSA was expressed as µmol Trolox equivalent (TE)/g dry extract.

2.4.5.5.3. Ferric reducing antioxidant power (FRAP)

FRAP was measured following the method of Sae-leaw *et al.* (2016). FRAP reagent was prepared by mixing acetate buffer (30 mM, pH 3.6), 10 mM TPTZ solution in 40 mM HCl and 20 mM iron (III) chloride solution in proportions of 10:1:1 (v/v/v). The extract at the desired concentration (150 µL) was mixed with 2.85 mL of working FRAP reagent and incubated in dark condition at room temperature for 30 min. The absorbance of the reaction mixture was read at 593 nm using a spectrophotometer. A standard curve was prepared using Trolox ranging from 0 to 500 µM. The activity was expressed as µmol Trolox equivalent (TE)/g dry extract.

2.4.5.5.4. Metal chelating activity (MCA)

The affinity of the extracts to chelate with Fe^{2+} will be measured using the method of Benjakul *et al.* (2014). The extract at the desired concentration (1.175 mL) was mixed with 25 µL of 2 mM FeCl2 and 50 µL of 5 mM ferrozine for 20 min. The absorbance was read at 562 nm. Distilled water was used as blank. A standard curve was prepared using EDTA ranging from 0 to 600 µM. Chelating activity was expressed as µmol EDTA equivalent (EE)/g dry extract.

2.4.5.5.5. Oxygen radical absorbance capacity (ORAC)

ORAC was performed as per the method of Sae-Leaw *et al.* (2016). Dry extracts were dissolved in 75 mM phosphate buffer (pH 7.0) to obtain a final concentration of 0.1 mg/mL. The prepared samples (25 μL) were loaded onto a polystyrene, nontreated 96-well microplate (Costar Corning Inc., Corning, NY, USA). Fifty μL of 0.04 μM fluorescein dissolved in 75 mM phosphate buffer (pH 7.0) was added to each well containing the samples. The loaded microplate was allowed to equilibrate at 37˚C for 20 min in a microplate reader (Thermo Scientific Varioskan® Flash Multimode Reader, Fisher Scientific UK Ltd., Leicestershire, UK). The reaction was initiated by the addition of 100 μL of 221 mM AAPH and was conducted at 37˚C. The fluorescence intensity was measured every 5 min for 90 min with excitation and emission filters of 485 and 535 nm, respectively. The control was prepared in the same manner, except that 75 mM phosphate buffer (pH 7.0) was used instead of the sample. The area under the fluorescence decay curve (AUC) of the samples was calculated by the normalized curves with the following equation:

$$AUC = 0.5 + (f_2/f_1) + (f_3/f_1) + (f_4/f_1) + \ldots + 0.5\ (f_n/f_1)$$

where f_1 is the fluorescence reading at the initiation of the reaction and f_n is the last measurement. The net AUC was obtained by subtracting the AUC of the blank from that of a sample or standard. Trolox (0 – 100 μM) was used as the standard. The ORAC values were expressed as μmol Trolox equivalents (TE)/g dry extract.

2.4.5.5.6. β-carotene/linoleic acid assay

β-carotene bleaching assay was performed as detailed by Miraliakbari and Shahidi (2008) with slight modifications. β-carotene solution (2.5 mg/5 mL) was prepared in chloroform. Then, it was pipetted into round bottom flask containing 60 mg of purified linoleic acid and 600 mg of Tween 40. Thereafter, chloroform was removed under vacuum using a rotary evaporator at 40˚C. Oxygenated distilled water (150 mL) was poured into the flask with vigorous shaking. Aliquots (4.8 mL) of this emulsion were transferred into a series of test tubes that contain 200 µL of the extracts. Distilled water (200 µL) was added instead of extracts and used as the control. Absorbance at 470 nm was read immediately after addition of the emulsion with the extract solution. Subsequently, readings were taken over 6 hr period at 15 min intervals, while maintaining the reaction tubes in a water-bath at 50˚C. Retardation of the decline in absorbance at 470 nm indicated the capability of preventing the oxidation of β-carotene by the extracts.

2.4.5.6. LC/MS profiling and identification

Extracts with the highest antioxidant activities and the lowest chlorophyll content with lowest greenness from both plants were selected for LC/MS profiling and identification as per the method of Shiekh *et al.* (2019). Liquid Chromatograph-Quadrupole Time-of Flight Mass Spectrometer LC-QTOF MS (1290 Infinity II LC-6545 Q-TOF, Agilent Technologies, USA) was used for the qualitative identification of the compounds in extracts. The chromatographic instrument was equipped with an auto sampler (G2179B), binary pump (G7120A), column compartment (G7116B), and diode array detector – DAD (G7117A). Acquisition method for mass spectrometer was performed using dual AJS ESI as ion source at 100 – 1700 MS range (m/z). The scan segment was performed in negative mode electron spray ionization (ESI) as it showed better resolution and higher sensitivity for identification compared with LC/MS run in positive mode. For identification of the constituents, the acquired data were processed using "Mass Hunter METLIN Metabolite PCD (Personal Compound Database)" software and "PCDL (Personal Compound Database and Library) version 8". Reference masses were used to verify the high resolution of mass spectrometry. This confirmed that the parent ion and the source-induced dissociation fragments could provide accurate mass information. The subfraction of ESI chromatogram was analyzed using LC/MS tool system (Formula calculator) to evaluate the mass value (m/z). On the chromatogram, mass and molecular formula of the selected peaks were determined from the system, while mass to charge ratios (m/z) of the selected peaks were analyzed using ESI scan.

2.4.5.7. Heat and pH stability

Stability of extracts toward heat and pH was tested following the method of Arabshahi-D *et al.* (2007) with minor modifications. For heat stability, extracts were heated in a water bath at 60, 80, and 100˚C for 10, 20, 30, and 60 min. After heating, the extracts were cooled in an iced water bath for 5 min. For pH stability, the extracts were incubated for 24 hr at pH 3, 5, 7, and 9 using 0.1 M phosphate buffer at room temperature. TPC, DPPH-RSA, and FRAP were measured as described previously.

2.4.6. Statistical analysis

Completely randomized design (CRD) was used for the whole study. All experiments were performed in triplicate. Data acquired were analyzed by one-way Analysis of Variance (ANOVA) and the Duncan's Multiple Range Test (DMRT) was used for mean comparison. SPSS package (SPSS 23.0 for Windows, SPSS Inc, Chicago, IL, USA) was applied for data analysis.

2.5. Results and discussion

2.5.1. Chlorophyll content of betel leaf ethanolic extract (BLEE) and chaphlu leaf ethanolic extract (CLEE) without and with dechlorophyllization using sedimentation process

Total chlorophyll contents of BLEE and CLEE were drastically reduced ($p < 0.05$) using sedimentation process as compared to those of the control (Table 4). Chlorophyll molecule contains a hydrophilic head of porphyrin ring centered with magnesium atom causing its hydrophilicity (Mukherjee, 2019) along with a hydrophobic long hydrocarbon tail bonded by an ester bond to the porphyrin ring, thus, simultaneously making the chlorophyll molecule water insoluble (Olatunde *et al.*, 2018). When water was added into the ethanolic extracts of both leaves, the system became more polar. Chlorophyll precipitation could occur, leading to the reduction of the chlorophyll content in the top phase. As a result, the supernatant possessed less chlorophyll. When considering the effect of extract/water ratios, no differences in the total chlorophyll content, chlorophyll A and B contents were observed ($p > 0.05$) in all the dechlorophyllized extracts. Therefore, the water quantity had no marked effect on lowering the chlorophyll content, but the difference might be obtained, depending on plant species. Generally, total chlorophyll content was much higher in BLEE than CLEE. This was mostly attributed to the difference in plants species, quantity of chlorophylls and maturity of the leaves (Li *et al.*, 2018). Furthermore, high mass of chlorophyll molecules (Chlorophyll A = 893.49 g/mol, Chlorophyll B = 907.47 g/mol) along with the gravitational forces could help in the sedimentation of the chlorophylls after keeping the extracts at 4˚C for 24 hr followed by centrifugation. Overall, chlorophylls were insolubilized in polar environment when water was excessive. Consequently, less green color of the extracts could be obviously visualized in the top phase.

The presence of chlorophyll residues in the samples after dechlorophyllization might be associated with hydrophilic porphyrin ring of the chlorophyll molecule. Total chlorophyll content of the dechlorophyllized guava leaf extracts using different organic solvents constituted from 0.04 to 0.37 mg/g as documented by Olatunde *et al.* (2018) while lead seed extract with prior dechlorophyllization by chloroform had a total chlorophyll content ranging from 0.05 to 0.75 mg/g (Benjakul *et al.,* 2014). In the present study, BLEE-DC1 and CLEE-DC1 had decreases in total chlorophyll content to 23.08 and 10.19%. Chlorophyll A and B contents of BLEE-DC1 were lowered to 21 and 24.54%, respectively. The decreases in chlorophyll A and B of CLEE-DC1 were found by 6.89 and 11.13%, respectively.

2.5.2. Color of betel leaf ethanolic extract (BLEE) and chaphlu leaf ethanolic extract (CLEE) without and with dechlorophyllization using sedimentation process

*L**, *a**, *b** values, chroma, and hue angle of the extracts are presented in Table 4. No difference in those parameters ($p > 0.05$) was observed between the dechlorophyllized fractions of BLEE and CLEE as influenced by extract/water ratios. However, the difference was clearly noticed between the control and dechlorophyllized fractions of both extracts. For greenness representing the presence of chlorophyll, it was dramatically lowered after dechlorophyllization using sedimentation method, regardless of extract/water ratios ascertained by the higher *a** value. The *b** values of both extracts were higher than those of the controls. This confirmed the removal of chlorophyll from the ethanolic extracts. A negative correlation was found between the reduction of chlorophyll A, chlorophyll B, and total chlorophyll with the increased lightness (*L**) of BLEE and CLEE, while positive correlation between the decreases in Hue angle as well as Chroma and the decrease in total chlorophyll, chlorophyll A and B contents were obtained. Therefore, sedimentation process was effective in removing the chlorophyll from the ethanolic extracts, however, the extract/ water ratio had no apparent effect on the color or the chlorophyll content of the dechlorophyllized extracts.

Table 4. Chlorophyll contents and color of betel leaf ethanolic extracts (BLEE) and chaplu leaf ethanolic extracts (CLEE) without and with dechlorophyllization using sedimentation process with different extract/water ratios

Samples	**Chlorophyll A (mg/g)**	**Chlorophyll B (mg/g)**	**Total chlorophyll (mg/g)**	***L****	***a****	***b****	**Chroma**	**Hue angle**	**ΔE***
BLEE	0.457 ± 0.005^{a}	0.717 ± 0.011^{a}	1.174 ± 0.008^{a}	0.69 ± 0.22^{b}	-0.93 ± 0.14^{b}	-3.83 ± 0.68^{b}	3.95 ± 0.68^{a}	256.06±2.47^{a}	92.24 ± 0.22^{a}
BLEE-DC 1	0.096 ± 0.005^{b}	0.176 ± 0.122^{b}	0.271 ± 0.015^{b}	1.60 ± 0.26^{a}	0.73 ± 0.22^{a}	-1.25 ± 0.28^{a}	1.45 ± 0.34^{b}	120 ± 4.24^{b}	91.26 ± 0.27^{b}
BLEE-DC 2	0.080 ± 0.009^{c}	0.179 ± 0.201^{b}	0.259 ± 0.014^{b}	1.32 ± 0.16^{a}	0.51 ± 0.40^{a}	-.1.25 ± 0.38^{a}	1.37 ± 0.47^{b}	112.19 ± 15.1^{b}	91.53 ± 0.15^{b}
BLEE-DC 3	0.077 ± 0.008^{c}	0.183 ± 0.169^{b}	0.261 ± 0.01^{b}	1.44 ± 0.12^{a}	0.62 ± 0.30^{a}	-1.43 ± 0.41^{a}	1.57 ± 0.46^{b}	113.29 ± 8.59^{b}	91.42 ± 0.13^{b}
CLEE	0.116 ± 0.004^{a}	0.404 ± 0.001^{a}	0.520 ± 0.005^{a}	1.03 ± 0.05^{b}	-0.49 ± 0.14^{b}	-2.08 ± 0.17^{a}	2.14 ± 0.2^{a}	245.43 ± 3.89^{a}	91.83 ± 0.05^{a}
CLEE-DC 1	0.008 ± 0.001^{b}	0.045 ± 0.01^{b}	0.053 ± 0.009^{b}	1.49 ± 0.33^{a}	0.43 ± 0.19^{a}	-1.78 ± 0.13^{a}	1.83 ± 0.14^{a}	103.57 ± 5.78^{b}	91.38 ± 0.33^{b}
CLEE-DC 2	0.005 ± 0.000^{b}	0.042 ± 0.008^{b}	0.048 ± 0.008^{b}	1.32 ± 0.13^{ab}	0.50 ± 0.39^{a}	-1.56 ± 1.20^{a}	1.85 ± 0.81^{a}	106.38 ± 4.52^{b}	91.55 ± 0.13^{ab}
CLEE-DC 3	0.004 ± 0.001^{b}	0.047 ± 0.013^{b}	0.051 ± 0.012^{b}	1.38 ± 0.23^{a}	0.40 ± 0.20^{a}	-1.36 ± 0.52^{a}	1.42 ± 0.55^{a}	106.39 ± 2.89^{b}	91.48 ± 0.23^{b}

Values are the mean ± standard deviation (n=3). Different superscripts within the same column under the same leaf indicate significant difference ($p < 0.05$). BLEE: betel leaf ethanolic extract without dechlorophyllization (control); BLEE-DC1, BLEE-DC2, and BLEE-DC3: betel leaf ethanolic extract dechlorophyllized using distilled water at 1:1, 1:2, and 1:3 ratio, respectively; CLEE: chaplu leaf ethanolic extract without dechlorophyllization (control); CLEE-DC1, CLEE-DC2, and CLEE-DC3: chaplu leaf ethanolic extract dechlorophyllized using distilled water at 1:1, 1:2, and 1:3 ratio, respectively; *L**: lightness/darkness; *a**: greenness/redness; *b**: yellowness/blueness; Δ*E**: change in color.

2.5.3. Extraction yield and TPC of extracts without and with dechlorophyllization using sedimentation process

The extraction yields of BLEE, and CLEE (Table 5) differed ($p < 0.05$). BLEE had higher extraction yield than CLEE ($p < 0.05$). This was attributed to the difference in plant species, leaf size, and environmental factors between both samples. However, the yield was not significantly decreased in the decholophyllized fractions for both BLEE and CLEE as the extract/water ratio was increased. The control on both extracts had the highest extraction yield, which was due to the presence of chlorophyll molecules in the ethanolic extracts.

TPC of BLEE was found to be higher ($p < 0.05$) than that of CLEE, showing a similar trend with the extraction yield. This result indicated that the decreased solid contents of the extracts were correlated with the removal of chlorophyll with coincidental augmentation of phenolic compound in the resulting extract. For both extracts, no difference in TPC was found when extract/water ratios were different ($p > 0.05$). It was found that TPC of the dechlorophyllized fractions was about 165.8 mg GAE/g dry extract for BLEE, which was higher than that determined by Nouri *et al.* (2014) who found that the TPC of betel leaves extracted in 70% of ethanol was 147.96 mg GAE/g dry extract. For CLEE, TPC of the dechlorophyllized fractions was around 62.6 mg GAE/g dry extract, which was lower than that reported by Hafizah *et al.* (2010) who found that TPC of *Piper sarmentosum* extracts was 90.8 mg GAE/g dry extract. Differences detected might be the results of varying extraction conditions, environmental factors, and species of leaves. It was noticed that TPC of the control in BLEE and CLEE was lower than that of the dechlorophyllized fractions ($p < 0.05$). This mostly resulted from the increased proportion of TPC after the chlorophyll was removed from the extract. Thus, the sedimentation process could augment the TPC of both extracts efficiently.

2.5.4. Antioxidant activity of extracts without and with dechlorophyllization using sedimentation process

Antioxidants activities (Table 5) of BLEE were generally higher than those of CLEE ($p < 0.05$). Antioxidants have different mode of actions and their response to the antioxidant assays will differ (Apak *et al.*, 2007; Francenia Santos-

Sánchez *et al.,* 2019). DPPH-RSA and ABTS-RSA of the dechlorophyllized fractions were higher ($p < 0.05$) than those of the control for both extracts. Nevertheless, there was no marked difference between the dechlorophyllized fractions using different extract/water ratios ($p > 0.05$). This reflected the insignificance of extract/water ratio on antioxidant activities of the extracts after dechlorophyllization. The results indicated the ability of the extracts to donate hydrogen atom or electron to both radicals. Correlation between TPC as well as DPPH-RSA and ABTS-RSA suggested that the phenolic contents of both extracts were responsible for their corresponding antioxidant activities, which were in line with many studies (Benjakul *et al.,* 2014; Chotphruethipong *et al.,* 2017; Olatunde *et al.,* 2018).

The ability of the extracts to reduce ferric ion into ferrous counterpart and to deactivate transition metals was determined by FRAP assay and metal chelating activity assay, respectively. The results (Table 5) showed similar trend to that of radical scavenging activities, in which there was no difference ($p > 0.05$) between the dechlorophyllized fractions of both BLEE and CLEE, regardless of extract/water ratios used. The profound difference was obvious between the control in both extracts and their dechlorophyllized counterparts ($p < 0.05$). This reconfirmed that water ratios used had no influence on the antioxidant activities of dechlorophyllized extracts during the sedimentation process. Therefore, the sedimentation process could effectively remove chlorophyll from the extracts but showed no detrimental effect on their antioxidant activities. The advantage of sedimentation process was noted over the conventional dechlorophyllization methods using organic solvents (Benjakul *et al.,* 2014; Olatunde *et al.,* 2018; Seo *et al.,* 2014). Moreover, the results showed a correlation between the metal chelating activity and FRAP with TPC, which affirmed the dependency of the antioxidant activities on the phenolic compounds present in the extracts. ORAC assay was applied to measure the ability of the extracts with antioxidant activities to inhibit peroxyl radicals produced by azo compounds like AAPH. The ORAC activity of BLEE-DC1 was higher than that of CLEE-DC1 (Table 5). This might be due to the high difference in TPC between both extracts. It was noticed that ORAC had a strong correlation with TPC of the extracts. This result confirmed the crucial role of phenolic compounds in determining the antioxidant activities of both extracts.

Table 5. Extraction yield, total phenolic content and antioxidant activities of betel leaf ethanolic extracts (BLEE) and chaplu leaf ethanolic extracts (CLEE) without and with dechlorophyllization using sedimentation process with different extract/water ratios.

Samples	Extraction yield (%)	TPC (mg GAE/g dry extract)	DPPH-RSA (µmol TE/g dry extract)	ABTS-RSA (µmol TE/g dry extract)	FRAP (µmol TE/g dry extract)	MCA (µmol EDTA dry extract)	ORAC (µmol TE/g dry extract)
BLEE	15.58 ± 0.04^{a}	137.6 ± 2.54^{b}	90.78 ± 0.78^{b}	1899.55 ± 11.64^{b}	1491.88 ± 4.53^{b}	126.13 ± 2.6^{b}	
BLEE-DC 1	13.7 ± 0.04^{b}	165.84 ± 1.48^{a}	105.82 ± 1.86^{a}	2708.88 ± 12.02^{a}	1669.44 ± 5.08^{a}	214.23 ± 0.08^{a}	11.83 ± 3.59
BLEE-DC 2	13.7 ± 0.08^{b}	165.64 ± 8.02^{a}	104.84 ± 0.25^{a}	2704.88 ± 10.69^{a}	1666.22 ± 2.45^{a}	214.09 ± 0.48^{a}	
BLEE-DC 3	13.38 ± 0.00^{c}	164.88 ± 6.36^{a}	104.18 ± 0.78^{a}	2700.44 ± 31.27^{a}	1667.11 ± 3.00^{a}	213.26 ± 1.09^{a}	
CLEE	9.61 ± 0.02^{a}	53.19 ± 2.16^{b}	74.59 ± 0.42^{b}	825.77 ± 16.88^{b}	275.22 ± 9.45^{b}	73.96 ± 9.36^{b}	
CLEE-DC 1	6.6 ± 0.02^{b}	63.008 ± 2.25^{a}	88.47 ± 1.18^{a}	1778.22 ± 31.50^{a}	352.77 ± 2.83^{a}	110.01 ± 1.75^{a}	6.02 ± 0.09
CLEE-DC 2	6.4 ± 0.02^{c}	62.29 ± 2.20^{a}	88.03 ± 2.83^{a}	1786.22 ± 37.05^{a}	351.88 ± 3.15^{a}	110.73 ± 0.12^{a}	
CLEE-DC 3	6.44 ± 0.02^{c}	62.31 ± 1.33^{a}	87.69 ± 3.23^{a}	1759.55 ± 15.45^{a}	351.22 ± 2.21^{a}	109.29 ± 4.27^{a}	

Values the are mean ± standard deviation (n=3). Different superscripts within the same column under the same leaf indicate significant difference ($p < 0.05$). TPC: Total phenolic content; DPPH-RSA: 2,2-diphenyl-1-picrylhydrazyl radical scavenging activity; ABTS-RSA: 2, 2'-Azino-Bis-3-Ethylbenzothiazoline-6-Sulfonic acid radical scavenging activity; FRAP: Ferric reducing antioxidant power; MCA: Metal chelating activity; ORAC: Oxygen radical absorbance capacity. For captions see Table 4.

2.5.5. Antioxidant activity in β-carotene/linoleic acid system

The ability of BLEE-DC1 and CLEE-DC1 to inhibit β-carotene oxidation was evaluated using the β-carotene/linoleic acid bleaching assay. Peroxyl free radicals are generated as a consequence of elimination of a hydrogen atom from the diallylic methylene groups of linoleic acid when oxidized (Ismail *et al.,* 2010). The produced free radicals will eventually oxidize the double bonds of the highly unsaturated β-carotene. This mainly causes the change from yellowish orange color to the colorless form (Olugbami *et al.,* 2014). β-carotene bleaching assay is a measure of the free radicals amount in the system and the rate of bleaching of the solution is referred to degradation rate (Juntachote and Berghofer, 2005). The presence of antioxidants will minimize the oxidation of β-carotene induced by hydroperoxides. Hydroperoxides formed in the system might be scavenged by antioxidants of the extracts (Ismail *et al.,* 2010). Antioxidant activity of BLEE-DC1 and CLEE-DC1 in comparison with the negative control (without extracts) is shown in Fig. 7.

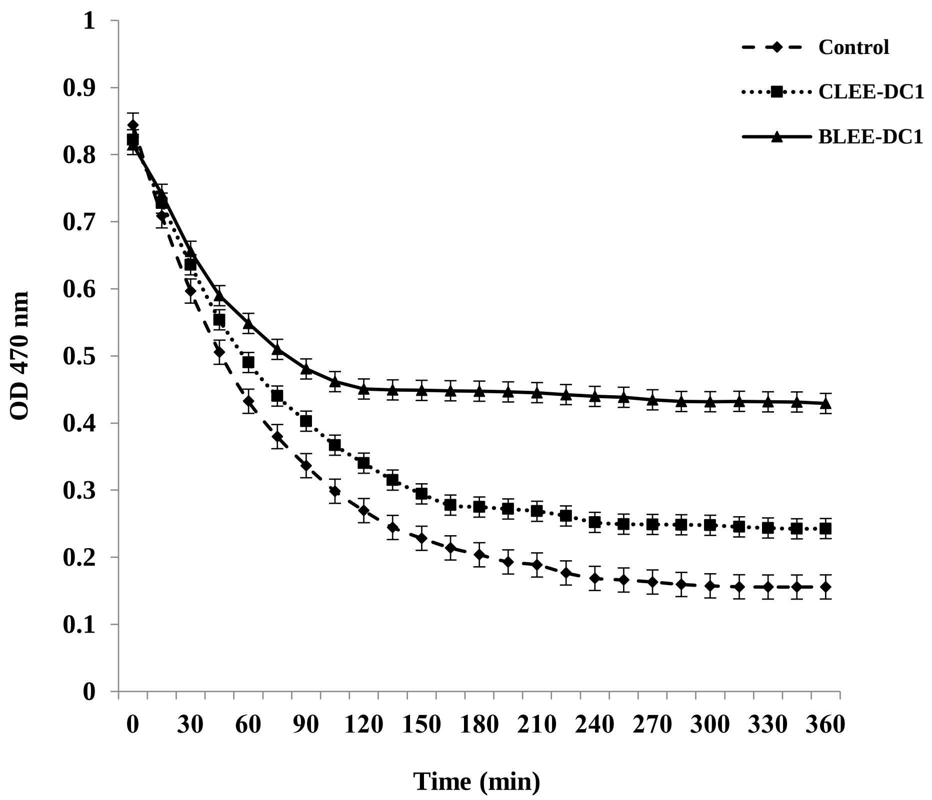

Figure 7. Degradation rate in β-carotene bleaching assay in the presence of BLEE-DC1 and CLEE-DC1. Concentration of 1 mg/ml of extract was used. Vertical bars in the curve represent standard deviation (n = 3).

Compared to the control, BLEE-DC1 had lower rate of degradation of β-carotene than CLEE-DC1. This confirmed that the ability of BLEE-DC1 to prevent oxidation of β-carotene was more effective than CLEE-DC1 in inhibiting the formation of linoleate free radicals. At the beginning of the assay, all the samples showed degradation of β-carotene at different rates. After approximately 90 min, the degradation rate of β carotene in the presence of BLEE-DC1 sample remained constant, while the degradation of the control and CLEE-DC1 still proceeded, ascertained by the continuous decrease in absorbance at 470 nm. This was plausibly attributed to the presence of phenolic compounds in BLEE-DC1 that had the ability to inhibit β-carotene degradation and could tolerate the temperature (50˚C) of the system over time, whereas CLEE-DC1 might have lower the antioxidant compounds, in which β-carotene degradation continuously take place.

2.5.6. Identification and profiling of compounds in dechlorophyllized extracts

Variations in the chemical constituents of BLEE-DC1 and CLEE-DC1 can be observed from their LC chromatograms (Fig. 8). The possible compounds were qualitatively identified based on their molecular ion peaks, mass to charge ratio (m/z), and fragment ions. Most polyphenols readily form negatively charged ions, especially in ESI (Shiekh *et al.*, 2019). Identification of the chemical constituents in the extracts revealed the presence of 102 compounds for BLEE-DC1 and 68 compounds for CLEE-DC1. Most of these compounds were identified as polyphenols or their glycosides. It was found that thirty compounds were in common between both extracts. The most prevalent compounds from the two leaf extracts including other common compounds are presented in Table 6. Although the difference between BLEE-DC1 and CLEE-DC1 was noticed, there were some similar compounds that could be found in both extracts, however, the abundance was varied. Among the compounds detected in BLEE-DC1, vitexin isomers, which are derivatives of apigenin and belong to the class of flavones, were found. Isovitexin was one of these isomers, which was the most abundant compound detected (24.9×10^6). However, it was not detected in the CLEE-DC1. Vitexin 4′-O-galactoside was the second most abundant compound in BLEE-DC1 (21.6×10^6). This compound was also found in CLEE-DC1 and was the most abundant compound in this extract (11.4×10^6). Vitexin and isovitexin have been extracted from several medicinal plants and showed remarkable biological activities including antioxidant, antimicrobial, and anticancer activities (Babaei *et al.*, 2020; He *et al.*, 2016; Khole *et al.*, 2016).

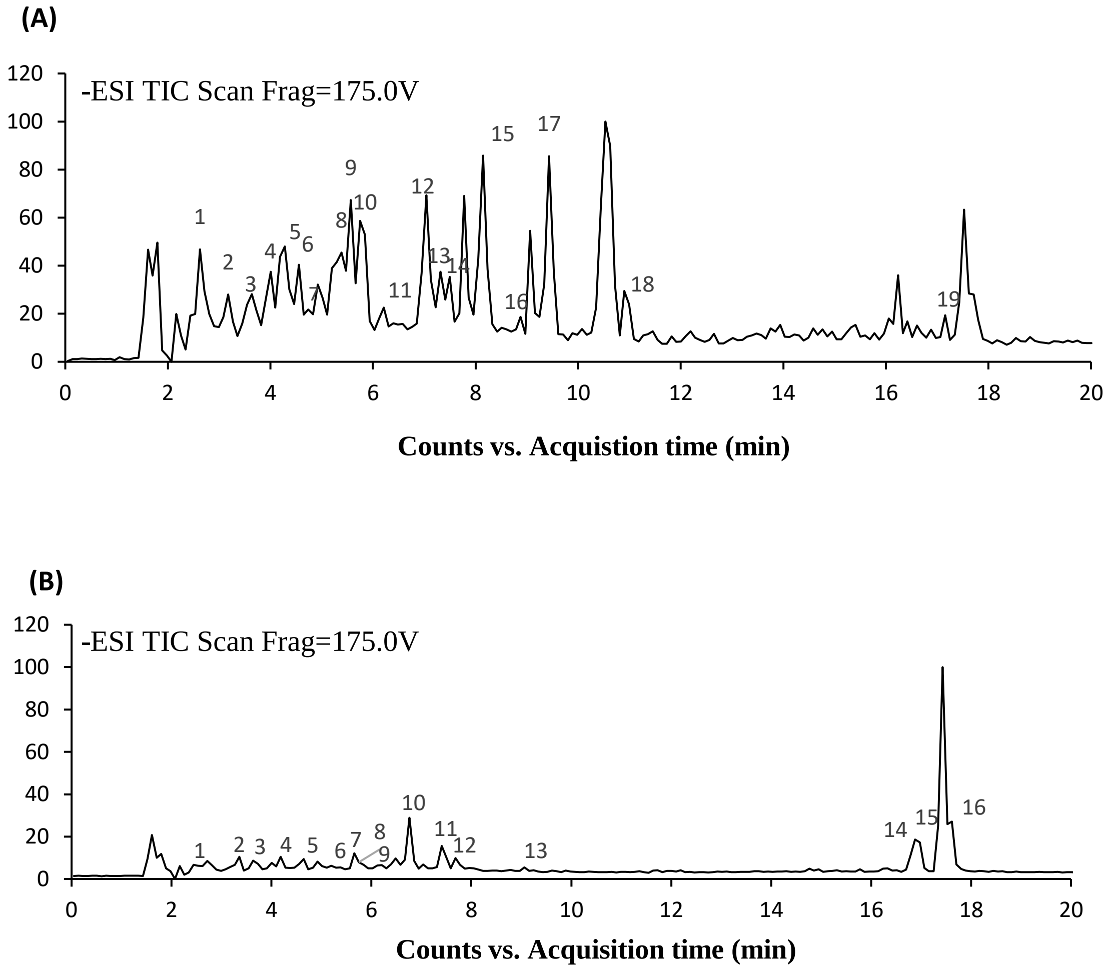

Figure 8. LC/MS chromatographic profiles of BLEE-DC1 (A) and CLEE-DC1 (B).

Kaempferol derivatives were detected in both extracts; however, BLEE-DC1 possessed the higher abundance. Such compounds were found in a variety of plants and were reported to possess antioxidant, anti-inflammatory, and antitumor activities (Jung *et al.*, 2009; Tatsimo *et al.*, 2012; Wang *et al.*, 2018). Other compounds along with their derivatives were also detected but in different abundances for both extracts. This included some naturally occurring organic acids such as hydrocinnamic acid, orthothymotinic acid, quinic acid, and citric acid with varying bioactivities (Halagarda *et al.*, 2020; Shen *et al.*, 2019; Teixeira *et al.*, 2013).

Table 6. LC/MS profiles of compounds in BLEE-DC1 and CLEE-DC1

BLEE-DC1

Peak no.	Identified compounds	Formula	m/z	Mass (g/mol)	Abundance ($x10^6$)
1	4-Glucogallic acid	$C_{13}H_{16}O_{10}$	331.06	332.07	3.00
2	m-Coumaric acid	$C_9H_8O_3$	163.04	164.04	1.00
3	Chlorogenic Acid	$C_{16}H_{18}O_9$	353.08	354.09	1.00
4	Citric acid	$C_6H_8O_7$	191.01	192.02	3.12
5	Hydrojuglone glucoside	$C_{16}H_{18}O_8$	337.09	338.10	10.31
6	Rutin	$C_{27}H_{30}O_{16}$	609.14	610.15	6.00
7	Epigallocatechin	$C_{15}H_{14}O_7$	305.06	306.07	0.18
8	Gulonic acid	$C_6H_{12}O_7$	195.05	196.05	5.24
9	Isovitexin 2"-(6'"-feruloylglucoside) 4 glucoside	$C_{43}H_{48}O_{23}$	931.25	932.25	2.00
10	Quinic acid	$C_7H_{12}O_6$	191.05	192.06	3.00
11	3',4'-Methylenedioxy epicatechin 5,7 dimethyl ether	$C_{18}H_{18}O_6$	329.10	330.11	0.90
12	Vitexin 4'-O-galactoside	$C_{27}H_{30}O_{15}$	593.15	594.16	21.62
13	cis-p-Coumaric acid	$C_9H_8O_3$	163.04	164.04	1.00
14	Kaempferol 3-rhamnoside-(1->2)-rhamnoside	$C_{27}H_{30}O_{14}$	577.15	578.16	1.00
15	Isovitexin	$C_{21}H_{20}O_{10}$	431.10	432.10	24.99
16	4'-Methyl-(-)-epigallocatechin 3'-glucuronide	$C_{22}H_{24}O_{13}$	495.11	496.12	0.26
17	Kaempferol 7-methyl ether 3-[3-hydro 3-methylglutaryl-(1->6)]-[apiosyl-(1-> galactoside]	$C_{33}H_{38}O_{19}$	737.19	738.20	20.27
18	Vitexin 6"-(3-hydroxy-3-methylglutara	$C_{27}H_{28}O_{14}$	575.14	576.14	8.16
19	Hydrocinnamic acid	$C_9H_{10}O_2$	149.06	150.06	2.00

CLEE-DC1

Peak no.	Identified compounds	Formula	m/z	Mass (g/mol	Abundance ($x10^6$)
1	m-Coumaric acid	$C_9H_8O_3$	163.04	164.04	0.33
2	Phenylethyl primeveroside	$C_{19}H_{28}O_{10}$	415.16	416.16	5.29
3	Citric acid	$C_6H_8O_7$	191.01	192.02	1.11
4	Hydrojuglone glucoside	$C_{16}H_{18}O_8$	337.09	338.10	2.95
5	Rutin	$C_{27}H_{30}O_{16}$	609.14	610.15	6.64
6	Epigallocatechin	$C_{15}H_{14}O_7$	305.06	306.07	0.16
7	Gulonic acid	$C_6H_{12}O_7$	195.05	196.05	4.01
8	Quinic acid	$C_7H_{12}O_6$	191.05	192.06	1.48
9	3',4'-Methylenedioxy epicatechin 5, dimethyl ether	$C_{18}H_{18}O_6$	329.10	330.11	0.68
10	Vitexin 4'-O-galactoside	$C_{27}H_{30}O_{15}$	593.15	594.16	11.45
11	Kaempferol 3-rhamnoside-(1->2) rhamnoside	$C_{27}H_{30}O_{14}$	577.15	578.16	3.67
12	Phenethyl Caffeiate	$C_{17}H_{16}O_4$	283.09	284.10	1.7
13	4'-Methyl-(-)-epigallocatechin 3'-glucuronide	$C_{22}H_{24}O_{13}$	495.11	496.12	0.12
14	2,5-Dimethoxycinnamic acid	$C_{11}H_{12}O_4$	207.06	208.07	4.89
15	Orthothymotinic Acid	$C_{11}H_{14}O_3$	193.08	194.09	4.25
16	Hydrocinnamic acid	$C_9H_{10}O_2$	149.06	150.06	5.60

BLEE-DC1: betel leaf ethanolic extract dechlorophyllized using distilled water at 1:1 ratio; CLEE-DC1: chaphlu leaf ethanolic extract dechlorophyllized using distilled water at 1:1 ratio

Epigallocatechin and some of its derivatives, which are well-known polyphenols for their bioactivities (Chu *et al.,* 2017), were also found at low quantities in both extracts. The abundance of such compounds was higher in BLEE-DC1 than CLEE-DC1. LC/MS results confirmed the presence of different polyphenolic compounds with different bioactivities in both extracts. Some of these compounds were in common between both BLEE-DC1 and CLEE-DC1. This was due to the fact that both plants belong to the same family. Generally, the differences in TPC and antioxidant activities between BLEE-DC1 and CLEE-DC1 were governed by varying compounds in the extracts related with different active components in both extracts.

2.5.7. Effect of heat and pH on the stability of the dechlorophyllized extracts

2.5.7.1. Thermal stability

Both BLEE-DC1 and CLEE-DC1 had the decrease in TPC as the heating temperature and time were augmented (Fig. 9). Increasing temperature caused a significant decrease in TPC ($p < 0.05$) in dechlorophyllized extracts up to 60 min ($p < 0.05$). BLEE-DC1 was more stable than CLEE-DC1 as 94.92, 93.51, and 89.59% of TPC were retained when BLEE-DC1 was incubated for 60 min at 60, 80, and 100˚C, respectively, while CLEE-DC1 showed higher degradation rate as 91.83, 74.35, and 64.67% of TPC were retained when exposed to heating at the same temperatures. The decrease in TPC might be caused by the degradation of some phenolic compounds in the extracts when exposed to heat, especially for the longer time. Different phenolic compounds found in the extracts and their response to heat treatment might differ from each other. These phenolic compounds could be responsible for antioxidant activity of the plant extracts (Jiménez *et al.,* 2018). A decrease in DPPH-RSA and FRAP as function of heating time was observed. Also, higher temperature resulted in the lower antioxidant activity of both extracts. Positive correlation between the antioxidant activities of the plant extracts and their TPC was documented by several studies (Dutta and Ray, 2020; Maghsoudlou *et al.,* 2019; Olatunde *et al.,* 2018). Consequently, a significant decrease ($p < 0.05$) in DPPH-RSA and FRAP might be caused by the decomposition of some phenolic compounds. Pearson's correlation coefficient was employed to establish the relationship between TPC and antioxidant activities (DPPH-RSA and FRAP) under different heating conditions.

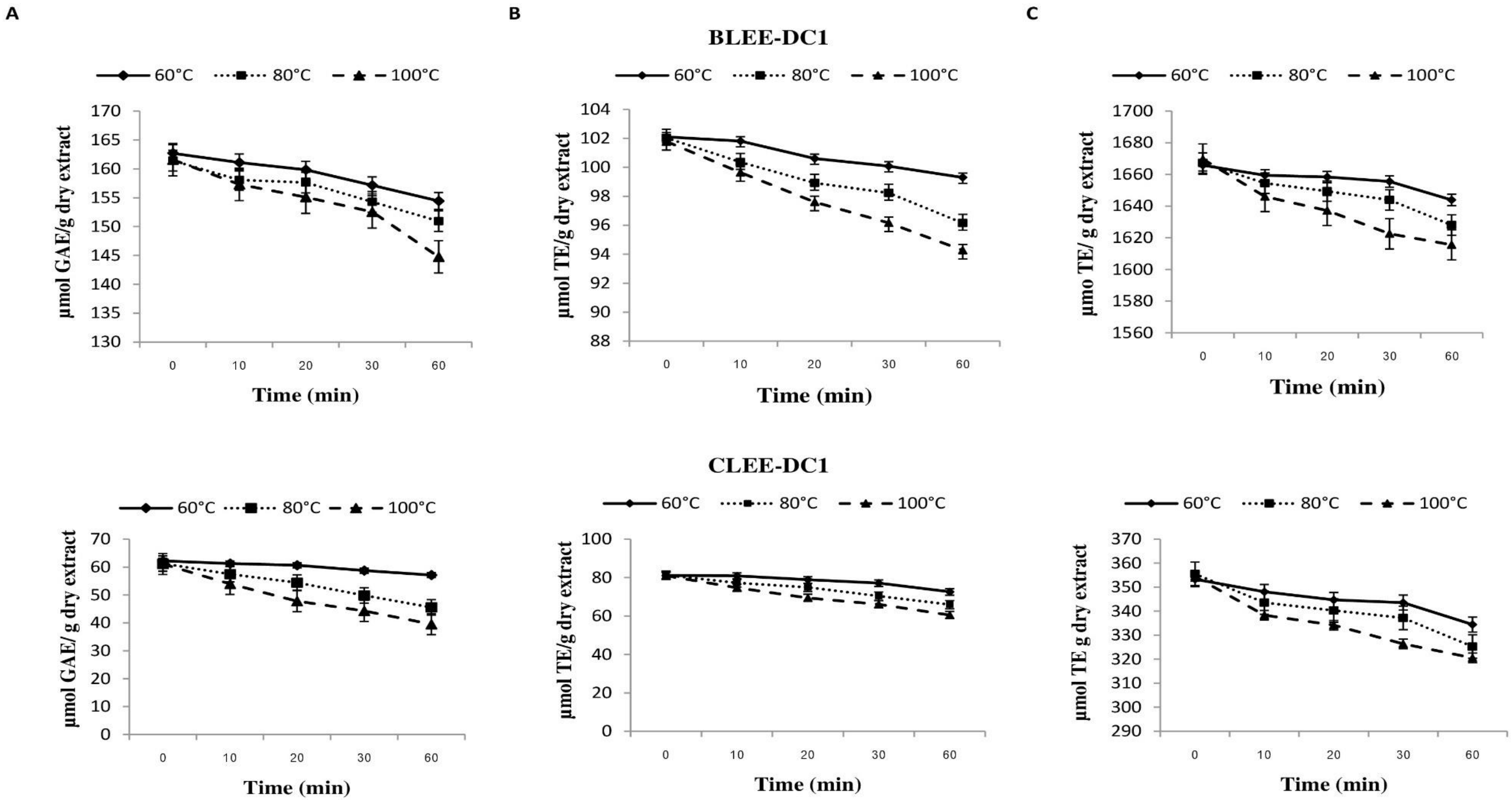

Figure 9. Heat stability of BLEE-DC1 and CLEE-DC1 as determined by total phenolic contents (TPC) (A), DPPH-RSA (B), and (FRAP) (C). Vertical bars in the curve represent the standard deviation (n = 3).

TPC/DPPH-RSA relation and TPC/FRAP relation were identified to be significant ($p < 0.01$) at value of 0.965 and 0.951, respectively, for BLEE-DC1 and 0.98 and 0.931 for CLEE-DC1, respectively. Thus, the decrease in TPC corresponded with the lower antioxidant activities of dechlorophyllized extracts during the heating. Correlation value (0.962) was observed by Sun *et al.* (2018) between TPC and DPPH-RSA of okara extracts when treated with subcritical water extraction. BLEE-DC1 was found to have higher retention of DPPH-RSA and FRAP than CLEE-DC1, which could be related to the higher abundance of certain heat stable phenolic compounds in BLEE-DC1. The retention of FRAP was observed to be higher than that of DPPH-RSA. Some phenolic compounds, which were able to scavenge the free radicals, were degraded at a higher extent than the other compounds which possessed the ability to reduce the ferric ion. Kim *et al.* (2019) observed a general decrease in TPC after heating for longer time, indicating the destruction of some phenolic compounds with a persistence of some free phenolic acids. Thus, phenolic compounds were more likely altered due to the cleavage of bonds within these compounds as induced by heat.

2.5.7.2. pH stability

The TPC, DPPH-RSA, and FRAP of BLEE-DC1 and CLEE-DC1 were influenced by pHs (Fig. 10). Pearson correlation coefficient indicated negative correlation ($p < 0.01$) between pH and TPC at the value of -0.673 in case of BLEE-DC1 and -0.724 for CLEE-DC1. Varying values at different pHs were observed ($p < 0.05$). Higher TPC was found for BLEE-DC1 than that of CLEE-DC1 ($p < 0.05$) at all pHs treated. When considering the impact of pHs on TPC and antioxidant activities, both extracts seemed to be negatively affected by increasing pH, especially pH 9 in which the extract had the lowest TPC. In other word, the extracts were more stable in slightly acidic pH range. Alkaline pH might cause degradation of active phenolic compounds to some degree. Chen *et al.* (2008) found that TPC of different yam species at pH 5 was the highest and a negative correlation between pH and TPC was observed. The chemical structure of the phenolic compounds had high impact on their stability (Goulas and Hadjisolomou, 2019). In general, hydroxyl groups will be shielded by protonation, while increasing pH will lead to the de-protonation of the hydroxyl groups, thus, decreasing their activities (Ghosh *et al.,* 2015).

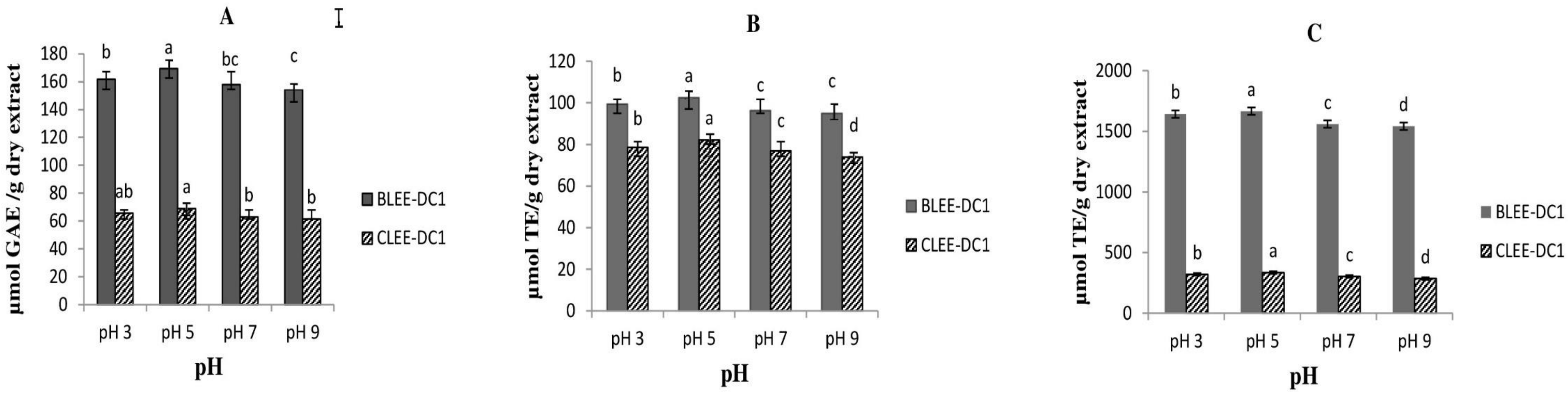

Figure 10. pH stability of BLEE-DC1 and CLEE-DC1 as determined by total phenolic contents (TPC) (A), DPPH-RSA (B), and (FRAP) (C). Vertical bars in the curve represent the standard deviation (n = 3). Letters on bars within the same extract indicate significant difference ($p < 0.05$).

It was noted that TPC and antioxidant activities were higher ($p < 0.05$) in acidic medium than in the alkaline medium. Decreased antioxidant activity in alkaline medium was attributed to the instability of some phenolic compounds (Bayliak *et al.,* 2016), change in pH or a certain pH may lead to conformational changes of some phenolic constituents in the plant extracts, thus, affecting TPC and antioxidant activities (Friedman and Jürgens, 2000). Results of DPPH-RSA and FRAP showed parallel trend to that of TPC, in which TPC and antioxidant activities were highest at pH 5 ($p < 0.05$). When Pearson's correlation coefficient was used to setup the relation between TPC and antioxidant activities under varying pHs, TPC/DPPH-RSA relation and TPC/FRAP relation were significant ($p < 0.01$) at value of 0.99 and 0.932, respectively, for BLEE-DC1 and at 0.984 and 0.976, respectively, for CLEE-DC1. Ghosh *et al.* (2015) reported that pH 5.5 was optimal for TPC of palm (*Borassus flabellifer*) wine. The DPPH-RSA also showed a positive correlation between TPC and antioxidant activity. Acidic medium had the higher TPC and antioxidant activities of the ethanolic extracts of Brazilian green propolis. Also, a correlation was observed between TPC and DPPH-RSA and between TPC and FRAB (Mello and Hubinger, 2012).

2.6. Conclusion

The sedimentation process showed remarkable effectiveness in chlorophyll removal with no negative influence on the phenolic content and antioxidant activities of ethanolic extracts of betel leaf and chaphlu leaf. Extract/water ratios showed insignificant impact on chlorophyll removal efficacy. They also had no impact upon total phenolic content or antioxidant activities of both extracts. It was found that BLEE had higher phenolic content and antioxidant activities than CLEE, and their antioxidant activities showed great dependency on total phenolic content. A higher number of phenolic compounds were found in BLEE, however, some similarities between the dechlorophyllized extracts were found. Heat and pH had notable effect on both extracts. Heat stability was higher in BLEE. Total phenolic content and antioxidant activities were optimum at pH 5 for both extracts. Therefore, BLEE dechlorophyllized by sedimentation had the potential to be used to improve food quality as it showed promising antioxidant activity and stability.

2.7. References

Apak, R., Güçlü, K., Demirata, B., Özyürek, M., Çelik, S. E., Bektaşoğlu, B., Berker, K. I., and Özyurt, D. 2007. Comparative evaluation of various total antioxidant capacity assays applied to phenolic compounds with the CUPRAC assay. Molecules 12(7): 1496 – 1547.

Arabshahi-D, S., Devi, D. V., and Urooj, A. 2007. Evaluation of antioxidant activity of some plant extracts and their heat, pH and storage stability. Food Chemistry. 100(3): 1100 – 1105.

Babaei, F., Moafizad, A., Darvishvand, Z., Mirzababaei, M., Hosseinzadeh, H., and Nassiri-Asl, M. 2020. Review of the effects of vitexin in oxidative stress-related diseases. Food Science and Nutrition. 8(6): 2569 - 2580.

Bayliak, M. M., Burdyliuk, N. I., and Lushchak, V. I. 2016. Effects of pH on antioxidant and prooxidant properties of common medicinal herbs. Open Life Sciences. 11(1): 298 – 307.

Benjakul, S., Kittiphattanabawon, P., Sumpavapol, P., and Maqsood, S. 2014. Antioxidant activities of lead (*Leucaena leucocephala*) seed as affected by extraction solvent, prior dechlorophyllisation and drying methods. Journal of Food Science and Technology. 51(11): 3026 – 3037.

Braga, T. V., Gonçalves, R., Ramos, C. S., Cristina, F., Evangelista, G., Márcia, L., Varotti, F. D. P., Carvalho, G., and Sabino, A. D. P. 2014. Antioxidant, antibacterial and antitumor activity of ethanolic extract of the *Psidium guajava* leaves. American Journal of Plant Sciences. 5(9): 3492 – 3500.

Brown, N., John, J. A., and Shahidi, F. 2019. Polyphenol composition and antioxidant potential of mint leaves. Food Production, Processing and Nutrition. 1(1): 1–14.

Chen, Y. T., Kao, W. T., and Lin, K. W. 2008. Effects of pH on the total phenolic compound, antioxidative ability and the stability of dioscorin of various yam cultivars. Food Chemistry. 107(1): 250 – 257.

Chotphruethipong, L., Benjakul, S., and Kijroongrojana, K. 2017. Optimization of extraction of antioxidative phenolic compounds from cashew (*Anacardium occidentale* L.) leaves using response surface methodology. Journal of Food Biochemistry. 41(4): 1-10.

Chu, C., Deng, J., Man, Y., and Qu, Y. 2017. Green tea extracts epigallocatechin-3-gallate for different treatments. BioMed Research International. 2017: 5615647.

Dutta, S., and Ray, S. 2020. Comparative assessment of total phenolic content and in vitro antioxidant activities of bark and leaf methanolic extracts of (*Manilkara hexandra* Roxb.) Dubard. Journal of King Saud University – Science. 32(1): 643 – 647.

Francenia Santos-Sánchez, N., Salas-Coronado, R., Villanueva-Cañongo, C., and Hernández-Carlos, B. 2019. Antioxidant compounds and their antioxidant mechanism. Antioxidants. IntechOpen: 85270 London, UK.

Friedman, M., and Jürgens, H. S. 2000. Effect of pH on the stability of plant phenolic compounds. Journal of Agricultural and Food Chemistry. 48(6): 2101 – 2110.

Gan, R. Y., Chan, C. L., Yang, Q. Q., Li, H. Bin, Zhang, D., Ge, Y. Y., Gunaratne, A., Ge, J., and Corke, H. 2018. Bioactive compounds and beneficial functions of sprouted grains. Sprouted Grains: Nutritional Value, Production, and Applications. AACC International Press. 2019: 191 – 246.

Ghosh, S., Chakraborty, R., and Raychaudhuri, U. 2015. Determination of pH-dependent antioxidant activity of palm (*Borassus flabellifer*) polyphenol compounds by photoluminol and DPPH methods: a comparison of redox reaction sensitivity. 3 Biotech. 5(5): 633 – 640.

Goulas, V., and Hadjisolomou, A. 2019. Dynamic changes in targeted phenolic compounds and antioxidant potency of carob fruit (*Ceratonia siliqua* L.) products during in vitro digestion. LWT - Food Science and Technology. 101(3): 269 – 275.

Hafizah, A. H., Zaiton, Z., Zulkhairi, A., Mohd Ilham, A., Nor Anita, M. M. N., and Zaleha, A. M. 2010. *Piper sarmentosum* as an antioxidant on oxidative stress in human umbilical vein endothelial cells induced by hydrogen peroxide. Journal of Zhejiang University: Science B. 11(5): 357 – 365.

Halagarda, M., Groth, S., Popek, S., Rohn, S., and Pedan, V. 2020. Antioxidant activity and phenolic profile of selected organic and conventional honeys from Poland. Antioxidants. 9(1): 1 – 19.

Hamad, G. M., Darwish, A. M. G., Abu-Serie, M. M., and Sohaimy, S. A. El. 2017. Antimicrobial, antioxidant and anti-inflammatory characteristics of combination

(*Cassia fistula* and *Ocimum basilicum*) extract as natural preservative to control and Prevent Food Contamination. Journal of Food and Nutrition Research. 5(10): 771 – 780.

He, M., Min, J. W., Kong, W. L., He, X. H., Li, J. X., and Peng, B. W. 2016. A review on the pharmacological effects of vitexin and isovitexin. Fitoterapia. 115(12): 74 – 85.

Hosikian, A., Lim, S., Halim, R., and Danquah, M. K. 2010. Chlorophyll extraction from microalgae: A review on the process engineering aspects. International Journal of Chemical Engineering 391632: 1 – 11.

Ismail, M., Mariod, A., Bagalkotkar, G., and Ling, H. S. 2010. Fatty acid composition and antioxidant activity of oils from two cultivars of Cantaloupe extracted by supercritical fluid extraction. Grasas y Aceites. 61(1): 37 – 44.

Ismail, S. M., Hui, C. K., Aminuddin, A., and Ugusman, A. 2018. *Piper sarmentosum* as an Antioxidant: A systematic review. Sains Malaysiana. 47(10): 2359 – 2368.

Jiménez, M., Juárez, N., Jiménez-Fernández, V. M., Monribot-Villanueva, J. L., and Guerrero-Analco, J. A. 2018. Phenolic compounds and antioxidant activity of wild grape (*Vitis tiliifolia*). Italian Journal of Food Science. 30(1): 128 – 143.

Jung, H. A., Woo, J. J., Jung, M. J., Hwang, G.-S., and Choi, J. S. 2009. Kaempferol glycosides with antioxidant activity from *Brassica juncea*. Archives of Pharmacal Research. 32(10): 1379 – 1384.

Juntachote, T., and Berghofer, E. 2005. Antioxidative properties and stability of ethanolic extracts of Holy basil and Galangal. Food Chemistry. 92(2): 193 – 202.

Karnjanapratum, S., and Benjakul, S. 2015. Characteristics and antioxidative activity of gelatin hydrolysates from unicorn leather jacket skin as affected by autolysis-assisted process. Journal of Food Processing and Preservation. 39(6): 915 – 926.

Khole, S., A Panat, N., Suryawanshi, P., Chatterjee, S., Devasagayam, T., and Ghaskadbi, S. 2016. Comprehensive assessment of antioxidant activities of apigenin isomers: vitexin and isovitexin. Free Radicals and Antioxidants. 6(2): 155 – 166.

Kim, M. Y., Lee, B. W., Lee, H. U., Lee, Y. Y., Kim, M. H., Lee, J. Y., Lee, B. K., Woo, K. S., and Kim, H. J. 2019. Phenolic compounds and antioxidant activity in sweet potato after heat treatment. Journal of the Science of Food and

Agriculture. 99(15): 6833 – 6840.

Leesombun, A., Boonmasawai, S., Shimoda, N., and Nishikawa, Y. 2016. Effects of extracts from thai piperaceae plants against infection with *Toxoplasma gondii*. PLoS ONE. 11(5): 1 – 13.

Li, T., Xu, J., Wu, H., Wang, G., Dai, S., Fan, J., He, H., and Xiang, W. 2016. A saponification method for chlorophyll removal from microalgae biomass as oil feedstock. Marine Drugs. 14(9): 162.

Li, Y., He, N., Hou, J., Xu, L., Liu, C., Zhang, J., Wang, Q., Zhang, X., and Wu, X. 2018. Factors influencing leaf chlorophyll content in natural forests at the biome scale. Frontiers in Ecology and Evolution. 6(6): 64.

Madhumita, M., Guha, P., and Nag, A. 2019. Extraction of betel leaves (*Piper betle* L.) essential oil and its bio-actives identification: Process optimization, GC-MS analysis and anti-microbial activity. Industrial Crops and Products. 138(10): 111578.

Maghsoudlou, Y., Asghari Ghajari, M., and Tavasoli, S. 2019. Effects of heat treatment on the phenolic compounds and antioxidant capacity of quince fruit and its tisane’s sensory properties. Journal of Food Science and Technology. 56(5): 2365 – 2372.

Maqsood, S., Benjakul, S., Abushelaibi, A., and Alam, A. 2014. Phenolic compounds and plant phenolic extracts as natural antioxidants in prevention of lipid oxidation in Seafood: A detailed review. Comprehensive Reviews in Food Science and Food Safety. 13(6): 1125 – 1140.

Maqsood, S., Benjakul, S., and Shahidi, F. 2013. Emerging role of phenolic compounds as natural food additives in fish and fish products. Critical Reviews in Food Science and Nutrition. 53(2): 162 – 179.

Martinez, V., Mestre, T. C., Rubio, F., Girones-Vilaplana, A., Moreno, D. A., Mittler, R., and Rivero, R. M. 2016. Accumulation of flavonols over hydroxycinnamic acids favors oxidative damage protection under abiotic stress. Frontiers in Plant Science. 7(6): 838.

Mello, B. C. B. S., and Hubinger, M. D. 2012. Antioxidant activity and polyphenol contents in Brazilian green propolis extracts prepared with the use of ethanol and water as solvents in different pH values. International Journal of Food Science and Technology. 47(12): 2510 – 2518.

Miraliakbari, H., and Shahidi, F. 2008. Antioxidant activity of minor components of tree nut oils. Food Chemistry. 111(2): 421 – 427.

Mukherjee, P. K. 2019. Evaluating natural products and traditional medicine. Quality Control and Evaluation of Herbal Drugs. Elsevier, Amesterdam, 2019: 784.

Nicoli, M. C., Anese, M., and Parpinel, M. 1999. Influence of processing on the antioxidant properties of fruit and vegetables. Trends in Food Science and Technology. 10(3): 94 – 100.

Nouri, L., Mohammadi Nafchi, A., and Karim, A. A. 2014. Phytochemical, antioxidant, antibacterial, and α-amylase inhibitory properties of different extracts from betel leaves. Industrial Crops and Products. 62(12): 47 – 52.

Olatunde, O. O., Benjakul, S., and Vongkamjan, K. 2018. Antioxidant and antibacterial properties of guava leaf extracts as affected by solvents used for prior dechlorophyllization. Journal of Food Biochemistry. 42(5): 1 - 12.

Olugbami, J. O., Gbadegesin, M. A., and Odunola, O. A. 2014. *In vitro* evaluation of the antioxidant potential, phenolic and flavonoid contents of the stem bark ethanol extract of *Anogeissus leiocarpus*. African Journal of Medicine and Medical Sciences. 43(1): 101 – 109.

Sae-leaw, T., and Benjakul, S. 2019. Prevention of quality loss and melanosis of Pacific white shrimp by cashew leaf extracts. Food Control. 95(1): 257 – 266.

Sae-leaw, T., O'Callaghan, Y. C., Benjakul, S., and O'Brien, N. M. 2016. Antioxidant activities and selected characteristics of gelatin hydrolysates from seabass (*Lates calcarifer*) skin as affected by production processes. Journal of Food Science and Technology. 53(1): 197 – 208.

Salehi, B., Amiruddin Zakaria, Z., Gyawali, R., Ibrahim, S. A., Rajkovic, J., Khan Shinwari, Z., Khan, T., Sharifi-Rad, J., Ozleyen, A., Turkdonmez, E., Valussi, M., Boyunegmez Tumer, T., Monzote Fidalgo, L., Martorell, M., and Setzer, W. N. 2019. Piper Species: A comprehensive review on their phytochemistry, biological activities and applications. Molecules. 24(7): 1364.

Seo, J., Lee, S., Elam, M. L., Johnson, S. A., Kang, J., and Arjmandi, B. H. 2014.

Study to find the best extraction solvent for use with guava leaves (*Psidium guajava* L.) for high antioxidant efficacy. Food Science and Nutrition. 2(2): 174 – 180.

Shen, Y., Song, X., Li, L., Sun, J., Jaiswal, Y., Huang, J., Liu, C., Yang, W., Williams, L., Zhang, H., and Guan, Y. 2019. Protective effects of p-coumaric acid against oxidant and hyperlipidemia-an *in vitro* and *in vivo* evaluation. Biomedicine and Pharmacotherapy. 111(3): 579 – 587.

Shiekh, K. A., Benjakul, S., and Sae-leaw, T. 2019. Effect of Chamuang (*Garcinia cowa* Roxb.) leaf extract on inhibition of melanosis and quality changes of Pacific white shrimp during refrigerated storage. Food Chemistry. 270(1): 554 – 561.

Sun, H., Yuan, X., Zhang, Z., Su, X., and Shi, M. 2018. Thermal processing effects on the chemical constituent and antioxidant activity of okara extracts using subcritical water extraction. Journal of Chemistry. 2018: 6823789.

Tatsimo, S. J. N., Tamokou, J. D. D., Havyarimana, L., Csupor, D., Forgo, P., Hohmann, J., Kuiate, J. R., and Tane, P. 2012. Antimicrobial and antioxidant activity of kaempferol rhamnoside derivatives from *Bryophyllum pinnatum*. BMC Research Notes. *5*(1): 1 - 6.

Teixeira, J., Gaspar, A., Garrido, E. M., Garrido, J., and Borges, F. 2013. Hydroxycinnamic acid antioxidants: An electrochemical overview. BioMed Research International. 2013(1): 1 – 11.

Wang, J., Fang, X., Ge, L., Cao, F., Zhao, L., Wang, Z., and Xiao, W. 2018. Antitumor, antioxidant and anti-inflammatory activities of kaempferol and its corresponding glycosides and the enzymatic preparation of kaempferol. PLoS ONE. 13(5): 0197563.

CHAPTER 3

BETEL (*PIPER BETLE* L.) LEAF ETHANOLIC EXTRACTS DECHLOROPHYLLIZED USING DIFFERENT METHODS: ANTIOXIDANT AND ANTIBACTERIAL ACTIVITIES, AND APPLICATION FOR SHELF-LIFE EXTENSION OF NILE TILAPIA (*OREOCHROMIS NILOTICUS*) SLICES

3.1. Abstract

Different methods for chlorophyll removal were used for betel leaf ethanolic extracts (BLEE). Chlorophyll content, color, antioxidant, and antibacterial activities of the resulting extracts were examined. Sedimentation process remarkably reduced the chlorophyll content and color of BLEE ($p < 0.05$), while antioxidant and antibacterial activities were enhanced ($p < 0.05$). Polyphenols content and bioactivities of the extracts dechlorophyllized using organic solvents were varied ($p < 0.05$). Antibacterial efficacy of BLEE dechlorophyllized by sedimentation method (BLEE-SED) depended on concentrations. Lower MIC and MBC of BLEE-SED toward 4 bacteria were obtained, compared to others. Lower microbiological and chemical changes were achieved when Nile tilapia slices were treated with BLEE-SED at 400 and 600 ppm after 12 days of storage at 4˚C. Therefore, sedimentation as a green process could be adopted for preparing a safe BLEE with augmented bioactivities and pale color, which could extend shelf-life of refrigerated Nile tilapia slices.

3.2. Introduction

Fish are highly perishable because of their biological composition (Neira *et al.,* 2019). Unfavorable enzymatic mediated reactions and protein decomposition induced by microbial proliferation contribute to undesirable changes e.g., off-flavor and unpalatable taste of fish during refrigerated storage (Bono *et al.,* 2017). Fish spoilage not only contributes to a serious public health hazard, but also causes economic losses. Synthetic preservatives have been extensively used to extend the shelf-life of fish (Hassoun and Emir Çoban, 2017). Nevertheless, safety concerns regarding the excessive usage of such preservatives required adopting alternative methods based on application of natural compounds to fish products (Hassoun and Emir Çoban, 2017). In this context, plant extracts possessing both antioxidant and antibacterial properties have been employed (Olatunde *et al.,* 2019; Shiekh *et al.*, 2019). Nile tilapia (*Oreochromis niloticus*) has been consumed globally owing to its high nutritive value with high protein content (15 – 20%) and considerably low fats (1 – 4%) (Srisapoome and Areechon, 2017). It was estimated that about 4.13 million tons were produced in 2017 globally with an expected growth raise in the future (Tacon, 2020).

Betel *(Piper betle* L.), known commonly as “phlu” in Thailand, has several uses in traditional medicine. High content of secondary metabolites such as polyphenols and essential oils in betel leaves could be responsible for their antioxidant and antibacterial activities (Salehi *et al.,* 2019). Polyphenols are naturally occurring organic compounds of plant origin with different chemical structures. They include various sub-compounds such as flavonoids which exhibit bioactivities including antioxidants, antimicrobial, and anti-cancer activities. As a response to the adverse effects caused by the synthetic compounds used in food and pharmaceutical applications, polyphenols were proposed as perfect alternative candidates to be used in such applications and in food and food preservation applications (Benjakul *et al.,* 2014; Pabon-Baquero *et al.*, 2018). This suggests the possible use of betel leaf ethanolic extract as an alternative to the synthetic preservatives for shelf-life extension of fish and fish products.

However, the presence of high chlorophyll content in betel leaves is a major obstacle for their use in foods, in which the change in color leads to rejection by consumers. Also, chlorophyll is unstable molecule when extracted due to substitution of its central magnesium ion with weak acids in food materials as well as its photo-oxidant characters. This could induce oxidation in foods, thus decreasing their storage stability and causing off-flavor, apart from discoloration in color (Li *et al.,* 2016; Udayan *et al.,* 2017). For these reasons, chlorophyll removal is a crucial step for maximized exploitation of plant extract, especially betel leaf extract for food applications.

Traditionally, different organic solvents were used for dechlorophyllization of different plant extracts. Nevertheless, the aforementioned process was not effective as the coloring pigments were still present in the extracts. Only 63% of the chlorophyll was removed from ethanolic guava leaf extract using some organic solvents as reported by Olatunde *et al.* (2018), while 76% was removed from brown lead seed as observed by Benjakul *et al.* (2014). Additionally, different bioactivities were negatively affected by the process. Toxicity of these organic solvents used for chlorophyll removal was another matter of consideration (Tagrida and Benjakul, 2020), especially when the plant extract was used in foods. Other techniques were also reported for the dechlorophyllization including the use of activated charcoal, liquid–liquid partitioning, and ChloroFiltr cartridges (Tzima *et al.,* 2020). Countercurrent separation (CCS) was used for chlorophyll removal form botanical crude extracts enriched in chlorophyll (Kim *et al.*, 2020). However, the complexity, time consumed, cost, and less availability of required materials and instruments may be drawbacks for the use of those techniques. The practical need is focused on a simple, affordable, and green process to remove chlorophyll from plant extracts, particularly leaves, while maintaining their bioactivities. Sedimentation induced by water has been shown as a satisfying means and is proposed as a potential and green method for dechlorophyllization (Tagrida and Benjakul, 2020; Olatunde *et al.*, 2021).

The investigation aimed to comparatively study antioxidant and antibacterial activities of betel leaf ethanolic extracts (BLEE) when dechlorophyllized using different methods. Different organic solvents with various polarities were used as the traditional method for chlorophyll removal, while sedimentation method was implemented as a novel green method for chlorophyll removal. The selected dechlorophyllized extract showing the highest antioxidant and antibacterial activities was applied on Nile tilapia slices as a preservative and quality changes were monitored during refrigerated storage (4˚C) for 12 days.

3.3. Objectives

To study the characteristics, antioxidant, and antibacterial activities of betel ethanolic extract dechlorophyllized using different methods and the application for shelf-life extension of Nile tilapia (*Oreochromis niloticus*) slices.

3.4. Materials and methods

3.4.1. Chemicals

All chemicals used were of analytical grade. Plate count agar was procured from Difco (Maryland, USA). Eosin methylene blue (EMP) agar, triple sugar iron agar, and Pseudomonas isolation agar were obtained from Himedia (Mumbai, India).

3.4.2. Preparation of betel leaf powder (BLP)

Betel (*Piper betle* L.) leaves were gathered from a plantation near Songkhla province, Thailand, between October and November 2020. Vines were approximately 3 to 5 years old and only mature and healthy leaves were used. Betel leaf powder was prepared as tailored by Tagrida and Benjakul (2020). Leaves were washed thoroughly using the running tap water. Subsequently, leaves were dried using a hot air oven overnight at 50˚C until the moisture content of the leaves was less than 10%. Dried leaves were collected, blended using a high-speed blender (Panasonic, Model MX-898N, Berkshire, UK), and sieved using 80 mesh stainless-steel sieve to obtain the fine powder. The betel leaf powder (BLP) was kept in zip-lock bags and placed in a desiccator at room temperature until further processing.

3.4.3. Preparation of BLEE without dechlorophyllization

The extraction process was performed following the method outlined by Tagrida and Benjakul (2020). Ethanol (70%) was used as extraction solvent at leaf powder/solvent ratio of 1:15. Ethanol was removed by a rotary evaporator before being lyophilized. Dried extract without removing the chlorophyll was used as the control termed 'BLEE-CON' and stored at -20˚C until use.

3.4.4. Preparation of BLEE with dechlorophyllization

3.4.4.1. Dechlorophyllization using different organic solvents

The procedure of Chotphruethipong *et al.* (2017) was adopted with minor modifications. Acetone, chloroform, and petroleum ether were selected as dechlorophyllizing solvents. Each solvent was mixed with BLP separately at a 1:10 powder/solvent ratio and stirred for 30 min, followed by filtering using Whatman filter paper No.1. The filtrate was discarded, and the retentate was subjected to dechlorophyllization in the same manner for another two times. The retentates were subsequently dried for 1 h at 60˚C in a hot air oven. Thereafter, the dried powders were subjected to ethanolic (70%) extraction as previously mentioned. The obtained extracts after lyophilization were termed BLEE-ACT, BLEE-CF, and BLEE-PET for BLP dechlorophyllized using acetone, chloroform, and petroleum ether, respectively. The resulting lyophilized powders were placed in vials, capped, and kept at -20˚C until use.

3.4.4.2. Dechlorophyllization using sedimentation

Sedimentation technique was used as tailored by Tagrida and Benjakul (2020) for the dechlorophyllization. Firstly, ethanolic extract was prepared from BLP as described previously, after removing the ethanol by a rotary evaporator at 40˚C, the distilled water was added to the concentrated extract at 1:1 ratio (v/v). Sedimentation was then allowed to occur at 4˚C for 24 h. After sedimentation and being centrifuged at 10,000 x g and 4˚C for 30 min, supernatant was collected and lyophilized. The dried extract termed "BLEE-SED" was placed in vial, capped, and kept at -20˚C before analysis.

3.4.5. Analyses

3.4.5.1. Extraction yield

The yield of the extracts was considered as the dry weight of the final extracts relative to the initial dry weight of their corresponding powder. Yield was calculated as per the method of Tagrida and Benjakul (2020).

3.4.5.2. Chlorophyll content and color

To determine chlorophyll content, dry extracts without and with dechlorophyllization were dissolved in 70% (v/v) ethanol to obtain a concentration of 2 mg/mL. Chlorophyll content was measured as guided by Olatunde *et al.* (2018). The same solutions were used for the determination of color attributes (*L**, *a**, *b**, chroma, and hue angle) with the aid of a colorimeter (Hunter Lab's Colorflex, Reston, USA).

3.4.5.3. Total phenolic content (TPC)

Folin-Ciocalteu's reagent (FCR) was employed for TPC determination of the extracts without and with dechlorophyllization. The assay outlined by Benjakul *et al.* (2014) was applied for determination of TPC. TPC was calculated and expressed as mg gallic acid equivalent (GAE)/g dry extract.

3.4.5.4. Determination of antioxidant activity

The procedure of Benjakul *et al.* (2014) was followed for estimating DPPH radical scavenging activity (DPPH-RSA), ABTS radical scavenging activity (ABTS-RSA), and Ferric reducing antioxidant power (FRAP). Trolox standard curve was used for the calculation of activities and the results were expressed as μmol Trolox equivalents (TE)/g dry extract. Metal chelating activity (MCA) was measured following the same procedure. Calculation was done using a standard curve of EDTA and expressed as μmol EDTA equivalents (EE)/g dry extract.

3.4.5.5. Determination of antibacterial activity

3.4.5.5.1. Bacterial strains

Selected Gram-positive bacteria (G+ve Bacteria) and Gram-negative bacteria (G-ve Bacteria) were assessed for inhibition by the extracts without and with dechlorophyllization. The bacteria used included *Escherichia coli* DMST 4122 and *Staphylococcus aureus* DMST 4547, obtained from the Department of Medical Science, Ministry of Health, Thailand. *Listeria monocytogenes* PSU.SCB.16S.13 and *Pseudomonas aeruginosa* PSU.SCB.16S.12, were gifted from Food Safety Laboratory, Department of Food Technology, Prince of Songkla University, Hat Yai, Thailand. Culture conditions and cell suspension were maintained as delineated by Olatunde *et al.* (2018).

3.4.5.5.2. Minimum inhibitory concentration (MIC) and minimum bactericidal concentration (MBC)

The method of Olatunde *et al.* (2019) was adopted to determine the MIC and MBC of BLEE without and with dechlorophyllization. Samples (100 μL) with diversified concentrations (50 to 0.097 mg/mL) prepared in tryptic soy broth (TSB), were placed into a sterile 96 flat shaped multi wells, and then 100 μl of a 0.5 McFarland standard (10^8 CFU/mL) bacterial suspension were inoculated into all the wells. Extracts at 50 mg/mL without bacterial suspension were served as negative control, while bacterial suspensions devoid of extracts were considered as positive control. After 24 h incubation period at 37˚C, resazurin solution (0.2 mM, 50 μL) was added to all the wells. MIC was assessed visually for color change, and it was defined as the lowest concentration, which completely inhibited bacterial growth. Before adding the resazurin solution, aliquots (15 μL) from wells showing no apparent bacterial growth were inoculated into tryptic soy agar (TSA) plates. Subsequently, the plates were incubated at 37˚C for 24 h. Least concentration with no bacterial growth was recorded as MBC.

3.4.5.5.3. Time-kill kinetics

BLEE with the lowest MIC and MBC was selected to study its killing rate against G+ve Bacteria and G-ve Bacteria. The experiment was conducted as tailored by Odedina, *et al.* (2015). The selected BLEE solutions (1.5 ml) at 0.5, 1, 2, and 4 MIC were inoculated with a 1.5 ml of 0.5 McFarland bacterial suspension from each growing culture (10^8 CFU/ml) prepared previously in TSB. All culture media were incubated for 24 h at 37˚C. Plate count method was used for enumerating the surviving cells at time 0, 2, 4, 6, 8, 12, and 24 h. Control culture with no extract was incubated and enumerated in the same manner. The experiment was performed in duplicate for three independent studies (Detection limit 10^2 CFU).

3.4.5.5.4. Scanning electron microscopy (SEM)

The BLEE showing the lowest MIC level on G+ve Bacteria and G-ve Bacteria was selected for treatment of bacteria (Olatunde *et al.*, 2019). All bacterial cells were visualized and photographed with the aid of scanning electron microscope (FEI Quanta 400-FEG SEM, Oregon, USA). Bacterial culture untreated with the selected BLEE was used as the control.

3.4.6. Influence of the selected BLEE on shelf-life extension of Nile tilapia (*Oreochromis niloticus*) slices during refrigerated storage

3.4.6.1. Preparation of Nile tilapia slices

Deceased Nile tilapia (around 4 kg, 1 ± 0.1 kg/fish) were purchased from the local market at Hat Yai, Songkhla, Thailand. Those fish (approximately 3 h after capture from fish farm in Ko Yo) were kept in ice (ice/fish ratio of 2:1 (w/w)) and transported within 30 min to the International Center of Excellence in Seafood Science and Innovation (ICE-SSI), Prince of Songkhla University, where they were immediately washed upon arrival. Subsequently, fish were decapitated, skinned, deboned, filleted, and sliced using sanitized stainless-steel knife. The average size of the slices was approximately 3 x 4 cm^2.

3.4.6.2. Pretreatment of tilapia slices with the selected BLEE extract

The selected extract "BLEE-SED" at known amount was dissolved in the minimum volume of distilled water. Tilapia slices were mixed manually with the prepared extract to get the levels of 200, 400, and 600 ppm. For slices treated with BLEE-SED (600 ppm), sensory evaluation was performed in comparison to the control (no treatment) by 50 untrained panelists. The fish slices were steamed as tailored by Olatunde *et al.* (2019) before serving. There was no difference in all attributes (color, odor, flavor, texture, and overall likeness) between the control and that treated with BLEE-SED ($p > 0.05$).

Untreated and treated slices were separately placed on polystyrene trays, wrapped tightly with shrink film, and stored at 4˚C. Sampling for analyses was done at day 0, 3, 6, 9, and 12 of storage.

3.4.6.3. Microbiological analyses

Firstly, slices (10 g) were added with 90 ml of sterilized saline solution (0.85%) in stomacher bag. Blending was done using a stomacher blender (M400, Seward Ltd., West Sussex, England) for 1 min at 220 rpm, followed by serial dilutions using 0.85% saline solution. Spread plate method with the appropriate dilutions was used for monitoring microbiological changes in tilapia slices (Shiekh *et al.*, 2019). Psychrophilic bacterial count and total viable count were enumerated on plate count agar after incubation at 4˚C for 10 days and 37˚C for 3 days, respectively. Triple sugar iron agar and pseudomonas isolation agar were used for evaluating H_2S producing bacteria and *pseudomonas* sp. counts, respectively, after 3 days incubation period at 25˚C. Counts of *Enterobacteriaceae* were evaluated after being incubated at 37˚C for 24 h using eosin methylene blue (EMB) agar.

3.4.6.4. Chemical analyses

Total volatile base (TVB) content was determined as tailored by Shiekh *et al.*, 2019 and reported as mg N/100 g fish meat. Peroxide value (PV) expressed as mg cumene hydroperoxide/ kg fish meat, was evaluated (Arfat *et al.*, 2015). Thiobarbituric acid reactive substances (TBARS) were examined as per the method of Olatunde *et al.* (2019). The values were expressed as mg MDA/kg fish meat. The pH of fish homogenate in distilled water (2:10, w/v) was measured using a pH meter (Lab 855, SI analytics, Weilheim, Germany).

3.4.7. Statistical analyses

Completely randomized design (CRD) was applied for the whole study. Experiments were carried out in triplicates (n=3). One-way Analysis of Variance (ANOVA) and the Duncan's Multiple Range Test (DMRT) for mean comparison were performed for the analysis of data using SPSS package (SPSS 23.0 for Windows, SPSS Inc, Chicago, IL, USA) software.

3.5. Results and discussion

3.5.1. Effect of different dechlorophyllization methods on chlorophyll content

Compared to the control, BLEE after dechlorophyllization showed varied chlorophyll contents (Table 7). BLEE dechlorophyllized using organic solvents showed the decreases in chlorophyll A, chlorophyll B and total chlorophyll contents ($p < 0.05$). No difference in total chlorophyll content was observed between BLEE-PET and BLEE-CF ($p > 0.05$). Among all the extracts with dechlorophyllization, BLEE-ACT had the highest total chlorophyll contents, indicating that petroleum ether and chloroform were more efficient for chlorophyll removal than acetone. Olatunde *et al.* (2018) also documented that non-polar solvents were more effective in chlorophyll removal than polar counterparts.

Chlorophyll is an amphiphilic compound containing a hydrophilic head of porphyrin ring, where magnesium atom is located at the center, and a long lipophilic hydrocarbon tail is linked by an ester bond to this porphyrin ring (Tagrida and Benjakul, 2020). Polarity of the organic solvents used for dechlorophyllization may affect the efficiency of the process. Organic solvents can access into plant cell *via* membrane, thus dissolving the lipids and lipoprotein of the plant cell organelles and releasing their contents (Olatunde *et al.*, 2018). Chloroform and petroleum ether are strong non-polar solvents, while acetone is a polar aprotic solvent. Therefore, more chlorophyll was dissolved in these non-polar solvents, which were further discarded. On the other hand, considerably higher chlorophyll content was remained in the extract dechlorophyllized using acetone.

When sedimentation process was used for chlorophyll removal, it was found that this process had more profound effect as compared to conventional dechlorophyllization methods using organic solvents ($p < 0.05$). Water added to the extract after ethanol removal made the medium more polar, causing the chlorophyll molecules to precipitate and leaving the top layers with negligible chlorophyll. It could be obviously detected by the difference in color between the top and lower layers of the extract. Extracts dechlorophyllized using organic solvents still had substantive amount of chlorophyll remaining after extraction. Therefore, BLEE-SED had less chlorophyll contents ($p < 0.05$) than the other extracts.

This finding was similar to results observed by Tagrida and Benjakul (2020) who found that betel leaf extract dechlorophyllized by sedimentation using all water/extract ratios (1:1, 1:2, and 1:3) had less chlorophyll content as compared to the control (without dechlorophyllization). Water was able to increase the polarity of the medium, thus allowing the chlorophyll molecules which are non-polar in nature to precipitate and subsequently removed. This process yielded the extract with less chlorophyll content. Similar trend was found with chlorophyll A and chlorophyll B, in which the control had the highest contents. Also, the extract dechlorophyllized using sedimentation process (BLEE-SED) had the lowest chlorophyll A and B contents ($p < 0.05$).

Chlorophyll A and B are types of chlorophyll that aid in absorbing the light required for photosynthesis, chlorophyll A is an electron donor in electron transport system, while chlorophyll B expands the absorption spectrum, thus converting a wider range of sun energy into chemical energy (Chen, 2014). Chlorophyll B was more dominant in all extracts, which was in tandem with the report of Olatunde *et al*. (2018). Usually, chlorophyll A content is higher than chlorophyll B content, however certain environmental conditions may lead to the difference in the chlorophyll A/B content ratio. The insufficient exposure to sunlight (shading) could make the betel leaves fight with other leaves from other plants or themselves over sunlight (Dai *et al.*, 2009). This would induce the production of higher levels of chlorophyll B in the leaves to capture as much sunlight as they could, whereas chlorophyll A cannot carry on photosynthesis (Ruban, 2009). Hence, betel leaves appear dark green and have higher content levels of chlorophyll B.

Table 7. Chlorophyll contents and color of betel leaf ethanolic extract (BLEE) before and after dechlorophyllization using different organic solvents and sedimentation process

Samples	**Chlorophyll A (mg/g)**	**Chlorophyll B (mg/g)**	**Total chlorophyll (mg/g)**	***L****	***a****	***b****	**Chroma**	**Hue angle**	**Δ*E****
BLEE-CON	0.488 ± 0.004^{a}	1.055 ± 0.028^{a}	1.543 ± 0.025^{a}	0.306 ± 0.08^{d}	-0.998 ± 0.07^{d}	-3.602 ± 0.49^{c}	3.74 ± 0.46^{a}	254.22 ± 2.96^{a}	91.62 ± 0.08^{a}
BLEE-ACT	0.388 ± 0.003^{b}	0.875 ± 0.012^{b}	1.263 ± 0.015^{b}	0.952 ± 0.06^{c}	-0.744 ± 0.16^{c}	-1.58 ± 0.14^{b}	1.75 ± 0.12^{b}	244.8 ± 6.02^{ab}	90.9 ± 0.06^{b}
BLEE-CF	0.313 ± 0.015^{c}	0.731 ± 0.003^{c}	1.044 ± 0.012^{c}	1.172 ± 0.06^{b}	-0.604 ± 0.06^{c}	-1.186 ± 0.17^{a}	1.33 ± 0.17^{c}	242.8 ± 2.91^{ab}	90.67 ± 0.06^{bc}
BLEE-PET	0.312 ± 0.018^{c}	0.712 ± 0.009^{c}	1.024 ± 0.019^{c}	1.196 ± 0.06^{b}	-0.552 ± 0.04^{b}	-1.008 ± 0.64^{a}	1.14 ± 0.06^{c}	229.3 ± 27.6^{b}	90.65 ± 0.06^{bc}
BLEE-SED	0.082 ± 0.007^{d}	0.184 ± 0.006^{d}	0.267 ± 0.009^{d}	1.82 ± 0.21^{a}	0.838 ± 0.11^{a}	-0.982 ± 0.41^{a}	1.29 ± 0.08^{c}	130.66 ± 6.56^{c}	90.48 ± 0.53^{c}

Values are the mean ± standard deviation (n = 3). Different lowercase superscripts within the same column indicate significant difference ($p < 0.05$). BLEE-CON: betel leaf ethanolic extract without dechlorophyllization; BLEE-ACT, BLEE-CF, BLEE-PET, and BLEE-SED: betel leaf ethanolic extract dechlorophyllized using acetone, chloroform, petroleum ether, and sedimentation method, respectively; *L**: lightness/darkness; *a**: greenness/redness; *b**: yellowness/blueness; Δ*E**: change in color.

3.5.2. Effect of different dechlorophyllization methods on the color of the extracts

When estimating the color of the extracts (Table 7), all the dechlorophyllized extracts had different colors from the control ($p < 0.05$). Among the extracts dechlorophyllized using organic solvents, BLEE-CF and BLEE-PET showed similar L^*, a^*, and b^* values ($p > 0.05$). However, both the extracts exhibited higher L^*, a^*, and b^* values than BLEE-ACT ($p < 0.05$). Lightness (L^*) was higher in BLEE-CF and BLEE-PET than BLEE-ACT, indicating ineffectiveness of acetone to remove pigments, mainly chlorophylls of the extracts, compared to chloroform or petroleum ether. This was also ascertained by greenness/redness (a^*) parameter, which showed less negative value in BLEE-CF and BLEE-PET than BLEE-ACT. This signified less greenness in both extracts than BLEE-ACT. Yellowness (b^*) was higher in BLEE-CF and BLEE-PET, reflecting more yellowness for both extracts than BLEE-ACT. It was noted that BLEE-SED had the highest L^*, a^*, and b^*, denoting that this extract was lighter with lesser greenness and slightly pale yellowish than other extracts dechlorophyllized by organic solvents ($p < 0.05$). This reconfirmed the ability of sedimentation process to reduce the color of betel leaf extract more efficiently than organic solvents.

A negative correlation was observed between chlorophyll content of the extracts and their color parameters (L^*, a^* and b^*), while it was positively correlated with the chroma and hue angle (h°). This indicated the influence of chlorophyll on the color of the extracts and implied that the higher the chlorophyll content in the extract, the color, especially greenness, was more dominant. The results reconfirmed that sedimentation process had the potential in removal of chlorophyll, thus lowering greenness caused by chlorophylls.

3.5.3. Extraction yield, total phenolic content (TPC), and antioxidant activities of BLEEs

Extraction yields were different ($p < 0.05$) among all the extracts and the control (Table 8). BLEE-CON showed the highest yield, mostly attributed to the abundance of chlorophyll, while differences in yields between BLEE-ACT, BLEE-CF and BLEE-PET could possibly be governed by solvents used. Different types of organic solvents used differ in polarity and penetration capacity into plant cell walls. Thus, the targeted products got solved and separated from the structural components differently (Miazek *et al.*, 2017). The lowest yield was observed in BLEE-SED, in which the settled chlorophyll was removed from the extract, thereby reducing its final yield. The extraction yield of the extracts dechlorophyllized using organic solvents was higher than that of BLEE-SED.

TPC of the extracts varied (Table 8). BLEE-SED had the highest TPC followed by BLEE-CON, whereas lower TPC was observed in the extracts dechlorophyllized using organic solvents. Previous studies also reported lower TPC of extracts from lead (*Leucaena leucocephala*) seeds and guava leaves, after dechlorophyllization using organic solvents (Benjakul *et al*., 2014; Olatunde *et al*., 2018). The reduction in TPC could be related to the loss in polyphenols from these extracts during dechlorophyllization process. The differences in TPC among BLEE-ACT, BLEE-CF and BLEE-PET were related to the varying polarities of different solvents along with their penetration capacity through the plant cells. Higher TPC in BLEE-SED than other extracts could be associated with high solubility of polyphenols in aqueous phase, while chlorophyll was precipitated (Cvetanović *et al.,* 2015). Therefore, addition of water to ethanolic extract at appropriate ratio could increase the polarity of the extraction medium, causing the chlorophyll molecules to settle and increase the proportion of polyphenols in the final extract. Loss of polyphenols during dechlorophyllization using solvents as well as remaining chlorophyll more likely reduced TPC of the extracts. These drawbacks were depleted in sedimentation process, making this technique more effective in chlorophyll removal as well as augmenting TPC.

Antioxidant activities of the dechlorophyllized extracts differed ($p < 0.05$) compared to those of BLEE-CON (Table 8). BLEE-SED exhibited the highest DPPH-RSA and ABTS-RSA ($p < 0.05$). It also had the most prominent FRAP and MCA ($p < 0.05$). This indicates the higher ability of BLEE-SED to donate electrons to ABTS and DPPH radicals with the profound capability to reduce ferric ions to ferrous ions as well as the higher capacity to chelate transition metals. The reduced activity of extracts dechlorophyllized using organic solvents was plausibly related to the high loss of polyphenols during the process.

Table 8. Extraction yield, total phenolic content (TPC), and antioxidant activities of BLEE before and after dechlorophyllization using different organic solvents and sedimentation process

Samples	Extraction yield (%)	TPC (mg GAE/g dry extract)	DPPH-RSA (μmol TE/g dry extract)	ABTS-RSA (μmol TE/g dry extract)	FRAP (μmol TE/g dry extract)	MCA (μmol EDTA dry extract)
BLEE-CON	14.93 ± 0.02^{a}	130.6 ± 3.86^{b}	105.7 ± 1.62^{a}	2164.2 ± 36.09^{b}	1213.04 ± 5.2^{b}	149.64 ± 5.32^{b}
BLEE-ACT	12.90 ± 0.09^{b}	98.72 ± 5.07^{c}	84.66 ± 0.44^{b}	1766.3 ± 16.16^{c}	998.43 ± 5.8^{c}	131.88 ± 1.75^{c}
BLEE-CF	12.38 ± 0.02^{c}	69.27 ± 4.92^{d}	80.45 ± 3.11^{c}	1529.6 ± 38.88^{d}	788.17 ± 7.7^{d}	92.46 ± 3.27^{d}
BLEE-PET	12.25 ± 0.01^{c}	53.54 ± 6.45^{e}	75.58 ± 2.08^{d}	1168.7 ± 36.02^{e}	693.04 ± 8.06^{e}	83.97 ± 2.25^{e}
BLEE-SED	11.06 ± 0.01^{c}	171.73 ± 4.42^{a}	108.7 ± 0.21^{a}	2503.03 ± 24.2^{a}	1394.14 ± 4.34^{a}	220.11 ± 2.3^{a}

Values are the mean ± standard deviation (n = 3). Different lowercase superscripts within the same column indicate significant difference ($p < 0.05$). TPC: Total phenolic content; DPPH-RSA: 2,2-diphenyl-1-picrylhydrazyl radical scavenging activity; ABTS-RSA: 2, 2'-Azino-bis-3-ethylbenzothiazoline-6-sulfonic acid radical scavenging activity; FRAP: Ferric reducing antioxidant power; MCA: Metal chelating activity. For captions see Table 7.

The difference in activity between these extracts was more likely associated with the differences in the polarity of different solvents used. Higher activity of BLEE-SED was connected to the low chlorophyll content and high TPC, thus augmenting its interactions with radicals. A high positive correlation was noticed between TPC and all the antioxidant activities, which suggested that polyphenols within the different extracts associated with antioxidant activities and the difference in their content determined antioxidant activity. Strong correlation between TPC and antioxidant activities confirmed that polyphenols are responsible for antioxidant activities of the extracts (Benjakul *et al.,* 2014; Olatunde *et al.,* 2018; Tagrida and Benjakul, 2020).

3.5.4. Antibacterial activities

3.5.4.1. MIC and MBC of the extracts

MICs and MBCs of BLEE without and with dechlorophyllization against some G+ve Bacteria and G-ve Bacteria are presented in Table 9. BLEE-SED had the lowest MIC against all bacteria tested, ranging from 0.39 to 3.12 mg/mL, followed by BLEE-CON. BLEE dechlorophyllized using organic solvents had the higher MIC against the tested bacteria, indicating lower antibacterial activity of these extracts. Differences in MIC values between all the extracts could be related to differences in content and types of polyphenols. These compounds were capable of interacting with the bacterial cell wall, thus causing disturbance to its constituents. This phenomenon promoted the leakage of bacterial cell and penetration of other compound and subsequently affected the internal organelles and nuclei. It caused growth inhibition or death to the bacterial cells (Olatunde *et al.,* 2019). Since BLEE-SED had the highest TPC, its antibacterial activity was greater than the others, which had lesser antibacterial activity ($p < 0.05$). The effects of the extracts varied among the different bacteria tested. All the extracts had lower inhibiting activity towards G+ve Bacteria. This could be due to the presence of more peptidoglycan layers in their cell wall, giving them higher resistance. MBC is the lowest concentration required from an antibacterial agent to completely kill certain bacterium (Olatunde *et al.,* 2019). Lowest MBC values were acquired by BLEE-SED ranging from 1.56 to 6.25 mg/mL. An antibacterial agent is considered as bactericidal if the MBC is 4 time higher than its corresponding MIC

(Yuniati *et al.,* 2018). Variations of MBCs among the different extracts were related with variations of MICs as well as the resistivity of the tested bacteria. Due to the higher antioxidant and antibacterial activities of BLEE-SED as well as its lowest chlorophyll content and highest color reduction, it was chosen for further study.

Table 9. Minimum inhibitory concentration (MIC) and minimum bactericidal concentration (MBC) of betel leaf ethanolic extracts (BLEE) before and after dechlorophyllization using different organic solvents and sedimentation process

Samples	**MIC* (mg/mL)**				**MBC* (mg/mL)**			
	SA	**EC**	**LM**	**PA**	**SA**	**EC**	**LM**	**PA**
BLEE-CON	3.12^{c}	1.56^{c}	3.12^{c}	0.78^{b}	6.25^{c}	6.25^{c}	6.25^{b}	1.56^{c}
BLEE-ACT	12.5^{b}	12.5^{a}	12.5^{a}	6.25^{a}	25^{a}	25^{a}	25^{a}	12.5^{b}
BLEE-CF	12.5^{b}	6.25^{b}	6.25^{b}	6.25^{a}	12.5^{b}	12.5^{b}	25^{a}	12.5^{b}
BLEE-PET	25^{a}	12.5^{a}	12.5^{a}	6.25^{a}	25^{a}	25^{a}	25^{a}	25^{a}
BLEE-SED	1.56^{d}	0.39^{d}	3.12^{c}	0.78^{b}	3.12^{d}	1.56^{d}	6.25^{b}	1.56^{c}

SA: *Staphylococcus aureus*, EC: *Escherichia coli*, LM: *Listeria monocytogenes*, PA: *Pseudomonas aeruginosa*, MIC: minimum inhibitory concentration, MBC: minimum bactericidal concentration. Different lowercase superscripts within the same column indicate significant difference ($p < 0.05$). Mean ($n = 3$). For captions see Table 7.

3.5.4.2. Time – kill kinetics

Different concentrations of BLEE-SED were employed to test its antibacterial efficacy against some G+ve Bacteria (*S. aureus* and *L. monocytogenes*) and G-ve Bacteria (*P. aeruginosa* and *E. coli*) using time – kill kinetics assay (Fig. 11). Distilled water with no extract was served as the control. Counts of the control and that treated with 0.5 MIC BLEE-SED continuously increased, however lower growth rate for BLEE-SED at 0.5 MIC was obtained compared to the control ($p < 0.05$) after 24 h of incubation, suggesting that BLEE-SED had quite low antibacterial activity at that concentration.

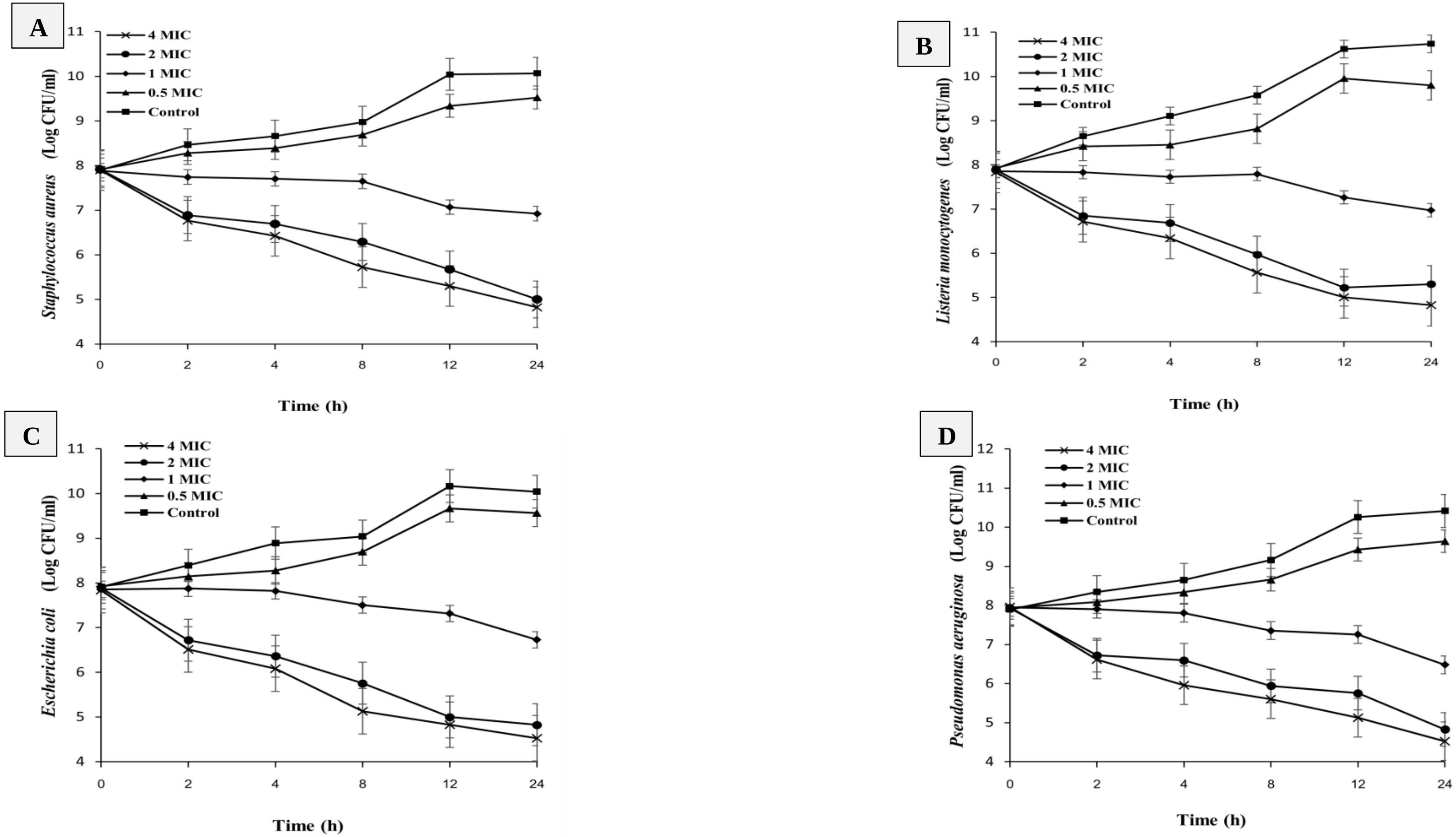

Figure 11. Time-kill curves toward different microorganisms including *Staphylococcus aureus* (A), *Listeria monocytogenes* (B), *Escherichia coli* (C) and *Pseudomonas aeruginosa* (D) without and with BLEE-SED treatment at different concentrations. Bars represent standard deviation (n = 3)

A reduction ≥ 3 log CFU/mL in bacterial count is defined as bactericidal activity, while reduction lower than that value is considered as bacteriostatic activity (Campanile *et al.*, 2019). At MIC level (1.56 mg/mL), BLEE-SED exhibited a bacteriostatic activity toward *S. aureus* with a 0.96 log CFU/mL reduction after 24 h of incubation, while it was about 0.88 log CFU/mL reduction for *L. monocytogenes* at MIC level (3.12 mg/mL). The reduction rate was 1.46 and 1.12 log CFU/mL for *P. aeruginosa* and *E. coli*, respectively, at their MIC level (0.78 and 0.39 mg/mL, respectively). Bactericidal activity was achieved after 24 h at 4 MIC for all the tested isolates as the reduction rate surpassed the 3 log CFU/mL limit. For S. aureus and *L. monocytogenes*, it was 3.07 and 3.01 log CFU/mL reduction, respectively. The reduction rate was 3.43 and 3.31 log CFU/mL for *P. aeruginosa* and *E. coli*, respectively. At 2 MIC level, BLEE-SED exhibited a bactericidal activity only on *P. aeruginosa* and *E. coli* with reduction rate of 3.1 and 3.06 log CFU/mL, respectively. The same level of BLEE-SED had bacteriostatic activity on *S. aureus* and *L. monocytogenes* with 2.91 and 2.5 log CFU/mL. The reduction rate is noted to be higher for the G-ve Bacteria (*P. aeruginosa* and *E. coli*) than that of the G+ve Bacteria at all concentrations used. This was mainly attributed to the lack of thick layers of peptidoglycan in the cell walls of the G-ve Bacteria, (Olatunde *et al.*, 2019) making those more sensitive towards BLEE-SED. Nevertheless, BLEE-SED showed notable antibacterial efficacy at various concentrations for inhibiting the growth of both selected G+ve Bacteriaand G-ve Bacteria.

3.5.4.3. Effect of BLEE-SED on morphology of bacterial cells

The effect of BLEE-SED on tested bacteria morphology was visualized by comparing the morphology of their cell walls before and after treatment with BLEE-SED at MIC level with the aid of scanning electron microscope (x 30,000). Bacterial cell walls without treatment (control) appeared intact with no apparent damage (Fig. 12A, B, C and D). On the other hand, the difference could be detected after treatment with BLEE-SED, as the cell walls of *S. aureus*, *L. monocytogenes*, *P. aeruginosa* and *E. coli* appeared shrunken or destroyed in addition to the several pours that were obtained as pointed by arrows (Fig. 12E, F, G and H).

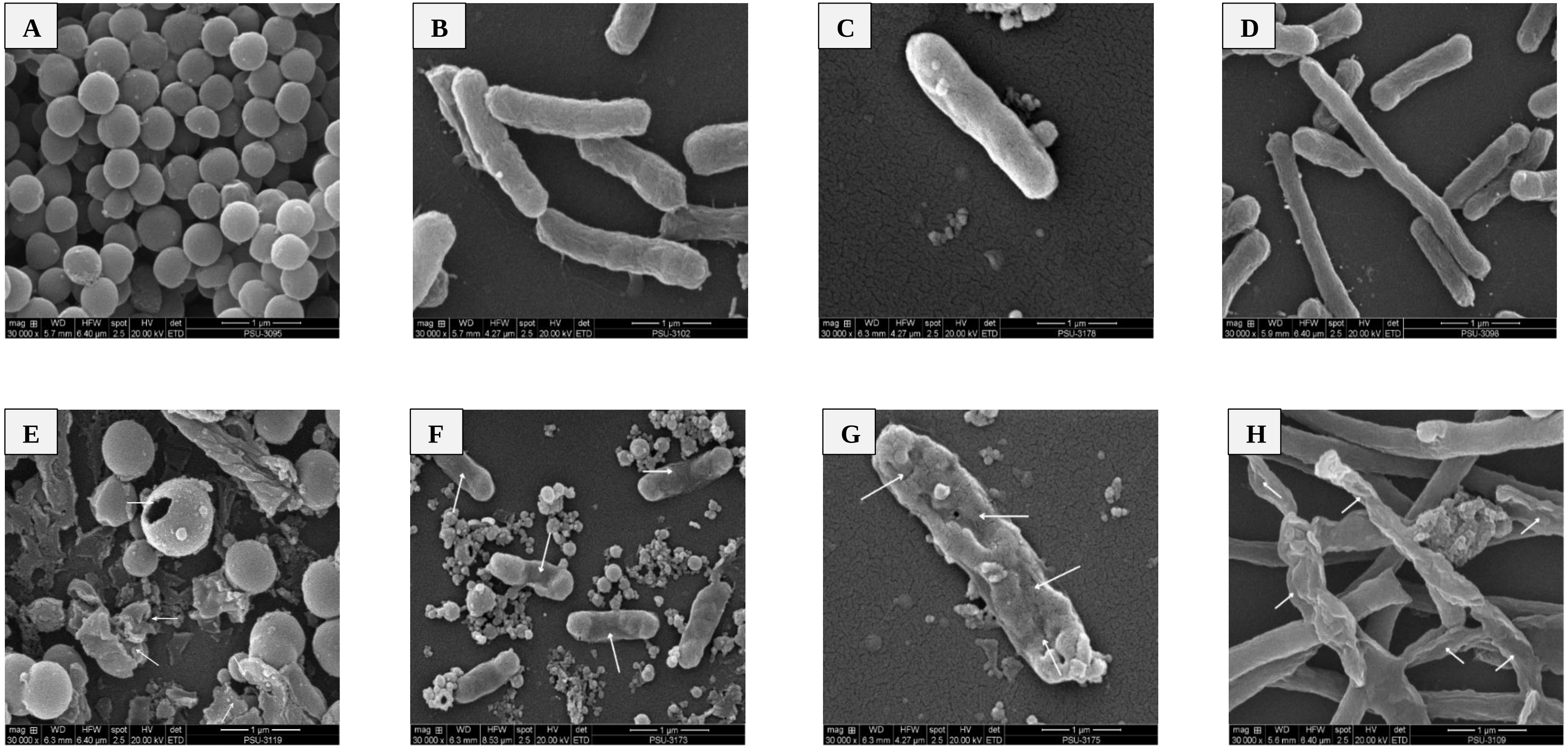

Figure 12. Scanning electron microscope photographs of untreated and treated *Staphylococcus aureus* (A and E), *Listeria monocytogenes* (B and F), *Escherichia coli* (C and G), and *Pseudomonas aeruginosa* (D and H). Magnification x 30,000.

Leakage of cytoplasmic substances from bacterial cells as a consequence of destruction of their cell walls by coconut husk ethanolic extract was also reported by Olatunde *et al*. (2019). When bacterial organelles and DNA were destroyed, their division and growth abilities as well as their cell wall repair mechanisms were negatively affected. Deformity of the bacterial cells took place when *Rhodomyrtus tomentosa* ethanolic leaf extract was applied (Odedina *et al*., 2015).

3.5.5. Influence of BLEE-SED on quality changes of tilapia slices during refrigerated storage

3.5.5.1. Changes in microbial load

Microbiological changes of tilapia slices treated with BLEE-SED at different concentrations were assessed by monitoring bacterial count during 12 days of storage (Fig. 13). TVC of the control and samples treated with BLEE-SED at various concentrations at day 0 ranged from 3.8 to 4.0 log CFU/g, indicating that a slight microbial contamination probably took place during the preparation of samples. Microbial load increased rapidly ($p < 0.05$) to 6.8 log CFU/g for the control at day 3. The growth continued to reach 8.3 log CFU/g on day 12 of storage. The marginal limit accepted for fresh and marine water species is 6.0 log CFU/g (Odedina *et al*., 2015). TVC of the treated samples still had the increase in bacterial count ($p < 0.05$). Nevertheless, the increase rate was lower than that of the control. After 6 days, samples treated with 200 ppm BLEE-SED had TVC of 6.2 log CFU/g, while samples treated with 400 and 600 ppm of the BLEE-SED had a load lower than the acceptable marginal limit after day 9, reaching 5.7 and 5.5 log CFU/g, respectively. These results implied the ability of BLEE-SED at 400 and 600 ppm to retard the microbial proliferation up to 9 days of storage at 4˚C. At day 12, the samples treated with BLEE-SED at 400 and 600 ppm had TVC of 6.21 and 6.13 log CFU/g, respectively.

Psychrophilic bacteria count (PBC) for the control and samples treated with BLEE-SED at various concentrations was augmented rapidly after day 3 ($p < 0.05$). However, this increase varied among the control and the treated samples ($p < 0.05$). PBC of the control exceeded the acceptable marginal limit of 6.0 log CFU/g, reaching 6.8 log CFU/g at day 9, while the treated samples had the microbial load within the acceptable range. All the treated samples exceeded the limit at day 12 except the sample treated with 600 ppm BLEE-SED, which had PBC of 6.01 log CFU/g. The result signified the effectiveness of BLEE-SED at high concentration to retard the growth of psychrophilic bacteria.

Lower *Pseudomonas* count was found as the concentration of BLEE-SED increased ($p < 0.05$). Untreated samples (control) had the highest count at day 12 with the count of 8.2 log CFU/g. *Pseudomonas* count reached 7.9, 6.7, and 6.1 log CFU/g at day 12 when treated with 200, 400, and 600 ppm BLEE-SED, respectively. Although the count was augmented for the treated samples ($p < 0.05$), the increasing rate was lesser than that of the control ($p < 0.05$), suggesting the capability of the extract especially at an elevated concentration to reduce the proliferation rate. *Pseudomonas* sp. were closely connected to food spoilage incidents (Arfat *et al.*, 2015). They are known for their high survival rate in chilled temperatures, majorly causing food spoilage. Different plant extracts were used for retardation of *Pseudomonas* growth, thus avoiding their contribution to spoilage (Sterniša *et al.*, 2020).

Hydrogen sulfide (H_2S) producing bacteria count in all the samples increased up to 12 days. It was noted that the samples treated with BLEE-SED at higher concentration ($p < 0.05$) had the lower increasing rate for H_2S producing bacteria. At day 12, untreated samples had the highest count (7.8 log CFU/g) followed by samples treated with BLEE-SED at 200, 400 and 600 ppm having the counts of 7.2, 6.8, 6.2 log CFU/g, respectively. The result confirmed the effectiveness of BLEE-SED for retarding the growth of spoilage bacteria such as the H_2S producing bacteria which is known for its ability to breakdown amino acids like methionine and L-cysteine along with other proteins found in fish meat, thus producing the unpleasant odor of H_2S (Szabo, 2018).

The presence of *Enterobacteriaceae* was associated with inappropriate or unhygienic preparation and handling of fish (Klanian *et al.*, 2018). Although, low count of *Enterobacteriaceae* was detected, the growth could take place when favorable conditions for their growth became dominant. The control samples had an increase in *Enterobacteriaceae* count by 6.06 log CFU/g, while the counts were 5.2, 4.7, and 4.1 log CFU/g for 200, 400, and 600 ppm BLEE-SED treated samples, respectivley, at day 12. An initial count ranging from 2.6 to 3 log CFU/g was noticeable. This suggested the ability of BLEE-SED to inhibit *Enterobacteriaceae* growth in tilapia slices during storage.

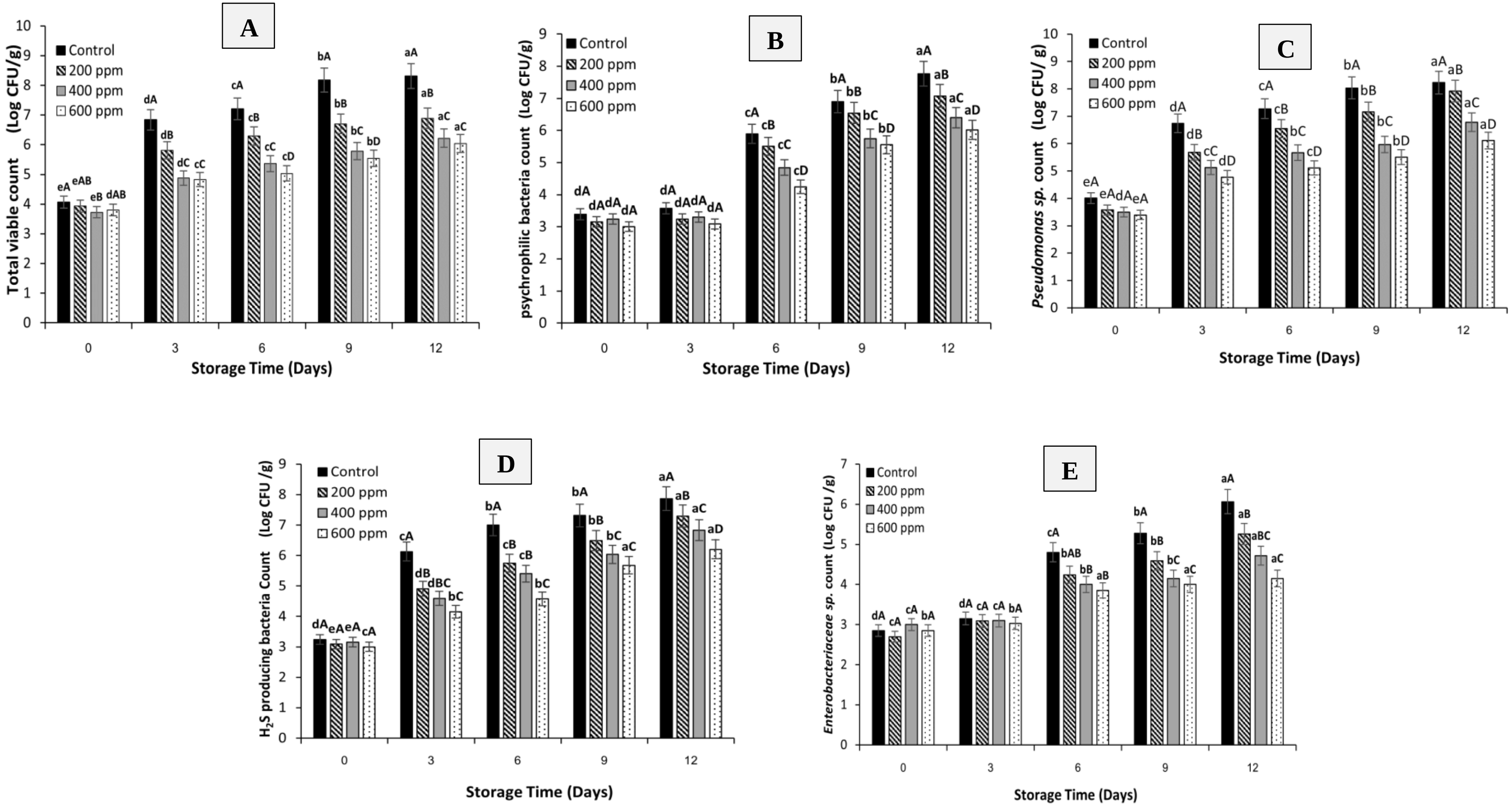

Figure 13. Total viable count (A), psychrophilic bacteria count (B), *Pseudomonas* sp. count (C), hydrogen sulfide producing bacteria count (D), and *Enterobacteriaceae* count (E) of Nile tilapia slices without and with the treatment by BLEE-SED at various concentrations during 12 days of storage at 4˚C. Bars represent standard deviation (n= 3). Different lowercase letters on bars within same treatment indicate significant difference ($p < 0.05$). Different uppercase letters on bars within the same storage time indicate significant difference ($p < 0.05$).

3.5.5.2. Changes in chemical characteristics

Total volatile base (TVB) content is an indicator for the quality of fish and fish products. The elevated TVB content reflects poor quality of fish as a consequence of spoilage, induced mainly by proliferation of microorganisms (Tacon, 2020). For the control and treated samples (Fig. 14A), TVB contents were in the range of 5.9 – 6.8 mg N/100g at day 0. At day 12, TVB content of the control was drastically increased and reached 62.8 mg N/100g ($p < 0.05$). TVB contents of the treated sample were also increased, however the increasing rate was lesser than the control ($p < 0.05$). After 12 days, samples treated with 200, 400, and 600 ppm BLEE-SED had TVB contents of 44.6, 30.5, and 22.3 mg N/100g, respectively. TVB content of 30 – 35 mg N/100g is considered as an accepted limit for fish freshness (Castro *et al.,* 2006). Therefore, treatment with BLEE-SED at 400 and 600 ppm could notably lower the formation of degradable products mediated by microorganisms.

During the storage, tilapia slices underwent lipid oxidation as ascertained by hydroperoxides formed (Fig. 14B). Untreated samples showed high PV as compared to the samples treated with BLEE-SED at high concentrations ($p < 0.05$) during storage. No difference ($p > 0.05$) between PVs of the control at days 9 and 12 of storage was noted, as it reached 7.88 and 7.83 mg cumene hydroperoxide/kg, respectively. This suggested that the formation of primary oxidation products was retarded, and decomposition occurred to a high extent. Similar observations were reported previously in fish slices treated with plant extracts (Olatunde *et al.,* 2019). Lower PVs were found in samples treated with 400 and 600 ppm BLEE-SED after 12 days of storage (6.68 and 6.48 mg cumene hydroperoxide/kg, respectively), while samples treated with 200 ppm BLEE-SED had similar PV to the control ($p > 0.05$). Thus, it can be concluded that BLEE-SED at 400 and 600 ppm could retard the auto-oxidation of fats in tilapia slices owing to its antioxidant activities.

At beginning of storage, TBARS values were in the range of 0.44 – 0.47 mg MDA/kg for the untreated and treated samples with BLEE-SED (Fig. 14C). TBARS are decomposition products of lipid peroxidation. Their formation is linked to high quantity of unsaturated fatty acids within samples, which underwent oxidation rapidly (Monserrat *et al.*, 2017).

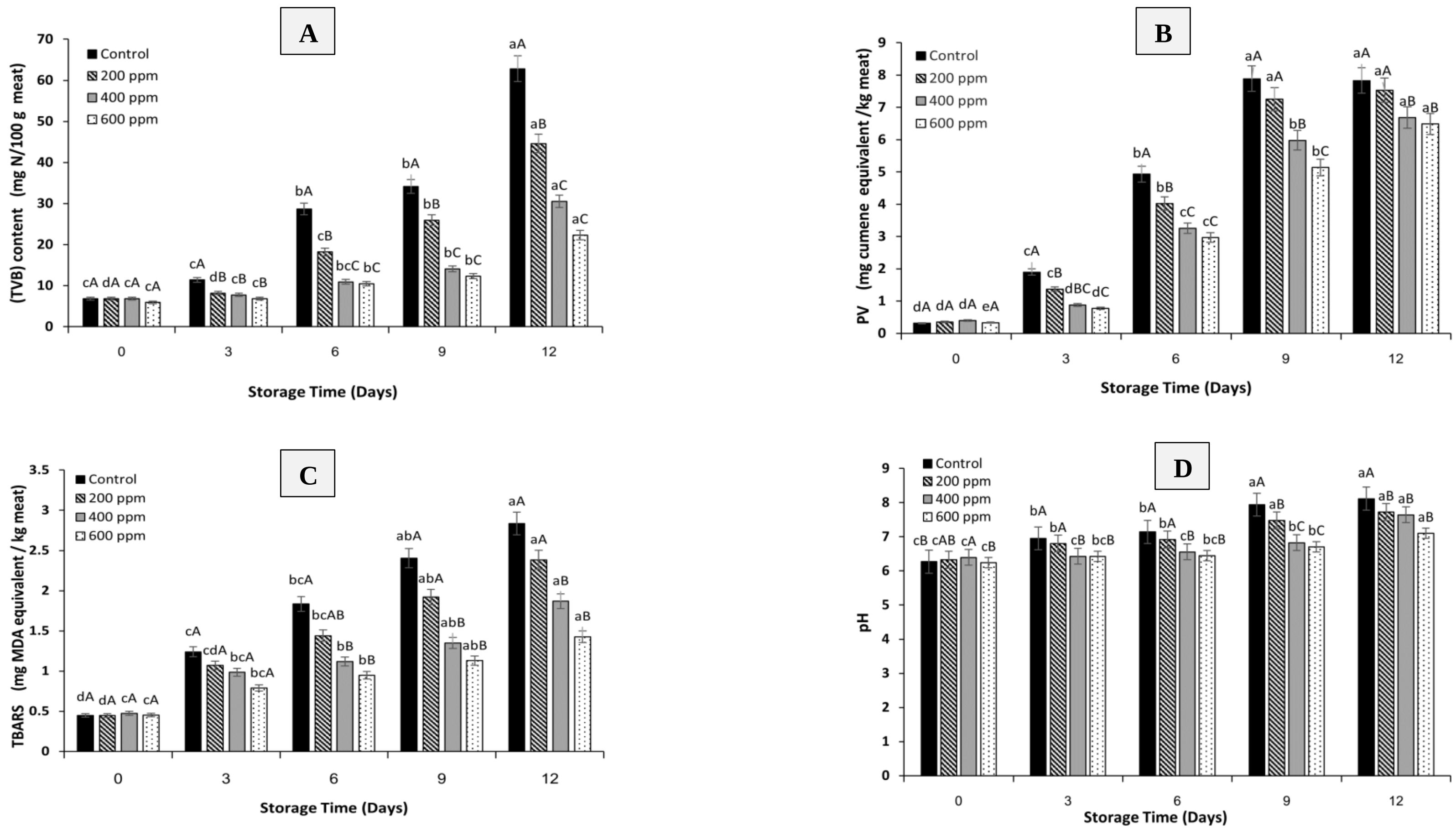

Figure 14. Total volatile base (TVB) content (A), peroxide value (PV) (B), thiobarbituric acid reactive substances (TBARS) (C), and pH (D) of Nile tilapia slices without and with the treatment by BLEE-SED at various concentrations during 12 days of storage at 4˚C. Bars represent standard deviation (n= 3). Different lowercase letters on bars within same treatments indicate significant difference ($p < 0.05$). Different uppercase letters on bars within the same storage time indicate significant difference ($p < 0.05$).

The presence of high microbial load could lead to enzymatic degradation, thus liberation of free fatty acids that are easily oxidized (Xu *et al*., 2018). The increasing rate of TBARS values was lesser in the treated samples than the control throughout storage ($p < 0.05$). At day 12, samples treated with BLEE-SED at 400 and 600 ppm had lower TBARS values (1.86 and 1.42 mg MDA/kg, respectively) than the control (2.83 mg MDA/kg). Treatment with 200 ppm BLEE-SED showed no difference in TBARS ($p > 0.05$) from the control (2.38 mg MDA/kg). Therefore, high oxidation of lipids induced by free radicals and enzymatic degradation mediated by microorganisms was retarded by the treatment of BLEE-SED at 400 or 600 ppm.

An increase in the pH was noted during storage of the control and the treated tilapia slices with BLEE-SED at different concentrations ($p < 0.05$). The increase in the pH could be related to the formation of basic compounds like ammonia and trimethylamine (TMA) as induced by proliferation of microorganisms during storage (Olatunde *et al.*, 2019). At day 0, the pH of the control and BLEE-SED treated samples was in the range of 6.2 – 6.3 ($p > 0.05$). At day 12, pH of the control increased rapidly to reach 8.1, while pH of samples treated with 600 ppm BLEE-SED was 7.1 which was slightly lower than those samples treated with 200 and 400 ppm BLEE-SED with pH of 7.72 and 7.64, respectively. The lower pH of the treated samples was in accordance with their lower TVB content and microbial load, affirming the ability of BLEE-SED to retard microbial proliferation associated with lower decomposition of the samples.

Based on the keeping quality of tilapia slices, BLEE-SED showed superior antioxidant and antibacterial properties to other extracts. That might be caused by the different types and contents of active components present in this extract. Recently, Tagrida and Benjakul (2020) found that compounds such as vitexin 4′-O-galactoside and isovitexin were the major components identified in betel leaf ethanolic extracts dechlorophyllized using sedimentation process. These compounds were reported to have antioxidant, antimicrobial and anticancer activities (Babaei *et al.,* 2020). Kaempferol derivatives, hydrocinnamic acid, citric acid and epigallocatechin were also detected. Those compounds are known for their high bioactivities including antimicrobial activity and can be used in several nutraceutical and pharmaceutical applications (Shen *et al.*, 2019).

3.6. Conclusion

Betel leaf ethanolic extract dechlorophyllized by sedimentation (BLEE-SED) showed superior antioxidant and antibacterial activities to other extracts dechlorophyllized using organic solvents. It had the lowest chlorophyll content and pale color. It was also rich in phenolic compounds, which led to higher antioxidant and antibacterial activities of BLEE-SED. Nile tilapia slices treated with BLEE-SED, especially at 400 and 600 ppm, had the retarded chemical changes as well as lowered microbial growth than the untreated samples during 12 days of storage at 4˚C, indicating the efficiency of BLEE-SED in lowering microbial proliferation during storage and reducing quality deterioration. Thus, BLEE-SED at 400 or 600 ppm could be used for shelf-life extension of Nile tilapia slices up to 9 days without any discoloration or change in taste. Moreover, BLEE-SED could be used as the natural antioxidant in foods rich in lipids, which are prone to the oxidation and as the natural preservative, which can be applied in perishable foods, such as shellfish, meat or poultry, etc., In addition, it could be applied in pharmaceutical industries, particularly nutraceutical or functional ingredients for health benefit in growing functional food market.

3.7. References

Arfat, Y. A., Benjakul, S., Vongkamjan, K., Sumpavapol, P., and Yarnpakdee, S. 2015. Shelf-life extension of refrigerated sea bass slices wrapped with fish protein isolate/fish skin gelatin-ZnO nanocomposite film incorporated with basil leaf essential oil. Journal of Food Science and Technology. 52(10): 6182 – 6193.

Babaei, F., Moafizad, A., Darvishvand, Z., Mirzababaei, M., Hosseinzadeh, H., and Nassiri-Asl, M. 2020. Review of the effects of vitexin in oxidative stress-related diseases. Food Science and Nutrition. 8(6): 2569 - 2580.

Benjakul, S., Kittiphattanabawon, P., Sumpavapol, P., and Maqsood, S. 2014. Antioxidant activities of lead (*Leucaena leucocephala*) seed as affected by extraction solvent, prior dechlorophyllisation and drying methods. *Journal of* Food Science and Technology. 51(11): 3026 – 3037.

Bono, G., Okpala, C. O. R., Vitale, S., Ferrantelli, V., Noto, A. Di, Costa, A., Di Bella, C., and Monaco, D. Lo. 2017. Effects of different ozonized slurry-ice treatments and superchilling storage (−1˚C) on microbial spoilage of two important pelagic fish species. Food Science and Nutrition. 5(6): 1049 – 1056.

Campanile, F., Bongiorno, D., Mongelli, G., Zanghì, G., and Stefani, S. 2019. Bactericidal activity of ceftobiprole combined with different antibiotics against selected Gram-positive isolates. Diagnostic Microbiology and Infectious Disease. 93(1): 77 – 81.

Castro, P., Padrón, J. C. P., Cansino, M. J. C., Velázquez, E. S., and Larriva, R. M. De. 2006. Total volatile base nitrogen and its use to assess freshness in European sea bass stored in ice. Food Control. 17(4): 245 – 248.

Chotphruethipong, L., Benjakul, S., and Kijroongrojana, K. 2017. Optimization of extraction of antioxidative phenolic compounds from cashew (*Anacardium occidentale* L.) leaves using response surface methodology. Journal of Food Biochemistry. 41(4): 1 – 10.

Chen, M. 2014. Chlorophyll modifications and their spectral extension in oxygenic photosynthesis. Annual Review of Biochemistry. 83(1): 317 – 340.

Cvetanović, A., Švarc-Gajić, J., Mašković, P., Savić, S., and Nikolić, L. 2015. Antioxidant and biological activity of chamomile extracts obtained by different techniques: Perspective of using superheated water for isolation of biologically active compounds. Industrial Crops and Products. 65(3): 582 – 591.

Dai, Y., Shen, Z., Liu, Y., Wang, L., Hannaway, D., and Lu, H. 2009. Effects of shade treatments on the photosynthetic capacity, chlorophyll fluorescence, and chlorophyll content of *Tetrastigma hemsleyanum Diels* et *Gilg*. Environmental and Experimental Botany. 65(2–3): 177 – 182.

Hassoun, A., and Emir Çoban, Ö. 2017. Essential oils for antimicrobial and antioxidant applications in fish and other seafood products. Trends in Food Science and Technology. 68(10): 26 – 36.

Kim, S. B., Bisson, J., Friesen, J. B., Pauli, G. F., and Simmler, C. 2020. Selective Chlorophyll Removal Method to “degreen” Botanical Extracts. Journal of Natural Products. 83(6): 1846 – 1858.

Klanian, M. G., Díaz, M. D., and Solís, M. J. S. 2018. Molecular characterization of histamine-producing psychrotrophic bacteria isolated from red octopus (*Octopus maya*) in refrigerated storage. High-Throughput. 7(3): 25.

Li, T., Xu, J., Wu, H., Wang, G., Dai, S., Fan, J., He, H., and Xiang, W. 2016. A saponification method for chlorophyll removal from microalgae biomass as oil feedstock. Marine Drugs. 14(9): 1 – 19.

Miazek, K., Kratky, L., Sulc, R., Jirout, T., Aguedo, M., Richel, A., and Goffin, D. 2017. Effect of organic solvents on microalgae growth, metabolism and industrial bioproduct extraction: A review. International Journal of Molecular Sciences. 18(7): 1429.

Monserrat, J. M., Seixas, A. L. R., Ferreira-Cravo, M., Bürguer-Mendonça, M., Garcia, S. C., Kaufmann, C. G., and Ventura-Lima, J. 2017. Interference of single walled carbon nanotubes (SWCNT) in the measurement of lipid peroxidation in aquatic organisms through TBARS assay. Ecotoxicology and Environmental Safety. 140(6): 103 – 108.

Neira, L. M., Agustinelli, S. P., Ruseckaite, R. A., and Martucci, J. F. 2019. Shelf life extension of refrigerated breaded hake medallions packed into active edible fish gelatin films. Packaging Technology and Science. 32(9): 471 – 480.

Odedina, G. F., Vongkamjan, K., and Voravuthikunchai, S. P. 2015. Potential bio-control agent from *Rhodomyrtus tomentosa* against *Listeria monocytogenes*. Nutrients. 7(9): 7451 – 7468.

Olatunde, O. O., Benjakul, S., and Vongkamjan, K. 2018. Antioxidant and antibacterial properties of guava leaf extracts as affected by solvents used for prior dechlorophyllization. Journal of Food Biochemistry. 42(5): 1 – 12.

Olatunde, O. O., Benjakul, S., and Vongkamjan, K. 2019. Coconut husk extract: antibacterial properties and its application for shelf-life extension of Asian sea bass slices. International Journal of Food Science and Technology. 54(3): 810 – 822.

Olatunde, O. O., Benjakul, S., and Vongkamjan, K. 2020. Microbial diversity, shelf-life and sensory properties of Asian sea bass slices with combined treatment of liposomal encapsulated ethanolic coconut husk extract and high voltage cold plasma. LWT- Food Science and Technology. 134(12): 1 – 10.

Olatunde, O. O., Della Tan, S. L., Shiekh, K. A., Benjakul, S., and Nirmal, N. P. 2021. Ethanolic guava leaf extracts with different chlorophyll removal processes: Anti-melanosis, antibacterial properties and the impact on qualities of Pacific white shrimp during refrigerated storage. Food Chemistry. 341(3): 128251.

Ruban, A. V. 2009. Plants in light. Communicative and Integrative Biology. 2(1): 50 – 55.

Salehi, B., Zakaria, Z. A., Gyawali, R., Ibrahim, S. A., Rajkovic, J., Shinwari, Z. K., Khan, T., Sharifi-Rad, J., Ozleyen, A., Turkdonmez, E., Valussi, M., Tumer, T. B., Fidalgo, L. M., Martorell, M., and Setzer, W. N. 2019. Piper species: A comprehensive review on their phytochemistry, biological activities and applications. Molecules. 24(7): 1364.

Shen, Y., Song, X., Li, L., Sun, J., Jaiswal, Y., Huang, J., Liu, C., Yang, W., Williams, L., Zhang, H., and Guan, Y. 2019. Protective effects of *p*-coumaric acid against oxidant and hyperlipidemia-an *in vitro* and *in vivo* evaluation. Biomedicine and Pharmacotherapy. 111(3): 579 – 587.

Shiekh, K. A., Benjakul, S., and Sae-leaw, T. 2019. Effect of Chamuang (*Garcinia cowa* Roxb.) leaf extract on inhibition of melanosis and quality changes of Pacific white shrimp during refrigerated storage. Food Chemistry. 270(1): 554 – 561.

Srisapoome, P., and Areechon, N. 2017. Efficacy of viable Bacillus pumilus isolated from farmed fish on immune responses and increased disease resistance in Nile tilapia (*Oreochromis niloticus*): Laboratory and on-farm trials. Fish and Shellfish Immunology. 67(8): 199 – 210.

Sterniša, M., Bucar, F., Kunert, O., and Smole Možina, S. 2020. Targeting fish spoilers *Pseudomonas* and *Shewanella* with oregano and nettle extracts. International Journal of Food Microbiology. 328(9): 1 – 8.

Szabo, C. 2018. A timeline of hydrogen sulfide (H_2S) research: From environmental toxin to biological mediator. Biochemical Pharmacology. 149(3): 5 – 19.

Tacon, A. G. J. 2020. Trends in Global Aquaculture and Aquafeed Production: 2000–2017. Reviews in Fisheries Science and Aquaculture. 28(1): 43 – 56.

Tagrida, M., and Benjakul, S. 2020. Ethanolic extract of Betel (*Piper betle* L.) and Chaphlu (*Piper sarmentosum* Roxb.) dechlorophyllized using sedimentation process: Production, characteristics, and antioxidant activities. Journal of Food Biochemistry. 44(12): e13508.

Tzima, K., Brunton, N. P., and Rai, D. K. 2020. Evaluation of the impact of chlorophyll removal techniques on polyphenols in rosemary and thyme by-products. Journal of Food Biochemistry. 44(3): e13148.

Udayan, A., Arumugam, M., and Pandey, A. 2017. Nutraceuticals From Algae and Cyanobacteria. Algal Green Chemistry. Recent Progress in Biotechnology. (11): 65 –89.

Xu, Y., Li, L., Mac Regenstein, J., Gao, P., Zang, J., Xia, W., and Jiang, Q. 2018. The contribution of autochthonous microflora on free fatty acids release and flavor development in low-salt fermented fish. Food Chemistry. 256(8): 259 – 267.

Yuniati, Y., Hasanah, N., Ismail, S., Anitasari, S., and Paramita, S. 2018. Antibacterial activity of dracontomelon dao extracts on methicillin-resistant *S. Aureus* (MRSA) and *E. Coli* multiple drug resistance (MDR). African Journal of Infectious Diseases, 12(1): 62 – 67.

CHAPTER 4

LIPOSOMES LOADED WITH BETEL LEAF (*PIPER BETLE* L.) ETHANOLIC EXTRACT PREPARED BY THIN FILM HYDRATION AND ETHANOL INJECTION METHODS: CHARACTERISTICS AND ANTIOXIDANT ACTIVITIES

4.1. Abstract

Betel leaf ethanolic extract (BLEE) dechlorophyllized by sedimentation process, was loaded in liposomes at 1 and 2% (w/v) concentrations using two different methods, namely thin film hydration (TF) and ethanol injection (EI) methods. Liposomes loaded with 1% BLEE and prepared by TF method (L/BLEE-T1) had the smallest particle size and paler color than L/BLEE-E1, L/BLEE-E2, and L/BLEE-T2 ($p < 0.05$). L/BLEE-T1 also showed strong stability as judged by its lowest zeta potential and polydispersity index. The highest encapsulation efficiency (EE) and lowest releasing efficiency (RE) were also found with L/BLEE-T1. No significant difference ($p > 0.05$) in the antioxidant activities was detected between the BLEE loaded liposomes and BLEE solutions, indicating that encapsulation had no adverse effect on the antioxidant potency. L/BLEE-T1 showed higher antioxidant stability than unencapsulated BLEE at the equivalent amount based on EE (U/BLEE-T1) during *in vitro* gastrointestinal tract digestion system. Therefore, L/BLEE-T1 could be an efficient delivery system for improving stability of antioxidant activities of BLEE.

4.2. Introduction

The rising awareness of hazards posed by synthetic food additives has driven food manufacturers to seek natural alternatives (Bouarab Chibane *et al.*, 2019). Plant extracts with high antioxidant properties have attracted attention as suitable candidates to be used as natural preservatives (Biesterbos *et al.*, 2019; Mohamed *et al.*, 2017). However, the antioxidant properties of these extracts are strongly attributed to their content and type of polyphenolic compounds (Guimarães *et al.*, 2014). Polyphenols are a diverse group of compounds, which include phenolic acids, flavonoids, and polyphenolic amides. Their amount, type and mode of action depend on the plant variety and extraction process used, in addition to other factors (Tsao, 2010).

Betel leaves (*Piper betle* L.) cultivated in Southeast Asian countries have been used for a long time as traditional medicine and as an ingredient in local cuisines (Rai *et al.*, 2011). Betel leaves have a strong aromatic smell, and several secondary metabolites were reported to have valuable biological activities including antioxidant, antibacterial, anti-inflammatory, and anticancer activities (Salehi *et al.*, 2019; Tan and Chan, 2014). Hydroxychavicol and eugenol were identified from the methanolic extracts of betel leaves and showed to have antibacterial activity (Syahidah *et al.*, 2017). LC/MS analysis of the dechlorophyllized betel leaf ethanolic extracts (BLEE) revealed that isovitexin and vitexin 4′-O-galactoside were the most abundant compounds (Tagrida and Benjakul, 2020). These compounds were documented to possess antimicrobial, anticancer, and antioxidant activities (Khole *et al.*, 2016). Therefore, betel leaf extract could be a promising natural preservative for food applications.

The effect of some polyphenolic compounds on their targeted sites may be hindered by inadequate solubility and poor stability in certain media, thus restricting the use of plant extracts in some applications (Chen *et al.*, 2019). Encapsulation is able to reduce the reactivity between the encapsulated active compounds and the surrounding medium in addition to controlling the release of active compounds to targeted sites (Madene *et al.*, 2006). Retardation of color changes and masking of undesirable flavors of the target compounds are important aspects of encapsulation techniques (Gortzi *et al.*, 2006). One of the commonly used encapsulation techniques is liposome entrapment. Liposomes are spherical vesicles, composed mostly of phospholipids prepared from natural resources, especially egg yolk, and soybean phospholipids (Taylor *et al.*, 2005). Liposomes have an amphiphilic characteristic along with beneficial properties including biocompatibility stability, and non-toxicity, which make them a suitable delivery agent for a variety of bioactive compounds that are compatible with a wide range of applications (Liu *et al.*, 2019).

Several methods have been employed for liposome formation, including mechanical dispersion methods such as thin film hydration, French pressure cell, and freeze-thawed technique. Solvent dispersion methods such as ethanol injection, ether injection, and double emulsion methods have also been used (Akbarzadeh *et al.*, 2013).

The choice of the proper method for liposomes preparation depends on several parameters such as physicochemical properties and concentrations of the compounds to be entrapped, nature of the dispersion medium, particle size and polydispersity of the liposomes, encapsulation efficiency, and target application of the resulting liposomes (Samad *et al.,* 2007). Thus, liposomes could be employed to entrap betel leaf ethanolic extract (BLEE) for enhanced stability, particularly after digestion.

This study, therefore, investigated the characteristics and antioxidant activities of liposomes prepared using thin film hydration and ethanol injection methods containing different concentrations of dechlorophyllized BLEE. Antioxidant activity of liposomes loaded with BLEE and subjected to *in vitro* gastrointestinal tract digestion system was also monitored.

4.3. Objective

To evaluate the antioxidative properties of betel ethanolic extract dechlorophyllized by sedimentation and encapsulated in liposome prepared by different methods.

4.4. Materials and methods

4.4.1. Chemicals

All chemicals used were of analytical grade. Ethanol was supplied by RCIlabscan Limited (Bangkok, Thailand). Soybean phosphatidylcholine was procured from Sigma Aldrich, Inc. (St. Louis, MO, USA). Cholesterol was purchased from Acros Organics (Fair lawn, NJ, USA). Tryptic soy broth was obtained from Difco Laboratories Inc. (Detroit, MI, USA). Other chemicals were procured from Sigma Aldrich, Inc. (St. Louis, MO, USA).

4.4.2. Preparation and dechlorophyllization of betel leaf ethanolic extracts (BLEE)

Mature healthy betel leaves were gathered from a garden near Songkhla province, Thailand. Leaves were transported to the laboratory for further processing. The method of Tagrida and Benjakul (2020) was adopted for the preparation of betel leaf powder. Extraction and chlorophyll removal from BLEE were carried out as tailored by Tagrida and Benjakul (2020). Ethanol (70%) was used as an extraction solvent at leaf powder/solvent ratio of 1:15 (w/v). The ethanolic extract was desolventized using a rotary evaporator and then dechlorophyllized using sedimentation, in which distilled water was added to the concentrated extract at a 1:1 ratio (v/v) and kept at 4˚C for 24 hr. After sedimentation, the extract was centrifuged for 30 min at 10,000 xg and 4˚C. The supernatant was collected, lyophilized as the BLEE and stored in a capped vial at -20˚C.

4.4.3. Preparation of BLEE loaded liposomes (L/BLEEs)

4.4.3.1. Ethanol injection method

The method described by Olatunde *et al.* (2020) was used for the preparation of L/BLEEs. Soybean phosphatidylcholine (SPC) and cholesterol (CHL) at a molar ratio of 4:1 was used as the lipid phase (LP). To the LP, ethanol (99%) was added to obtain a final LP concentration of 60 μmol/ml. The mixture was heated at 50˚C and stirred at 500 rpm on a magnetic heat stirrer until complete solubilization was achieved. BLEE was prepared at 1% and 2% (w/v) in distilled water as the aqueous phase (AQ) and heated at 37˚C in a water bath. Prepared LP solution was rapidly injected into the AQ through a fine needle (diameter of 1.6 mm) and the mixtures were stirred for 10 min at 50˚C and 500 rpm. Ethanol was removed using a rotary evaporator followed by nitrogen purging. The liposomal mixtures were then sonicated for 30 min using an ultrasonic bath to obtain uniform liposomes. The prepared liposomes were named as L/BLEE-E1 and L/BLEE-E2 for liposomes with 1% and 2% BLEE, respectively.

4.4.3.2. Thin film hydration method

The method described by Chotphruethipong *et al.* (2020) was followed for the preparation of L/BLEEs. The above formulation was used to make the LP solution. Subsequently, ethanol was evaporated using a rotary evaporator until the formation of film in the round bottom flasks took place. These flasks were kept in a desiccator for 12 hr for drying. Distilled water containing BLEE (AQ) at concentrations of 1% and 2% (w/v) was used to disperse the lipid films with vigorous agitation followed by sonication in an ultrasonic bath for 30 min. The resulting liposomes with 1% and 2% BLEE were termed as L/BLEE-T1 and L/BLEE-T2, respectively.

The resultant liposomes from both methods were separated into two portions, in which one part was lyophilized and stored at -20˚C.

4.4.4. Characterization of L/BLEEs prepared by different methods

4.4.4.1. Particle size, zeta potential, and poly-dispersity index (PDI)

Dynamic light scattering technique (Zeta potential analyzer, ZetaPALS, Brookhaven, Holtsville, NY, USA) was used for determination of particle size, zeta potential, and PDI of the liposomes at 25˚C. Sample preparation and instrument conditions were adapted from the method of Chotphruethipong *et al.* (2020).

4.4.4.2. Encapsulation efficiency (EE)

To determine EE of the resulting liposomes, the method described by Miere *et al.* (2021) was followed with minor modifications. Aliquots (1 mL) of the liposomes were subjected to disruption using 10% (v/v) triton X-100 (0.1 mL), followed by centrifugation at 10,000 x g and 4˚C for 20 min. The supernatant was collected and total phenolic content (TPC) of each prepared liposomes was determined according to the method of Benjakul *et al.* (2014). TPC of BLEE initially loaded into the liposomes was determined and EE was calculated as follows:

$$\text{EE (\%)} = \left(1 - \frac{\text{TPC}_{out}}{\text{TPC}_{initial}}\right) \times 100$$

where TPC_{out} is TPC of the supernatant obtained from the disruption of the liposomes and $\text{TPC}_{initial}$ is total TPC of BLEE initially loaded into the liposomes.

4.4.4.3. Color

The method of Tagrida and Benjakul (2020) was followed for measuring lightness (L^*), greenness/redness (a^*), and yellowness/blueness (b^*) of the prepared liposomes. A colorimeter (ColorFlex, Hunter Lab Reston, VA, USA) was used for the determination of the color attributes.

4.4.4.4. *In vitro* releasing efficiency (RE)

The dialysis method reported by Nounou *et al.* (2006) was adopted for evaluating RE of the prepared liposomes. Two milliliters of different liposomes (1 mg/mL) were pipetted into dialysis bags (2.5 × 7 cm^2, MW cut-off of 12 kDa) previously activated by immersing in 1 mM EDTA solution for 5 min, followed by boiling in distilled water. The bags were clamped and dialyzed against 200 mL of distilled water for 72 hr at 4˚C with continuous stirring (100 rpm). For control, 2 mL of 1% and 2% BLEE was placed separately in dialysis bags and subjected to dialysis under similar conditions used for the liposomes. Aliquots (2 mL) were taken from the dialysis solution of all the samples and the controls at 0, 2, 4, 8, 12, 24, 36, 48, 60, and 72 hr, and their TPC was determined. The following equation was used to calculate the *In vitro* RE at each interval:

$$\text{RE (\%)} = \left(1 - \frac{\text{TPC}_{released}}{\text{TPC}_{initial}}\right) \times 100$$

where $\text{TPC}_{released}$ is the TPC released from the liposomes at the given time, and $\text{TPC}_{initial}$ is the TPC of BLEE initially loaded to the each of the prepared liposomes. Results were presented as the average percentage of the release.

4.4.4.5. Antioxidant properties of liposomes

Prior to analysis, all the liposomal samples were subjected to disruption as described previously, using 10% (v/v) triton X-100. The resultant supernatant after centrifugation at 10,000 x g and 4˚C for 20 min. was used for the determination of antioxidant activity. Metal chelating activity (MCA) was determined following the method of Rattaya *et al.* (2014) and expressed as µmol EDTA equivalent (EE)/g solid. DPPH radical scavenging activity (DPPH-RSA), ABTS radical scavenging activity (ABTS-RSA), and ferric reducing antioxidant power (FRAP) were evaluated using the methods described by Benjakul *et al.* (2014). Oxygen radical absorbance capacity (ORAC) was measured as per the method of Sae-leaw *et al.* (2016). These activities were expressed as µmol Trolox equivalent (TE)/g solid. Unencapsulated BLEE was prepared at a concentration corresponding to that of encapsulated BLEE based on EE and used as the control.

4.4.5. *In vitro* gastrointestinal tract (GIT) digestion

Changes in the antioxidant activities of the selected liposome (L/BLEEs) based on EE, RE, and antioxidant activities in comparison with the equivalent free form (BLEE) were monitored by measuring DPPH-RSA and FRAP after being subjected to *in vitro* GIT digestion system. The GIT system was prepared according to the procedure of Brodkorb *et al.* (2019). To simulate oral phase, 500 mg of the samples was mixed with 35 mL of simulated salivary fluid (SSF) (KCl, 15.1 mM; KH_2PO_4, 3.7 mM; $NaHCO_3$, 13.6 mM; $MgCl_2$, 0.15 mM; $(NH_4)2CO_3$, 0.06 mM). Thereafter, 5 mL of heat stable α-amylase (10 mg/g solid sample) and 0.25 mL of $CaCl_2$ (0.3 M) were added. The volume of oral solution was made up to 50 mL by the addition of 9.75 ml distilled water to the mixture. This solution was incubated in a shaking water bath at 37˚C for 2 min after adjusting to pH 7.0 using 1 M NaOH.

For gastric phase simulation, 20 mL of the oral bolus was taken after oral phase incubation and mixed with 15 mL of simulated gastric fluid (SGF) (KCl, 6.9 mM; KH_2PO_4, 0.9 mM; $NaHCO_3$, 25 mM; NaCl, 47.2 mM; $MgCl_2$, 0.1 mM; $(NH_4)_2CO_3$, 0.5 mM). Subsequently, 3.2 mL of porcine pepsin solution (40 mg/g solid sample) was added to the mixture along with 10 μL of $CaCl_2$ (0.3 M). The gastric mixture was adjusted to pH 3.0 using 1 M HCl and the solution made up to 40 mL using distilled water. The vessels containing the gastric mixture were immediately incubated in a shaking water bath for 2 hr at 37˚C while maintaining at pH 3.0 with the addition of 1 M HCl during the digestion.

After gastric digestion, 20 mL of the gastric chyme was taken to initiate the intestinal digestion by mixing with 11 mL of simulated intestinal fluid (SIF) (KCl, 6.8 mM; KH_2PO_4, 0.8 mM; $NaHCO_3$, 85 mM; NaCl, 38.4 mM; $MgCl_2$, 0.33 mM) and then 5 mL of pancreatin solution (20 mg/g solid sample) was added along with 2.5 mL bile salts (160 mM) and 40 μL of $CaCl_2$ (0.3 M). The mixture was adjusted to pH 7.0 using 1 M NaOH and distilled water added to make up the volume to 40 mL. The solution was incubated at 37˚C for 2 hr in a shaking water bath with the mixture maintained at pH 7.0 using 1 M NaOH. Aliquots were taken before digestion, after oral phase and every 30 min during the digestion process. DPPH-RSA and FRAP of all these aliquots were determined.

4.4.6. Transmission electron microscopy (TEM)

Liposomes that showed the highest EE, antioxidant activity, and lowest RE were selected for visualization using transmission electron microscopy (TEM). Conditions and parameters of the visualization were adapted from the method of Zhao *et al.* (2017).

4.4.7. Statistical analysis

Completely randomized design (CRD) was applied for the whole study. All the experiments were conducted in triplicates (n = 3) and results are presented as mean ± standard deviation. One-way analysis of variance (ANOVA) and the Duncan's Multiple Range Test (DMRT) for mean comparison were performed. Analysis of data was done using SPSS package (SPSS 22.0 for Windows, SPSS Inc, Chicago, IL, USA) software.

4.5. Results and discussion

4.5.1. Characteristics of L/BLEEs prepared by different methods

4.5.1.1. Particle size, zeta potential, and polydispersity index (PDI)

Particle sizes of the liposomes were varied, depending on preparation methods and amount of BLEE loaded (Table 10). L/BLEE-T1 had the smallest particle size (195.8 nm), followed by L/BLEE-E1 (282 nm). L/BLEE-T2 and L/BLEE-E2 had the particle sizes of 387.8 and 450.7 nm, respectively. Liposomes prepared using thin film hydration method had lower particle size as compared to those prepared by ethanol injection method ($p < 0.05$), when the same amount of BLEE was used. Differences in particle size could be because of difference in phase transition temperature (T_m) between the liposomes prepared by various methods (Zhang, 2017). T_m is a very important parameter influencing encapsulation efficiency (EE) and storage stability of the liposomes. Liposomes containing 2% BLEE had a larger particle size ($p < 0.05$) when compared with those loaded with 1% BLEE, irrespective of preparation methods. Concentration of the bioactive compounds entrapped within the liposomes generally affects their particle size, which consequently impacts on encapsulation efficiency, releasing capacity, and stability. Chotphruethipong *et al.* (2020) found that different particle sizes of hydrolysate-loaded liposomes were associated with differences in the quantity of the entrapped hydrolysates. Liposomes loaded with 2% coconut husk extract had the largest particle size compared to those with a lower percentage of the loaded extract (Olatunde *et al.*, 2019).

All the obtained liposomes exhibited negative zeta potential (Table 10), indicating the negative charge on their surface. This could be mainly owed to the phosphate groups of the phosphatidylcholine, which possessed a negative charge. Regardless of the preparation method, liposomes that contained 1% BLEE had higher zeta potential as compared to those with 2% ($p < 0.05$). L/BLEE-T1 and L/BLEE-E1 had zeta potentials of -68.17 and -60.19 mV, respectively, while zeta potentials of -41.86 and -40.52 mV were attained for L/BLEE-T2 and L/BLEE-E2, respectively. Highly negative charges of liposomes were related to smaller particle size, which had higher surface area. Zeta potential is an indication of the physical stability of the liposomes. Liposomes are considered stable when their zeta potential is higher than 30 mV, regardless of charge (Jovanović *et al.,* 2018). Particle size appears to affect the charge distribution on liposome surfaces (Fröhlich, 2012). Since L/BLEE-T1 had the lowest particle size, this allowed the distribution or exposure of polar head of phospholipids to a higher extent. Increasing concentration of the BLEE to 2% augmented the particle size of the liposomes, thus lowering zeta potential. This could lessen the stability of liposomes. These findings are in line with Olatunde *et al.* (2019) who reported a lower zeta potential for liposomes containing 2% coconut husk extract in comparison with those loaded with a lower amount of the extract.

PDI is a measure of the heterogenicity of a sample based on its particle size. Non-harmonious size distribution of liposomes could occur after preparation as indicated by lower PDI (Danaei *et al.,* 2018). Among all the liposomes, L/BLEE-T1 possessed the lowest PDI (Table 10), suggesting the highest uniformity or homogeneity. The distribution of negative charges on the surface of the liposomes may have led to strong repulsions between the particles, thus lowering the possibilities of coagulation or collision of particles. As a result, a low PDI was observed in L/BLEE-T1. The particle size of the liposomes also played an important role in the uniform distribution of their surface charge, which is related to homogenous dispersion of liposomal vesicles in a medium. Increased BLEE concentration resulted in an enlarged particle size that led to an uneven distribution of charges on the surface of the liposomes along with the lower zeta potential. This more likely lowered the repulsive forces between the particles and increased the aggregation of liposomal vesicles, which eventually led to higher PDI in L/BLEE-T2 and L/BLEE-E2.

4.5.1.2. Encapsulation efficiency (EE)

EE is the percentage of successfully entrapped BLEE molecules in the liposomes relative to total unentrapped or free BLEE added to the encapsulation system. EE of the prepared liposomes varied from 58.5% to 79.86% ($p < 0.05$) (Table 10). L/BLEE-T1 had the highest EE (79.86%) than other liposomes ($p < 0.05$).

Table 10. Particle size, zeta potential, polydispersity index, encapsulation efficiency, and color of liposomes loaded with betel leaf ethanolic extract (BLEE) at different levels and prepared by different methods

Samples	Particle size (nm)	Zeta potential (mV)	Polydispersity Index (PDI)	Encapsulation Efficiency (EE) %	Lightness (*L**)	Redness/Greenness (*a**)	Yellowness/Blueness (*b**)
L/BLEE-E1	282.0 ± 3.2^{c}	-60.19 ± 1.33^{a}	0.21 ± 0.01^{ab}	71.79 ± 1.74^{b}	31.69 ± 0.04^{a}	0.28 ± 0.04^{a}	9.49 ± 0.03^{a}
L/BLEE-E2	450.7 ± 5.8^{a}	-40.52 ± 0.88^{b}	0.29 ± 0.05^{a}	58.50 ± 0.12^{d}	22.96 ± 0.10^{b}	0.19 ± 0.04^{bc}	6.88 ± 0.02^{c}
L/BLEE-T1	195.8 ± 0.5^{d}	-68.17 ± 1.12^{a}	0.17 ± 0.004^{b}	79.86 ± 1.84^{a}	31.92 ± 0.47^{a}	0.25 ± 0.30^{ab}	7.89 ± 0.59^{b}
L/BLEE-T2	387.8 ± 0.7^{b}	-41.86 ± 1.3^{b}	0.22 ± 0.019^{ab}	63.66 ± 1.30^{c}	22.70 ± 0.08^{b}	0.15 ± 0.11^{c}	5.47 ± 0.03^{d}
BLEE-1	NA	NA	NA	NA	7.35 ± 0.03^{c}	0.03 ± 0.02^{d}	-0.69 ± 0.04^{e}
BLEE-2	NA	NA	NA	NA	3.09 ± 0.14^{d}	-0.94 ± 0.08^{e}	-0.95 ± 0.07^{e}

Values are the mean ± standard deviation (n = 3). Different lowercase superscripts within the same column indicate significant difference ($p < 0.05$). L/BLEE-E1 and L/BLEE-E2 are liposomes loaded with BLEE at 1% and 2%, respectively, prepared by ethanol injection method. L/BLEE-T1 and L/BLEE-T2 are liposomes loaded with BLEE at 1% and 2%, respectively, prepared by thin film hydration method. BLEE-1 and BLEE-2 are free nonencapsulated BLEE at 1% and 2%, respectively.

NA: not applicable.

This could be related to its high stability with high negative charge and homogeneity as measured by zeta potential and PDI, respectively. L/BLEE-E1 showed EE of 71.79%. Liposomes with 2% BLEE had decreased EE for both preparation methods used. The augmented concentration of the extract enlarged their particle size, which eventually affected surface charge and ability to encapsulate BLEE in the core as indicated by lowered EE. Liposomes prepared using thin film hydration method were observed to have higher EE than those prepared using ethanol injection method. Ethanol removal after preparation of the liposomes might cause some disruption of bilayer wall, leading to the leakage of BLEE from the core. Evaporation process could also affect the integrity of liposome walls prepared by ethanol injection method, in which the vesicle structure is eventually compromised, resulting in a lower EE (Trucillo *et al.*, 2020).

4.5.1.3. Color

An improvement in color parameters was achieved when BLEE was loaded in liposomes as compared to the unencapsulated or free BLEE (Table 10). At the same amount of BLEE used, the preparation method had no influence on L* value ($p > 0.05$). However, an increased *L** value of the liposomes was found when compared with that of control. This may be due to the entrapment of BLEE in the liposomal vesicles, thus masking its color. Liposomes loaded with 1% BLEE showed a higher *L** value than those containing 2% BLEE. The *a** and *b** values were generally augmented in liposomes, mainly due to the yellow color of soy phosphatidylcholine localized in the wall of the liposomes (Olatunde *et al.*, 2019). Liposomes prepared by the thin film method had a lower *b** value than those prepared by ethanol injection method ($p < 0.05$). It is possible that oxidation might have taken place for the ethanol injection, particularly during injection, in which some oxygen could be incorporated, hence higher *b** value was obtained when compared with the thin film method. Nevertheless, no differences in *a** values were found between liposomes prepared with both methods when the same amount of BLEE was used. Overall, liposomes were yellowish in color but lighter than BLEE (free form).

4.5.1.4. *In vitro* releasing efficiency

Releasing efficiency (RE) of various liposomes with different formulations and the control (unentrapped 1% and 2% BLEE) is depicted in Fig. 15. Compared to the controls, BLEE release rate from the liposomes was much slower. The release profile of both 1% and 2% unentrapped BLEE showed an approximately 81% and 89% RE, respectively, after 8 hr of dialysis. Encapsulation of BLEE into liposomes greatly reduced RE, in which RE of 19%, 25%, 30%, and 38% were obtained for L/BLEE-T1, L/BLEE-E1, L/BLEE-T2, and L/BLEE-E2, respectively, within 8 hr. The liposomes containing 1% BLEE were observed to exhibit a lower release rate. Among all the liposome samples, L/BLEE-T1 showed the lowest release rate, in which RE of 48% was attained after 72 hr followed by L/BLEE-E1 (61%). The results confirmed that the difference in their release rates was mediated by preparation methods.

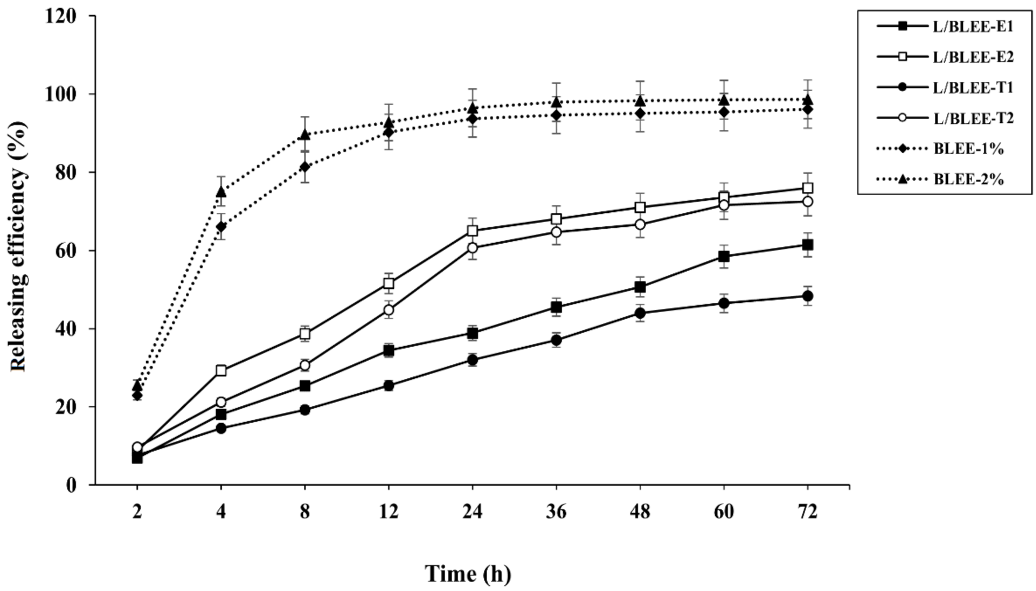

Figure 15. Release profiles of liposomes loaded with betel leaf ethanolic extract (BLEE) at different levels prepared using thin film hydration (L/BLEE-T1 and L/BLEE-T2) and ethanol injection (L/BLEE-E1 and L/BLEE-E2) methods in comparison with non-encapsulated BLEE at 1% and 2%, respectively, during a 72 hr dialysis period at 4˚C. Bars represent standard deviation (n = 3).

The lower release rate in liposomes containing 1% BLEE was in tandem with high EE, indicating that BLEE was entrapped, and the release occurred gradually. With augmented concentration of BLEE used for loading into liposomes, higher release rates were noted. Release profiles of the prepared liposomes were biphasic, as they showed a burst effect over time. This effect was relatively moderate for all the liposomes, but a lesser phenomenon was found in those containing 1% BLEE. Different liposomal types, lipid composition of their outer wall, and inclusion of cholesterol into the wall composition had a direct effect on the release rate of BLEE located in the core of liposomes. In general, phosphatidylcholine imparted a negative charge on the wall of the liposomes owing to the phosphate groups, thus increasing their stability, while lowering the release rate (Nounou *et al.,* 2006). It has been shown that controlled release is a highly favored property for encapsulated compounds (Olatunde *et al.,* 2019). Therefore, encapsulation of BLEE into liposomes drastically lowered diffusion rate and controlled their release through varied rates, depending on the amount of BLEE used and the manner of preparation.

4.5.1.5. Antioxidant properties of L/BLEEs prepared using different methods

Unencapsulated BLEE had similar antioxidant activities to the encapsulated counterpart ($p > 0.05$) (Table 11) since the amount corresponding to that entrapped in liposomes based on EE was used for determination. When comparing the amount of BLEE entrapped in liposomes, it was found that liposomes prepared by thin film method had higher BLEE amount than that of ethanol injection method. This indicated that not all the extract was fully loaded in the liposomal particles and the amount of BLEE loaded was varied, depending on the method used. However, the prepared liposomes could retain a considerable amount of the antioxidant activity of BLEE. Overall, liposomes prepared using the thin film method showed higher antioxidant activity, due to their higher EE, in which antioxidative compounds were loaded to a higher extent. Liposomes prepared by ethanol injection method had a lower antioxidant activity ($p < 0.05$).

Although liposomes containing 2% BLEE showed higher antioxidant activity due to the elevated concentration, EEs were lower and therefore, their free BLEE might undergo destruction caused by environment such as light, etc, which could later lead to decreases in activity. Free BLEE and all the liposomes loaded with BLEE showed DPPH-RSA, ABTS-RSA, MCA, and FRAP. This indicated that active compounds in BLEE had the ability to scavenge free radicals, both hydrophobic (DPPH) and amphiphilic (ABTS) (Benjakul *et al.,* 2014; Tagrida and Benjakul, 2021).

Table 11. Antioxidant activities of non-encapsulated betel leaf ethanolic extract (BLEE) and liposomes loaded with BLEE at different concentrations

		1%				2%			
		DPPH-RSA (µmol TE/g solid)	**ABTS-RSA (µmol TE/g solid)**	**FRAP (µmol TE/g solid)**	**MCA (µmol EDTA/g solid)**	**DPPH-RSA (µmol TE/g solid)**	**ABTS-RSA (µmol TE/g solid)**	**FRAP (µmol TE/g solid)**	**MCA (µmol EDTA/g solid)**
Ethanol injection	**U/BLEE**	73.43 ± 1.96^{b}	1737.4 ± 1.1^{b}	963.9 ± 6.9^{b}	176.8 ± 1.18^{b}	104.7 ± 1.61^{b}	2637.4 ± 8.8^{b}	1418.9 ± 2.0^{b}	269.7 ± 0.74^{b}
	L/BLEE	72.80 ± 2.05^{b}	1732.3 ± 2.7^{b}	958.1 ± 1.7^{b}	176.0 ± 0.34^{b}	102.9 ± 1.02^{b}	2634.8 ± 1.1^{b}	1412.8 ± 3.6^{b}	269.1 ± 0.70^{b}
Thin Film hydration	**U/BLEE**	80.91 ± 1.20^{a}	1989.7 ± 3.2^{a}	1066.1 ± 5.7^{a}	190.4 ± 0.26^{a}	112.8 ± 1.88^{a}	2953.3 ± 6.9^{a}	1565.1 ± 4.7^{a}	291.1 ± 0.38^{a}
	L/BLEE	79.80 ± 1.62^{a}	1983.3 ± 6.6^{a}	1061.1 ± 5.0^{a}	190.0 ± 1.74^{a}	110.2 ± 1.34^{a}	2947.4 ± 2.9^{a}	1562.6 ± 4.1^{a}	290.8 ± 0.32^{a}

Values are the mean ± standard deviation (n = 3). Different lowercase superscripts within the same column indicate significant difference ($p < 0.05$). L/BLEE: liposomes loaded with BLEE; U/BLEE: non-encapsulated BLEE with the equivalent amount to that present in the core (based on EE). DPPH-RSA: 2,2-diphenyl-1-picrylhydrazyl radical scavenging activity; ABTS-RSA: 2, 2'-Azino-bis-3-ethylbenzothiazoline-6-sulfonic acid radical scavenging activity; FRAP: Ferric reducing antioxidant power; MCA: Metal chelating activity.

Additionally, they could donate electrons to free radicals as determined by the FRAP assay. BLEE also exhibited metal chelating activity, which indicates binding or sequestering of metal ions, which are prooxidants in the lipid oxidation process. Similar findings were reported by Yuan *et al.* (2017) who found that hydroxytyrosol (HT) loaded liposomes had similar DPPH-RSA with free HT solution at the same concentration, indicating the ability of the resulted liposomes to retain DPPH-RSA via encapsulation. The results showed the ability of the prepared liposomes containing 1% and 2% BLEE to scavenge radicals as well as to reduce the ferric into ferrous ions and to chelate metals. Therefore, BLEE-loaded liposomes may be able to retard the oxidation process that take place in foods with high lipid contents.

These antioxidant abilities are probably because of the high content of polyphenols present in BLEE. LC/MS profile of a betel leaf ethanolic extract dechlorophyllized by sedimentation showed the presence of large amounts of polyphenolic compounds including vitexin 4′-O-galactoside and isovitexin (Tagrida and Benjakul, 2020). These two compounds were regarded as the major components in BLEE and were reported to have antioxidant, antimicrobial, and anticancer activities. Other compounds such as hydrocinnamic acid, citric acid, and kaempferol derivatives were also detected. These compounds are known for their high bioactivities including antioxidant and antimicrobial activities (Tagrida and Benjakul, 2020, 2021). ORAC fluorescence decay diagram of BLEE-loaded liposomes and their corresponding BLEE solution is shown in Fig 16. ORAC has been used to measure the antioxidant activity of bioactive compounds against the oxidative degradation of fluorescein when mixed with free radical generators such as the azo-initiators compounds (Sae-leaw *et al.,* 2016). The lowest decay of fluorescein was found in U/BLEE-T2, whereas the fastest decay was noted for L/BLEE-E1, U/BLEE-E1, and L/BLEE-T1. For liposomes loaded with 2% BLEE, those prepared by the thin film method (L/BLEE-T2) showed a lower rate of decay than those prepared via ethanol injection method. This was in accordance with the outcome of other antioxidant assays (Table 11). Since L/BLEE-T1 showed the highest EE with the lowest RE, it was selected to monitor the changes in antioxidant activities using a GIT digestion system and compared with free BLEE.

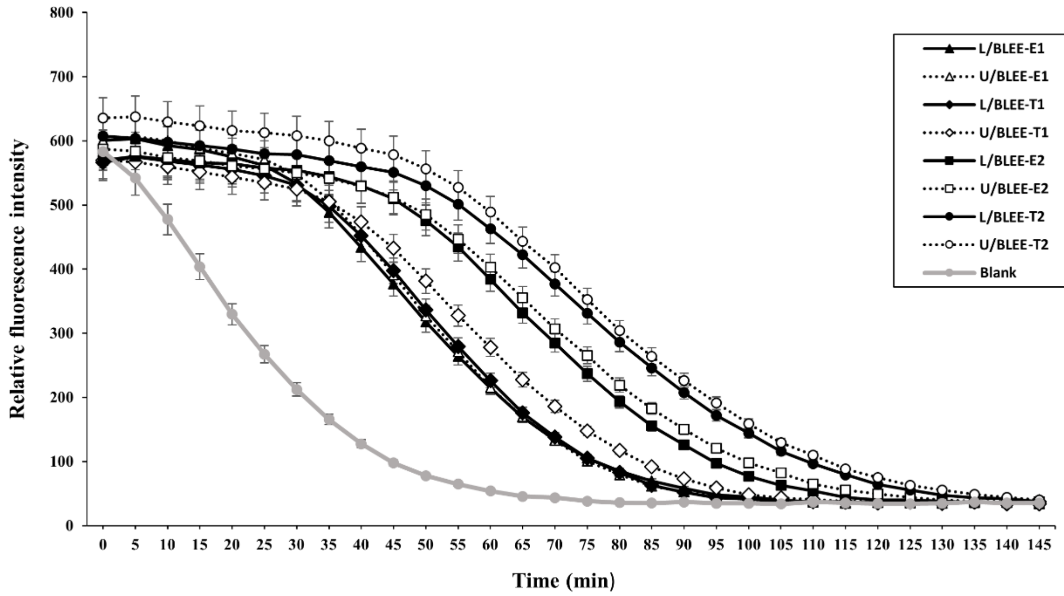

Figure 16. Fluorescence decay curves of L/BLEEs and non-encapsulated BLEE at a similar amount corresponding EE. Bars represent standard deviation (n = 3). L/BLEE-E1 and L/BLEE-E2: liposomes prepared by ethanol injection method containing 1% and 2% BLEE, and U/BLEE-E1 and U/BLEE-E2: 1% and 2% non-encapsulated BLEE with the equivalent amount based on EE, respectively. L/BLEE-T1 and L/BLEE-T2: liposomes prepared by thin film hydration method containing 1% and 2% BLEE and U/BLEE-T1 and U/BLEE-T2: 1% and 2% nonencapsulated BLEE with the equivalent amount based on EE, respectively.

4.5.2. Antioxidant activities of L/BLEE-T1 upon *in vitro* GIT digestion

A simulated GIT digestion system has been used to examine the stability and changes in the antioxidant activities of L/BLEE-T1 and free (non-encapsulated) BLEE (U/BLEE-T1) with the equivalent amount based on EE (Fig. 17). Such an *in vitro* system has been extensively employed because of their safety and speed. Also, ethical restrictions concerning the *in vivo* procedures can be avoided (Sae-leaw *et al.*, 2016). Antioxidant activities of the samples were monitored before and during the digestion process using DPPH-RSA and FRAP assays. No reduction ($p > 0.05$) in DPPH-RA was observed after oral phase for both samples (Fig. 17A). However, after 30 min of gastric digestion, U/BLEE-T1 exhibited a slight reduction ($p < 0.05$) in the DPPH-RSA, while L/BLEE-T1 remained unchanged ($p > 0.05$). After 60 min of gastric digestion, L/BLEE-T1 showed a slight increase ($p < 0.05$) in DPPH-RSA, which could be probably because of some release of BLEE after the partial rupture of the liposomal vesicles. U/BLEE-T1 had a continuous reduction ($p < 0.05$) in DPPH-RSA.

After 90 min of gastric digestion and until the end of the digestion process, both samples showed a continuous decrease in DPPH-RSA ($p < 0.05$). Nevertheless, encapsulation of BLEE using liposomes retarded the reduction rate in DPPH-RSA when compared with the non-encapsulated BLEE, which had a much higher reduction. A similar trend was noticeable with FRAP (Fig. 17B), in which no changes ($p > 0.05$) were observed after the oral phase or after 30 min of gastric digestion for both U/BLEE-T1 and L/BLEE-T1. An increase in FRAP ($p < 0.05$) was observed in L/BLEE-T1 after 60 min of gastric digestion. This increase was probably due to the release of some BLEE compounds having high FRAP, leading to the augmented activity. On the other hand, the activity of U/BLEE-T1 continued to sharply decrease ($p < 0.05$) until the end of gastric digestion period. Both samples had a marked decrease ($p < 0.05$) in FRAP activity after 90 min of gastrointestinal digestion onward until the end of the process. However, the reduction rate of L/BLEE-T1 was ($p < 0.05$) lower than that of U/BLEE-T1. The results confirmed that encapsulation of BLEE into liposomes maintained its activity and lowered the rate of loss of antioxidant activity during GIT digestion.

Changes in pH during the digestive process, especially at acidic pH, might have affected the stability of BLEE. Tagrida and Benjakul (2020) reported that variations in pH led to conformational changes in the phenolic constituents of the dechlorophyllized betel leaf ethanolic extract, which adversely affected their antioxidant activity. Also, the destruction of some phenolic compounds at 37˚C might occur after 4 hr, thus lowering antioxidant activity. When BLEE was loaded in liposome, lesser decomposition rate was observed, which may be due to ability of the phospholipids bilayer to protect the BLEE from the GIT environment. Similar findings were reported by Li *et al.* (2018) who found that curcumin-loaded liposomes with enhanced stability prevented the extract from interacting with the surroundings in a GIT simulation, thus reducing the degradation rate of the curcumin extract. Therefore, encapsulation of BLEE in liposomes prepared by thin film hydration method could maintain the antioxidant activity up to 60 min after gastric digestion and delayed the loss in antioxidant activity throughout the entire period of digestion.

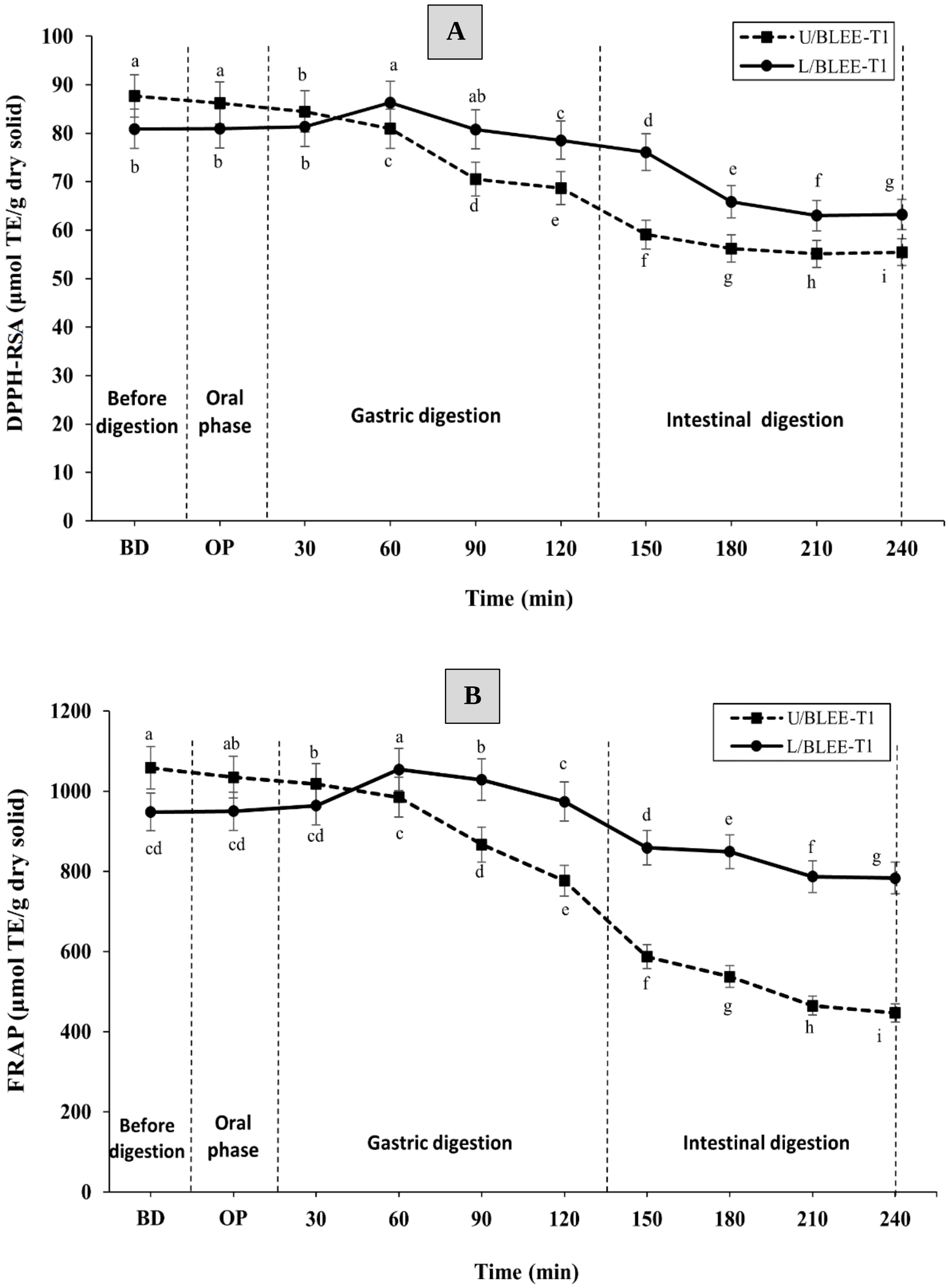

Figure 17. Changes in DPPH-RSA (A) and FRAP (B) of L/BLEE-T1) and U/BLEE-T1 at equivalent amount during *in vitro* gastrointestinal tract digestion (GIT). Bars represent standard deviation (n = 3). Different lowercase letters in each line indicate significant difference among the samples ($p < 0.05$).

4.5.3. Transmission electron microscopic (TEM)

When BLEE/L-T1 was visualized using TEM, the liposomal vesicles appeared to have a spherical morphology (Fig. 18). The image also showed that the liposomes could be classified as double bilayer vesicles (DBV) type. Double bilayer vesicles showed better controllable release and had higher stability when compared with other types of vesicles such as the uni-lamellar (ULV) and multi-lamellar (MLV) vesicles (Danaei *et al.,* 2018). The liposomes contained spherical dark particles in their cores, more likely representing the BLEE. Phospholipid molecules naturally form bilayers to minimize contact of their hydrophobic tails with the aqueous medium where they were dispersed. As a result, the tail is directed to an opposite side of the head, which interacts with the aqueous phase. With heat treatment, they form a bilayer structure (liposomes) to protect their hydrophobic end and during this process, active compounds present in the aqueous medium become trapped (Olatunde *et al.,* 2019). Therefore, BLEE was effectively encapsulated into liposomes of the DBV type, which were spherical in shape with high stability.

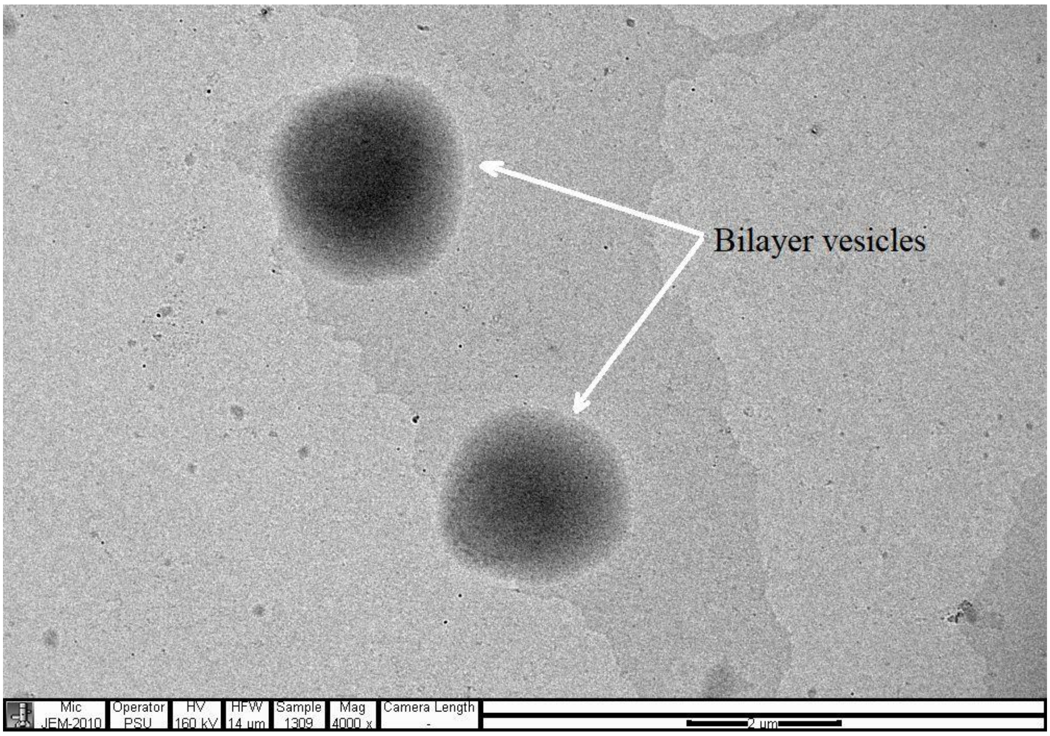

Figure 18. Transmission electron microscopic (TEM) image of 1% BLEE-loaded liposomes prepared by thin film hydration method (L/BLEE-T1).

4.6. Conclusion

The thin film hydration method could be adopted to produce liposomes with smaller particle sizes and paler color. Strong encapsulation efficiency with slow release, especially when liposomes were loaded with 1% BLEE, was achieved when compared with the 2% concentration. Encapsulation of BLEE in liposomes had no adverse effect on antioxidant activities, but to the contrary, it delayed the diffusion or release of the extract. The 1% BLEE-loaded liposomes prepared by thin film method showed higher ability in maintaining antioxidant activities when subjected to a GIT digestion system. Therefore, liposomes prepared by thin film hydration method loaded with 1% BLEE could be used as a vehicle in food applications for reducing the color and preserving the antioxidant activity of BLEE during processing or GIT digestion.

4.7. References

Akbarzadeh, A., Rezaei-Sadabady, R., Davaran, S., Joo, S. W., Zarghami, N., Hanifehpour, Y., Samiei, M., Kouhi, M., and Nejati-Koshki, K. 2013. Liposome: classification, preparation, and applications. Nanoscale Research Letters. 8(102): 433 - 442.

Benjakul, S., Kittiphattanabawon, P., Sumpavapol, P., and Maqsood, S. 2014. Antioxidant activities of lead (*Leucaena leucocephala*) seed as affected by extraction solvent, prior dechlorophyllisation and drying methods. Journal of Food Science and Technology. 51(11): 3026 – 3037.

Biesterbos, J. W. H., Sijm, D. T. H. M., van Dam, R., and Mol, H. G. J. 2019. A health risk for consumers: the presence of adulterated food supplements in the Netherlands. Food Additives and Contaminants - Part A Chemistry, Analysis, Control, Exposure and Risk Assessment. 36(9): 1273 – 1288.

Bouarab Chibane, L., Degraeve, P., Ferhout, H., Bouajila, J., and Oulahal, N. 2019. Plant antimicrobial polyphenols as potential natural food preservatives. Journal of the Science of Food and Agriculture. 99(4):1457 – 1474.

Brodkorb, A., Egger, L., Alminger, M., Alvito, P., Assunção, R., Ballance, S., Bohn, T., Bourlieu-Lacanal, C., Boutrou, R., Carrière, F., Clemente, A., Corredig, M., Dupont, D., Dufour, C., Edwards, C., Golding, M., Karakaya, S., Kirkhus, B., Le

Feunteun, S., and Recio, I. 2019. INFOGEST static *in vitro* simulation of gastrointestinal food digestion. Nature Protocols. 14(4): 991 – 1014.

Chen, L., Gnanaraj, C., Arulselvan, P., El-Seedi, H., and Teng, H. 2019. A review on advanced microencapsulation technology to enhance bioavailability of phenolic compounds: Based on its activity in the treatment of Type 2 Diabetes. Trends in Food Science and Technology. 85:149 – 162.

Chotphruethipong, L., Battino, M., and Benjakul, S. 2020. Effect of stabilizing agents on characteristics, antioxidant activities and stability of liposome loaded with hydrolyzed collagen from defatted Asian sea bass skin. Food Chemistry. 328: 127127.

Danaei, M., Dehghankhold, M., Ataei, S., Hasanzadeh Davarani, F., Javanmard, R., Dokhani, A., Khorasani, S., and Mozafari, M. R. 2018. Impact of particle size and polydispersity index on the clinical applications of lipidic nanocarrier systems. Pharmaceutics. 10(2): 57.

Fröhlich, E. 2012. The role of surface charge in cellular uptake and cytotoxicity of medical nanoparticles. International Journal of Nanomedicine. 7: 5577 – 5591.

Gortzi, O., Lalas, S., Chinou, I., and Tsaknis, J. 2006. Reevaluation of antimicrobial and antioxidant activity of *Thymus* spp. extracts before and after encapsulation in liposomes. Journal of Food Protection. 69(12): 2998 – 3005.

Guimarães, R., Barros, L., Calhelha, R. C., Carvalho, A. M., Queiroz, M. J. R. P., and Ferreira, I. C. F. R. 2014. Bioactivity of different enriched phenolic extracts of wild fruits from northeastern Portugal: A comparative study. Plant Foods for Human Nutrition. 69(1): 37 – 42.

Jovanović, A. A., Balanč, B. D., Ota, A., Ahlin Grabnar, P., Djordjević, V. B., Šavikin, K. P., Bugarski, B. M., Nedović, V. A., and Poklar Ulrih, N. 2018. Comparative effects of cholesterol and β-sitosterol on the liposome membrane characteristics. European Journal of Lipid Science and Technology. 120(9): 1800039.

Khole, S., A Panat, N., Suryawanshi, P., Chatterjee, S., Devasagayam, T., and Ghaskadbi, S. 2016. Comprehensive assessment of antioxidant activities of apigenin isomers: Vitexin and Isovitexin. Free Radicals and Antioxidants. 6(2): 155 – 166.

Li, Z. ling, Peng, S. feng, Chen, X., Zhu, Y. qing, Zou, L. qiang, Liu, W., and Liu, C.

mei. 2018. Pluronics modified liposomes for curcumin encapsulation: Sustained release, stability and bioaccessibility. Food Research International. 108: 246 - 253.

Liu, W., Ye, A., Han, F., and Han, J. 2019. Advances and challenges in liposome digestion: Surface interaction, biological fate, and GIT modeling. Advances in Colloid and Interface Science. 263: 52 – 67.

Madene, A., Jacquot, M., Scher, J., and Desobry, S. 2006. Flavour encapsulation and controlled release - A review. International Journal of Food Science and Technology. 41(1): 1 – 21.

Mohamed, M. S., Khalil, M. S., Tagrida, M. A. and Mawgoud, Y. A. 2017. Purification of gelatinase from the bacteria contaminating gelatin production process. Research Journal of Pharmaceutical Biological and Chemical Sciences. 8: 914 - 930.

Miere, F., Vicas, S. I., Timar, A. V., Ganea, M., Zdrinca, M., Cavalu, S., and Pallag, A. 2021. Preparation and characterization of two different liposomal formulations with bioactive natural extract for multiple applications. Processes. 9(3): 432.

Nounou, M. M., El-Khordagui, L. K., Khalafallah, N. A., and Khalil, S. A. 2006. *In vitro* release of hydrophilic and hydrophobic drugs from liposomal dispersions and gels. Acta Pharmaceutica. 56(3): 311 – 324.

Olatunde, O. O., Benjakul, S., Vongkamjan, K., and Amnuaikit, T. 2019. Liposomal encapsulated ethanolic coconut husk extract: Antioxidant and antibacterial properties. Journal of Food Science. 84(12): 3664 – 3673.

Olatunde, O. O., Benjakul, S., Vongkamjan, K., and Amnuaikit, T. 2020. Influence of stabilising agents on the properties of liposomal encapsulated ethanolic coconut husk extract. International Journal of Food Science and Technology. 55(2): 702 – 711.

Rai, M. P., Thilakchand, K. R., Palatty, P. L., Rao, P., Rao, S., Bhat, H. P., and Baliga, M. S. 2011. *Piper betel* Linn (betel vine), the maligned southeast asian medicinal plant possesses cancer preventive effects: Time to reconsider the wronged opinion. Asian Pacific Journal of Cancer Prevention. 12(9): 2149 – 2156.

Rattaya, S., Benjakul, S., and Prodpran, T. 2014. Extraction, antioxidative, and antimicrobial activities of brown seaweed extracts, *Turbinaria ornata* and *Sargassum polycystum*, grown in Thailand. International Aquatic Research. 7(1): 1–16.

Sae-leaw, T., O'Callaghan, Y. C., Benjakul, S., and O'Brien, N. M. 2016. Antioxidant activities and selected characteristics of gelatin hydrolysates from seabass (*Lates calcarifer*) skin as affected by production processes. Journal of Food Science and Technology. 53(1): 197 – 208.

Salehi, B., Zakaria, Z. A., Gyawali, R., Ibrahim, S. A., Rajkovic, J., Shinwari, Z. K., Khan, T., Sharifi-Rad, J., Ozleyen, A., Turkdonmez, E., Valussi, M., Tumer, T. B., Fidalgo, L. M., Martorell, M., and Setzer, W. N. 2019. *Piper* species: A comprehensive review on their phytochemistry, biological activities and applications. Molecules. 24(7): 1364.

Samad, A., Sultana, Y., and Aqil, M. 2007. Liposomal drug delivery systems: An update review. Current Drug Delivery. 4(4): 297 – 305.

Syahidah, A., Saad, C. R., Hassan, M. D., Rukayadi, Y., Norazian, M. H., and Kamarudin, M. S. 2017. Phytochemical analysis, identification and quantification of antibacterial active compounds in betel leaves, *piper betle* methanolic extract. Pakistan Journal of Biological Sciences. 20(2): 70 – 81.

Tagrida, M., and Benjakul, S. 2020. Ethanolic extract of betel (*Piper betle* L.) and Chaphlu (*Piper sarmentosum* Roxb.) dechlorophyllized using sedimentation process: Production, characteristics, and antioxidant activities. Journal of Food Biochemistry. 44(12): e13508.

Tagrida, M., and Benjakul, S. 2021. Betel (*Piper betle* L.) leaf ethanolic extracts dechlorophyllized using different methods: antioxidant and antibacterial activities, and application for shelf-life extension of Nile tilapia (*Oreochromis niloticus*) fillets. RSC Advances. 11(29): 17630 - 17641.

Tan, Y. P., and Chan, E. W. C. 2014. Antioxidant, antityrosinase and antibacterial properties of fresh and processed leaves of *Anacardium occidentale* and *Piper betle*. Food Bioscience. 6(6): 17 – 23.

Taylor, T. M., Davidson, P. M., Bruce, B. D., and Weiss, J. 2005. Liposomal nanocapsules in food science and agriculture. Critical Reviews in Food Science and Nutrition. 45(7–8): 587 – 605.

Trucillo, P., Campardelli, R., and Reverchon, E. 2020. Liposomes: From bangham to supercritical fluids. Processes. 8(9):332 - 341.

Tsao, R. 2010. Chemistry and biochemistry of dietary polyphenols. Nutrients 2(12): 1231 – 1246.

Yuan, J. J., Qin, F. G. F., Tu, J. L., and Li, B. 2017. Preparation, characterization, and antioxidant activity evaluation of liposomes containing water-soluble hydroxytyrosol from olive. Molecules. 22(6): 870 .

Zhang, H. 2017. Thin-film hydration followed by extrusion method for liposome preparation. Methods in Molecular Biology. 1522: 17 – 22.

Zhao, L., Temelli, F., Curtis, J. M., and Chen, L. 2017. Encapsulation of lutein in liposomes using supercritical carbon dioxide. Food Research International. 100: 168 – 179.

CHAPTER 5

LIPOSOMES LOADED WITH BETEL LEAF (*PIPER BETLE* L.) EXTRACT: ANTIBACTERIAL ACTIVITY AND PRESERVATIVE EFFECT IN COMBINATION WITH HURDLE TECHNOLOGIES ON TILAPIA SLICES

5.1. Abstract

Betel (*Piper betle* L.) leaf ethanolic extract (BLEE) has shown to possess antibacterial activities. However, the use of BLEE is still limited due to the instability and remaining chlorophylls even after dechlorophyllization. Encapsulation using liposomes might enhance its stability and reduce the color of BLEE, but antibacterial properties of liposomes have not been elucidated. Hence, this study was conducted to determine the antibacterial activity of liposome loaded with BLEE (L/BLEE). Microbial challenge tests using the selected bacteria (*Staphylococcus aureus*, *Escherichia coli*, *Pseudomonas aeruginosa*, and *Shigella sonnei*) were also conducted to evaluate the preservative properties of L/BLEE at different concentrations combined with modified atmosphere packaging (MAP) and non-thermal plasma (NTP) treatment on tilapia slices stored at 4˚C. Antibacterial activity of BLEE was enhanced ($p < 0.05$) after loading into liposomes, as witnessed by lower ($p < 0.05$) MIC and MBC than those of the unencapsulated BLEE. L/BLEE also showed larger inhibition zones, lower triphenyl-2H tetrazolium chloride (TTC) dehydrogenase activity, and higher release rates of K^+ and Mg^{2+} ions ($p < 0.05$) of bacteria. Additionally, scanning electron microscopic (SEM) images showed deformations and perforation on cell walls of bacteria after treatment with L/BLEE. L/BLEE at 400 ppm combined with MAP (CO_2: Ar: O_2 = 60: 30: 10) and NTP (80 KV-RMS for 5 min) exhibited the highest inhibition effect ($p < 0.05$) toward all the challenged bacteria over 15 days of storage at 4˚C. The use of L/BLEE at 400 ppm combined with MAP and NTP treatments could preserve tilapia slices for up to 12 days.

5.2. Introduction

Fish having high contents of proteins, polyunsaturated fatty acids, and other components undergo rapid deterioration as induced mostly by spoilage microorganisms. One of the most cultivated and consumed fish in Asia due to its high nutritional value is Nile tilapia (*Oreochromis niloticus*). The presence of high protein (15 – 20%) with low fat (1 – 4%) contents make tilapia very popular for consumers (Srisapoome and Areechon, 2017). Also, tilapia is known for its rapid growth, usage of different feeds, and adaptation in diverse environmental conditions, making it a profitable fish for the producers (Yuasa *et al.,* 2008). Despite COVID-19 pandemic, Asian production of tilapia was estimated to be around 4.55 million tons in 2020 (FAO, 2020). In Thailand, the production was more than 210,000 tons in 2016 with expectations of continuous growth (Wijitpun *et al.,* 2021).

Increasing numbers of consumers have sought out easy-to-cook fish products. For this purpose, tilapia has been introduced to the markets as fillets or slices rather than the whole fish (Watanabe *et al.,* 2002). To avoid spoilage of such products, synthetic preservatives have been used (Albertos *et al.,* 2019). However, excessive usage will lead to the accumulation of such chemicals in fish, lowering the acceptability of the fish owing to safety concerns (Bouarab-Chibane *et al.,* 2019). Additionally, the increased resistance of microorganisms against these preservatives has been taken in consideration. To alleviate the problem, food manufacturers have sought for natural effective alternatives for preserving fish.

Plant extracts with valuable bioactivities have drawn the attention as possible natural alternatives to synthetic preservatives (Carocho *et al.,* 2015). Betel leaves (*Piper betle* L.), cultivated in Southeastern Asian countries, were frequently used in traditional medicine owing to their copious content of different polyphenols that exhibit bioactivities such as antioxidant and antimicrobial activities (Salehi *et al.,* 2019). Therefore, betel leaf extract could be used to substitute synthetic or chemical preservatives for fish (Tagrida and Benjakul, 2020). However, due to the green color of leaf extract caused by chlorophyll, the removal of chlorophyll could lower the greenness. Sedimentation is a green process used for chlorophyll removal from the ethanolic extract of betel leaves (Tagrida and Benjakul, 2021). Nevertheless, some components as well as remaining chlorophylls could bring about the lowered acceptability of treated fish or other foods, thus restricting its use as a preservative.

These obstacles could be conquered using liposomes, which are spherical vesicles with amphiphilic characteristic that are composed of phospholipids bilayer (Liu *et al.,* 2019). Liposomes can reduce the reactivity between the encapsulated active compounds and the surroundings. Moreover, they could minimize the color and mask any undesirable flavors of the active compound known as 'core'. In addition, liposomes can maintain the sensorial attributes of treated food products at satisfactory levels (Kamkar *et al.,* 2021; Tagrida *et al.,* 2021b; Tometri *et al.*, 2020). Additionally, liposomes are known for their stability and non-toxicity, making them become a potential vesicle for a variety of bioactive compounds or plant extracts (Gortzi *et al.,* 2006).

Non-thermal technologies including non-thermal plasma, irradiation, and pulsed electric field have been applied for shelf-life extension of several food products (Bourke *et al.*, 2018). Non-thermal plasma (NTP) has been demonstrated to have promising impact in maintaining the quality of many foods including fish owing to its antibacterial activity with minimum or no adverse changes in the nature of the food products (Gavahian *et al.,* 2018). NTP is generated when the gases within the food containers are ionized by high electric field, thus inducing the formation of several reactive species (RS) such as reactive oxygen radials, excited molecules, and ions, which can inhibit bacterial growth (Zhao *et al.*, 2019). Lipid oxidation may be induced by NTP, hence the usage of betel leaf extract, which can scavenge the excessive RS and lower the induced oxidation. Usually, air is involved for the generation of NTP, however for better exploitation of plasma, appropriate mixture of gases has been used. Also modified atmospheric packaging (MAP), in which the ratio of gases is altered from atmospheric gas, can contribute to retardation of bacterial growth, thus prolonging the shelf-life of products (Olatunde *et al.*, 2020). MAP can prevent the re-proliferation of microorganisms when RS disappear due to their short half-life.

The current study aimed to investigate antibacterial activity of liposomes loaded with betel leaf ethanolic extract dechlorophyllized by sedimentation (L/BLEEs) compared with unencapsulated betel extract at equivalent amount (U/BLEE). In addition, the preservative efficiency of L/BLEEs on refrigerated tilapia slices coupled with MAP and NTP treatments using microbiological challenge test was also investigated.

5.3. Objectives

To evaluate the antimicrobial properties of betel ethanolic extract dechlorophyllized by sedimentation and encapsulated in liposome.

To determine the preservative effect of liposomes loaded with betel ethanolic extract using microbiological challenge test.

5.4. Materials and methods

5.4.1. Chemicals

All chemicals were of analytical grade. Soybean phosphatidylcholine, cholesterol, and resazurin sodium salt were procured from Sigma Aldrich, Inc. (St. Louis, MO, USA). Triphenyl-2H tetrazolium chloride was purchased from AppliChem (Darmstadt, Germany). All microbial media were obtained from Oxoid (Hampshire, England).

5.4.2. Preparation of betel leaf ethanolic extracts (BLEE) and BLEE loaded liposome (L/BLEE)

Extraction and dechlorophyllization of BLEE were carried out as tailored by Tagrida and Benjakul (2020). 70% ethanol was used as the solvent for extraction, in which a leaf powder/solvent ratio of 1:15 (w/v) was selected. After solvent removal by a rotary evaporator, the concentrated extract was dechlorophyllized by sedimentation method. Dechlorophyllized extract was used for liposomes preparation, following thin film hydration method as described by Tagrida *et al.* (2021b). The resulting liposomes containing 1% BLEE (L/BLEE) had particle size, polydispersity, and zeta potential of 196 nm, 0.170, and -68.1 mV, respectively as determined by the methods of Tagrida *et al.* (2021b). The encapsulation efficiency (EE) of the prepared liposomes was found to be 79.8%, while the releasing efficiency (RE) after 8 h of dialysis was 19%. The color attributes of the liposomes were improved, in which lightness (L^*), redness/greenness (a^*), and yellowness/blueness (b^*) were 31.9, 0.251, and 7.89, respectively, while the corresponding attributes of unencapsulated BLEE with concentration at 1% were 7.35, 0.0301, and -0.692, respectively. L/BLEEs were then freeze-dried, transferred into aluminum foil bag, sealed, and stored at 4˚C until use.

5.4.3. Antibacterial activity of L/BLEE

5.4.3.1. Bacterial strains, culture conditions and cell suspension

The bacteria used in this study were *Pseudomonas aeruginosa* PSU.SCB.16S.12, *Escherichia coli* PSU.SCB.16S.22, *Staphylococcus aureus* PSU.SCB.16S.41, and *Shigella sonnei* PSU.SCB.16S.33, gifted from Food Safety Laboratory, Faculty of Agro-Industry, Prince of Songkla University. Each culture was separately grown for 24 h in tryptic soy broth (TSB). Thereafter, the bacterial cells were suspended in fresh TSB and incubated at 37˚C for 4 h. Bacterial suspensions were serially diluted to obtain 10^8 CFU/mL (0.5 McFarland standard).

5.4.3.2. Minimum inhibitory concentration (MIC) and minimum bactericidal concentration (MBC)

For the determination of MIC and MBC, the method of Tagrida and Benjakul (2021) was adopted. L/BLEEs and U/BLEE were serially diluted (50.0 – 0.0977 mg equivalent of BLEE/mL) in a sterile 96-well microplate. The wells were then inoculated with 100 μL of bacterial solution (10^6 CFU/mL) and incubated for 24 h at 37˚C. MIC was reported as the lowest concentration that completely inhibited bacterial growth and was confirmed by testing with resazurin solution (2 mM, 50 μL) after incubation for 1 – 2 h at 37˚C. MBC was defined as the lowest concentration that completely killed the bacterial isolates and determined by using spot plate technique, in which 10 μL of aliquots from wells having no apparent bacterial growth without the addition of resazurin solution, were seeded on tryptic soy agar (TSA) plates.

5.4.3.3. Well diffusion method

Antibacterial activity of L/BLEEs compared to U/BLEE was evaluated by well diffusion method (Jayeoye *et al.*, 2020) against S. aureus, E. coli, *P. aeruginosa*, and *S. sonnei*. Bacterial suspensions previously cultured in TSB for 24 h at 37˚C were diluted and adjusted to 10^6 CFU/mL before use. These bacterial suspensions (100 μL) were inoculated and spread on TSA plates. Wells (diameter: 6 mm) were then made by a cork borer and filled with L/BLEEs and U/BLEE solutions at 2 MIC. Sterile distilled water was served as negative control.

5.4.3.4. Triphenyl-2H tetrazolium chloride (TTC) dehydrogenase activity

Living bacterial cells are known for their ability to produce TTC dehydrogenase, which could be used as an indication of cell viability. TTC dehydrogenase activity of bacterial cells treated without (control) and with L/BLEEs or U/BLEE at 2 MIC was determined following the method of Olatunde *et al.* (2019a). Absorbance was recorded at 510 nm and the TTC dehydrogenase relative activity (TRA) was calculated using the following equation:

$$\text{TRA (\%)} = \frac{A_T}{A_U} \times 100$$

where AT and AU are the absorbance of the treated and untreated bacterial cells, respectively.

5.4.3.5. Potassium (K^+) and magnesium (Mg^{2+}) ions leakage

The method of Jayeoye *et al.* (2020) was adopted to study the effect of L/BLEEs and U/BLEE on the cell membranes of the selected bacterial by measuring K^+ and Mg^{2+} contents released from the bacterial cells after treatment with L/BLEEs and U/BLEE at 2 MIC. K^+ and Mg^{2+} contents were measured using inductively coupled plasma optical emission spectroscopy (ICP-OES) and expressed as mg/L.

5.4.3.6. Scanning electron microscopy (SEM)

Bacterial cell morphology as affected by L/BLEEs at 2 MIC was visualized and photographed using a scanning electron microscope (FEI Quanta 400-ESEM FEG, Oregon, USA). Preparation and conditions of bacterial cells smeared on the slides for visualization were carried out following the procedure of Odedina *et al*. (2015). Untreated bacterial cells were photographed and served as the control.

5.4.4. Evaluation of L/BLEE preservative effectiveness in tilapia slices by microbial challenge test

5.4.4.1. Preparation of tilapia slices

Freshly deceased tilapias (around 3 kg, 1 ± 0.1 kg/fish) were purchased from a local market in Hat Yai, Songkhla, Thailand, and transported in ice (fish/ice: 1:2) to laboratory within 20 min. Fish were washed using clean water, descaled, gutted, and washed using sterilized cold water. The cleaned fish were filleted in complete aseptic condition (exposed to UV light) using a sterilized stainless-steel knife. Slices (4×2 cm^2) were further cut into an average thickness of 1.5 ± 0.3 cm.

5.4.4.2. Preparation of bacterial suspension and inoculation to the slices

Bacterial suspensions of *S. aureus, E. coli, P. aeruginosa,* and *S. sonnei*, at 10^8 CFU/mL were prepared separately in a sterilized 0.85% saline solution from a 24 h cultures grown in TSB at 37˚C. The bacterial suspensions were further diluted independently to 10^7 CFU/mL. Thereafter, 1 mL of each bacterial suspension was inoculated into 10 g of slices by surface spreading to obtain a final level of about 10^6 CFU/g. Such an inoculum level was selected to mimic fish samples that were heavily contaminated during processing, to ensure survival of the bacterial inoculum, and for proper determination of the log reductions (Komitopoulou, 2011; NACMCF, 2010).

Samples were incubated for 60 min at 37˚C, in which bacterial inoculums could adapt and proliferate in the slices. Subsequently, fish samples were treated as described by Tagrida and Benjakul (2021) with L/BLEEs at 200 and 400 ppm. Samples treated only with bacterial suspension without any treatment were served as positive control. All samples (10 g) were placed in polyethylene bags and MAP was carried out as tailored by Olatunde *et al.* (2020) using 2 different gas mixtures, G1 (CO_2: Ar: O_2 = 60: 30: 10) and G2 (CO_2: Ar: O_2 = 30: 60: 10). Oxygen level in the bags was determined using Oxybaby headspace analyzer (WITT Gasetechnik, Witten, Germany). Samples packed in G1 or G2 and added with 200 ppm L/BLEEs were termed as "L200/G1" and "L200/G2", respectively. Samples added with 400 ppm L/BLEEs packed using the corresponding gases were named as "L400/G1" and "L400/G2", respectively. NTP treatment was subsequently conducted as specified by Tagrida *et al.* (2021a) in which all the packed samples were placed between the ground cathode and quartz. NTP treatment was then conducted at 80 KV-RMS for 5 min at room temperature. Slices inoculated with bacterial suspensions without any hurdle treatments were placed in polyethylene trays, wrapped with shrinking film, and considered as control. All treated samples and the control were stored at 4˚C for 15 days.

All the samples were taken for bacterial enumeration every 3 days up to 15 days. For samples inoculated with *S. aureus,* Baird Parker agar (BPA) was used for their enumeration. Samples (5 g) were added to 45 mL of 0.85% saline solution and homogenized using a stomacher. One hundred μL of appropriate dilution were cultured on the BPA and incubated for 24 – 48 h at 37˚C. The formation of shiny black colonies with a thin white edge and transparent zone around was characteristic of *S. aureus*. For samples inoculated with *E. coli*, *S. sonnei* and *P. aeruginosa*, samples were prepared as mentioned previously, but Eosin methylene blue (EMB) agar, Pseudomonas agar base (PAB), and Hektoen enteric agar (HEA) were used for the enumeration of *E. coli*, *P. aeruginosa*, and *S. sonnei*, respectively. The bacterial colonies formed after 24 h incubation at 37˚C with a metallic sheen having a dark center on EMB were the characteristic of *E. coli*. Large, opaque, flat colonies with irregular margins showing greenish coloration on PAB were an indication for *P. aeruginosa*, while the green colonies on HEA were indication of *S. sonnei*. Counts were taken in triplicate for each treatment and three separated challenge experiments were performed. The detection limit of 10^2 CFU was implemented. Log reduction was calculated using the following formula:

$$\text{Log reduction} = \text{Log}_{10}\ (A) - \text{Log}_{10}\ (B)$$

where A is the bacterial count at the day 0 of storage and B is the count at different storage time. Based on log reduction, the percentage reduction (% reduction) was calculated using the following formulation:

$$\text{Reduction (\%)} = (1 - 10^{-L}) \times 100.$$

where L is the log reduction (Microchem Laboratory, 2021).

5.4.4.3. Chemical analyses of slices

For lipid oxidation in slices, thiobarbituric acid reactive substances (TBARS) and peroxide value (PV) were measured as detailed by Jin *et al.* (2020). The values were expressed as mg malondialdehyde (MDA)/kg fish meat and as mg cumene hydroperoxide/kg fish meat, respectively. Total volatile base (TVB) content was determined as spoilage index following the method of Yu *et al.* (2018) and was reported as mg N/100 g fish meat. The pH was measured for all the samples throughout the storage at 4˚C for 15 days.

5.4.5. Statistical analysis

Completely randomized design (CRD) was applied for all studies. All the experiments were conducted in triplicates (n = 3) and the results were presented as mean ± standard deviation. One-way Analysis of Variance (ANOVA) was conducted, and Duncan's Multiple Range Test (DMRT) was done for mean comparison. SPSS package (SPSS 22.0 for Windows, SPSS Inc, Chicago, IL, USA) software was used for data analysis.

5.5. Results and discussion

5.5.1. Antibacterial activities of L/BLEE and U/BLEE

5.5.1.1. Minimum inhibitory concentration (MIC) and minimum bactericidal concentration (MBC)

MIC results (Table 12) showed similar antibacterial activity ($p > 0.05$) between L/BLEE and U/BLEE against *S. aureus* indicating that BLEE could be released from the liposomes and acted as antimicrobial agent. However, MICs of L/BLEEs were lower than that of U/BLEE against *E. coli*, *S. sonnei* and *P. aeruginosa* ($p < 0.05$), denoting an enhanced antibacterial activity of BLEE when entrapped in liposomes particularly against the Gram-negative bacteria. This enhancement could be related to the surface polarity of liposomes that facilitated the association with bacterial cell wall. This led to the better diffusion and interaction of the active compound released from the liposomal core across the bacterial cell walls, thus favoring their permeability and affecting the bacterial organelles. This phenomenon eventually resulted in the inhibition of bacterial growth (McAllister *et al.*, 1999; Nacucchio *et al.*, 1988). Such effects seemed to be more profound in the Gram-negative bacteria over the Gram-positive counterparts. Gram-positive bacteria possessing thick layers of peptidoglycan in the cell wall had more resistance against several active compounds (Mai-Prochnow *et al.*, 2016). MBCs of L/BLEEs and U/BLEE against the same bacteria were in tandem with MICs results. MBCs of L/BLEE were 3.12, 0.39, 0.78 and 0.39 mg/mL, while those of U/BLEE were 6.25, 0.78, 1.56, and 0.78 mg/mL against *S. aureus*, *E. coli*, *P. aeruginosa*, and *S. sonnei*, respectively. These findings confirmed the enhancement of the antibacterial activity of BLEE when loaded in liposomes. Mugabe *et al.* (2006) reported an improvement in antibacterial properties of aminoglycosides loaded liposomes against *P. aeruginosa* due to the association of the negatively charged liposome vesicles with the outer bacterial membrane. Similarly, Solleti *et al.* (2015) recorded an increased bactericidal activity of liposomes loaded with azithromycin, compared with free azithromycin.

Table 12. MIC, MBC, and inhibition zones (IZ) of L/BLEE and the equivalent amount of unencapsulated BLEE (U/BLEE) based on encapsulation efficiency (EE) toward *S. aureus*, *E. coli*, *P. aeruginosa*, and *S. sonnei*.

	L/BLEE			**U/BLEE**		
	MIC (mg/mL)	**MBC (mg/mL)**	**IZ (mm)**	**MIC (mg/mL)**	**MBC (mg/mL)**	**IZ (mm)**
S. aureus	3.12^{aA}	3.12^{aB}	15.3 ± 0.5^{cA}	3.12^{aA}	6.25^{aA}	13.8 ± 0.7^{cB}
E. coli	0.19^{cB}	0.39^{cB}	20.8 ± 0.2^{aA}	0.39^{cA}	0.78^{cA}	18.5 ± 0.2^{aB}
P. aeruginosa	0.39^{bB}	0.78^{bB}	18.8 ± 0.7^{bA}	0.78^{bA}	1.56^{bA}	16.8 ± 0.2^{bB}
S. sonnei	0.19^{cB}	0.39^{cB}	21.3 ± 0.5^{aA}	0.39^{cA}	0.78^{cA}	18.6 ± 0.5^{aB}

Different lowercase superscripts within the same column indicate significant difference ($p < 0.05$). Different uppercase superscripts within the same row under the same parameter tested, indicated significant difference ($p < 0.05$). Mean ± SD (n = 3).

5.5.1.2. Well diffusion method

This method is based on the diffusion of antibacterial compounds through agar medium previously inoculated with certain bacterial isolates. The activity of the tested compound is determined by the dimension of the inhibition zones caused by these compounds. The larger the inhibition zones, the higher antimicrobial activity of active compound was achieved (Balouiri *et al.*, 2016). L/BLEEs (Table 12) had a superior antibacterial activity to U/BLEE ($p < 0.05$) against all the tested bacteria. L/BLEE had inhibition zones of 15.3, 20.8, 18.8 and 21.3 mm against *S. aureus*, *E. coli*, *P. aeruginosa*, and *S. sonnei*, respectively. Inhibition zones of U/BLEE were 13.8, 18.5, 16.8 and 18.6 mm against the corresponding bacteria. These results reconfirmed the improved antibacterial activity of L/BLEE, more likely caused by the efficient fusion between the bacterial cell membrane and the liposomes walls, resulting from the decreased surface hydrophobicity (McAllister *et al.*, 1999). The efficiency of the liposome-bacterial wall fusion might be governed by several factors, such as the nature of bacterial membrane, liposomes fluidity, pH, temperature, and monovalent and divalent cations in the surrounding medium (Wang *et al.*, 2016). Thus, these factors could affect the inhibition zone diameters of BLEE loaded in liposomes.

5.5.1.3. TTC dehydrogenase activity

Treatment with L/BLEEs or U/BLEE affected the viability of the bacterial cells as witnessed by the change in TTC dehydrogenase activity (Fig. 19A). TTC is a low molecular weight compound that could be absorbed by viable bacterial cells and then reduced in their cell walls to the insoluble red colored 2,3,5-triphenylformazan (TF). Dehydrogenase is important for bacterial respiration (Olatunde *et al.*, 2019a). When this enzyme reduces TTC, TF is then produced. Therefore, it could be presumed that the decrease in TTC dehydrogenase activity of bacterial isolates was strongly related to the antibacterial activity of either L/BLEEs or U/BLEE. Both L/BLEE and U/BLEE could affect their respiration as well as their metabolism, leading eventually to their death as indicated by the lowered TTC dehydrogenase activity. The activities of L/BLEE and U/BLEE appeared to be similar ($p > 0.05$), however, L/BLEE tended to show lower TTC dehydrogenase activity, indicating more bactericidal effect of the former.

TTC dehydrogenase activities of L/BLEE were decreased to 27.9, 12.1, 10.3, and 10.9% against *S. aureus*, *E. coli*, *P. aeruginosa*, and *S. sonnei*, respectively, while the relative activities of 29.3, 13.2, 11.9, and 13.01% were found for U/BLEE. The result suggested that more viable bacteria were retained after treatment with U/BLEE, which denoted the lower antibacterial activity of U/BLEE. *S. aureus* exhibited the highest TTC dehydrogenase activity ($p < 0.05$) among all tested bacteria, regardless of treatment with either L/BLEEs or U/BLEE. High content of peptidoglycan in their cell walls made them more resistant against the antibacterial compounds. On the other hand, TTC dehydrogenase activity of the untreated bacterial cells ranged between 87.8 and 91.0%, denoting high viable bacteria and the absence of any antibacterial compound. The difference in activity between L/BLEE and U/BLEE signified an enhancement of antibacterial activity of BLEE when encapsulated in liposomes.

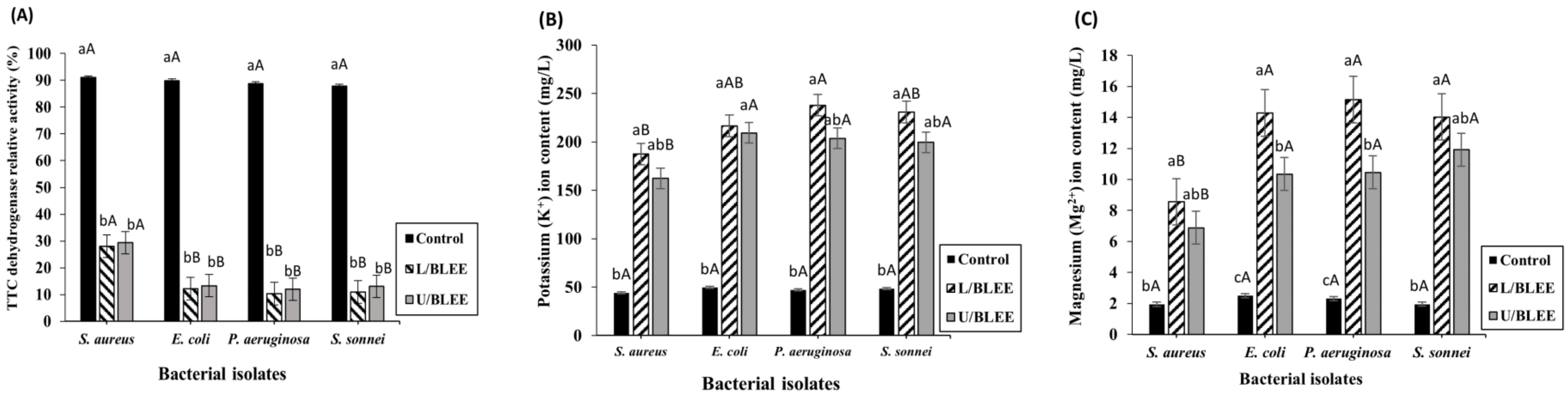

Figure 19. Triphenyl-2H tetrazolium chloride (TTC) dehydrogenase activity (A), potassium ion (K^+) content (B) and magnesium ion (Mg^{+2}) content (C) of *S. aureus*, *E. coli*, *P. aeruginosa*, and *S. sonnei* without treatment (control), with treatments of liposomes loaded with betel leaf ethanolic extract (L/BLEE) and unencapsulated BLEE (U/BLEE) at equivalent amount based on encapsulation efficiency at concentrations of 2 MIC. Bars represent standard deviation (n = 3). Different lowercase letters on the bars for the same bacteria indicate significant difference ($p < 0.05$). Different uppercase letters on the bars for same treatment indicate significant difference ($p < 0.05$).

5.5.1.4. Potassium (K^+) and magnesium (Mg^{2+}) ions leakage

The effects of L/BLEE and U/BLEE on the bacterial cells were also studied by determining K^+ and Mg^{2+} contents released after treatment of both samples at 2 MIC (Fig. 19B and C). Plasma membrane plays a crucial role in the regulation of influx and efflux of the different molecules into the bacterial cells. Maintaining the integrity of the plasma membrane is an important function of the bacterial cells. The loss in this integrity would lead to privation of the molecules essential for the metabolic activities of the bacterial cells, leading to the ultimate death of the bacteria (Davin-Regli *et al.,* 2008). Potassium is one of the major elements in the bacterial cells required for its intercellular enzyme activities. It also acts as intercellular messenger and is required for the maintenance of membrane potential and a constant internal pH (Gründling, 2013). Magnesium is essential for glycolysis, peptidoglycan synthesis and is also required for DNA enzymatic replication (Thomas and Rice, 2014; Wang *et al.,* 2019).

Treatments with L/BLEE or U/BLEE led to the increased ($p < 0.05$) leakage of the K^+ as compared to the control (untreated cells). L/BLEE was generally noticed to cause more K^+ leakage for all treated bacteria than U/BLEE ($p < 0.05$). L/BLEE at 2 MIC led to the release of 187, 217, 238, and 231 mg/L of K^+ from *S. aureus*, *E. coli*, *P. aeruginosa*, and *S. sonnei*, respectively, whereas the K^+ releases of 162, 209, 204, and 199 mg/L were found when treated with U/BLEE at the same concentration. K^+ content for the control was in the range of 44.2 – 48.4 mg/L. Leakage of $Mg2^+$ from treated bacterial cells was in tandem with that of K^+, in which L/BLEE had the higher effect on the leakage of Mg^{2+} from all the treated bacteria. Mg^{2+} contents after treatment with L/BLEE were 8.55, 14.3, 15.1, and 14.0 mg/L from *S. aureus*, *E. coli*, *P. aeruginosa*, and *S. sonnei*, respectively. The same bacteria treated with U/BLEE had Mg^{2+} contents of 6.88, 10.3, 10.4, and 11.9 mg/L, respectively. The control had contents ranging from 1.94 to 2.5 mg/L.

Generally, K^+ content was observed to be higher than that of Mg^{2+} in the bacterial cells, which came in line with Epstein (2003) and Nierhaus (2014) who found that K^+ prevailed over other cations in the bacterial cells and was the major intracellular cation in bacteria as well as in eucaryotic cells. Again, the presence of high content of peptidoglycan reflected the resistance of *S. aureus* to L/BLEE or U/BLEE, which was ascertained by lesser contents of K^+ or Mg^{2+} released from their cells. These results suggested that membrane disruption could be a major antimicrobial mechanism of L/BLEE. The results also confirmed the improved antibacterial effect of L/BLEE as the K^+ or Mg^{2+} released from the bacteria were higher ($p < 0.05$) than those found in bacteria treated with U/BLEE.

5.5.1.5. Scanning electron microscopy (SEM)

The impacts on morphology of *S. aureus*, *E. coli*, *P. aeruginosa*, and *S. sonnei* without and with L/BLEE treatment at 2 MIC are depicted in Fig. 20. The morphologies of untreated bacterial cells (Fig. 20A, B, C, and D) appeared intact and unharmed without any apparent damage. The treated bacterial cells, however, were shown to be deformed, shrunken, and full of perforation as pointed by arrow signs (Fig. 20E, F, G, and H). Apart from heavily disturbing the permeability of the bacterial cell walls, these damages caused by L/BLEE clearly led to leakage of cytoplasmic substances as well as other molecules including bacterial organelles and DNA. This directly affected their metabolism, division, and cell wall repair abilities. This resulted in the lowered resistance to antibacterial compounds and eventually inevitable death. Similar morphological changes were observed previously on bacterial cells that were treated with liposomes loaded with antibacterial agents (Jung *et al.,* 2015; Nicolosi *et al.,* 2010).

Antibacterial activity of the extract or active compounds was enhanced when loaded in liposomes, when compared with the free form. The mostly agreed mode of action of these liposomes involves two main steps, firstly, active compounds are protected in the core from the surrounding abiotic environment and the bacterial enzymes, which could lower its activity. Secondly, a reduction of surface hydrophobicity or electrostatic repulsion occurs between the wall of the liposomes and the bacterial cell membrane, thus allowing an efficient fusion and rapid release of the active compound which will alter the bacterial membrane permeability. This leads to uncontrolled leakage of the cell constituents, metabolic failures and eventually the death of the bacterial cells (Khatibi *et al.,* 2018; McAllister *et al.,* 1999; Umagiliyage *et al.,* 2017).

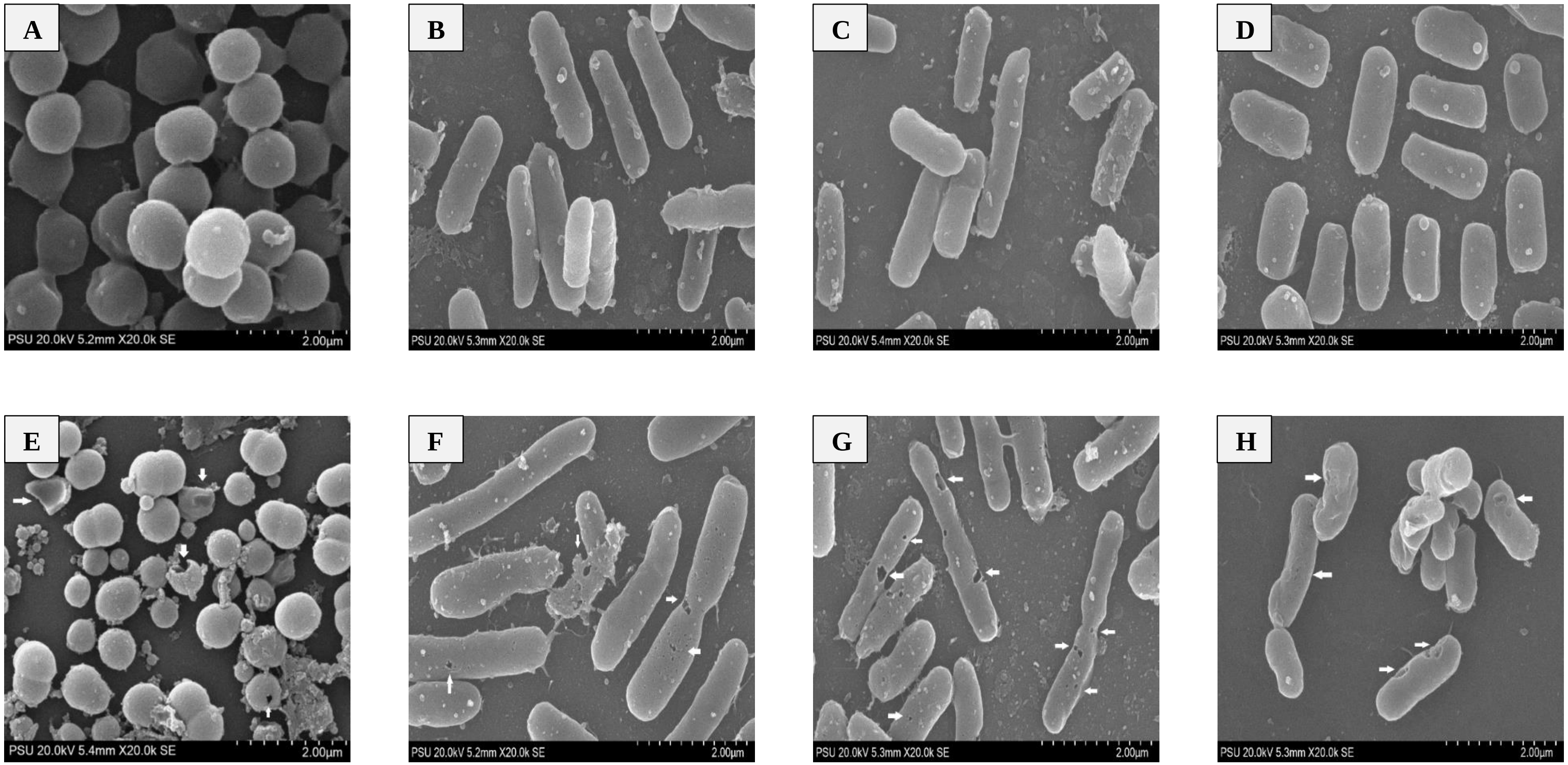

Figure 20. Scanning electron microscopic (SEM) photographs of *S. aureus* (A and E), *E. coli* (B and F), *P. aeruginosa* (C and G), and *S. sonnei* (D and H) without (control) and treated with liposomes loaded with betel leaf ethanolic extract (L/BLEE) at concentration of 2 MIC. Magnification x 20,000.

In addition to the biocompatibility of the liposomes with the bacterial cell walls which enhanced bactericidal effect, antibacterial activity of BLEE was also related to the polyphenols within the extract such as vitexin 4′-O-galactoside, isovitexin, hydrocinnamic acid, kaempferol derivatives, and epigallocatechin known for their remarkable antibacterial activities (Tagrida and Benjakul, 2020).

5.5.2. Preservative effectiveness of L/BLEE combined with NTP and MAP on tilapia slices during refrigerated storage

Challenge test is a useful tool for evaluating the efficiency of specific hurdles to inhibit the growth of certain microorganisms inoculated intentionally on food products for a certain period. The extent of microbial inhibition determines the preservation ability as well as the shelf-life of the target product (Komitopoulou, 2011). The efficiencies of L/BLEE at different concentrations (200 and 400 ppm) coupled with NTP treatment (80 KV-RMS for 5 min) and MAP using 2 different gas formulations, G1 (CO_2: Ar: O_2 = 60: 30: 10) and G2 (CO_2: Ar: O_2 = 30: 60: 10) were varied against *S. aureus*, *E. coli*, *P. aeruginosa*, and *S. sonnei*, inoculated into tilapia slices. At the initial day of storage (Fig. 21), the counts of all challenged bacteria were high (5.97–6.06 log CFU/g) due to the high inoculum used at the beginning of the test, to ensure the proliferation of the target bacteria in slices. Also, the log reduction could be effectively calculated. These counts also indicated the adaptation of the challenged bacteria on slices.

At day 3, the count of the controls of each challenged bacteria continued to increase and exceeded the initial limit for contamination (>6.0 log CFU/g). Varied efficiencies ($p < 0.05$) in the log reduction of the challenged bacteria as affected by the hurdles implemented were observed (Fig. 21A, B, C, and D). L400/G1 and L400/G2 showed the highest inhibition effect on all the challenged bacteria ($p > 0.05$). However, L400/G1 had slightly higher log reduction with values of 2.47, 2.94, 3.12, and 3.35 log CFU/g against *S. aureus*, *E. coli*, *P. aeruginosa*, and *S. sonnei*, respectively, while L400/G2 had the values of 2.16, 2.66, 2.90, and 3.06 against the same tested bacteria. This difference in log reduction for L400/G1 was possibly due to the elevated CO_2 (60%) used in the packaging. Masniyom *et al.* (2002) reported that bacterial inhibition was enhanced when CO_2 at high ratio was present, associated with alteration of the metabolic activities of bacteria. Additionally, the dissolution of CO_2 in water generated carbonic acid which caused the bacterial inhibition (Olatunde *et al.,* 2019b).

The log reduction of L200/G1 was 1.15, 2.10, 1.74, and 2.25 log CFU/g, while that of L200/G2 was 1.06, 1.83, 1.62, and 2.05 log CFU/g against *S. aureus*, *E. coli*, *P. aeruginosa*, and *S. sonnei*, respectively. Thus, the growth retardation of bacteria by L/BLEE was in dose-dependent manner. Log reduction can be defined as the difference of the log CFU/g of the tested microorganisms before and after the treatments and it gives an indication of how effective the antibacterial compound or hurdles in reducing the load of microorganisms (De Vries and Hamilton, 1999). From the log reduction, the percent reduction, which is more simplified expression, can be calculated. For a post-lethality treatment to be validated, at least 1 log reduction (90% reduction) must be achieved, while a reduction of 5 log (99.9% reduction) is regarded as full lethality treatment (Spanu *et al.,* 2014). The percent reduction after 3 days for L400/G1 was in the range of 99.6 – 99.9% and for L400/G2, it was in the range of 99.3 – 99.9% against the aforementioned bacteria, indicating high efficiency in eliminating those bacteria, particularly when L/BLEEs at 400 ppm were used. Also, G1 showed slightly higher log reduction than G2, which was associated with higher CO_2 level in G1. At 200 ppm, the percentage reduction was in the range of 93.0 – 99.4% for L200/G1 and in the range of 91.4–99.1% for L200/G2, indicating that lower effectiveness was found with lower level of L/BLEE used. In general *S. aureus* (Fig. 21A) was more resistant against L/BLEE as ascertained by the lower percent reduction, while the other Gram-negative bacteria, particularly *S. sonnei* (Fig. 21D) were the most affected. As previously discussed, this lower percent reduction for *S. aureus* could be attributed to their thick cell walls of peptidoglycans, providing more resistance to L/BLEE (Mai Prochnow *et al.*, 2016). Additionally, the morphology of the targeted bacteria might play an important role in their resistance to the actions of many hurdles. Coccus bacteria were more resistant than rods (Raso *et al.,* 2014).

At day 6, the log reduction dropped ($p < 0.05$) drastically for L200/G1 and L200/G2, ranging between 0.753 and 0.946 log reduction (82.3 and 88.7% reduction) for the former and 0.497 – 0.849 log reduction (68.1 and 85.8% reduction) for the latter, signifying that these treatments after 6 days of refrigerated storage were below the post-lethality limit. The result revealed the inability of those treatments to effectively retard the bacterial growth. On the other hand, L400/G1 and L400/G2 remained effective and above the post-lethality limit after 6 days as the log reduction still ranged between 2.19 and 2.97 log reduction (99.3 – 99.9% reduction) and between 1.94 and 2.51 log reduction (98.9 – 99.7% reduction), respectively. This effect could be attributed to the slow release of the L/BLEEs into slices, thus effectively inhibiting bacterial growth. L200/G1 and L200/G2 treatments at day 9 were no longer effective in retarding bacterial growth as the log reduction was below the post-lethality limit, however the counts were still lower than the initial inoculation counts ($p < 0.05$) which reflected a mild antibacterial activity for these treatments after 9 days of storage. The log reduction was also decreased for L400/G1 and L400/G2 treatments, however it remained above the post-lethality limit with values of 1.17–1.31 log reduction (93.4–95.2% reduction) for L400/G1 and 1.00–1.19 log reduction (90.0–93.6% reduction) for L400/G2. This confirmed satisfactory effectiveness in inhibiting the growth of the challenged bacteria after 9 days of storage. L400/G1 continued to show slightly higher efficacy in bacterial inhibition due to its elevated CO_2 in the packages.

By day 12, L200/G1 and L200/G2 lost entirely their effectivity in inhibiting the bacterial growth as the counts of all challenged bacteria surpassed the initial counts at day 0. The counts of L400/G1 and L400/G2 treatments were still below the limit, however, the log reduction of these treatments dropped markedly to be in the range of 0.211 – 0.519 log reduction (38.4 and 69.7% reduction) for L400/G1 and 0.0413 – 0.255 log reduction (9.08 – 44.3% reduction) for L400/G2, denoting a steady efficacy in bacterial growth retardation after 12 days of storage. The increase in the bacterial counts was related to many factors, including the loss of effectiveness of BLEE due to the disintegration or decomposition of active components. The elevated quantity of CO_2 caused higher exudate or free water, which favored the increased growth of bacteria (Masniyom, 2011). On day 0, the water activity (a_w) of slices was in the range of 0.977 – 0.980 and a_w was increased to 1.002 – 1.007 after 12 days. Such an increase was related to the poor water holding capacity of the slices, which could enhance bacterial growth. At day 15, the counts of both L400/G1 and L400/G2 treatments exceeded the initial limit (6 log CFU/g), indicating the complete loss of the antibacterial activity and in turn the end of storage.

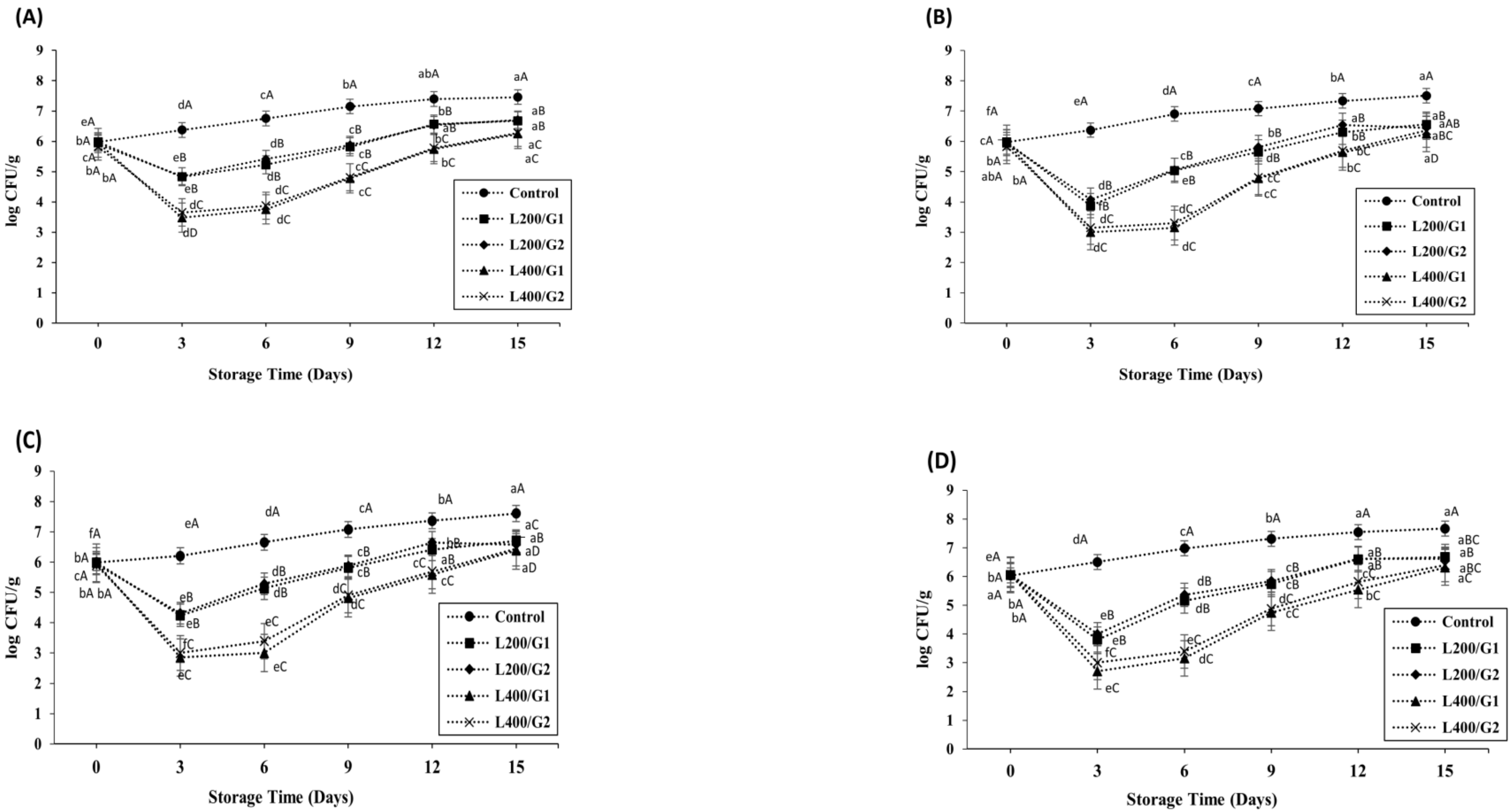

Figure 21. Growth curves of S. *aureus* (A), *E. coli* (B), *P. aeruginosa* (C), and *S. sonnei* (D) inoculated on tilapia slices without any treatment (control), with treatments of liposomes loaded with betel leaf ethanolic extract (L/BLEE) at 200 or 400 ppm and packaged under two different modified atmosphere G1 (CO_2: Ar: O_2 = 60: 30: 10) or G2 (CO_2: Ar: O_2 = 30: 60: 10), during 15 days of storage at 4˚C. Bars represent the standard deviation (n = 3). Different lowercase letters on bars within same treatment indicate significant difference ($p < 0.05$). Different uppercase letters on bars within the same storage time indicate significant difference ($p < 0.05$).

5.5.3. Chemical changes of tilapia slices

5.5.3.1. Lipid oxidation

Lipid oxidation generally takes place in fish rich in polyunsaturated fatty acids (PUFAs) by the actions of the free radicals and reactive oxygen species, leading to nutritional loss and the formation of hydroperoxides that are responsible for the rancidity (Masniyom *et al.,* 2002). Bacterial proliferation in fish can cause lipolysis, which results in the release of free fatty acids (FFAs), which can be used by the bacteria as an energy source and for other functional processes (Rameshwaram *et al.,* 2018). These FFAs are highly susceptible to oxidation, especially in the presence of heavy microbial load. PV has been used to mainly indicate the formation of peroxide and hydroperoxide (Jin *et al.*, 2020). At day 0, PV was in the ranges of 0.613 – 0.746, 0.581 – 0.764, 0.594 – 0.675, and 0.575 – 0.654 mg cumene hydroperoxide/kg ($p > 0.05$) for the samples inoculated with *S. aureus*, *E. coli*, *P. aeruginosa*, and *S. sonnei*, respectively (Fig. 22A). A relatively elevated rate of hydroperoxide generation at beginning of the storage could be attributed to both NTP radicals and bacterial activity. Overall, the control sample containing each challenged bacterium had a higher increase in PV than others during the storage of 15 days. For L200/G1 and L200/G2 treated samples, lower PV was found than the control during the storage. No marked changes were found within the first 3 days of storage. However, a continuous increase was noted up to day 12, followed by constant value until the end. This might be related to the antioxidant activities of L/BLEE.

It was noted that O_2 (10%) was lower than atmospheric O_2 (21%). This could lower oxidation taken place in the packages. MAP also contained CO_2, acting as antimicrobial agent. Ar, an inert gas could displace the O_2, thus preventing the growth of aerobic bacteria, and O_2 in lower quantities was able to prevent the growth of anaerobic bacteria. All these gases were also required by NTP to generate the radicals that could retard the bacterial growth (Olatunde *et al.,* 2019a). In addition, L/BLEE was able to scavenge the excessive radicals to some extent, thus preventing further lipid oxidation. At day 6, the control samples, had an increased PVs ($p < 0.05$) in the range of 6.15 – 6.93 mg cumene hydroperoxide/kg, considered as an indication of slight rancidity (Feiner, 2006). On the other hand, L400/G1 and L400/G2 treated samples had no pronounced change in PV, indicating more effectiveness of treatments, especially L/BLEEs at 400 ppm, to prevent lipid oxidation. After day 6, both L400/G1 and L400/G2 treated samples had a continuous increase in PV up to day 15. At day 15, samples L400/G1 and L400/G2 exceeded the accepted limits (>9 mg cumene hydroperoxide/kg) (Feiner, 2006), indicating that these treatments could retard lipid oxidation no longer than 12 days.

TBARS is an indicator to assess the extent of lipid oxidation by determination of the secondary products such as malonaldehyde, aldehydes, and ketones (Chen *et al.*, 2017). Like PV results, TBARS values of all the samples at day 0 were similar ($p > 0.05$) and were noticed to be slightly high because of bacterial inoculation and NTP treatments (Fig. 22B). Throughout the storage, the control samples had the marked increase in TBARS ($p < 0.05$), probably because of the augmented activity of the inoculated bacteria in liberating FFAs, which were prone to oxidation. After 3 days, TBARS of both L200/G1 and L200/G2 treated samples had the increase in TBARS but the values were lower than ($p < 0.05$) the control at all storage times. For L400/G1 and L400/G2 treated samples, negligible change ($p > 0.05$) in their values was found within the first 6 days. This might be due to the efficiency in retarding the lipid oxidation as well as delaying the growth of the inoculated bacteria. After 9 days of storage, the control samples had TBARS values ranging between 4.01 and 4.15 mg MDA/kg, which exceeded the limit (4 mg MDA/kg) in slices (Ozogul *et al.*, 2010). At the same period, the rest of the samples still had the values in the accepted margins, which reflected the effectiveness of the hurdles and L/BLEE used. Overall, the lower increasing rate ($p < 0.05$) was noticed in L400/G1 and L400/G2 treated samples, while values of L200/G1 and L200/G2 treated samples were close to the lower limit of acceptability (4 mg MDA/kg) at the end of storage. Based on both PV and TBARS, treatments of L200/G1 and L200/G2 against all the challenged bacteria were effective in retarding the bacterial growth and lowering lipid oxidation for up to 9 days, while treatments of L400/G1 and L400/G2 were effective up to 12 days.

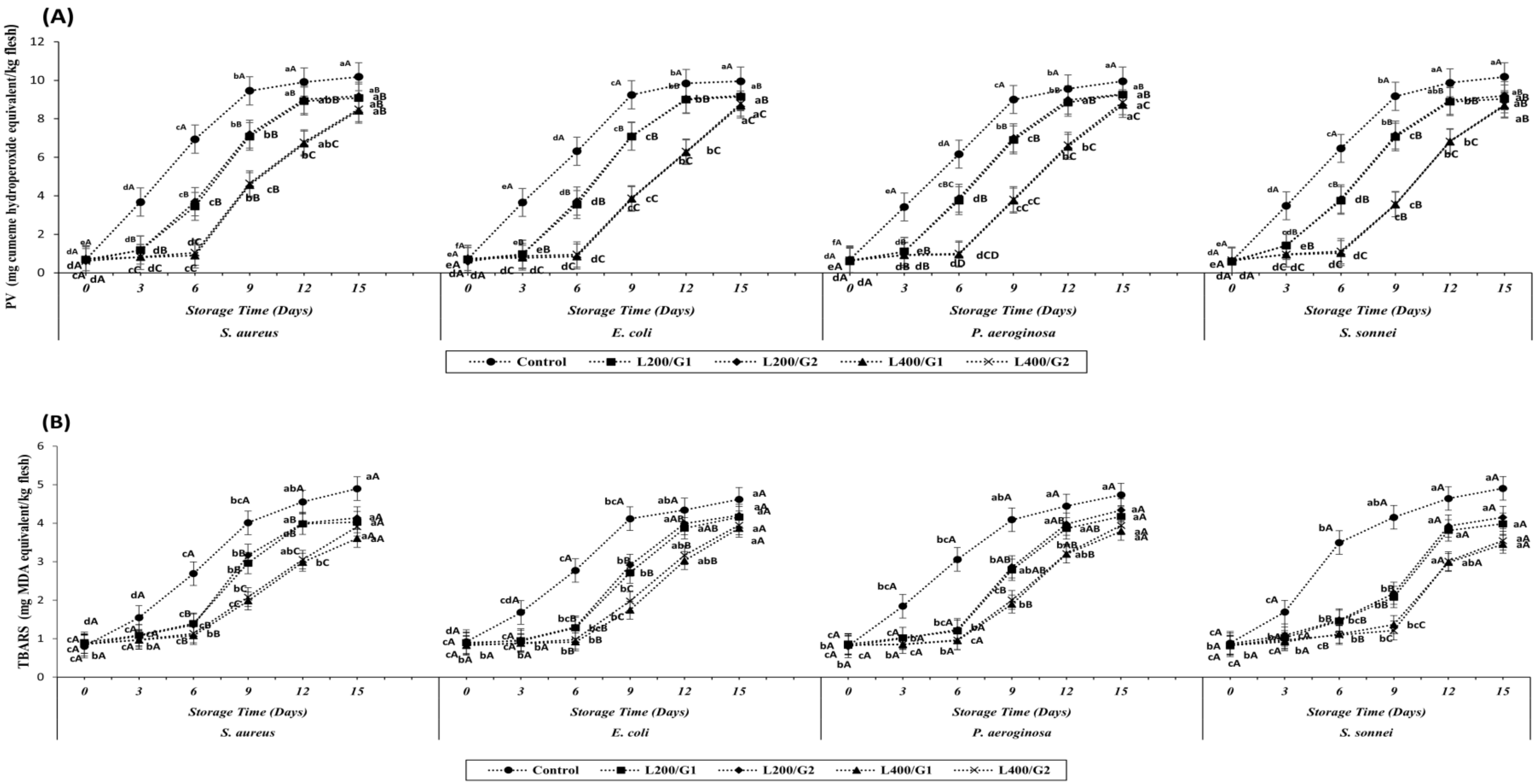

Figure 22. Peroxide value (PV) (A) and thiobarbituric acid reactive substances (TBARS) (B) of tilapia slices inoculated separately with *S. aureus*, *E. coli*, *P. aeruginosa*, and *S. sonnei*, without any treatment (control), with treatments of L/BLEE at 200 or 400 ppm and packaged under two different modified atmosphere G1 (CO_2: Ar: O_2 = 60: 30: 10) or G2 (CO_2: Ar: O_2 = 30: 60: 10), during 15 days of storage at 4˚C. Bars represent the standard deviation (n = 3). Different lowercase letters on bars within same treatment indicate significant difference ($p < 0.05$). Different uppercase letters on bars within the same storage time indicate significant difference ($p < 0.05$).

Irrespective of gas formulations or NTP treatment, the quantity of L/BLEE used had the profound effect in retarding the lipid oxidation. This effect can be explained by the remarkable antioxidant and antibacterial activities of L/BLEE and the slow release of the BLEE into slices, which is a valued feature of the liposomes. The prepared L/BLEE had a releasing efficiency of 19% after 8 h dialysis against distilled water, while it was 81% for the same amount of unencapsulated BLEE based on the encapsulation efficiency (79.8%) after the same period. After 72 h of dialysis, the releasing efficiency for L/BLEE was 48%, while the unencapsulated BLEE was completely released into the medium. The slow release of L/BLEE assured a continuous bioactivity of the BLEE for longer time, thus showing better preservative activity and extended shelf-life for the treated samples.

5.5.3.2. TVB content and pH

TVB content is a quality indicator for fish and fish products and is based on the quantification of total nitrogenous compounds including ammonia (NH_3), dimethylamine (DMA), and trimethylamine (TMA) generated by bacteria (Leisner and Gram, 2000). High TVB levels indicate spoilage and usually augmenting levels are accompanied by an increase in pH of the samples. In general, major compounds formed are basic. In addition, the optimum pH of many bacteria, particularly the challenged bacteria, is in basic pH range (Sanchez-Clemente *et al.,* 2018). No difference in TVB content was detected ($p > 0.05$) between all the samples at day 0 (Fig. 23A). Similarly, pHs of the samples showed no difference ($p > 0.05$) in their values (6.00–6.20) (Fig. 23B). TVB content of the controls increased markedly ($p < 0.05$) at day 3 and continuously increased up to 15 days. This increase was coincidental with the increase in pH. L200/G1 and L200/G2 treated samples had no apparent change ($p > 0.05$) in both TVB content and pH within the first 3 days, whereas L400/G1 and L400/G2 had no change in TVB content within the first 6 days ($p > 0.05$). The lower formation of nitrogenous compounds was due to lower bacterial growth. Thereafter, TVB content as well as pH of all the samples continued to increase ($p < 0.05$). L200/G1 and L200/G2 treated samples had an increase in both parameters ($p < 0.05$) but showed the lower rate than that of the controls.

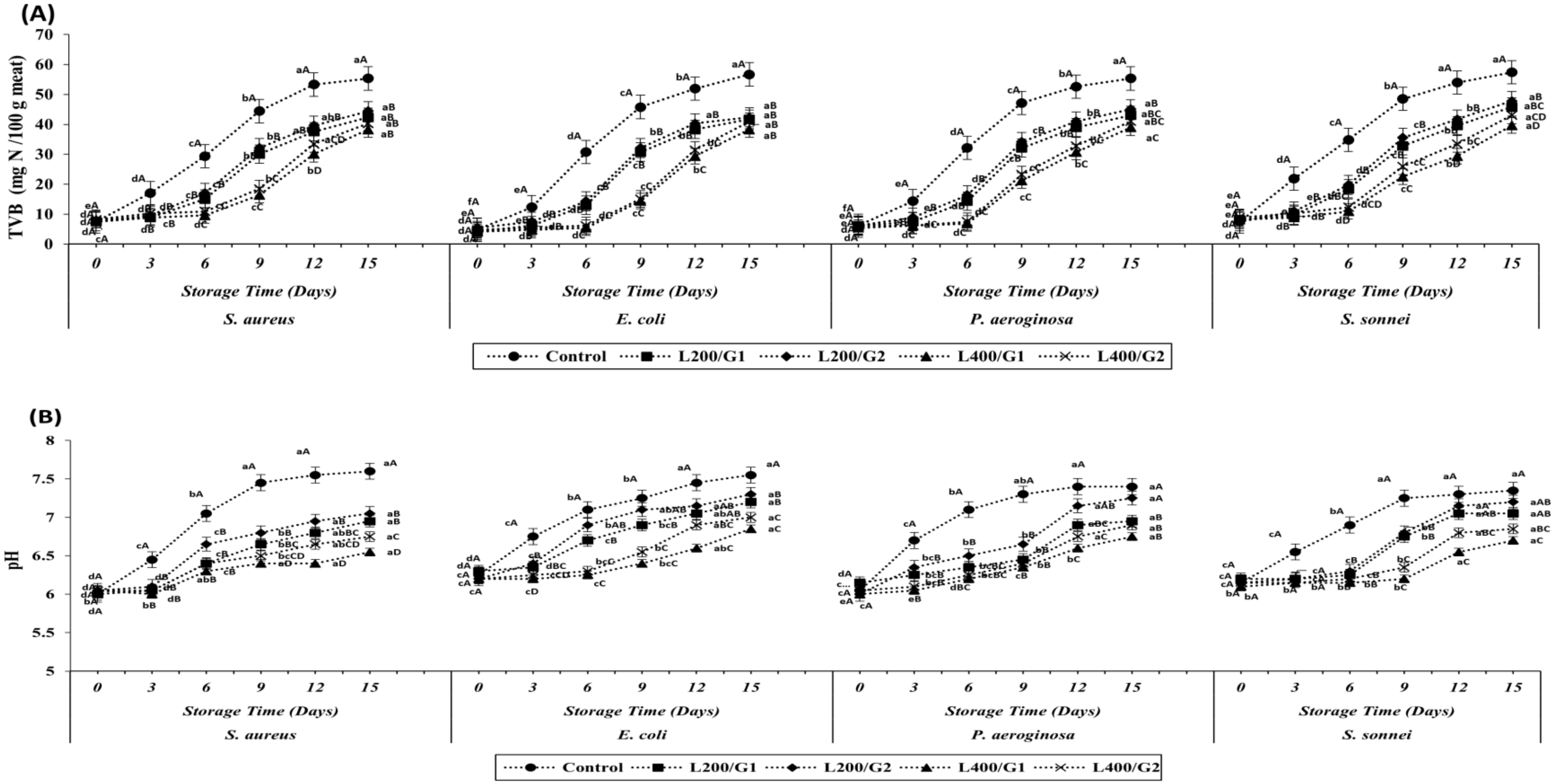

Figure 23. Total volatile base (TVB) content (A) and pH (B)of tilapia slices inoculated separately with *S. aureus*, *E. coli*, *P. aeruginosa*, and *S. sonnei*, without any treatment (control), with treatments of L/BLEE at 200 or 400 ppm and packaged under two different modified atmosphere G1 (CO_2: Ar: O_2 = 60: 30: 10) or G2 (CO_2: Ar: O_2 = 30: 60: 10), during 15 days of storage at 4˚C. Bars represent the standard deviation (n = 3). Different lowercase letters on bars within same treatment indicate significant difference ($p < 0.05$). Different uppercase letters on bars within the same storage time indicate significant difference ($p < 0.05$).

L400/G1 and L400/G2 treated samples exhibited the lowest increasing rate of TVB content ($p > 0.05$). When comparing TVB content and pH between G1 and G2 atmospheres, G1 treated samples tended to have lower TVB content and pH than G2 counterparts. This reconfirmed the crucial role of CO_2 in helping in retardation of microbial growth in slices. Also, the synergistic effect between L/BLEE and CO_2 was presumed. L400/G1 generally showed lower TVB content or pH than others throughout the storage of 15 days. TVB contents of control samples at day 9 were in the range of 44.4 – 48.5 mg N/100 g. TVB content above 35 mg N/100 g is regarded as an indication of spoilage (European Regulation, 2008). Therefore, it can be postulated that the control underwent spoilage within day 9.

pH of the control kept a steady increase and was in the range of 7.25 – 7.45 during 15 days of storage. Both TVB content and pH of L400/G1 and L400/G2 treated samples were lower than others and control, denoting the profound effectiveness of these treatments to prevent the formation of the nitrogenous compounds mainly mediated by spoilage bacteria. By day 12, TVB content of L200/G1 and L200/G2 treated samples surpassed the accepted limit with a marked increase in their pH. This indicated that these treatments were able to delay the formation of the nitrogenous compounds for 9 days. L400/G1 and L400/G2 treated samples still had TVB contents within the limit. Additionally, pHs were lower than the other samples. On day 15, TVB contents of L400/G1 and L400/G2 treated samples exceeded the accepted limits, signifying that their effectiveness of delaying the formation of basic compounds lasted up to 12 days. pHs of L400/G1 treated sample was increased from day 12 to day 15 ($p < 0.05$), probably because of the accumulation of the previously formed nitrogenous compounds and the slow formation of new basic compounds (Olatunde *et al.*, 2019b).

5.6. Conclusion

Encapsulation of BLEE into liposomes enhanced their antibacterial activities as ascertained by lower MIC, MBC, and larger zones of inhibition against *S. aureus*, *E. coli*, *P. aeruginosa*, and *S. sonnei*. Bacterial cells treated with L/BLEE had lower TTC dehydrogenase activity than those treated with U/BLEE, revealing their augmented bactericidal activity. L/ BLEE also led to increased leakage of K^+ and

Mg^{2+}, suggesting that their antibacterial mechanism was based on the attack on bacterial cell wall and alteration of permeability as shown by deformed and perforated cell walls. The use of challenge tests demonstrated that treatments with L/BLEE at 400 ppm combined with MAP (CO_2: Ar: O_2 = 60: 30: 10) and NTP (80 KV-RMS for 5 min) had the profound preservative efficiency on tilapia slices for up to 12 days of storage at 4˚C against all bacteria inoculated. Therefore, these treatments could be adopted as a promising hurdle for preventing bacterial growth and extending the shelf-life of tilapia slices.

5.7. References

Albertos, I., Martin-Diana, A., Cullen, P. J., Tiwari, B. K., Ojha, K. S., Bourke, P., and Rico, D. 2019. Shelf-life extension of herring (*Clupea harengus*) using in-package atmospheric plasma technology. Innovative Food Science and Emerging Technologies. 53: 85 - 91.

Balouiri, M., Sadiki, M., and Ibnsouda, S. K. 2016. Methods for *in vitro* evaluating antimicrobial activity: A review. Journal of Pharmaceutical Analysis, 6(2): 71 - 79.

Bouarab Chibane, L., Degraeve, P., Ferhout, H., Bouajila, J., and Oulahal, N. 2019. Plant antimicrobial polyphenols as potential natural food preservatives. Journal of the Science of Food and Agriculture. 99(4): 1457 - 1474.

Bourke, P., Ziuzina, D., Boehm, D., Cullen, P. J., and Keener, K. 2018. The potential of cold plasma for safe and sustainable food production. Trends in Biotechnology. 36(6): 615 - 626.

Carocho, M., Morales, P., and Ferreira, I. C. 2015. Natural food additives: Quo vadis? Trends in Food Science and Technology. 45(2): 284 - 295.

Chen, Q., Kong, B., Han, Q., Xia, X., and Xu, L. 2017. The role of bacterial fermentation in lipolysis and lipid oxidation in Harbin dry sausages and its flavour development. LWT- Food Science and Technology. 77: 389 - 396.

Davin-Regli, A., Bolla, J.-M., James, C. E., Lavigne, J.-P., Chevalier, J., Garnotel, E., and Molitor, A. 2008. Membrane permeability and regulation of drug “influx and efflux” in enterobacterial pathogens. Current Drug Targets. 9(9): 750 - 759.

De Vries, T. A. and Hamilton, M. A. 1999. Estimating the antimicrobial log reduction: part 1. quantitative assays. Quantitative Microbiology. 1: 29 - 45.

Epstein, W. 2003. The roles and regulation of potassium in bacteria. Progress in Nucleic Acid Research and Molecular Biology. 75: 293 - 320.

European Regulation. 2008. European Commission Regulation (EC) No 1022/2008 of 17 October 2008 amending Regulation (EC) No 2074/2005 as regards the total volatile basic nitrogen (TVB-N) limits. L277/18 EN Official Journal the European Union.

FAO. 2020. GLOBEFISH—Information and Analysis on World Fish Trade. Retrived fromhttps://www.fao.org/in-action/globefish/market-reports/resource detail/en/c/1416636/

Feiner, G. 2006. Meat products handbook: Practical science and technology. Boca Raton: Woodhead Publishing Limited. Elsevier. 19 - 32.

Gavahian, M., Chu, Y.-H., Khaneghah, A. M., Barba, F. J. and Misra, N. 2018. A critical analysis of the cold plasma induced lipid oxidation in foods. Trends in Food Science and Technology. 77: 32 - 41.

Gortzi, O., Lalas, S., Chinou, I., and Tsaknis, J. 2006. Reevaluation of antimicrobial and antioxidant activity of *Thymus* spp. extracts before and after encapsulation in liposomes. Journal of Food Protection. 69(12): 2998 - 3005.

Gründling, A. 2013. Potassium uptake systems in *Staphylococcus aureus*: new stories about ancient systems. MBio. 4: e00784-13.

Jayeoye, T. J., Nwabor, O. F. and Rujiralai, T. 2020. Synthesis of highly stable and dispersed silver nanoparticles/poly (vinyl alcohol-co-ethylene glycol)/poly (3-aminophenyl boronic acid) nanocomposite: Characterization and antibacterial, hemolytic and cytotoxicity studies. Journal of Industrial and Engineering Chemistry. 89: 288 - 300.

Jin, S., Pang, Q., Liu, R., Yang, H., Liu, F., Wang, M., Wang, Y., Feng, X. and Shan, A. 2020. Dietary curcumin decreased lipid oxidation and enhanced the myofibrillar protein structure of the duck (*Anas Platyrhynchos*) breast muscle when subjected to storage. LWT- Food Science and Technology. 133: 109986.

Jung, S. W., Thamphiwatana, S., Zhang, L., and Obonyo, M. 2015. Mechanism of antibacterial activity of liposomal linolenic acid against *Helicobacter pylori*. PloS One. 10(3): e0116519.

Kamkar, A., Molaee-Aghaee, E., Khanjari, A., Akhondzadeh-Basti, A., Noudoost, B., Shariatifar, N., Sani, M. A. and Soleimani, M. 2021. Nanocomposite active packaging based on chitosan biopolymer loaded with nano-liposomal essential oil: Its characterizations and effects on microbial, and chemical properties of refrigerated chicken breast fillet. International Journal of Food Microbiology. 342: 109071.

Khatibi, S., Misaghi, A., Moosavy, M., Akhondzadeh-Basti, A., Mohamadian, S. and Khanjari, A. 2018. Effect of nanoliposomes containing *Zataria multiflora* Boiss. essential oil on gene expression of Shiga toxin 2 in *Escherichia coli* O157: H7. Journal of Applied Microbiology. 124: 389 - 397.

Komitopoulou, E. 2011. Microbiological challenge testing of foods. Food and Beverage Stability and Shelf Life. Woodhead Publishing Series in Food Science, Technology and Nutrition. Elsevier. 507 - 523.

Leisner, J., and Gram, L. 2000. Spoilage of fish. Encyclopedia of food microbiology. Academic Press. 2000: 813 - 820.

Liu, W., Ye, A., Han, F., and Han, J. 2019. Advances and challenges in liposome digestion: Surface interaction, biological fate, and GIT modeling. Advances in Colloid and Interface Science. 263: 52 - 67.

Mai-Prochnow, A., Clauson, M., Hong, J. and Murphy, A. B. 2016. Gram positive and Gram-negative bacteria differ in their sensitivity to cold plasma. Scientific Reports. 6: 1 - 11.

Masniyom, P., Benjakul, S., and Visessanguan, W. 2002. Shelf-life extension of refrigerated seabass slices under modified atmosphere packaging. Journal of the Science of Food and Agriculture. 82(8): 873 - 880.

Masniyom, P. 2011. Deterioration and shelf-life extension of fish and fishery products by modified atmosphere packaging. Songklanakarin Journal of Science and Technology. 33(2): 181 - 192.

McAllister, S., Alpar, H. and Brown, M. 1999. Antimicrobial properties of liposomal polymyxin B. Journal of Antimicrobial Chemotherapy. 43: 203 - 210.

Microchem Laboratory. 2021. Log and Percent Reductions in Microbiology and Antimicrobial Testing. https://microchemlab.com/information/log-and-percent-reductions-microbiology-and-antimicrobial-testing

Mugabe, C., Halwani, M., Azghani, A. O., Lafrenie, R. M. and Omri, A. 2006. Mechanism of enhanced activity of liposome-entrapped aminoglycosides against resistant strains of *Pseudomonas aeruginosa*. *A*ntimicrobial Agents and Chemotherapy. 50: 2016 - 2022.

NACMCF. 2010. National advisory committee on microbiological criteria for foods. Parameters for determining inoculated pack/challenge study protocols. Journal of Food Protection, 73:140-202.

Nacucchio, M. C., Gatto Bellora, M. J., Sordelli, D. O., and D'aquino, M. 1988. Enhanced liposome-mediated antibacterial activity of piperacillin and gentamicin against gram-negative bacilli *in vitro*. Journal of Microencapsulation. 5(4): 303 - 309.

Nicolosi, D., Scalia, M., Nicolosi, V. M., and Pignatello, R. 2010. Encapsulation in fusogenic liposomes broadens the spectrum of action of vancomycin against Gram-negative bacteria. International Journal of Antimicrobial Agents. 35(6): 553 - 558.

Nierhaus, K. H. 2014. Mg^{2+}, K^{+}, and the ribosome. Journal of Bacteriology. 196(22): 3817 - 3819.

Odedina, G. F., Vongkamjan, K., and Voravuthikunchai, S. P. 2015. Potential bio-control agent from *Rhodomyrtus tomentosa* against *Listeria monocytogenes*. Nutrients. 7(9): 7451 - 7468.

Olatunde, O. O., Benjakul, S. and Vongkamjan, K. 2019a. Dielectric barrier discharge cold atmospheric plasma: Bacterial inactivation mechanism. Journal of Food Safety. 39: e12705.

Olatunde, O. O., Benjakul, S., and Vongkamjan, K. 2019b. Combined Effect of ethanolic coconut husk extract and modified atmospheric packaging (MAP) in extending the shelf life of Asian sea bass slices. Journal of Aquatic Food Product Technology. 28(6): 689 - 702.

Olatunde, O. O., Benjakul, S. and Vongkamjan, K. 2020. Shelf-life of refrigerated Asian sea bass slices treated with cold plasma as affected by gas composition in packaging. International Journal of Food Microbiology. 324: 108612.

Ozogul, Y., Ayas, D., Yazgan, H., Ozogul, F., Boga, E. K., and Ozyurt, G. 2010. The capability of rosemary extract in preventing oxidation of fish lipid. International Journal of Food Science and Technology. 45(8): 1717 – 1723

Rameshwaram, N. R., Singh, P., Ghosh, S., and Mukhopadhyay, S. 2018. Lipid metabolism and intracellular bacterial virulence: key to next-generation therapeutics. Future Microbiology. 13(11): 1301 - 1328.

Raso, J., Condón, S., and Álvarez, I. 2014. Non-thermal processing-pulsed electric field. Encyclopedia of Food Microbiology (Second Edition), Academic Press. 966-973.

Salehi, B., Zakaria, Z. A., Gyawali, R., Ibrahim, S. A., Rajkovic, J., Shinwari, Z. K., Khan, T., Sharifi-Rad, J., Ozleyen, A. and Turkdonmez, E. 2019. Piper species: A comprehensive review on their phytochemistry, biological activities and applications. Molecules. 24: 1364.

Sánchez-Clemente, R., Igeño, M. I., Población, A. G., Guijo, M. I., Merchán, F., and Blasco, R. 2018. Study of pH changes in media during bacterial growth of several environmental strains. Multidisciplinary Digital Publishing Institute. Proceedings. 2(20): 1297.

Solleti, V. S., Alhariri, M., Halwani, M., and Omri, A. 2015. Antimicrobial properties of liposomal azithromycin for *Pseudomonas* infections in cystic fibrosis patients. Journal of Antimicrobial Chemotherapy. 70(3): 784 - 796.

Spanu, C., Scarano, C., Ibba, M., Pala, C., Spanu, V. and De Santis, E. P. L. 2014. Microbiological challenge testing for *Listeria monocytogenes* in ready-to-eat food: a practical approach. Italian Journal of Food Safety. 3(4): 4518.

Srisapoome, P., and Areechon, N. 2017. Efficacy of viable Bacillus pumilus isolated from farmed fish on immune responses and increased disease resistance in Nile tilapia (*Oreochromis niloticus*): Laboratory and on-farm trials. Fish and Shellfish Immunology. 67(8): 199 – 210.

Tagrida, M., and Benjakul, S. (2020). Ethanolic extract of Betel (*Piper betle* L.) and Chaphlu (*Piper sarmentosum* Roxb.) dechlorophyllized using sedimentation process: Production, characteristics, and antioxidant activities. Journal of Food Biochemistry. 44(12): e13508.

Tagrida, M. and Benjakul, S. 2021. Betel (*Piper betle* L.) leaf ethanolic extracts dechlorophyllized using different methods: antioxidant and antibacterial activities, and application for shelf-life extension of Nile tilapia (*Oreochromis niloticus*) fillets. RSC Advances. 11: 17630 - 17641.

Tagrida, M., Prodpran, T., Zhang, B., Aluko, R. E. and Benjakul, S. 2021a. Liposomes loaded with betel leaf (*Piper betle* L.) ethanolic extract prepared by thin film hydration and ethanol injection methods: Characteristics and antioxidant activities. Journal of Food Biochemistry. 45(12): e14012.

Tagrida, M., Benjakul, S. and Zhang, B. 2021b. Use of betel leaf (*Piper betle* L.) ethanolic extract in combination with modified atmospheric packaging and nonthermal plasma for shelf-life extension of Nile tilapia (*Oreochromis niloticus*) fillets. Journal of Food Science. 86(12): 5226 – 5239.

Thomas, K. J., and Rice, C. V. 2014. Revised model of calcium and magnesium binding to the bacterial cell wall. BioMetals. 27(6): 1361 - 1370.

Tometri, S. S., Ahmady, M., Ariaii, P. and Soltani, M. S. 2020. Extraction and encapsulation of *Laurus nobilis* leaf extract with nano-liposome and its effect on oxidative, microbial, bacterial and sensory properties of minced beef. Journal of Food Measurement and Characterization. 14: 3333 - 3344.

Umagiliyage, A. L., Becerra-Mora, N., Kohli, P., Fisher, D. J. and Choudhary, R. 2017. Antimicrobial efficacy of liposomes containing d-limonene and its effect on the storage life of blueberries. Postharvest Biology and Technology. 128: 130 - 137.

Wang, Z., Ma, Y., Khalil, H., Wang, R., Lu, T., Zhao, W., Zhang, Y., Chen, J. and Chen, T. 2016. Fusion between fluid liposomes and intact bacteria: study of driving parameters and in vitro bactericidal efficacy. International Journal of Nanomedicine. 11: 4025.

Wang, T., Flint, S. and Palmer, J. 2019. Magnesium and calcium ions: roles in bacterial cell attachment and biofilm structure maturation. Biofouling. 35: 959 - 974.

Watanabe, W. O., Losordo, T. M., Fitzsimmons, K. and Hanley, F. 2002. Tilapia production systems in the Americas: technological advances, trends, and challenges. Reviews in Fisheries Science. 10: 465 - 498.

Wijitpun, Y., Chomnawang, P., Huaisan, K., Sootsuwan, K. and Chomnawang, C. 2021. Chemical characteristics changes associated with extracted protein and salt addition and effect of different additives in the curing process on sensory acceptance of liquid fermented fish from tilapia frame. Aquaculture and Fisheries. 7(4): 405 - 410.

Yu, D., Regenstein, J. M., Zang, J., Jiang, Q., Xia, W. and Xu, Y. 2018. Inhibition of microbial spoilage of grass carp (*Ctenopharyngodon idellus*) fillets with a chitosan-based coating during refrigerated storage. International Journal of Food Microbiology. 285: 61 - 68.

Yuasa, K., Kamaishi, T., Hatai, K., Bahnnan, M. and Borisutpeth, P. 2008. Two cases of streptococcal infections of cultured tilapia in Asia. Diseases in Asian Aquaculture VI. 505: 259 - 268.

Zhao, Y.-M., de Alba, M., Sun, D.-W., and Tiwari, B. 2019. Principles and recent applications of novel non-thermal processing technologies for the fish industry-A review. Critical Reviews in Food Science and Nutrition. 59(5): 728 - 742.

CHAPTER 6

USE OF BETEL LEAF (*PIPER BETLE* L.) ETHANOLIC EXTRACT IN COMBINATION WITH MODIFIED ATMOSPHERIC PACKAGING AND NONTHERMAL PLASMA FOR SHELF-LIFE EXTENSION OF NILE TILAPIA (*OREOCHROMIS NILOTICUS*) SLICES

6.1. Abstract

Fish is perishable and has a short shelf-life. To maintain its quality, it is necessary to implement the appropriate technology, particularly nonthermal processing along with safe additive from plant origin under the concept of "hurdle technology". The use of potential vesicle including liposome for loading the plant extract could be a means to enhance the stability and activities of the extract. The current study aimed to evaluate the effect of liposomes loaded with betel leaf ethanolic extract (L/BLEEs) or unencapsulated BLEE (U/BLEE) in conjunction with modified atmospheric packaging (MAP) and nonthermal plasma (NTP) on the quality changes and shelf-life of Nile tilapia slices (TSs) stored under refrigerated condition (4˚C). TSs treated with L/BLEE or U/BLEE at 400 ppm, packed under modified atmosphere (CO_2: Ar: O_2 = 60:30:10) and subjected to NTP for 5 min (L/BLEE-400/MAP-NTP and U/BLEE-400/MAP-NTP, respectively) had the lowest microbial and chemical changes during storage, while the control showed the highest changes ($p < 0.05$). Lipid oxidation was lower in these samples, ascertained by more retained polyunsaturated fatty acids and lower lipid oxidation based on fourier transform infrared (FT-IR) spectra. Overall likeness scores were similar ($p > 0.05$) between all the samples at day 0 of storage. Only L/BLEE-400/MAP-NTP and U/BLEE-400/MAP-NTP were still sensorially acceptable after 12 days at 4˚C. Therefore, L/BLEE or U/BLEE combined with MAP/NTP treatment could be adopted as a potent hurdle for shelf-life extension of TSs.

6.2. Introduction

Because of their copious content of proteins and polyunsaturated fatty acids, fish are prone to rapid spoilage. Undesirable chemical reactions induced by indigenous enzymes as well as proliferation of food-spoilage microorganisms contribute to fish spoilage (Albertos *et al.,* 2019a). Both natural and synthetic preservatives have been employed for minimizing fish spoilage, thus extending their shelf-life. With increasing health concerns on synthetic preservatives, food manufacturers have sought for safe natural alternatives (Bouarab-Chibane *et al.,* 2019). Recently, nonthermal processes such as nonthermal plasma, pulsed electric field, and irradiation were applied for shelf-life extension of many food products (Bourke *et al.,* 2018). Among those technologies, nonthermal plasma (NTP) technology has drawn attention as a promising nonthermal process because of its antibacterial properties. Different factors such as type of gases used, voltage and frequency of electric current applied, and treatment time determine antimicrobial abilities of NTP (Miyamoto *et al.,* 2016). Nowadays, NTP has been used for shelf-life extension of many foods (Giannoglou *et al.,* 2020). NTP is achieved when a gas or mixture of gases is ionized with the aid of high electric field, leading to the formation of several reactive species (RS). These RS have the ability of bacterial inhibition. Those include reactive oxygen radials, positive and chemical ions, excited molecules, and electrons (Kim *et al.,* 2014). Air is commonly involved for NTP, in which reactive oxygen and nitrogen species including peroxide, ozone, and several forms of nitrogen oxides, are produced (Moutiq *et al.,* 2020).

For the optimum exploitation of plasma, the appropriate mixture of gases must be chosen in combination with other hurdle technologies, particularly the modified atmospheric packaging (MAP). This aims to compensate the unstable RS with excited state that may lead to the re-proliferation of microorganisms (Olatunde *et al.,* 2020). Despite its benefits, NTP could initiate lipid oxidation in seafoods rich in fats by the action of RS. Lipid oxidation is associated with severe loss of nutrients, unsavory flavor formation, and health risk in fish (Gavahian *et al.,* 2018). The use of antioxidants from natural origin especially plant extracts combined with NTP has been proposed not only to mitigate the effects of lipid oxidation induced by NTP treatment but also to elevate the antimicrobial properties of NTP (Olatunde *et al.,* 2020).

Betel leaves (*Piper betle* L.) grown in Southeast Asian countries were reported to have several secondary metabolites with valuable biological activities including antioxidant and antibacterial activities (Tagrida and Benjakul, 2020).

Therefore, betel leaf extract could be a promising natural preservative for food applications. However, discoloration and flavor change of the treated samples as well as the poor stability of some polyphenolic compounds, may restrict the use of plant extracts (Chen *et al.*, 2019). Liposome encapsulation may tackle such limitations due to its ability to reduce the reactivity between the encapsulated active compounds and the surrounding. More importantly, it could minimize the color changes and mask the undesirable flavors (Gortzi *et al.*, 2006). Liposomes are spherical vesicles, composed of phospholipids prepared from natural sources, especially egg yolk, soybean lipids and other sources. They have an amphiphilic characteristic along with beneficial properties including biocompatibility, stability, and non-toxicity which made them a suitable delivery agent for a variety of bioactive compounds including plant extracts (Liu *et al.*, 2019).

Therefore, the study aimed to elucidate the effects of liposomes containing dechlorophyllized betel leaf ethanolic extracts (L/BLEE) and unencapsulated BLEE (U/BLEE) with the same amount of extract in combination of MAP and NTP on the quality and shelf-life of tilapia fillets stored at refrigerated temperature (4˚C). Sensorial properties of the treated samples with the selected treatments were also examined.

6.3. Objectives

To study the synergistic effects of liposomal encapsulated betel leaf ethanolic extract and non-thermal plasma on the prevention of lipid oxidation and shelf-life extension of refrigerated Nile tilapia slices packaged under modified atmospheres.

6.4. Materials and methods

6.4.1. Chemicals

All chemicals used were of analytical grade. Ethanol was supplied by RCI labscan Limited (Bangkok, Thailand). Soybean phosphatidylcholine was procured from Sigma Aldrich, Inc. (St. Louis, MO, USA). Cholesterol was purchased from Acros Organics (Fair lawn, NJ, USA). Other chemicals were procured from Sigma Aldrich, Inc.

6.4.2. Preparation of BLEE and L/BLEE

Extraction and dechlorophyllization of BLEE was carried out as tailored by Tagrida and Benjakul (2020). Ethanol (70%) was employed as the extraction solvent using a leaf powder/solvent ratio of 1:15 (w/v). After solvent removal by a rotary evaporator, the concentrated betel extract was dechlorophyllized using sedimentation method. The thin film hydration method as described by Chotphruethipong *et al*. (2020) was adopted for the preparation of L/BLEEs. The resulting liposomes had particle size, zeta potential, polydispersity of 195.8 nm, −68.17, and 0.17, respectively. The encapsulation efficiency (EE) was 79.8%, while the releasing efficiency (RE) was 19% after 8 hr of dialysis. L/BLEEs were subsequently freeze-dried, placed in aluminum foil bag, sealed, and kept at 4˚C until further use.

6.4.3. Effect of L/BLEE or U/BLEE combined with MAP and NTP on shelf-life extension of Nile tilapia slices during storage at 4˚C

6.4.3.1. Preparation of slices and treatment with hurdles

Nile tilapia (freshly deceased, about 6 kg; 1 ± 0.1 kg per fish) were bought from a local market in Hat Yai, Songkhla, Thailand. Nile tilapia slices (TSs) were prepared as tailored by Tagrida and Benjakul (2021). Afterward, TSs were divided into six portions, in which the first and second portions were added with L/BLEE and U/BLEE at 400 ppm, respectively. Third and fourth portions were treated with L/BLEE and U/BLEE at 200 ppm, respectively. Fifth and sixth portions were left without any treatment. All the samples were placed in polystyrene foam trays, inserted in low-density polyethylene laminated with polyamide (80 µm thickness) bags (15 × 22 cm^2). The thickness of bag was 0.080 mm, and the oxygen permeability was 48.72 cm^3/m^2 24 hr atm).

Modified atmospheric packaging (MAP) using the mixture gases (CO_2: Ar: O_2 = 60: 30: 10) was applied and a slices/gases ratio of 1:3 (w/v) was used. Oxygen level in the bags was determined using Oxybaby headspace analyzer (WITT Gasetechnik, Witten, Germany). Samples packed and added with 400 ppm L/BLEE and U/BLEE were termed as “L/BLEE-400″ and “U/BLEE-400″, respectively.

Samples added with 200 ppm were named as “L/BLEE-200″ and “U/BLEE-200″, respectively. Sample packed under MAP (fifth portion), without BLEE or L/BLEE, was termed as “MAP”. For control, TSs without any treatment (sixth portion) were packed and wrapped with a shrink film.

NTP treatment was done as specified by Olatunde *et al.* (2020). To avoid any microbial contamination particularly after treatments, the in-bag dielectric barrier discharge NTP was applied. Sealed bags containing samples including L/BLEE-400, U/BLEE-400, L/BLEE-200, U/BLEE-200, and MAP were placed between the ground cathode and quartz. Thereafter, NTP treatment was conducted at 80 KV-RMS for 5 min at room temperature. Ozone content was measured using GASTEC gas tube detector immediately after treatment. All the samples were renamed to be L/BLEE-400/MAP-NTP, U/BLEE-400/MAP-NTP, L/BLEE-200/MAP-NTP, U/BLEE-200/MAP-NTP, and MAP-NTP, respectively. All the samples, including the control without any treatments, were stored at 4˚C. Quality changes were monitored every 3 days for 15 days.

6.4.3.2. Microbiological analyses

Total viable count (TVC), psychrophilic bacterial count (PBC), H_2S producing bacteria count (H_2S-BC), *Enterobacteriaceae* count (EC), and *Pseudomonas* sp. count (PC) were evaluated using spread plate method with the appropriate dilutions and the selected media to monitor microbiological changes in TSs during refrigerated storage following the procedures of Tagrida and Benjakul (2021).

6.4.3.3. Chemical analyses

Total volatile base (TVB) content was determined as per the method of Yu *et al.* (2018) and were expressed as mg N/100 g fish meat. Thiobarbituric acid reactive substances (TBARS) and peroxide value (PV) were measured as detailed by Jin *et al.* (2020) and were expressed as mg malondialdehyde (MDA) equivalent/kg flesh, and as mg cumene hydroperoxide/kg flesh, respectively. pHs of samples were taken at day 0 and during storage at 4˚C for 15 days.

6.4.3.4. Fatty acid profile

Lipids were extracted as per the method of Folch *et al.* (1957) from the control and treated samples at day 0 and those samples stored for 12 days with TVC lower than 6.0 log CFU/g, which is the accepted microbiological limit for fish product (ICMSF, 2002). Fatty acid profile was determined from the extracted lipids following the method described by Muhammed *et al.* (2015). Fatty acid methyl esters (FAME) were prepared by transmethylation of the extracted lipids (10 mg) by methanolic sodium hydroxide (2 M) and methanolic hydrochloric acid (2 M). Gas chromatography system (Agilent 7890B, Santa Clara, CA, USA) equipped with flame ionization detector (FID) was used for analysis of the prepared FAME. Peaks were identified according to the retention time of standards and the results were expressed as g/100 g of lipid.

6.4.3.5. Fourier transform infrared spectroscopy (FT-IR)

The control (untreated) and treated TSs at day 0 and day 12 were evaluated for FT-IR spectra following the method of Chaijan *et al.* (2006). Samples were freeze-dried and spectra of the dried samples were acquired with the aid of Bruker INVENIO S FT-IR spectrometer (Bruker Co., Ettlingen, Germany) equipped with a A225/Q Platinum attenuated total reflectance (ATR) unit with single reflection diamond crystal cell. IR absorption in 400 – 4000 cm^{-1} region was determined using 32 scans with 4 cm^{-1} resolution. OPUS v8.5 software (Bruker Optik GmbH 2020©, Ettlingen, Germany) was used to analyze the data.

6.4.3.6. Sensory evaluation

The 9-point hedonic scale was used for the sensory analysis of the untreated (control) and treated TSs at day 0 and the stored samples with TVC less than 6.0 log CFU/g (Olatunde *et al.*, 2020). Fifty untrained panelists, the students and staffs at the Faculty of Agro-Industry, Prince of Songkhla University, Hat Yai, Thailand, who had no apparent allergies to fish consumption, were selected for the sensory evaluation. A separate sample was wrapped with aluminum foil, steamed for 5 min, and served to each panelist. The acceptable limit for the sensory score was 5.

6.4.4. Statistical analysis

Completely randomized design (CRD) was applied for the whole study. All the experiments were conducted in triplicates (n = 3) and the results were presented as mean ± standard deviation. One-way analysis of variance (ANOVA) was conducted, and Duncan's multiple range test (DMRT) was performed for mean comparison. SPSS package (SPSS 22.0 for Windows, SPSS Inc, Chicago, IL, USA) software was used for data analysis.

6.5. Results and discussion

6.5.1. Effect of L/BLEE or U/BLEE combined with MAP/NTP on shelf-life extension of TSs during storage at 4˚C

6.5.1.1. Microbial changes of TSs during storage

Changes in microbial load of TSs without any treatment (control), those with NTP treatment only (MAP-NTP), L/BLEE-400/MAP-NTP, U/BLEE-400/MAP NTP, L/BLEE-200/MAP-NTP, and U/BLEE-200/MAP-NTP samples are depicted in Fig. 24. On day 0, TVC (Fig. 24A) of samples without any treatment ranged from 3.38 to 4.06 log CFU/g, indicating freshness of the fish samples. However, TVC of the samples exposed to NTP treatment was lower than that of the control ($p < 0.05$), regardless of treatment with L/BLEE or U/BLEE, in which counts were between 3.38 and 3.73 log CFU/g. Lowering of microbial load was more likely attributed to the NTP treatment. NTP caused gas excitation that initiated the generation of different RS, most profoundly ozone molecules (O_3) which were reported to have antimicrobial properties (Albertos *et al.*, 2019b). Thus, a higher decrease in TVC was found than the control. Efficiency of O_3 in bacterial inhibition was demonstrated previously (Albertos *et al.*, 2019b; Olatunde *et al.*, 2020). In the current study, the content of O_3 generated inside the bags was in the range of 2420 – 2530 ppm. Han *et al.* (2016) reported that NTP generated using atmospheric air had a remarkable antimicrobial activity, in which O_3 in the range of 120 – 4400 ppm was produced.

TVC of all the samples was raised with augmentation of storage time ($p < 0.05$). However, the raising rate was lower for samples treated with NTP, especially those added with L/BLEE or U/BLEE at 400 ppm. Generally, fish and other marine species are consumable when TVC was within the accepted marginal, which is 6.0 log CFU/g (ICMSF, 2002). After the third day of storage, TVC of the control exceeded this limit (6.58 log CFU/g), while TVC of other samples remained below the limit. On day 6 of storage, TVC of MAP-NTP surpassed the limit (6.17 log CFU/g). This indicated the ability of NTP in conjunction with MAP to reduce TVC up to approximately 6 days of refrigerated storage. Apart from antimicrobial activities of plasma, the reduction in TVC could be owing to bacterial inhibition abilities of carbonic acid formed after dissolution of CO_2 present in the packaging bags with water in the slices (Olatunde *et al.,* 2020). TVC of L/BLEE-200/MAP-NTP and U/BLEE-200/MAP-NTP exceeded 6.0 log CFU/g at day 9 with TVC of 6.03 log CFU/g and 6.14 log CFU/g, respectively. L/BLEE-400/MAP-NTP and U/BLEE-400/MAP-NTP had TVC of 5.77 log CFU/g and 5.87 log CFU/g, respectively, which were still below the accepted limit after 12 days of storage. However, at day 15, TVC of all the samples surpassed the acceptable limit. These results indicated the ability of MAP/NTP combined with pretreatment with L/BLEEs or U/BLEEs in extending the shelf-life of TSs by 9 days when L/BLEE or U/BLEE at 200 ppm was used. Shelf-life of 12 days was found when L/BLEE or U/BLEE at 400 ppm was added.

Antibacterial activity of BLEE was due to phenolic compounds such as vitexin 4′-O-galactoside and isovitexin present in the extract known for their antimicrobial properties (Tagrida and Benjakul, 2021). The results also suggested similar effect ($p > 0.05$) between L/BLEE and U/BLEE at different concentrations, signifying a success of the encapsulation process and indicating that the amount of the extract was employed at the same level, in addition to no apparent loss in the antimicrobial activity of the BLEE. PBC for all the samples was low at day 0 (Fig. 24B), however, the count was increased continuously with the augmenting storage time ($p < 0.05$). Only L/BLEE-400/MAP-NTP and U/BLEE-400/MAP-NTP showed PBC below 6.0 log CFU/g at day 12 with the values of 5.21 and 5.19 log CFU/g, respectively. The role of psychrophilic bacteria in spoilage of fish and fish products was extensively studied (Mol *et al.,* 2007). MAP/NTP in combination with L/BLEE or U/BLEE at 400 ppm could enhance the keeping qualities of TSs by retarding the proliferation of both mesophilic and psychrophilic bacteria for 12 days, while the control could be stored less than three days at 4˚C.

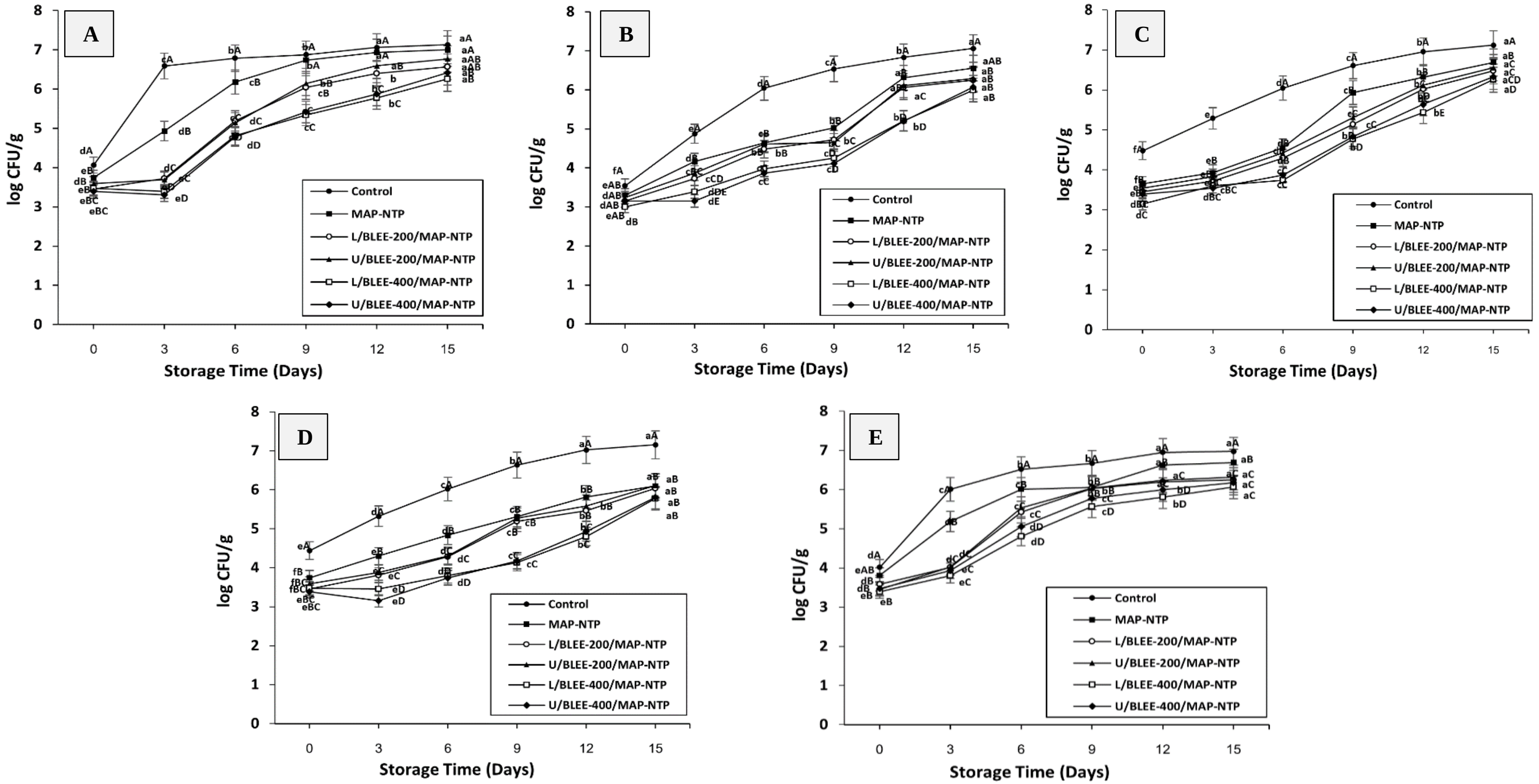

Figure 24. Total viable count (TVC) (A), psychrophilic bacteria count (PBC) (B), hydrogen sulfide producing bacteria count (H_2S-BC) (C), *Enterobacteriaceae* count (EC) (D), and *Pseudomonas* sp. count (PC) (E) of tilapia slices without any treatment (control), with MAP/NTP treatment, and with MAP/NTP treatment combined with addition of L/BLEE or U/BLEE at various concentrations during 15 days of storage at 4˚C. Bars represent standard deviation (n = 3). Different lowercase letters on bars within same treatment indicate significant difference ($p < 0.05$). Different uppercase letters on bars within the same storage time indicate significant difference ($p < 0.05$).

On day 0, all NTP treated samples had low H_2S-BC and EC, 3.38–3.65 and 3.33–3.77 log CFU/g, respectively (Fig. 24C and D), denoting the remarkable efficiency of MAP/NTP in bacterial inhibition. On the other hand, H_2S-BC and EC were slightly higher ($p < 0.05$) for the control (4.49 and 4.44 log CFU/g, respectively). Proliferation of bacteria probably took place during sample preparation. H_2S producing bacteria and *Enterobacteriaceae* are known for their vital roles in fish spoilage. H_2S producing bacteria can breakdown different amino acids such as methionine and L-cysteine found abundantly in fish muscles, thus producing H_2S with its repellent odor. *Enterobacteriaceae* relates to food poisoning and many nosocomial infections (Tagrida and Benjakul, 2021). H_2S-BC and EC were recorded at day 3 for MAP-NTP (3.92 and 4.29 log CFU/g, respectively), while the counts were still negligible for the other samples. At day 9 of storage, all the samples except L/BLEE-400/MAP-NTP and U/BLEE-400/MAP-NTP, surpassed 5 log CFU/g, considered as the maximum accepted limit of H_2S-BC (Olatunde *et al.,* 2020). At day 12, the counts for the aforementioned samples were still within the accepted limit for H_2S-BC (4.93 and 4.99 log CFU/g), while it was 4.80 and 4.92 log CFU/g for EC in L/BLEE 400/MAPNTP and U/BLEE-400/MAP-NTP samples, respectively. On day 15, the counts exceeded the H_2S-BC accepted limit and were high for EC. These findings remark the ability of L/BLEE or U/BLEE combined with MAP/NTP treatment for prolonging the shelf-life of TSs up to 12 days by retarding the growth of both H_2S producing bacteria and *Enterobacteriaceae*.

Pseudomonas sp. majorly contributed to fish spoilage accompanied by the unpleasant odor (Albertos *et al.,* 2019b). PC was lower for all samples treated with MAP/NTP as compared to that of the control ($p < 0.05$) (Fig. 24E). This confirmed the high potency of MAP/NTP for inhibiting the growth of *Pseudomonas* sp. Bacteriostatic activity of NTP particularly against *Pseudomonas* sp. has been reported (Albertos *et al.,* 2019b; Olatunde *et al.,* 2020). In addition, high CO_2 in MAP used in conjunction with NTP could inhibit the microorganisms including *Pseudomonas* sp. The PC reached 6.01 log CFU/g within day 6 for MAP-NTP. On day 9, L/BLEE-200/MAP-NTP and U/BLEE- 200/MAP-NTP samples had PC of 6.02 and 6.03 log CFU/g, respectively. L/BLEE-400/MAP-NTP and U/BLEE-400/MAP-NTP could maintain PC below such elevated counts for 12 days, as the counts of 5.80 and 5.99 log CFU/g were detected, respectively. The retardation in PC in these samples was related to many factors including the RS, which were formed because of NTP, the antimicrobial actions of CO_2 present in the bags, and the high phenolic content of BLEE.

Overall, no difference ($p > 0.05$) in antimicrobial activity between L/BLEE and U/BLEE was observed when the same level of extract in both treated slices was used, irrespective of encapsulation. Therefore, it was postulated that liposomes could release the extract located in the core and exhibited antimicrobial activity similar to the free unencapsulated BLEE prepared in amount equivalent to that loaded into the liposomes based on EE.

6.5.1.2. Chemical changes of TSs during storage

TVB content is an indicator of quality loss for fish and fish products, and it is determined by the quantification of the total nitrogenous compounds including ammonia (NH_3), dimethylamine (DMA), and trimethylamine (TMA) formed by either bacterial or enzymatic reactions. TMA is the product of the bacterial reduction of trimethylamine oxide (TMAO). TMAO does not serve as a substrate for their catabolism but act as an alternative electron acceptor, thus accelerating their growth especially under anaerobic condition (Leisner and Gram, 2000). TMA and the other nitrogenous compounds have an important role in the fishy odor of the stored fish and the increase in their contents is considered as an indicator of fish spoilage.

No difference ($p > 0.05$) was observed in TVB content among all the samples (Fig. 25A) at day 0, in which the ranges of 4.55 – 5.64 mg N/100 g was recorded. TVB content below 10 mg N/100 g indicates freshness of fish (Olatunde *et al.*, 2020). Overall, TVB content increased for all the samples within the first 6 days ($p < 0.05$). The control exhibited the highest increasing rate in TVB at day 6 with the value of 36.8 mg N/100 g, which exceeded the acceptable limit of 35 mg N/100 g (European Regulation, 2008). TVB content of the rest of TSs remained in the acceptable limits up to 6 days. However, at day 9, MAP-NTP, L/BLEE-200/MAP-NTP, and U/BLEE- 200/MAP-NTP samples exceeded the limit, in which TVB values of 44.6, 38.6, and 41.8 mg N/100 g, respectively. These findings affirmed the efficiency of MAP/NTP in reduction of microbial proliferation up to nine days. Nevertheless, L/BLEE or U/BLEE at 200 ppm did not show obvious combined effect with MAP/NTP, especially as the storage time augmented. At day 12, TVB contents of L/BLEE-400/MAP-NTP and U/BLEE-400/MAP-NTP samples were below the limit (31.4 and 33.2 mg N/100 g, respectively). Increased TVB content for the aforementioned samples was related to increasing microbial load (Fig. 24). Since L/BLEE-400/MAP-NTP and U/BLEE-400/MAP-NTP samples showed the lowest increasing rate of TVB content, the combined treatment of MAP/NTP with L/BLEE or U/BLEE at 400 ppm could retard the formation of the nitrogenous compounds for 12 days.

All samples at day 0 had no difference in their pHs ($p > 0.05$). The values were in the range of 6.23 – 6.27 (Fig. 25B). At day 3, the control had a slight increase ($p < 0.05$) in its pH (6.95), while MAP/NTP treated samples had a decrease ($p < 0.05$) in their pH (6.02–6.16), which was probably related to the formation of carbonic acid, caused by dissolution of CO_2 in the TSs. From day 6 onward until the end of storage (15 days), pH of all the samples was increased rapidly ($p < 0.05$). The control had the highest increasing rate, followed by MAP-NTP, L/BLEE-200/MAP-NTP, and U/BLEE-200/MAP-NTP. Lowest increasing rate of pH ($p < 0.05$) was observed for L/BLEE-400MAP-NTP and U/BLEE-400/MAP-NTP, in which the pH values were 7.12 and 7.20, respectively at day 12. In general, the increase in pH relates to the formation of nitrogenous basic compounds produced by microorganisms in the TSs. Thus, MAP/NTP combined with L/BLEE or U/BLEE at 400 ppm could lower the upsurge of pH in TSs by retarding bacterial growth. Moreover, there was no difference ($p > 0.05$) in pH of the samples treated with L/BLEE and U/BLEE at both levels. This was in line with the results of TVB content.

Lipid oxidation took place in the TSs as ascertained by hydroperoxides formed (Fig. 26A). It was noted that PV differed among the samples at day 0 ($p < 0.05$). TSs packed under MAP and treated with NTP (MAP-NTP) had higher PVs (0.29 – 0.35 mg cumene hydroperoxide/kg) than the control, which had PV of 0.18 mg cumene hydroperoxide/kg. This was more likely because of the actions of NTP, which induced lipid oxidation in fish slices.

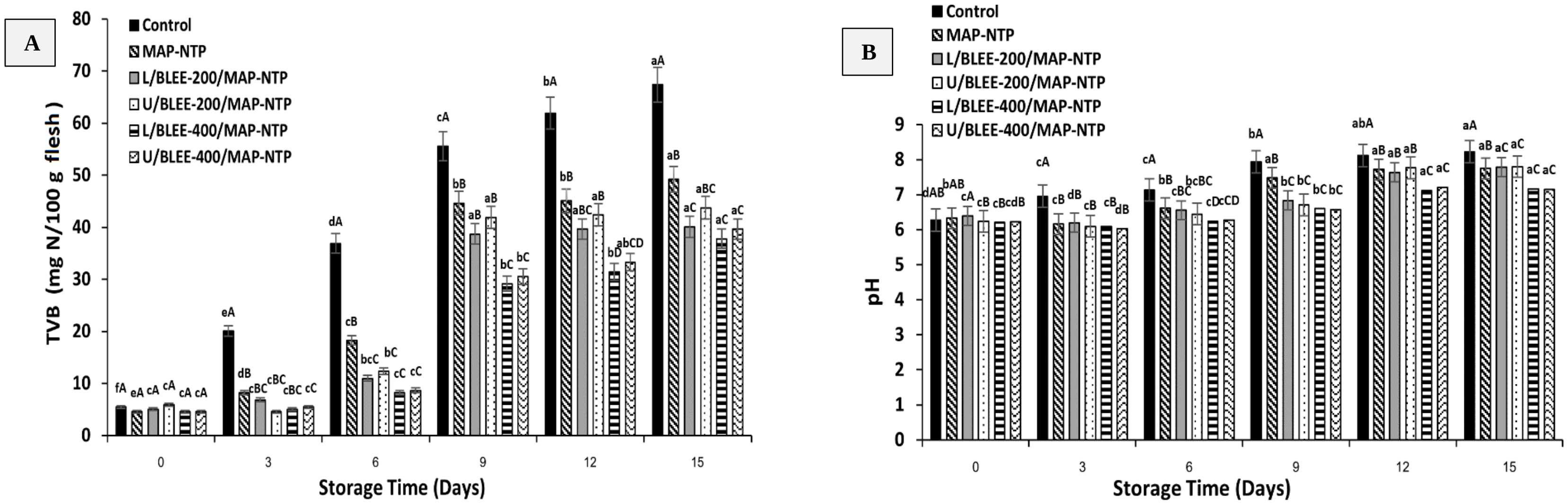

Figure 25. Total volatile base (TVB) content (A) and pH (B) of tilapia slices without any treatment (control), with MAP/NTP treatment and with MAP/NTP treatment combined with addition of L/BLEE or U/BLEE at various concentrations during 15 days of storage at 4˚C. Bars represent standard deviation (n = 3). Different lowercase letters on bars within same treatment indicate significant difference ($p < 0.05$). Different uppercase letters on bars within the same storage time indicate significant difference ($p < 0.05$).

Numerous active species could accelerate lipid oxidation, Gao *et al.* (2019) reported the increased lipid oxidation caused by cold plasma in processed ground chicken patties. In addition, CO_2 in MAP could be dissolved in water and carbonic acid formed was able to denature heme protein, thus releasing free non-heme iron known as prooxidant (Thiansilakul *et al.*, 2010). When storage time progressed, PV of control and MAP-NTP augmented rapidly ($p < 0.05$). The samples pretreated with L/BLEE or U/BLEE, particularly L/BLEE-400/MAP-NTP and U/BLEE-400/MAP-NTP also had the increase in PVs, but at lower rate than the control or MAP-NTP ($p < 0.05$), in which PVs of 5.91 and 6.26 mg cumene hydroperoxide/kg after 12 days were obtained. BLEE with antioxidant activities could scavenge the RS, thus reducing the oxidation rate, acquired, or induced initially by NTP.

TBARS represent the secondary products of lipid peroxidation induced by high microbial load or autolytic degradation and autooxidation (Dasgupta and Klein, 2014). Regardless of pretreatment with L/BLEE or U/BLEE, all TSs at day 0, packed under MAP and treated with NTP exhibited higher ($p < 0.05$) TBARS values (0.52 – 0.58 mg MDA/kg) than that of the control (0.42 mg MDA/kg) (Fig. 26B). This was related to increased lipid oxidation induced by NTP treatment. RS, particularly O_3 and other active species were able to accelerate the oxidation of food samples, especially those with high polyunsaturated fatty acid (PUFA) content (Olatunde *et al.*, 2020). TBARS value increased markedly for the control and MAP-NTP sample ($p < 0.05$) with augmentation of storage time, but the increasing rate of TBARS was much lower ($p < 0.05$) in samples treated with L/BLEE or U/BLEE, especially at 400 ppm. This result confirmed antioxidant activities of BLEE, that could reduce oxidation by scavenging a variety of RS. TBARS value lower than 4 mg MDA/kg in stored fish samples was considered an indication of acceptable quality (Ozogul *et al.*, 2010; Sousa *et al.*, 2018). At day 12, TBARS values of L/BLEE-400/MAP-NTP and U/BLEE-400/MAP-NTP were 3.01 and 3.25 mg MDA/kg, respectively. The remaining samples had TBARS content ranging from 4.19 to 4.83 mg MDA/kg. Therefore, MAP/NTP could be used along with pretreatment of L/BLEE or U/BLEE at 400 ppm to reduce lipid oxidation, thus decreasing undesirable odor or other side effects in TSs stored at 4˚C for 12 days.

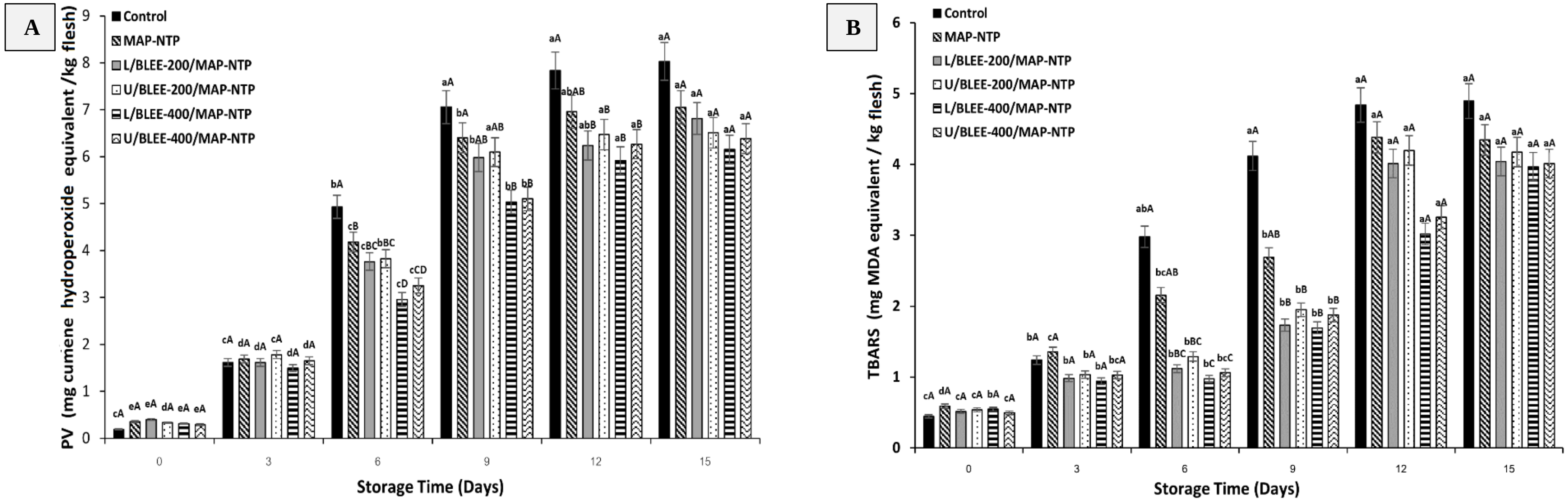

Figure 26. Peroxide value (PV) (A) and thiobarbituric acid reactive substances (TBARS) (B) of tilapia slices without any treatment (control), with MAP/NTP treatment and with MAP/NTP treatment combined with addition of L/BLEE or U/BLEE at various concentrations during 15 days of storage at 4˚C. Bars represent standard deviation (n = 3). Different lowercase letters on bars within same treatment indicate significant difference ($p < 0.05$). Different uppercase letters on bars within the same storage time indicate significant difference ($p < 0.05$).

6.5.2. Characteristics and sensory properties of the selected samples

6.5.2.1. Fatty acid profile

Fatty acid compositions of TSs without and with hurdle treatments are presented in Table 13. At day 0, similar fatty acids compositions were found among the samples ($p > 0.05$). Nevertheless, there were differences in some fatty acids between TSs with different treatments ($p < 0.05$). Palmitic, oleic, and linoleic acids were identified as the most abundant fatty acids in TSs at amounts of 15.6 – 16.7, 16.6 – 17.9, and 13.9–14.3 g/100 g, respectively. Palmitic acid is a saturated fatty acid (SFA) that could be used by some body cells for energy generation; however, it can cause adverse health impact if consumed excessively (Agostoni *et al.,* 2016). Oleic and linoleic acids are unsaturated fatty acids. The former belongs to the monounsaturated fatty acid (MUFA) and the latter is polyunsaturated fatty acid (PUFA). Both fatty acids are known for their beneficial health effects (Khan *et al.,* 2003). Eicosapentaenoic acid (EPA) and docosahexaenoic acid (DHA) were also detected at the first day of storage, with the ranges of 0.95 – 1.12 and 3.13 – 3.54 g/100 g, respectively. These PUFAs are renowned for their important roles in preventing heart disease, decreasing asthma and cancer, and overcoming some lung diseases (Erdman *et al.,* 2011). Overall, the amount of SFA, MUFA, and PUFA in the TSs were in the range of 25.33 – 26.87, 22.49 – 24.94, and 20.68 – 21.75 g/100 g, respectively. After MAP/NTP treatment, there was a noticeable increase ($p < 0.05$) in the amount of the SFA for all the treated samples, while the contents of MUFA and PUFA were decreased ($p < 0.05$). This was plausibly attributed to lipid oxidation induced by the RS. The result was in line with Olatunde *et al.* (2020) who reported the lower amount of both MUFA and PUFA in Asian seabass slices as a consequences of cold plasma treatment. Addition of either L/BLEE or U/BLEE had no marked impact on prevention of PUFA caused by MAP/NTP treatments at day 0.

On day 12, SFA continued to increase, while MUFA and PUFA further decreased. However, those changes were more pronounced in the control. L/BLEE-400/MAP-NTP and U/BLEE-400/MAP-NTP samples showed lower changes, confirming the effect of L/BLEE or U/BLEE in retardation of lipid oxidation by scavenging the RS and inhibiting bacterial growth in the TSs. No difference in fatty acid profile as influenced by both L/BLEE and U/BLEE was observed. This result was in accordance with PV and TBARS values (Figure 26A and B), reconfirming the effectiveness of the hurdles.

Table 13. Fatty acid profile of tilapia slices without and with MAP/NTP treatment combined with addition of L/BLEE or U/BLEE at day 0 and 12 of refrigerated storage

	Day 0						Day 12		
Fatty acid (g/100 g)	**Control**	**MAP-NTP**	**L/BLEE-200/ MAP-NTP**	**U/BLEE-200/ MAP-NTP**	**L/BLEE-400/ MAP-NTP**	**U/BLEE-400/ MAP-NTP**	**Control**	**L/BLEE-400/ MAP-NTP**	**U/BLEE-400/ MAP-NTP**
Saturated fatty acids (SFA)									
C12:0 (Lauric)	0.11^{aB}	0.12^{a}	0.11^{a}	0.12^{a}	0.12^{aB}	0.11^{aB}	0.37^{aA}	0.22^{abA}	0.19^{bA}
C14:0 (Myristic)	3.93^{cB}	4.02^{ab}	4.08^{a}	4.00^{b}	4.08^{aB}	4.05^{abB}	7.15^{aA}	5.01^{bA}	5.16^{bA}
C15:0 (Pentadecanoic)	0.63^{cA}	0.66^{b}	0.63^{c}	0.68^{a}	0.65^{bA}	0.60^{cB}	3.06^{bA}	2.77^{aA}	2.97^{abA}
C16:0 (Palmitic)	15.6^{cA}	16.9^{a}	16.5^{ab}	16.7^{b}	16.4^{abB}	16.6^{bB}	24.2^{aA}	20.9^{bA}	21.0^{bA}
C17:0 (Heptadecanoic)	0.07^{aB}	0.08^{a}	0.07^{a}	0.07^{a}	0.08^{aB}	0.08^{aB}	0.54^{aA}	0.38^{bA}	0.39^{bA}
C18:0 (Stearic)	1.86^{cB}	1.83^{c}	2.01^{b}	2.02^{b}	2.04^{aB}	2.04^{aB}	5.07^{aA}	4.64^{bA}	4.57^{bA}
C20:0 (Arachidic)	0.10^{cB}	0.28^{a}	0.16^{bc}	0.21^{b}	0.17^{bB}	0.19^{bB}	1.42^{aA}	0.99^{cA}	1.01^{bA}
C23:0 (Tricosanoic)	2.93^{cB}	3.03^{b}	3.18^{a}	2.99^{bc}	3.05^{bB}	3.14^{aB}	7.29^{aA}	5.56^{bA}	5.62^{bA}
Total	$\mathbf{25.33^{cB}}$	$\mathbf{26.66^{b}}$	$\mathbf{26.74^{ab}}$	$\mathbf{26.79^{ab}}$	$\mathbf{26.59^{bB}}$	$\mathbf{26.87^{aB}}$	$\mathbf{49.1^{aA}}$	$\mathbf{40.47^{bA}}$	$\mathbf{40.91^{bA}}$
Monounsaturated fatty acids (MUFA)									
C14:1 (Myristoleic)	0.06^{aA}	0.05^{a}	0.05^{a}	0.06^{a}	0.05^{aA}	0.06^{aA}	ND	0.02^{aB}	0.02^{aB}
C16:1 (Palmitoleic)	6.32^{aA}	5.19^{b}	5.12^{c}	5.20^{b}	5.17^{bcA}	5.21^{bA}	5.85^{aB}	4.91^{bB}	4.96^{bB}
C17:1 cis 10 (cis-10- Heptadecanoic)	0.25^{bA}	0.26^{b}	0.28^{a}	0.19^{c}	0.28^{aA}	0.20^{cA}	0.08^{aB}	0.10^{aB}	0.09^{aB}
C18:1 cis 9 (Oleic)	17.9^{aA}	17.2^{b}	16.9^{c}	16.7^{db}	16.6^{dA}	16.8^{cA}	14.8^{bB}	15.8^{abB}	16.0^{aB}
C20:1 cis 11 (cis-11- Eicosenoic)	0.41^{aA}	0.34^{b}	0.36^{b}	0.39^{a}	0.39^{aA}	0.39^{aA}	0.01^{bB}	0.06^{aB}	0.07^{aB}
Total	$\mathbf{24.94^{aA}}$	$\mathbf{23.01^{b}}$	$\mathbf{22.71^{c}}$	$\mathbf{22.54^{d}}$	$\mathbf{22.49^{dA}}$	$\mathbf{22.66^{cdA}}$	$\mathbf{20.74^{bB}}$	$\mathbf{20.89^{abB}}$	$\mathbf{21.14^{aB}}$
Polyunsaturated fatty acids (PUFA)									
C18:2 cis 9,12 (Linoleic)	14.3^{aA}	14.0^{ab}	14.1^{ab}	14.0^{ab}	13.9^{bA}	14.0^{abA}	10.4^{bB}	12.0^{aB}	12.5^{aB}
C18:3 cis 6,9,12 (gramma-Linolenic)	0.61^{aA}	0.61^{a}	0.58^{b}	0.54^{c}	0.58^{bA}	0.53^{cA}	0.16^{bB}	0.25^{aB}	0.23^{aB}
C18:3 cis 9,12,15 (alpha-Linolenic)	0.45^{aA}	0.42^{ab}	0.43^{ab}	0.41^{b}	0.38^{cA}	0.41^{bA}	0.03^{bB}	0.07^{aB}	0.08^{aB}
C20:2 cis 11, 14 (cis-11,14-Eicosadienoic)	0.81^{aA}	0.83^{a}	0.77^{a}	0.79^{a}	0.80^{aA}	0.79^{aA}	ND	ND	ND
C20:3 cis 8,11,14 (cis-8,11,14-Eicosatrienoic)	0.92^{aA}	0.87^{ab}	0.86^{b}	0.89^{ab}	0.85^{bA}	0.88^{abA}	0.09^{bB}	0.21^{aB}	0.24^{aB}
C20:5 cis 5, 8,11,14,17 EPA (cis-5,8,11,14,17-Eicosapentaenoic)	1.12^{aA}	0.95^{b}	1.00^{ab}	1.01^{ab}	1.02^{abA}	1.07^{abA}	0.39^{bB}	0.78^{aB}	0.74^{aB}
C22:6 cis 4,710,13,16,19 DHA (cis-4,710,13,16,19-Docosahexaenoic)	3.54^{aA}	3.13^{b}	3.15^{b}	3.13^{b}	3.15^{bA}	3.15^{bA}	2.07^{bB}	2.40^{aB}	2.39^{aB}
Total	$\mathbf{21.75^{aA}}$	$\mathbf{20.81^{b}}$	$\mathbf{20.89^{b}}$	$\mathbf{20.77^{b}}$	$\mathbf{20.68^{bA}}$	$\mathbf{20.83^{bA}}$	$\mathbf{13.14^{bB}}$	$\mathbf{15.71^{aB}}$	$\mathbf{16.18^{aB}}$

Different lowercase superscripts in the same row within the same storage time indicate significant differences ($p < 0.05$). Different uppercase superscripts in the same row within the same treatment indicate significant differences ($p < 0.05$). ND: not detected.

6.5.2.2. FT-IR spectra

L/BLEE-400/MAP-NTP and U/BLEE-400/MAP-NTP, which showed the promising keeping quality, were selected to investigate their structural changes after 12 days of refrigerated storage using FT-IR in comparison to the control and corresponding samples at day 0 (Fig. 27**)**. Spectral region of 400 – 4000 cm^{-1} will provide information about the vibrational modes linked to the different functional groups and molecular composition (Volpe *et al.*, 2019). At day 0, all the samples showed similar patterns, nevertheless MAP/NTP treated samples had a slight increased intensity of peaks at 3011 cm^{-1}, while it was absent in the control. Usually, lipid oxidation can be indicated by variations of peaks with absorbance at 3009 – 3011 cm^{-1} (═ CH olefinic stretch), which are related with ethyl esters, at 2920 – 2924 cm^{-1} (CH_2 asymmetric stretch) and 2852 – 2854 cm^{-1} (CH_2 symmetric stretch). These peaks can be found in saturated lipids, phospholipids, and side chains of proteins, while wavenumbers of 1743 – 1745 cm^{-1} linked to carbonyl formation (Volpe *et al.*, 2019). An increased intensity was also observed at 1745 cm^{-1}, confirming that oxidation took place in those samples subjected to MAP/NTP treatment.

At day 12, the control had a noticeable increase in peak intensity of the aforementioned wavenumbers. Less change was observed in peak intensity of L/BLEE-400/MAP-NTP and U/BLEE-400/MAP-NTP samples. This indicated that lipid oxidation occurred in the control to a higher extent. The oxidation was prevented in treated samples because of the dual action of MAP/NTP and BLEE that retarded the bacterial growth and acted as antioxidant. At day 12, an increase in peak intensity was observed for the control in amide I band located at 1638 – 1640 cm^{-1} (C ═ O stretch), in amide II band at 1530 – 1535 cm^{-1} (N ─ H bend, C ─ N stretch), and in amide III band at 1380 – 1385 cm^{-1} (C ═ O ─ N bend). The increased intensity of these peaks located in regions corresponding to amides and amines could be attributed to microbial proteolytic activity, in which free amide or amine could be produced. Govari *et al.* (2021) reported that the increased FT-IR absorption peaks observed for seabass fillets at similar regions was possibly because of the production of spoilage metabolites by *Pseudomonas* sp.

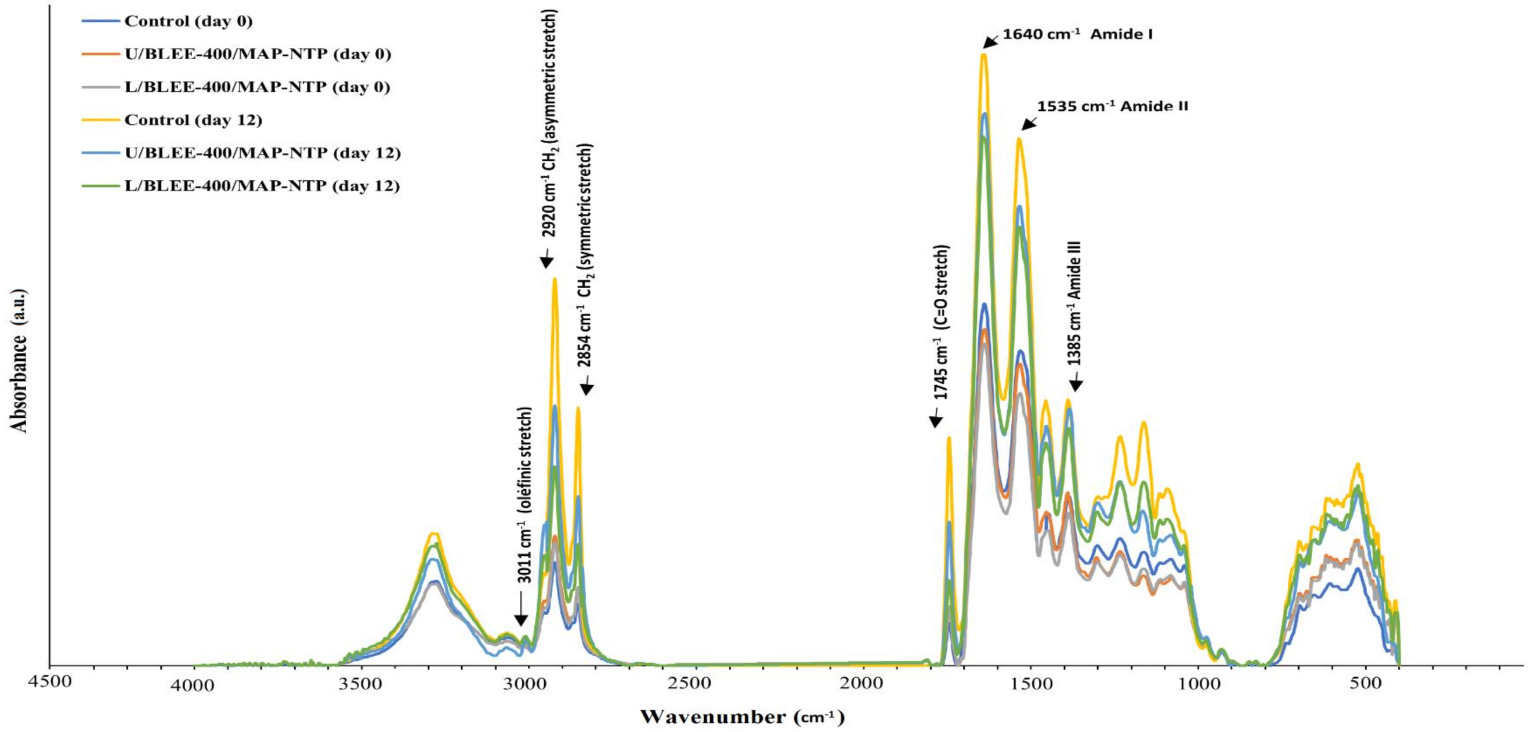

Figure 27. FT-IR spectra of tilapia slices (TSs) without treatment (control) and with MAP/NTP treatment combined with addition of L/BLEE (L/BLEE-400/MAP-NTP) and unencapsulated BLEE (U/BLEE-400/MAP-NTP) at day 0 and day 12 of refrigerated storage.

From the FT-IR spectra, the increase in absorbance of peaks at the same regions and the shift of the wavenumbers were lower in L/BLEE-400/MAP-NTP and U/BLEE-400/MAP-NTP samples than the control, suggesting that MAP/NTP combined with L/BLEE or U/BLEE could slow down lipid oxidation and proteolytic activities, thus minimizing the structural changes of TSs. These findings were in tandem with the lower microbiological and chemical alterations of TSs subjected to MAP/NTP in conjunction with BLEE during refrigerated storage for 12 days. Similar spectra were observed between L/BLEE-400/MAP-NTP and U/BLEE-400/MAP-NTP samples at the same storage time.

6.5.2.3. Acceptability

No difference ($p > 0.05$) was detected in appearance, color, and texture likeness scores between the control, MAP-NTP, L/BLEE-200/MAP-NTP, and L/BLEE-400/MAP-NTP at day 0 of storage (Table 14), but a minor difference ($p < 0.05$) was apparent between the control, U/BLEE-200/MAPNTP and U/BLEE-400/MAP-NTP. This difference could be related to the characteristic color of the BLEE, which could affect the color and appearance of the samples. Higher likeness scores in color and appearance for samples pretreated with L/BLEE confirmed the efficiency of liposome encapsulation for masking the color of BLEE. A slight difference ($p < 0.05$) in odor, taste, and flavor likeness scores was found between the control and the MAP-NTP treated samples, but similar overall likeness scores were obtained between those samples ($p > 0.05$).

This difference was more likely because of the RS generated by MAP/NTP, which led to minor changes in these samples. Lipid oxidation induced by MAP/NTP could be responsible for such lower likeness scores in flavor, taste, and odor at day 0 of storage, which was strongly correlated with the TBARS and PV results. Likeness scores for all attributes were decreased after 12 days of storage for L/BLEE-400/MAP-NTP and U/BLEE-400/MAP-NTP samples, in which TVC was still below the accepted limit. The lower scores were mostly because of the elevated formation of lipid oxidation products and nitrogenous compounds. L/BLEE-400/MAP-NTP exhibited slightly higher ($p < 0.05$) overall likeness scores than U/BLEE-400/MAPNTP, which might be attributed to the slow release of BLEE into

Table 14. Likeness scores of tilapia slices without and with MAP/NTP treatment combined with addition of L/BLEE or U/BLEE at day 0 and 12 of refrigerated storage

Sample	Day 0						Day 12	
	Control	MAP-NTP	L/BLEE-200/ MAP-NTP	U/BLEE-200/ MAP-NTP	L/BLEE-400/ MAP-NTP	U/BLEE-400/ MAP-NTP	L/BLEE-400/ MAP-NTP	U/BLEE-400/ MAP-NTP
Appearance	8.71 ± 0.45^{a}	8.69 ± 0.41^{a}	8.71 ± 0.41^{a}	8.61 ± 0.48^{b}	8.70 ± 0.48^{b}	8.59 ± 0.35^{b}	7.11 ± 0.17^{a}	7.18 ± 0.59^{a}
Color	8.66 ± 0.72^{a}	8.65 ± 0.67^{a}	8.68 ± 0.75^{a}	8.48 ± 0.72^{b}	8.66 ± 0.79^{a}	8.51 ± 0.79^{b}	6.13 ± 0.74^{a}	6.19 ± 0.75^{a}
Texture	8.66 ± 0.45^{a}	8.63 ± 0.82^{a}	8.62 ± 0.77^{a}	8.61 ± 0.25^{a}	8.62 ± 0.77^{a}	8.63 ± 0.88^{a}	6.06 ± 0.88^{a}	6.13 ± 0.86^{a}
Odor	8.76 ± 0.45^{a}	8.51 ± 0.72^{b}	8.56 ± 0.71^{b}	8.55 ± 0.63^{b}	8.46 ± 0.77^{b}	8.45 ± 0.83^{b}	5.22 ± 0.77^{a}	5.26 ± 0.79^{a}
Taste	8.73 ± 0.51^{a}	8.56 ± 0.74^{b}	8.52 ± 0.67^{b}	8.58 ± 0.63^{b}	8.46 ± 0.88^{b}	8.53 ± 0.83^{b}	5.26 ± 1.16^{a}	5.26 ± 1.12^{a}
Flavor	8.68 ± 0.48^{a}	8.55 ± 0.63^{b}	8.53 ± 0.77^{b}	8.51 ± 0.67^{b}	8.47 ± 0.67^{b}	8.33 ± 0.59^{c}	5.06 ± 0.37^{a}	5.03 ± 0.74^{a}
Overall likeness	8.69 ± 0.51^{a}	8.63 ± 0.66^{a}	8.65 ± 0.68^{a}	8.62 ± 0.61^{a}	8.64 ± 0.56^{a}	8.62 ± 0.71^{a}	5.87 ± 0.82^{a}	5.73 ± 0.81^{b}

Values represent the mean and standard deviation (n = 50). Different lowercase superscripts in the same row within the same storage time indicate significant differences ($p < 0.05$). Control: tilapia slices without any treatment, MAP-NTP: tilapia slices with MAP/NTP treatments only; L/BLEE-200/MAP-NTP and L/BLEE-200/MAP-NTP: tilapia slices with addition of L/BLEE or U/BLEE, respectively at 200 ppm and with MAP/NTP treatments; L/BLEE-400/MAP-NTP and L/BLEE-400/MAP-NTP: tilapia slices with addition of L/BLEE or U/BLEE, respectively at 400 ppm and with MAP/NTP treatments during 15 days of storage at 4˚C.

the TSs from liposomes, thus preserving the antioxidant activities of the extract for a longer period. Also, liposomes could mask the color of BLEE, thus lowering negative impact on TSs. Nevertheless, all the scores were above the acceptable limit (5.00), indicating the ability of these treatments to maintain the sensorial acceptability of TSs up to 12 days.

6.6. Conclusion

When nonthermal plasma was applied on TSs packaged under MAP and pretreated with L/BLEE or U/BLEE particularly at 400 ppm, the shelf-life of TSs could be extended to 12 days under refrigerated storage. Based on spoilage and lipid oxidation indices, such a treatment yielded lower lipid oxidation and provided better keeping qualities. The overall likeness of L/BLEE-400/MAP-NTP and U/BLEE-400/MAP-NTP showed no difference from the control at day 0, and they were still acceptable after 12 days of refrigerated storage, when the microbial load was still lower than the accepted limit. Therefore, MAP/NTP combined with L/BLEE or U/BLEE pretreatment could be a promising means for shelf-life extension of TSs.

6.7. References

Agostoni, C., Moreno, L. and Shamir, R. 2016. Palmitic acid and health: Introduction. Critical Reviews in Food Science and Nutrition. 56: 1941 - 1942.

Albertos, I., Martin-Diana, A., Burón, M. and Rico, D. 2019a. Development of functional bio-based seaweed (*Himanthalia elongata* and *Palmaria palmata*) edible films for extending the shelf-life of fresh fish burgers. Food Packaging and Shelf Life. 22: 100382.

Albertos, I., Martin-Diana, A., Cullen, P. J., Tiwari, B. K., Ojha, K. S., Bourke, P. and Rico, D. 2019b. Shelf-life extension of herring (*Clupea harengus*) using in-package atmospheric plasma technology. Innovative Food Science and Emerging Technologies. 53: 85 - 91.

Bouarab-Chibane, L., Degraeve, P., Ferhout, H., Bouajila, J., and Oulahal, N. 2019. Plant antimicrobial polyphenols as potential natural food preservatives. Journal of the Science of Food and Agriculture. 99(4):1457 – 1474.

Bourke, P., Ziuzina, D., Boehm, D., Cullen, P. J. and Keener, K. 2018. The potential of cold plasma for safe and sustainable food production. Trends in Biotechnology. 36: 615 - 626.

Chaijan, M., Benjakul, S., Visessanguan, W. and Faustman, C. 2006. Changes of lipids in sardine (*Sardinella gibbosa*) muscle during iced storage. Food Chemistry. 99: 83 - 91

Chen, L., Gnanaraj, C., Arulselvan, P., El-Seedi, H., and Teng, H. 2019. A review on advanced microencapsulation technology to enhance bioavailability of phenolic compounds: Based on its activity in the treatment of Type 2 Diabetes. Trends in Food Science and Technology. 85: 149 – 162.

Chotphruethipong, L., Battino, M., and Benjakul, S. 2020. Effect of stabilizing agents on characteristics, antioxidant activities and stability of liposome loaded with hydrolyzed collagen from defatted Asian sea bass skin. Food Chemistry. 328: 127127.

Dasgupta, A. and Klein, K. 2014. Methods for measuring oxidative stress in the laboratory. Antioxidants in food, vitamins and supplements. Prevention and treatment of disease. Elsevier. ISBN: 978-0-12-405872-9: 19 - 40.

EC. 2008. European Commission Regulation (EC) No 1022/2008 of 17 October 2008 amending Regulation (EC) No 2074/2005 as regards the total volatile basic nitrogen (TVB-N) limits. L277/18 EN Official Journal the European Union.

Erdman, J., Oria, M. and Pillsbury, L. 2011. Eicosapentaenoic acid (EPA) and docosahexaenoic acid (DHA). Nutrition and traumatic brain injury: Improving acute and subacute health outcomes in military personnel. National Academies Press (US). PMID: 24983072.

Folch, J., Lee, M. and Sloane, S. 1957. A simple method for isolation and purification of total lipids from animal tissues. The Journal of Biological Chemistry. 226: 497 - 509.

Gao, Y., Zhuang, H., Yeh, H.-Y., Bowker, B. and Zhang, J. 2019. Effect of rosemary extract on microbial growth, pH, color, and lipid oxidation in cold plasma-processed ground chicken patties. Innovative Food Science and Emerging Technologies. 57: 102168.

Gavahian, M., Chu, Y.-H., Khaneghah, A. M., Barba, F. J. and Misra, N. 2018. A critical analysis of the cold plasma induced lipid oxidation in foods. Trends in Food Science and Technology. 77: 32 - 41.

Giannoglou, M., Stergiou, P., Dimitrakellis, P., Gogolides, E., Stoforos, N. G. and Katsaros, G. 2020. Effect of Cold Atmospheric Plasma processing on quality and shelf-life of ready-to-eat rocket leafy salad. Innovative Food Science and Emerging Technologies. 66: 102502.

Gortzi, O., Lalas, S., Chinou, I., and Tsaknis, J. 2006. Reevaluation of antimicrobial and antioxidant activity of *Thymus* spp. extracts before and after encapsulation in liposomes. Journal of Food Protection. 69(12): 2998 – 3005.

Govari, M., Tryfinopoulou, P., Parlapani, F. F., Boziaris, I. S., Panagou, E. Z. and Nychas, G.-J. E. 2021. Quest of intelligent research tools for rapid evaluation of fish quality: FTIR spectroscopy and multispectral imaging versus microbiological analysis. Foods. 10: 264.

Han, L., Patil, S., Boehm, D., Milosavljević, V., Cullen, P. and Bourke, P. 2016. Mechanisms of inactivation by high-voltage atmospheric cold plasma differ for *Escherichia coli* and *Staphylococcus aureus*. Applied and Environmental Microbiology. 82: 450 - 458.

ICMSF 2002. International commission on microbiological specifications for foods. Microbiological testing in food safety management in microorganisms in foods *7*, London: Kluwer Academic /Plenum.

Jin, S., Pang, Q., Liu, R., Yang, H., Liu, F., Wang, M., Wang, Y., Feng, X. and Shan, A. 2020. Dietary curcumin decreased lipid oxidation and enhanced the myofibrillar protein structure of the duck (*Anas Platyrhynchos*) breast muscle when subjected to storage. LWT- Food Science and Technology. 133: 109986.

Khan, F., Elherik, K., Bolton-Smith, C., Barr, R., Hill, A., Murrie, I. and Belch, J. J. 2003. The effects of dietary fatty acid supplementation on endothelial function and vascular tone in healthy subjects. Cardiovascular Research. 59: 955 - 962.

Kim, Y. H., Hong, Y. J., Baik, K. Y., Kwon, G. C., Choi, J. J., Cho, G. S., Uhm, H. S. and Choi, E. H. 2014. Measurement of reactive hydroxyl radical species inside the biosolutions during non-thermal atmospheric pressure plasma jet bombardment onto the solution. Plasma Chemistry and Plasma Processing. 34: 457 - 472.

Leisner, J. and Gram, L. 2000. Spoilage of fish. Encyclopedia of food microbiology. Academic Press. 2000: 813 - 820.

Liu, W., Ye, A., Han, F., and Han, J. 2019. Advances and challenges in liposome digestion: Surface interaction, biological fate, and GIT modeling. Advances in Colloid and Interface Science. 263: 52 – 67.

Miyamoto, K., Ikehara, S., Takei, H., Akimoto, Y., Sakakita, H., Ishikawa, K., Ueda, M., Ikeda, J.-I., Yamagishi, M. and Kim, J. 2016. Red blood cell coagulation induced by low-temperature plasma treatment. Archives of Biochemistry and Biophysics. 605: 95 - 101.

Mol, S., Erkan, N., Uecok, D. and Tosun, Ş. Y. 2007. Effect of psychrophilic bacteria to estimate fish quality. Journal of Muscle Foods. 18: 120 - 128.

Moutiq, R., Misra, N., Mendonca, A. and Keener, K. 2020. In-package decontamination of chicken breast using cold plasma technology: Microbial, quality and storage studies. Meat Science. 159: 107942.

Muhammed, M., Domendra, D., Muthukumar, S., Sakhare, P. and Bhaskar, N. 2015. Effects of fermentatively recovered fish waste lipids on the growth and composition of broiler meat. British Poultry Science. 56: 79 - 87.

Olatunde, O. O., Benjakul, S. and Vongkamjan, K. 2020. Cold plasma combined with liposomal ethanolic coconut husk extract: A potential hurdle technology for shelf-life extension of Asian sea bass slices packaged under modified atmosphere. Innovative Food Science and Emerging Technologies. 65: 102448.

Ozogul, Y., Ayas, D., Yazgan, H., Ozogul, F., Boga, E. K., and Ozyurt, G. 2010. The capability of rosemary extract in preventing oxidation of fish lipid. International Journal of Food Science and Technology. 45(8): 1717 - 1723.

Sousa, R., Pedrosa, R., and Gil, M. M. 2018. Lipid oxidation inhibition by natural tocopherols increases the nutritional value of tuna salami. Advances in Food Technology and Nutritional Science. 4(1): 4 - 9.

Tagrida, M., and Benjakul, S. 2020. Ethanolic extract of betel (*Piper betle* L.) and Chaphlu (*Piper sarmentosum* Roxb.) dechlorophyllized using sedimentation process: Production, characteristics, and antioxidant activities. Journal of Food

Biochemistry. 44(12): e13508.

Tagrida, M. and Benjakul, S. 2021. Betel (*Piper betle* L.) leaf ethanolic extracts dechlorophyllized using different methods: antioxidant and antibacterial activities, and application for shelf-life extension of Nile tilapia (*Oreochromis niloticus*) fillets. RSC Advances. 11: 17630 - 17641.

Thiansilakul, Y., Benjakul, S. and Richards, M. P. 2010. Changes in heme proteins and lipids associated with off-odour of seabass (*Lates calcarifer*) and red tilapia (*Oreochromis mossambicus*× *O. niloticus*) during iced storage. Food Chemistry. 121: 1109 - 1119.

Volpe, M. G., Coccia, E., Siano, F., Di Stasio, M. and Paolucci, M. 2019. Rapid evaluation methods for quality of trout (*Oncorhynchus mykiss*) fresh fillet preserved in an active edible coating. Foods. 8: 113.

Yu, D., Regenstein, J. M., Zang, J., Jiang, Q., Xia, W. and Xu, Y. 2018. Inhibition of microbial spoilage of grass carp (*Ctenopharyngodon idellus*) fillets with a chitosan-based coating during refrigerated storage. International Journal of Food Microbiology. 285: 61 - 68.

CHAPTER 7

FISH GELATIN/CHITOSAN BLEND FILMS INCORPORATED WITH BETEL (*PIPER BETLE* L.) LEAF ETHANOLIC EXTRACTS: CHARACTERISTICS, ANTIOXIDANT AND ANTIMICROBIAL PROPERTIES

7.1. Abstract

Mechanical, barrier, and thermal properties of biodegradable films prepared using different gelatin/chitosan blends without and with betel leaf ethanolic extract (BLEE) at 1 and 2% were investigated. Incorporation of BLEE enhanced elasticity and heat-seal ability of the films. However, the seal ability was diminished with increasing chitosan proportion ($p < 0.05$). Ultraviolet and visible light barrier abilities along with water vapor permeability were improved ($p < 0.05$) for films containing 2% BLEE. Swelling and water solubility of the films were lessened with augmenting BLEE concentrations ($p < 0.05$). Antioxidant and antibacterial activities were augmented as BLEE levels incorporated increased. SEM images of selected films showed smooth homogenous surface and cross-section in film sample devoid of BLEE, while those incorporated with BLEE had slightly rough surface and cross-section. FT-IR spectra revealed the difference in peaks and patterns between films without and with BLEE. Addition of BLEE enhanced thermal stability of film associated with lowered structure of film. Thus, gelatin/chitosan films containing BLEE could serve as active packaging with satisfactory properties.

7.2. Introduction

Among the important issues raised by the United Nations (UN) climate change conference (COP26), the unaccepted increasing rate of plastic usage was pointed out as the major cause for the severe changes to the global climate. Therefore, innovative solutions are needed urgently. Plastics alone were estimated to account for 15% of the world’s carbon emission, which is approximately equivalent to 1.7 gigatons of CO_2. This number is expected to quadruple by 2050 if no strict actions are implemented (Abelson, 2021). Moreover, plastic pollution particularly in oceans and other water sources can be doubled by 2030 due to the current heavy consumption and the low rate of recycling, which is now less than 10% (UNEP, 2021).

Development of novel biodegradable packaging materials from natural polymers (e.g., proteins, polysaccharides, and lipids) to replace the commonly used plastics has been continuously done as green process for environment protection (Gómez-Estaca, *et al.,* 2010). Among biodegradable packaging materials, gelatin and chitosan have potential to form films with excellent barrier properties (Nowzari *et al.,* 2013). Gelatin, partially denatured or hydrolyzed collagen, has been used for film preparation due to excellent oxygen barrier property (Karim and Bhat, 2009). Due to some limiting properties of gelatin film such as swelling and poor water vapor barrier properties, modifications on gelatin forming solutions through cross-linking with other polymers chains is needed to improve the resulting film (Nowzari *et al.,* 2013). Chitosan, on the other hand, is a linear β-1,4-D-glucosamine semicrystalline polysaccharide obtained by deacetylation of chitin (Tian and Liu, 2020). Chitosan has been used as film forming material because of its biocompatibility, non-toxicity, low oxygen permeability, and antimicrobial properties (Bonilla and Sobral, 2016). Blend films made from gelatin and chitosan blends had an improved mechanical and physiochemical properties over those made only from a single component (Qiao *et al.,* 2017). This improvement was based on polyelectrolyte complexes formed and interconnection via the protonated amino groups of chitosan and the negatively charged carboxylate groups of gelatin under a controlled pH (Pereda *et al.,* 2011).

To enhance the composite film properties, especially antioxidant and antibacterial properties, plant-based products having both antioxidant (AO-A) and antibacterial activities (AB-A) could be incorporated in film forming solution instead of the synthetic additives. As a consequence, biodegradable active packaging can be produced using composite films with augmented preservative activities and minimized usage of synthetic chemicals (Moradi *et al.,* 2012). Betel, a leafy plant grown in Southeast Asian countries, was used previously in traditional medicine and as a food due to its bioactivities. Betel leaf ethanolic extract (BLEE) dechlorophyllized by sedimentation (green process) contained a relatively high content of polyphenols and flavonoids including isovitexin, vitexin 4′-O-galactoside, epigallocatechin, and kaempferol derivatives known for their immense AO-A and AB-A (Tagrida and Benjakul, 2020). Therefore, BLEE could be a suitable candidate as a natural extract, in which biodegradable active packaging can be developed.

The current work therefore aimed to investigate mechanical and physical properties of gelatin/chitosan blend films incorporated with BLEE at different levels. AO-A and AB-A of resulting films were also determined.

7.3. Objectives

To investigate the antioxidant, antimicrobial, and mechanical properties of gelatin/chitosan blend films incorporated with betel leaf ethanolic extracts.

7.4. Materials and methods

7.4.1. Chemicals

Fish gelatin powder (bloom: 250; molecular weight (MW): ~5.1 × 10^4 Da; moisture content: 9.99%) was purchased from Vinh Hoan Corp. (Dong Thap, Vietnam). Chitosan (MW: ~2.1× 10^3 KDa; degree of deacetylation (DDA): ~82%; viscosity: 1000 – 2000 cps) was supplied by Marine Bioresources Co. Ltd. (Samut-Sakhon, Thailand). Acetic acid and ethanol were procured from RCI labscan Limited (Bangkok, Thailand). Glycerol was acquired from Ajax Finechem Pty. Ltd. (Taren Point, Australia). Folin–Ciocalteu reagent (FCR) was brought from Merck Ltd. (Bangkok, Thailand).

7.4.2. Preparation and dechlorophyllization of BLEE

Extraction of BLEE was performed (Tagrida and Benjakul, 2020), in which betel leaf powder was mixed with 70% ethanol (v/v) at the ratio of 1:15 (w/v). After removal of the solvent with the aid of a rotary evaporator, dechlorophyllization of concentrated extract was done by sedimentation method (Tagrida and Benjakul, 2020). The extract was freeze-dried, and the powder was placed in a capped vial and kept at -20˚C until use.

7.4.3. Preparation of blend films

Casting technique was adopted for film preparation. Fish gelatin film forming solution (GFS) was prepared (Nilsuwan *et al.*, 2018). Gelatin powder (3.5 g) was mixed with distilled water (100 mL) and heated for 15 min at 65˚C with continuous stirring until complete solubilization. The method of Mittal *et al.* (2021) was followed for preparing chitosan film forming solution (CFS). Chitosan (1 g) was mixed with 100 mL of 1% (v/v) acetic acid and then stirred overnight at room temperature. GFS and CFS were mixed to obtain different gelatin/chitosan ratios (9:1, 7.5:2.5, and 5:5 (w/w)). Glycerol, as the plasticizer, was added at 30% (w/w, based on total solid content). The pH of film forming solutions (FF-S) was adjusted to 3.0 to avoid the precipitation of chitosan. Subsequently, the blends were further stirred for 1 h. BLEE was incorporated into all the blends at 1 or 2% and stirred until BLEE was completely dissolved.

FF-S with different GFS/CFS ratios were termed as G9:C1-1%, G7.5:C2.5-1%, and G5:C5-1% for FF-S containing 1% BLEE and G9:C1-2%, G7.5:C2.5-2%, and G5:C5-2% for FF-S added with 2% BLEE. Film blends without BLEE were also prepared and termed as G9:C1-0%, G7.5:C2.5-0%, and G5:C5-0%. The prepared FF-S (without and with BLEE) were degassed for 10 min in a sonication bath (Elmasonic S 70 H, Elma Schmidbauer, Singen, Germany). Four grams of each of the FF-S were casted onto the cells (5 × 5 cm^2) of rimmed silicone resin plates. Air drying of films was carried out overnight with the aid of an air-blower at the relative humidity (RH) of 65 – 70% and 25˚C. Subsequently, casted plates were equilibrated in an environmental chamber (Binder GmbH, Tuttlingen, Germany) with RH of 50 ± 5% at 25 ± 0.5˚C for 48 h. After being peeled off, films were conditioned in the environmental chamber before analyses.

7.4.4. Characterization of blend films without and with BLEE at different levels

7.4.4.1. Thickness

Thickness of film was measured using a micrometer (Mitutoyo, Model ID-C112PM, Serial No. 00330, Mitutoyo Corp., Kawasaki-shi, Japan). For each treatment, nine random spots on each of ten film samples were measured for thickness.

7.4.4.2. Mechanical properties

Tensile strength (TS) and elongation at break (EAB) were determined as tailored by Nilsuwan *et al.* (2018). TS (MPa) was calculated by dividing the maximum force (N) required to break down film with designated cross-section area

(m^2). EAB was computed by dividing the elongation of film by the initial grip length of samples and reported as percentage.

7.4.4.3. Seal ability

Seal strength (SS) and seal efficiency (SE) were examined (Nilsuwan *et al.,* 2018) using the peel test. Sealed films were subjected to tensile loaded at 100 N till the seal was broken apart. Both SS and SE were computed using the following equations:

$$\text{SS (N/m)} = \frac{\text{Peak force}}{\text{Film width}}$$

$$\text{SE (\%)} = \left(\frac{\text{Peak force}}{\text{Tensile force}}\right) \times 100$$

where tensile force is the force (N) acquired from tensile strength testing of a single film and peak force (N) is the maximum force gotten from the seal testing.

7.4.4.4. Color

Color measurements of the films were conducted (Mittal *et al.*, 2021) using a colorimeter (Hunterlab, Reston, VA, USA). L^* (lightness), a^* (redness/greenness) and b^* (yellowness/blueness) were recorded. Total color difference (ΔE^*) was computed as follows:

$$\Delta E^* = \sqrt{(\Delta L^*)^2 + (\Delta a^*)^2 + (\Delta b^*)^2}$$

where ΔL^*, Δa^* and Δb^* are the differences between the color parameter of the samples and those of the white standard (L^* = 92.83, a^* = -1.23, b^* = 0.48).

7.4.4.5. Light transmission and transparency

The method of Shiku *et al.* (2004) was adopted for determination of light transmission of the films in both ultraviolet (200 – 280 nm) and visible (350 – 800 nm) ranges with the aid of an UV-vis spectrophotometer (UV-1800, Shimadzu, Kyoto, Japan). The transparency value of films was computed (Han and Floros, 1997):

$$\text{Transparency value} = \frac{-\log T_{600}}{X}$$

where T_{600} is the fractional transmission at 600 nm and X is film thickness (mm). Lower film transparency is indicated by higher transparency value.

7.4.4.6. Swelling

Film swelling was evaluated following the procedure of Kumar *et al.* (2019) with slight modifications. Film specimens (2 x 2 cm^2) were dried in a hot air oven (105˚C for 24 h) and weighed. Dried samples were submersed in 50 mL of distilled water for 1 h, removed and the excess water was eliminated by placing on a filter paper for 5 min. The swollen specimens were weighed, and swelling was calculated as follows:

$$\text{Swelling (\%)} = \left(\frac{W_2 - W_1}{W_1}\right) \times 100$$

where W_1 and W_2 are the weight of the dried film specimen and the weight of the specimen after swelling and eliminating the excess water, respectively.

7.4.4.7. Water solubility

Solubility of the films was assessed at 25˚C (Liu *et al.*, 2020). After drying (section 7.4.4.6.) to a constant weight, specimens were continuously stirred with 50 mL of distilled water overnight. Thereafter, the mixture was filtered through stainless steel mesh (size: 40) and the remaining residues were dried at 105˚C for 24 h and weighed. The solubility of film was computed using the following equation:

$$\text{Water solubility (\%)} = \left(\frac{W_i - W_r}{W_i}\right) \times 100$$

where W_i and W_r are the initial weight of the dried film specimen and the weight of dried film residues after water immersion, respectively.

7.4.4.8. Water vapor permeability (WVP)

The method described by Nilsuwan *et al.* (2018) was adopted. Films were placed on the aluminum permeation cups containing 0% RH dried silica gel, silicon vacuum grease and a rubber gasket were used to tightly sealed the films on the cups. The cups were displayed in an environmental chamber (25 ± 2˚C and 50 ± 5% RH), and then were weighed every 1 h over a 10 h period. WVP was subsequently computed:

$$\text{WVP } (g\ m^{-1}\ s^{-1}\ Pa^{-1}) = \left(\frac{WVTR \times L}{\Delta P \times A}\right)$$

where WVTR is the water vapor transmission rate obtained from the slope of plot of cup weight gain vs time (g/s), L is thickness of the film (m), ΔP is water vapor pressure difference across the film (1583.74 Pa at 25˚C), and *A* is the exposed area of the film (m^2).

7.4.4.9. Bioactivities of composite films

7.4.4.9.1. Antioxidant activities (AO-A)

Small pieces of film (0.1 g) were mixed with distilled water (10 mL) and stirred overnight. The mixture was centrifuged for 20 min at 8000 x g, and the supernatants were collected and used for determination of AO-A following the method of Tagrida *et al.* (2021). DPPH and ABTS radical-scavenging activities (DPPH-RSA and ABTS-RSA, respectively), and ferric-reducing antioxidant power (FRAP) were examined and reported as μmol Trolox equivalent (TE)/g sample. Metal-chelating activity (MCA) was expressed as μmol EDTA equivalent (EE)/g sample

7.4.4.9.2. Antibacterial activity (AB-A)

Agar diffusion method described by Giménez *et al.* (2013) was implemented for evaluation of AB-A of different blend films against *Staphylococcus aureus*, *Escherichia coli*, *Listeria monocytogenes*, and *Pseudomonas aeruginosa* gifted from the Food Safety Laboratory, Prince of Songkhla University, Hat Yai, Thailand. One hundred μL of bacterial suspension (10^6 CFU/mL) were spread on tryptic soy agar (TSA) plates under aseptic condition. Subsequently, film samples cut into discs (diameter: 5 mm) were placed on the surface of the inoculated TSA plates. Plastic polyethylene films of the same size were used as control. All the plates were incubated for 24 h at 37˚C. Then the inhibition zone dimeter including the film sample was determined in millimeters.

7.4.5. Characterization of selected films

7.4.5.1. Scanning electron microscopy (SEM)

Morphology of the surface and cross-section of the selected film samples was visualized using Quanta 400-FEI scanning electron microscope (Eindhoven, The Netherlands). Film samples were fractured using liquid nitrogen for cross-sectional visualization. All the samples were mounted on bronze stub and sputtered with gold particles (Sputter coater SPI-Module, PA, USA) for conductivity. The acceleration voltage at 20 kV was selected for taking of the photographs.

7.4.5.2. Fourier transform infrared (FT-IR) spectroscopy

FT-IR spectra of the selected films were recorded using a horizontal ATR Trough plate crystal cell (45˚ ZnSe; 80 mm long, 10 mm wide and 4 mm thick) (PIKE Technology Inc., Madison, WI, USA) assembled to Bruker Model Equinox 55 FTIR spectrometer (Bruker Co., Ettlingen, Germany) at 25˚C (Nuthong *et al.*, 2009). Normalization was conducted for all the obtained spectra prior to interpretation.

7.4.5.3. Thermogravimetric analysis (TGA)

Thermostability of the selected films was evaluated with the aid of a simultaneous thermal analyzer (STA-8000, PerkinElmer, Norwalk, CT, USA) using the heating flow rate of 10˚C/min from 30 to 800˚C. Thermal degradation temperature and weight loss of selected film samples were determined. Nitrogen as the purge gas was used at a flow rate of 20 mL/min.

7.4.6. Statistical analysis

Completely randomized design (CRD) was applied for all studies. Data were reported as mean ± standard deviation (SD). One-way Analysis of Variance (ANOVA) was conducted, and Duncan's Multiple Range Test (DMRT) was done for mean comparison. SPSS package (SPSS 23.0 for Windows, SPSS Inc, Chicago, IL, USA) software was used for data analysis.

7.5. Results and discussion

7.5.1. Characteristics of gelatin/chitosan blend films prepared without and with BLEE at different levels

7.5.1.1. Thickness

Film thickness is a decisive parameter influencing mechanical and barrier properties of films. All control films with different gelatin/chitosan proportions showed similar thickness ($p > 0.05$). Regardless of the gelatin/chitosan ratio used, the incorporation of BLEE at different concentrations showed similar effect ($p > 0.05$) on thickness of the prepared films, in which the thickness ranged from 0.040 to 0.048 mm (Table 15). Blend films based on gelatin/chitosan without BLEE were thinner than those with BLEE ($p < 0.05$). This might be owing to the increased solid content in the films containing BLEE. Additionally, the interaction and alignment of gelatin and

Table 15. Thickness, mechanical properties, seal strength, seal efficiency, and color of blend films based on gelatin/chitosan at different proportions added with BLEE at various concentrations

Samples	**Thickness (mm)**	**TS (MPa)**	**EAB (%)**	**Seal strength (N/m)**	**Seal efficiency (%)**	***L****	***a****	***b****	**∆*E******
G9:C1-0%	0.034 ± 0.008^{c}	30.33 ± 7.06^{b}	12.72 ± 3.27^{cd}	NA*	NA	90.57 ± 0.21^{a}	-1.58 ± 0.03^{a}	1.85 ± 0.04^{d}	2.66 ± 0.20^{a}
G9:C1-1%	0.045 ± 0.003^{ab}	6.70 ± 1.25^{de}	88.43 ± 2.44^{b}	83.92 ± 14.41^{c}	46.33 ± 1.43^{c}	87.43 ± 0.21^{b}	-4.47 ± 0.06^{b}	34.8 ± 3.70^{bc}	34.9 ± 3.63^{bc}
G9:C1-2%	0.048 ± 0.002^{a}	3.62 ± 1.56^{e}	176.46 ± 6.4^{a}	254.43 ± 32.71^{a}	75.88 ± 1.75^{a}	77.56 ± 2.35^{e}	-6.90 ± 0.12^{c}	55.2 ± 1.61^{a}	57.1 ± 2.13^{a}
G7.5:C2.5-0%	0.033 ± 0.008^{c}	33.95 ± 6.35^{b}	5.58 ± 1.97^{d}	NA	NA	89.95 ± 0.18^{a}	-1.51 ± 0.02^{a}	1.61 ± 0.04^{d}	3.10 ± 0.18^{a}
G7.5:C2.5-1%	0.042 ± 0.002^{ab}	8.11 ± 2.90^{d}	33.71 ± 1.39^{c}	NA	NA	85.33 ± 0.42^{c}	-4.60 ± 0.51^{b}	34.5 ± 1.46^{bc}	35.1 ± 1.49^{bc}
G7.5:C2.5-2%	0.047 ± 0.004^{ab}	5.62 ± 1.10^{de}	70.55 ± 1.51^{b}	175.07 ± 31.74^{b}	62.23 ± 1.28^{b}	77.22 ± 4.34^{e}	-6.74 ± 0.54^{c}	54.3 ± 1.16^{a}	56.5 ± 1.30^{a}
G5:C5-0%	0.032 ± 0.008^{c}	44.24 ± 5.69^{a}	4.07 ± 0.60^{d}	NA	NA	89.29 ± 0.27^{ab}	-1.35 ± 0.1^{a}	1.87 ± 0.12^{d}	3.80 ± 0.26^{a}
G5:C5-1%	0.040 ± 0.006^{ab}	14.89 ± 3.17^{c}	7.54 ± 5.40^{d}	NA	NA	85.34 ± 0.60^{c}	-4.46 ± 0.56^{b}	37.2 ± 1.45^{b}	37.6 ± 1.54^{b}
G5:C5-2%	0.046 ± 0.003^{ab}	6.13 ± 2.68^{de}	23.54 ± 4.56^{cd}	NA	NA	79.96 ± 0.26^{d}	-6.86 ± 0.39^{c}	55.3 ± 0.32^{a}	56.6 ± 0.38^{a}

Values are mean ± SD. Different lowercase superscripts in the same column denote significant difference ($p < 0.05$). TS: tensile strength; EAB: elongation at break; BLEE: betel leaf ethanolic extract. G9:C1-1%, G7.5:C2.5-1%, and G5:C5-1% indicated film forming solutions (FF-S) with gelatin/chitosan ratios at 9:1, 7.5:2.5, and 5:5, respectively and containing 1% BLEE. G9:C1-2%, G7.5:C2.5-2%, and G5:C5-2% for FF-S added with 2% BLEE. G9:C1-0%, G7.5:C2.5-0%, and G5:C5-0% for FF-S without BLEE.

*NA: not applicable.

chitosan molecules as well as their matrix arrangements could have been impeded or rearranged by BLEE molecules, resulting in a relatively protruded network.

Similar observations were documented by Tongnuanchan *et al.* (2015) who found an increase in the thickness of gelatin films when the levels of the incorporated palm oil increased and Kumar *et al.* (2019) who observed that incorporation of citric acid to composite films of gelatin and starch led to an increased thickness due to reorientation of the films' matrix. Films without BLEE showed relatively higher thickness ($p < 0.05$) when the gelatin proportion increased. The increased hydrophilicity of gelatin associated with its hydroxyl groups attracted and trapped greater amount of water molecules, resulting in the swollen network. Also, gelatin is amorphous in structure, in which the compact structure of chain alignment rarely occurred.

7.5.1.2. Mechanical properties

Mechanical strength is a vital property of the prepared films in keeping their integrity when used as food packages and during their handling, transportation, or storage. Blend film sample (G5:C5-0%) without BLEE had the highest TS (44.24 ± 5.69 MPa) but lowest EAB (4.07 ± 0.60%) ($p < 0.05$) than others (Table 15). When the proportion of gelatin increased, TS was decreased, while EAB was augmented ($p < 0.05$). Generally, gelatin film is more flexible and softer than chitosan film due to its amorphous structure. On the contrary, chitosan is semi-crystalline structure which yields stiffer and stronger film (Mittal *et al.,* 2021). This result indicated that biomaterials with varying molecular structure and composition or chain length had a high impact on property of films, mainly by the alignment or interconnection between molecules in different fashions. For the same gelatin/chitosan ratio, films showed lower TS but higher EAB with increasing BLEE concentration ($p < 0.05$). This could be due the formation of higher amount of junction zones as well as denser and more ordered network in films devoid of BLEE associated with elevated crosslinking. This made the films more rigid as witnessed by the higher TS with lower EAB. The films with BLEE, on the other hand, showed lesser TS since the extract might impede the interaction or entanglement of both gelatin and chitosan chains to form the ordered network. As a consequence, films became more flexible as seen by higher EAB.

Bonilla and Sobral (2016) showed that films made from either gelatin or chitosan had relatively higher TS and lower EAB than films containing different plant extracts. Varying cross-linking activities of different compounds in various plant extracts were postulated. It was noted that gelatin was less in lysine and had no cysteine (Monsur *et al.*, 2014). Those amino acids were the cross-linking sites induced by plant polyphenols (Cao *et al.*, 2007). Wu *et al.* (2014) documented the decreased TS and the augmented EAB due to the disturbance of the gelatin/chitosan film network by oregano essential oil, making film matrix discontinuous or uneven. Films with higher chitosan proportion showed higher TS but lower EAB than those with lower chitosan proportion ($p < 0.05$). The increased interactions between chitosan chains could occur to a higher extent. Chitosan can provide more reactive groups, especially amino ($-NH_2$) groups and hydroxyl (-OH) groups, which favored intermolecular interaction via hydrogen bonds and hydrophobic interactions, resulting in the formation of polyanion-polycation complexes, which eventually strengthened the films (Liu *et al.*, 2012). However, gelatin with amino acid side chain might interact with chitosan to some degree, leading to the composite matrix. This result indicated that chitosan could yield a stronger film than gelatin.

7.5.1.3. Seal ability

Efficient heat-sealing ability is highly regarded in any prepared biodegradable film, as it is required to prevent the leakage of products, especially if they are in liquid state. It is also important in deciding the efficiency of the package whether as bag or pouch during handling or storage. Surface of two films was melted by the applied heat which could enhance interfacial interactions or merging across the contacted surfaces. This resulted in efficient sealing between two films. The preliminary study showed that heating temperature of $150 \pm 0.5^{\circ}C$ for 1.25 s, with subsequent cooling for 1.50 s could provide the sufficient melting and fusion for most tested films. Among all the prepared gelatin/chitosan blend films, only three samples showed successful heat-sealing ability (Table 15).

The failure in sealing was probably attributed to the presence of chitosan at relatively elevated level within the blend films. Chitosan has poor thermoplastic properties and can be degraded before the melting point. In general, chitosan cannot be molded, or extruded and films containing high amount of chitosan were not sealable (Cazón and Vázquez, 2020). This was observed clearly in films containing a higher amount of chitosan. Furthermore, seal strength of films tended to be weakened due to poor interfacial adhesion when an elevated hydrophobic polymer became incompatible with hydrophilic polymer, even at low level (Fathima *et al.*, 2018). G9:C1-2% sample had the highest seal strength and efficiency (254.43 N/m and 75.88%) followed by G7.5:C2.5-2% (175.07 N/m and 62.23%) and G9:C1-1% (83.92 N/m and 46.33%) ($p < 0.05$), respectively. Several factors determine the strength and efficiency of sealed films (Qiao *et al.*, 2017). Electrostatic interactions between the functional groups of both gelatin and chitosan coupled with the hydrogen bonds between the gelatin molecules and the plasticizer could be disrupted by heat, thus favoring the melting during heat sealing. G9:C1-2% sample plausibly had well-balanced electrostatic interactions between the gelatin and chitosan molecules via weak bond such as hydrogen bonding between gelatin molecules and plasticizer together with BLEE, resulting in looser network. This could facilitate the melting of film network, leading to interdiffusion of gelatin or chitosan molecules, improving the seal ability of this film. For G9:C1-1% films, seal ability markedly decreased as BLEE decreased; this could be due to the higher rigidity and compact network. This rigid film could not be melted effectively, thus lowering seal ability. The G7.5:C2.5-2% sample showed moderate seal ability, possibly due to the weak or moderate interactions between gelatin and chitosan molecules. Additionally, higher BLEE concentration (2%) presumably lowered the interaction among polymer chains in the film matrix. This could allow the films to be melted and sealed with ease. Nouri and Nafchi (2014) noted the importance of betel extract in providing efficient seal ability to films made from sago starch by increasing the hydrogen bonds between film components, which were easily destroyed by heat during sealing. Nevertheless, chitosan levels in other films (G7.5:C2.5-0% and G7.5:C2.5-1%) were relatively higher, thus failed in sealing by heat. Overall, the more rigid the film network, the inability to melt, and as a result, sealing could not be achieved.

7.5.1.4. Color

The visual observation showed that homogenous gelatin/chitosan blend films with no apparent insoluble particles were obtained, regardless of BLEE concentrations (Fig. 28). However, the color of the films was changed to yellowish color when BLEE was incorporated, and its intensity increased with augmenting BLEE concentration ($p < 0.05$). L^* and a^* values of films without BLEE were highest ($p < 0.05$), while their b^* and ΔE^* values were the lowest ($p < 0.05$) (Table 15). With increasing concentration of BLEE, L^* and a^* values decreased markedly ($p < 0.05$), indicating the decrease in film lightness and increase in its greenness, while b^* and ΔE^* values were increased ($p < 0.05$), reflecting the increases in both yellowness and total color change of these films containing BLEE. Such a change was more likely attributed to remaining pigmented compounds, especially chlorophyll, even though dechlorophyllization was applied.

Similarly, Bitencourt *et al.* (2014) reported that the color change in the gelatin-based films containing curcuma ethanol extract was related to the increasing concentration of the extract, which contains curcuminoid with a distinctive yellow color. Also, the decreases in L^* value and upsurges in both a^* and b^* values for the chitosan-based films were observed when tea polyphenols were incorporated in these films (Wang *et al.,* 2013). In general, gelatin/chitosan proportions had a negligible effect on the color of the films. Nevertheless, the difference became more pronounced when BLEE, particularly at higher level, was incorporated.

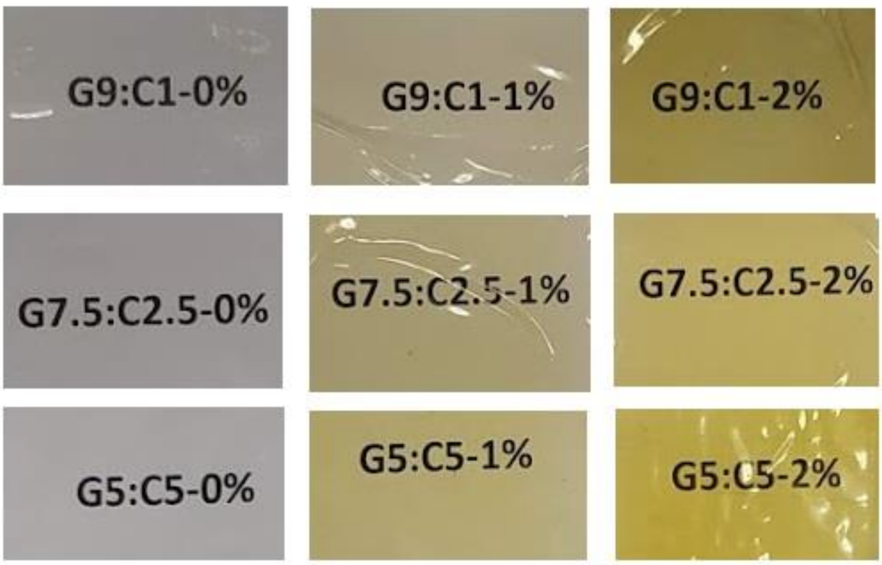

Figure 28. Blend films based on gelatin/chitosan at different proportions added with BLEE at various concentrations. For captions see Table 15.

7.5.1.5. Light transmission and transparency value

Films with excellent ultraviolet and visible (UV/Vis) light barrier abilities are strongly desired for the prevention of the adverse effects of light toward quality changes such as pigment degradation, enzymes denaturation, lipid oxidation, and vitamins destruction. For films without BLEE incorporated, higher transmission was found for films having higher proportion of chitosan (Fig. 29). On the other hand, lower transmission was obtained with blend films having higher proportion of gelatin. Protein based films including gelatin film were documented to have an excellent UV barrier property (Sobral and Habitante, 2001). UV shows the negative impact in food systems, especially enhancement of oxidation process at initiation stages. Gelatin containing amino acid residues, especially those containing aromatic rings with double bonds, can absorb UV light (Sobral and Habitante, 2001). Bonilla and Sobral (2016) observed that films containing higher concentration of gelatin showed better barrier to UV than films containing elevated levels of chitosan. Incorporation with BLEE markedly enhanced the UV/Vis light barrier abilities of gelatin/chitosan blend films ($p < 0.05$), as compared to films without BLEE (Fig. 29). Film samples containing either 1 or 2% BLEE showed low transmission values close to zero in the wavelength range of 200 – 400 nm (UV region), indicating a remarkable barrier ability towards the UV light. This finding could be related to the diverse phenolic compounds or other components in BLEE such as vitexin and isovitexin (Tagrida and Benjakul, 2020), which contain abundant unsaturated bonds in their structures. Compounds with many unsaturated bonds can absorb UV light, thus preventing harmful effects to the products (Damodaran *et al.*, 2007). UV/Vis light barrier property was attributed to the curcumin with many double bonds found in gelatin-based films added with ethanolic extract from curcuma (Bitencourt *et al.*, 2014). High transmission was found with most films; however, the lowest values were found in films with 2% BLEE, signifying higher acquisition of polyphenols acting as visible light barrier.

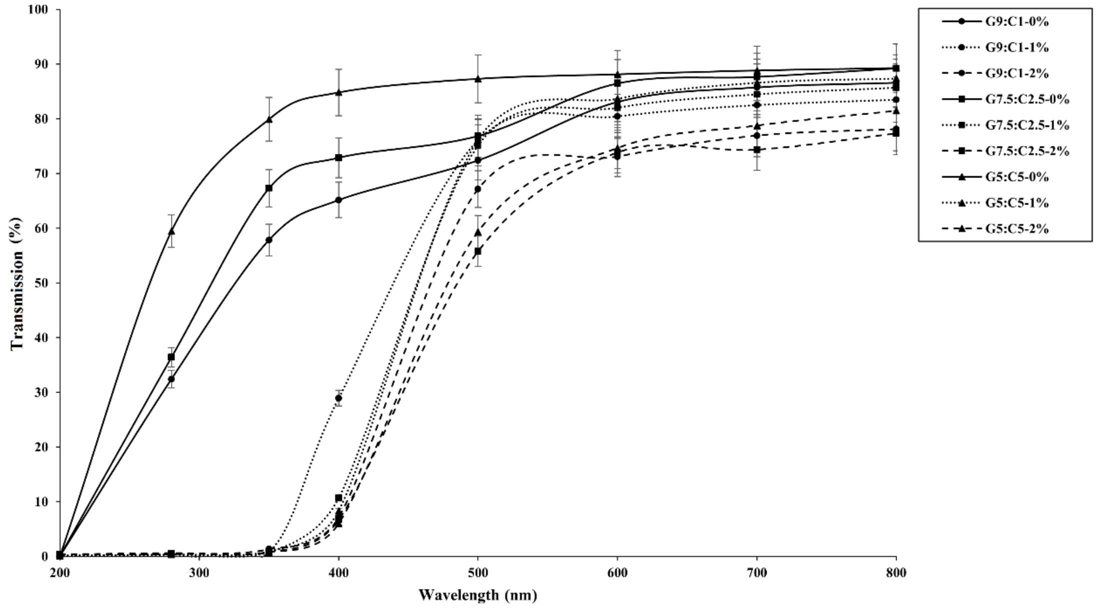

Figure 29. Transmission of blend films based on gelatin/chitosan at different proportions added with BLEE at various concentrations in UV and visible ranges. For captions see Table 15.

Visual observation (Fig. 28) showed that all the prepared gelatin/chitosan blend films without and with BLEE were transparent, indicating their homogeneity. No phase separation among the components of the prepared films was noticeable. Nonetheless, the transparency values increased with augmenting BLEE concentration ($p < 0.05$), regardless of the gelatin/chitosan proportions used (Table 16). Lower values indicate more transparency. Higher transparency values coincided with the less L* values. BLEE incorporation into the films therefore affected their transparency to some degrees.

7.5.1.6. Swelling

The swelling of films is related to their components. Usually, films with low swelling are more applicable and desired particularly for food products with high moisture content (Senturk-Parreidt *et al.,* 2018). Gelatin/chitosan ratios as well as BLEE concentration greatly affected the swelling of the prepared films (Table 16). In general, films with high gelatin proportion had higher swelling ($p < 0.05$). This was strongly attributed to the hydrophilic nature of gelatin, which attracted more water molecules and had more electrostatic repulsion between the chains, leading to swollen film (Ling *et al*., 2004). When BLEE was present in the films, the swelling was

Table 16. Transparency value, swelling, solubility, and water vapor permeability of blend films based on gelatin/chitosan at different proportions without and with BLEE at various concentrations.

Sample	Transparency value	Swelling (%)	Water solubility (%)	WVP ($\times 10^{-11}$ g m^{-1} s^{-1} Pa^{-1})
G9:C1-0%	1.93 ± 0.55^{b}	80.43 ± 1.24^{a}	74.41 ± 2.15^{a}	9.62 ± 0.15^{a}
G9:C1-1%	2.07 ± 0.24^{b}	41.68 ± 2.93^{c}	62.99 ± 1.98^{ab}	3.62 ± 0.22^{d}
G9:C1-2%	2.81 ± 0.18^{a}	24.66 ± 0.68^{d}	47.42 ± 1.18^{cd}	3.97 ± 0.13^{d}
G7.5:C2.5-0%	1.90 ± 0.52^{b}	77.01 ± 1.63^{a}	57.12 ± 1.68^{bc}	6.66 ± 0.56^{b}
G7.5:C2.5-1%	2.02 ± 0.15^{b}	36.86 ± 3.58^{c}	53.78 ± 2.73^{bc}	3.89 ± 0.83^{d}
G7.5:C2.5-2%	2.80 ± 0.67^{a}	23.39 ± 0.02^{d}	35.44 ± 1.19^{de}	3.79 ± 0.76^{d}
G5:C5-0%	1.87 ± 0.07^{b}	60.53 ± 2.43^{b}	26.54 ± 2.85^{ef}	5.32 ± 0.79^{c}
G5:C5-1%	1.92 ± 0.20^{b}	36.66 ± 0.82^{c}	23.13 ± 1.79^{ef}	3.79 ± 0.09^{d}
G5:C5-2%	2.77 ± 0.69^{a}	20.81 ± 0.65^{d}	19.53 ± 2.66^{f}	3.68 ± 0.39^{d}

Values are mean ± SD. Different lowercase superscripts in the same column denote significant difference ($p < 0.05$). WVP: water vapor permeability. For captions see Table 15.

markedly decreased, particularly at higher amount added ($p < 0.05$). This was probably related to the homogenous insertion of BLEE polyphenols or other components between chitosan or gelatin molecules, and might interact with hydrophilic chains, resulting in the reduction of the availability of hydroxyl or charged residues, which could bind with water molecules. Similar findings were observed by Kumar *et al*. (2019), in which the swelling was reduced in gelatin-starch blend films added with 5% citric acid as compared to films without citric acid.

7.5.1.7. Water solubility

High solubility indicates high affinity for water, which is considered a major drawback in some biodegradable films. The solubility of gelatin/chitosan blend films showed a similar trend to swelling (Table 16). Films with higher gelatin proportion had the higher solubility ($p < 0.05$). With increasing chitosan proportion, the solubility was noticeably decreased ($p < 0.05$). The presence of gelatin, which was hydrophilic, allowed easy accessibility for the water molecules, thus increasing the solubility of films. Conversely, the hydrophobic nature of chitosan improved the water resistance by disrupting the electrostatic interactions and hydrogen bonding with water molecules, resulting in decreased solubility (Xu *et al.*, 2021).

Incorporation with BLEE greatly affected the solubility of the films and this effect was in concentration dependent manner ($p < 0.05$). This was probably due to the competing effect of BLEE polyphenols with water molecules, while phenolic domain could serve as hydrophobic domain with poor water absorption. Some phenolic compounds could interact with gelatin chains, this making them more aggregated and less available for water binding. Bitencourt *et al.* (2014) reported a decrease in solubility of gelatin-based films with elevated concentration of curcuma ethanol extract. Rattaya *et al.* (2009) also found that the lowered solubility of gelatin films was associated with the enhanced crosslinking of gelatin after incorporation of 6% seaweed extract into the film.

7.5.1.8. Water vapor permeability (WVP)

Water vapor permeability is a measure of the rate of water vapor that passes through the surface of the film. Films with low WVP are preferable as they could maintain the moisture content of the food products as stable as possible (Kester and Fennema, 1989). Gelatin/chitosan proportion affected the WVP of resulting films (Table 16). Among film samples devoid of BLEE, G9:C1-0% had the highest WVP, while G5:C5-0% had the lowest WVP ($p < 0.05$). The hydrophilic nature of gelatin allowed higher quantities of water vapor to migrate through the film. When the proportion of gelatin decreased and chitosan proportion increased, WVP was suppressed, because of both decrease in hydrophilic gelatin and increased hydrophobic chitosan. Kumar *et al.* (2019) reported an increased WVP when more gelatin was present in film.

A noticeable decrease in WVP ($p < 0.05$) was found for all the film samples when BLEE was incorporated. However, WVP was not different ($p > 0.05$) between films containing BLEE at both concentrations, regardless of gelatin/chitosan proportion used. This reduction in WVP when BLEE was incorporated could be attributed to the enhancement of the gelatin and chitosan cross-linking, which led to decreased hydrophilic functional groups, thus decreasing the hydrophilicity of the matrix of film. As a consequence, the decrease in permeation of water vapor through the films was attained (Rattaya *et al.,* 2009). Giménez *et al.* (2013) found the lower WVP of agar-gelatin films added with green tea extract, in which a less permeable film network was formed. In addition, the BLEE might consist of essential oil, which was hydrophobic and acted as barrier for water vapor migration. Betel leaf was reported to be rich in essential oil containing eugenol, estragole, chavicol, linalool, etc., (Madhumita *et al.*, 2019).

7.5.1.9. Bioactivities of blend films

7.5.1.9.1. Antioxidant activities (AO-A)

Active packaging covers films added with components with bioactivities such as AO-A or AB-A that will help in the better prevention of food deterioration by preventing lipid oxidation and retarding the growth of microorganisms (de Campos *et al.,* 2019). Incorporation of BLEE to the gelatin/chitosan blend increased their AO-A ($p < 0.05$) (Table 17), and the increases were in a concentration-dependent manner. The gelatin/chitosan blend films containing BLEE at the same concentration showed similar AO-A. Films without BLEE showed low DPPH-RSA and ABTS-RSA. Residual amino groups of chitosan molecules and $-NH_2$ or -OH groups of side chains of gelatin molecules might contribute to radical scavenging activities (Moradi *et al.,* 2012). No FRAP and MCA were detected for all the films without BLEE. Xu *et al*. (2021) found that films made from either gelatin or chitosan alone had no reducing power. Films without BLEE also had low ORAC as shown by the rapid decay in fluorescence intensity (Fig. 30).

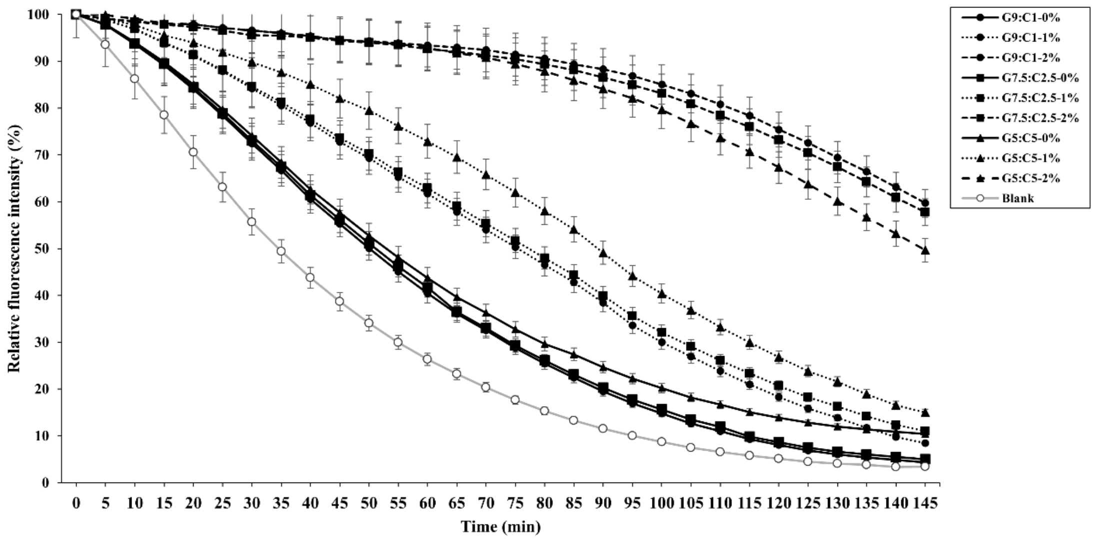

Figure 30. Fluorescence decay curves of blend films based on gelatin/chitosan at different proportions added with BLEE at various concentrations. For captions see Table 15.

The increased AO-A in films containing elevated concentration of BLEE was linked to the polyphenols or reducing components in BLEE such as isovitexin, epigallocatechin, and kaempferol derivatives, which could behave as antioxidants. In which they acted as electron donor or free radical acceptor, and exhibited the reduction of ferric into ferrous ion, metal chelating, and peroxyl radical scavenging (Tagrida and Benjakul, 2021). Similarly, increasing curcuma ethanol extract in gelatin-based films led to the augmentation of AO-A (Bitencourt *et al.,* 2014). Additionally, Giménez *et al.* (2013) observed an increase in AO-A of agar-gelatin films when the concentration of the incorporated green tea extract was increased. At the same level of BLEE incorporated, the film having higher proportion of chitosan showed no difference ($p > 0.05$) in all activities tested in comparison with those containing lower proportion of chitosan (higher proportion of gelatin). Thus, antioxidants could be released during extraction from film matrix effectively, regardless of gelatin/chitosan ratios.

Table 17. Antioxidant and antibacterial activities of blend films based on gelatin/chitosan at different proportions added with BLEE at various concentrations

Sample	**Antioxidant activities**				**Antibacterial activity (mm)**			
	DPPH-RSA (µmol TE/g sample)	**ABTS-RSA (µmol TE/g sample)**	**FRAP (µmol TE/g sample)**	**MCA (µmol EDTA/g sample)**	***S. aureus***	***E. coli***	***L. monocytogenes***	***P. aeruginosa***
G9:C1-0%	4.90 ± 2.04^{c}	32.5 ± 1.22^{c}	ND*	ND	ND	ND	ND	ND
G9:C1-1%	98.84 ± 1.27^{b}	2357.1 ± 14.6^{b}	1550.8 ± 6.9^{b}	183.65 ± 8.2^{b}	6.33 ± 0.27^{b}	6.5 ± 0.33^{b}	6.25 ± 0.41^{b}	6.01 ± 0.38^{b}
G9:C1-2%	125.18 ± 0.89^{a}	2757.7 ± 34.4^{a}	1844.6 ± 10.8^{a}	237.85 ± 4.8^{a}	10.08 ± 0.93^{a}	10.58 ± 1.91^{a}	9.67 ± 1.32^{a}	10.51 ± 1.21^{a}
G7.5:C2.5-0%	5.12 ± 3.71^{c}	34.4 ± 1.8^{c}	ND	ND	ND	ND	ND	ND
G7.5:C2.5-1%	99.01 ± 0.72^{b}	2377.1 ± 30.7^{b}	1546.2 ± 10.1^{bc}	185.66 ± 0.8^{b}	6.25 ± 0.78^{b}	6.5 ± 0.87^{b}	6.33 ± 0.38^{b}	6.52 ± 0.43^{b}
G7.5:C2.5-2%	125.88 ± 0.67^{a}	2768.1 ± 37.2^{a}	1851.1 ± 10.1^{a}	241.78 ± 0.5^{a}	10.51 ± 1.03^{a}	11.75 ± 1.34^{a}	9.91 ± 2.33^{a}	11.08 ± 1.07^{a}
G5:C5-0%	5.21 ± 1.37^{c}	34.8 ± 1.06^{c}	ND	ND	ND	ND	ND	ND
G5:C5-1%	99.96 ± 1.25^{b}	2382.9 ± 31.5^{b}	1533.4 ± 15.3^{c}	186.02 ± 3.1^{b}	6.51 ± 0.63^{b}	6.61 ± 0.68^{b}	6.51 ± 0.19^{b}	6.91 ± 0.51^{b}
G5:C5-2%	127.29 ± 1.73^{a}	2771.4 ± 39.5^{a}	1860.1 ± 13.9^{a}	243.35 ± 1.6^{a}	10.67 ± 0.91^{a}	12.08 ± 1.52^{a}	10.01 ± 1.01^{a}	11.33 ± 1.56^{a}

Values are the mean ± SD (n=3). Different lowercase superscripts in the same column denote significant difference ($p<0.05$). DPPH-RSA: 2,2-diphenyl-1-picrylhydrazyl radical scavenging activity; ABTS-RSA: 2, 2'-Azino-bis-3-ethylbenzothiazoline-6-sulfonic acid radical scavenging activity; FRAP: Ferric reducing antioxidant power; MCA: Metal chelating activity. For captions see Table 15.

*ND: Not detected.

7.5.1.9.2. Antibacterial activities (AB-A)

AB-A of gelatin/chitosan films are presented by inhibition zones (Table 17). Only films incorporated with BLEE showed AB-A against all tested bacteria and the activity increased with augmenting concentration of BLEE ($p < 0.05$). AB-A of gelatin/chitosan blend films was strongly connected with the presence of BLEE, which could diffuse through films into the agar surface and inhibited bacterial growth. The AB-A of BLEE was associated with copious amounts of polyphenols and other components, such as essential oil, etc. within BLEE that had the profound ability to inhibit bacterial growth (Nouri and Nafchi, 2014; Tagrida and Benjakul, 2021). Gram-positive bacteria (*S. aureus* and *L. monocytogenes*) generally showed more resistance towards BLEE than Gram-negative bacteria (*E. coli* and *P. aeruginosa*). This could be explained by the presence of thick layer of peptidoglycan in the Gram-positive bacteria, which showed more resistance against the actions of antibacterial agents (Mai-Prochnow *et al.,* 2016).

The BLEE's antibacterial mode of action might be due to the hydroxyl groups of polyphenols in BLEE which acted as proton exchanger and destabilized the cytoplasmic membrane of the bacterial cells. This could reduce the pH gradient and disturb the membrane ion permeability and further disrupt the electron flow and proton motive forces. Leading eventually to the discharge of ATPs along with other constituents needed for the metabolism of the bacterial cells, and finally to the bacterial death (Burt, 2004; Nouri and Nafchi, 2014). Films containing high amount of BLEE exhibited higher AB-A as witnessed by larger inhibition zones. However, no marked differences in clear zones were found between films with different proportions of gelatin and chitosan.

7.5.2. Characteristics of selected films

Based on the characteristics of the prepared gelatin/chitosan blend film samples, G7.5:C2.5-2% showed the most satisfactory physical, barrier and bioactive properties, especially heat seal ability. Therefore, it was selected along with film sample G7.5:C2.5-0% (devoid of BLEE) to evaluate the effect of BLEE on some properties of gelatin/chitosan blend films.

7.5.2.1. Scanning electron microscopic (SEM)

SEM micrographs showed smoother and more homogenous surface and cross-section for G7.5:C2.5-0% sample devoid of BLEE (Fig. 31A and B) than that

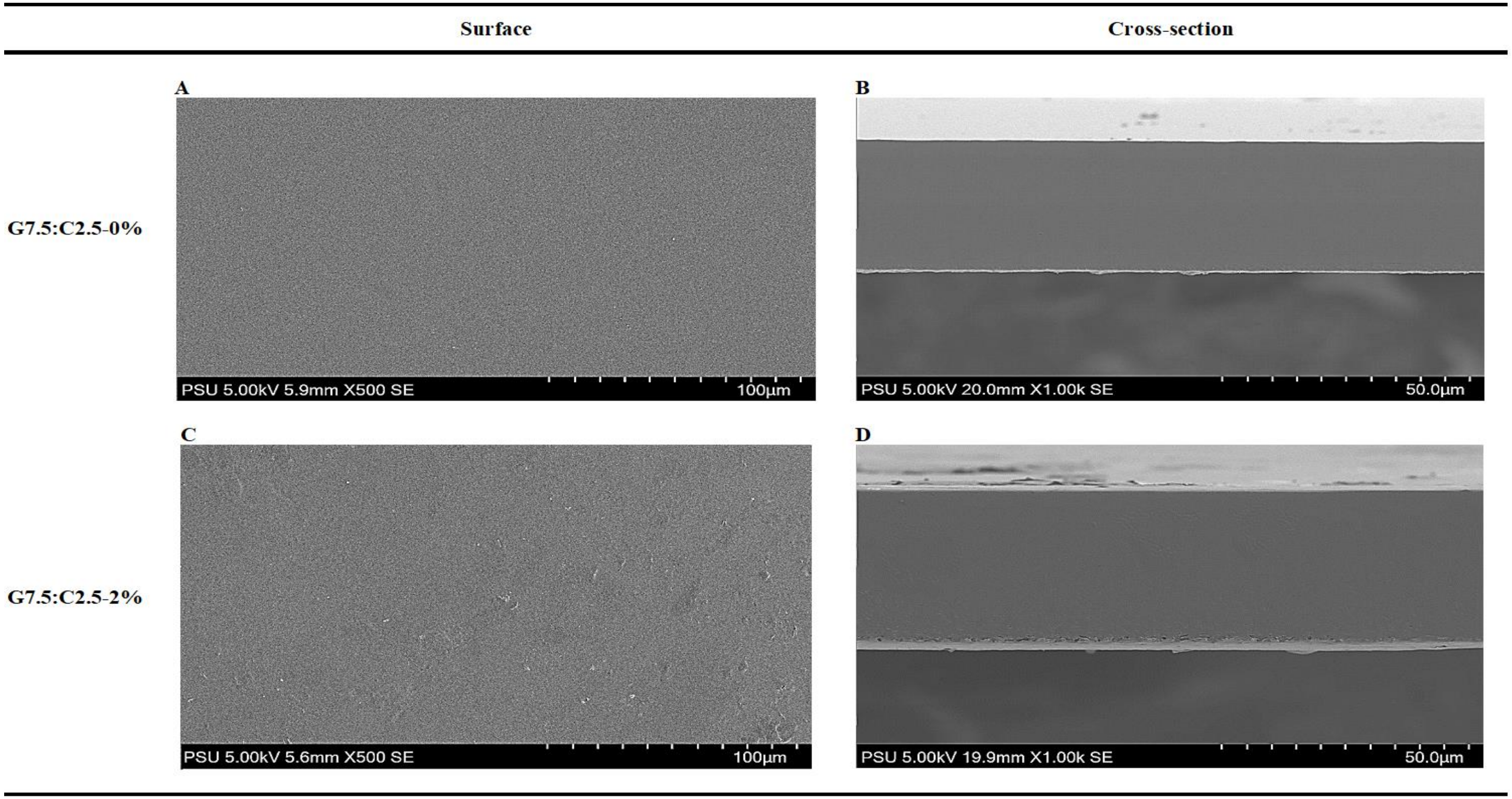

Figure 31. SEM micrographs of surface (500 x) (A and C) and cross-section (1000 x) (B and D) of the selected gelatin/chitosan blend films without (G7.5:C2.5-0%) and with 2% BLEE (G7.5:C2.5-2%)

containing BLEE (Fig. 31C and D). There was no apparent phase separation, indicating the interaction and high compatibility between two polymers in the blend. Generally, surface and cross-section of G7.5:C2.5-2% sample were rougher and slightly non-uniform (Fig. 31C and D). Nevertheless, no phase separation could be detected, indicating a high degree of compatibility between all the components in the film matrix. Polyphenols or other components in BLEE probably disturbed the alignment of both gelatin and chitosan chains into the ordered network. Also, they might lower the electrostatic interactions between those molecules, leading to the increased tortuosity of G7.5:C2.5-2% matrix as evidenced by rougher network and surface compared to those of G7.5:C2.5-0% sample. This less compact and non-uniform morphology might contribute to the lower TS and higher EAB of blend films incorporated with BLEE as compared to those without BLEE (Table 15). Bitencourt *et al.* (2014) found that gelatin-based films added with curcuma ethanol extract had less compact and uniform surface, due to the interactions between polyphenols of the extract and gelatin molecules. Similar observation was reported by Mittal *et al.* (2021) who reported the roughness of chitosan films incorporated with epigallocatechin gallate (EGCG).

7.5.2.2. Fourier transform infrared (FT-IR)

FT-IR spectra of G7.5:C2.5-0% and G7.5:C2.5-2% samples (Fig. 32) revealed the presence of peak at around 3255 cm^{-1} (Amide A), which was characteristic for inter- and intramolecular H-bonding as well as O-H and N-H stretching (Sun *et al.*, 2017). The higher amplitude of this peak in G7.5:C2.5-2% sample was possibly attributed to -OH groups of polyphenols in BLEE. Higher intensity of peak at 1040 cm^{-1}, corresponding to -OH groups mainly from plasticizers such as glycerol (Tongnuanchan *et al.*, 2015) was observed for G7.5:C2.5-2% sample. Such an increase could also be connected to the -OH group of polyphenols in BLEE. Bitencourt *et al.* (2014) reported the shift of Amide A peak at wavenumber of 3280 cm^{-1} due to the interactions between curcuma extract and gelatin chains. G50:C50-2% sample had the decrease in intensity at wavenumbers 1630, 1540, and 1230 cm^{-1} assigned for Amide I (C=O stretch), Amide II (N-H and C-N vibrations), and Amide III bands, respectively, typical characteristic of gelatin molecules (Bergo *et al.*, 2013).

Also, a decrease was observed at wavenumbers 1450 cm^{-1} assigned to vibrations of the -OH groups from gelatin and 1155 cm^{-1} representing the C-OH stretch, a characteristic band for saccharide structure found in chitosan (Bonilla *et al.*, 2014).

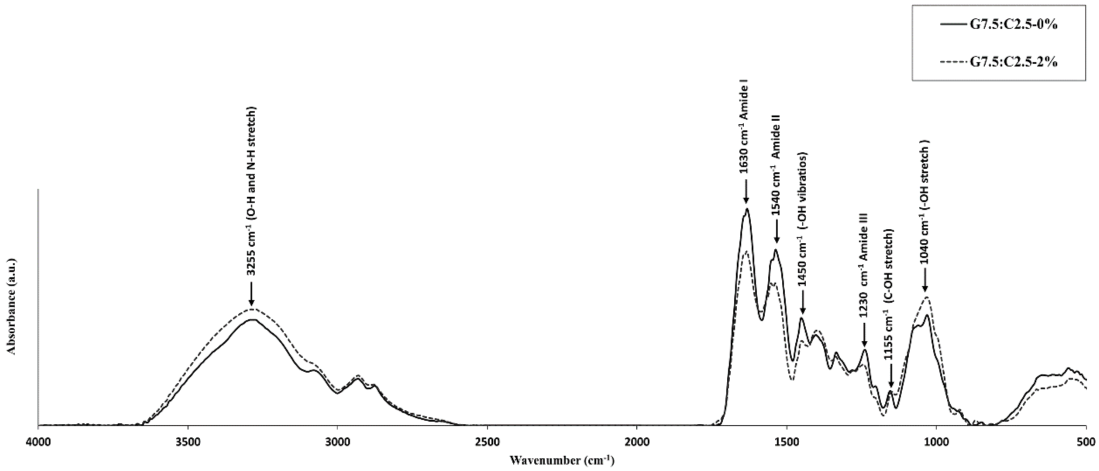

Figure 32. ATR-FTIR spectra of the selected gelatin/chitosan blend films without (G7.5:C2.5-0%) and with 2% BLEE (G7.5:C2.5-2%).

This decrease in intensities could be associated with the presence of 2% BLEE, which could dilute both polymers. Additionally, the slight decrease in the vibrational wavelength and broadening of OH and NH bands indicated hydrogen bonding interaction between the polymers (Liu *et al.*, 2012; Bonilla and Sobral, 2016). Overall, differences in the FT-IR spectra between G7.5:C2.5-0% and G7.5:C2.5-2% were strongly connected to the presence of BLEE, which could lower the concentration of blend polymers. However, some shift of peaks at wavenumbers of 1629, 1531, 1226, and 1140 cm^{-1} indicated the interaction between polyphenols and gelatin or between polyphenols and chitosan.

7.5.2.3. Thermogravimetric analysis (TGA)

Thermal degradation behavior of G7.5:C2.5-0% and G7.5:C2.5-2% samples was evaluated by TGA thermograms (Fig. 33). Both G7.5:C2.5-0% and G7.5:C2.5-2% samples underwent multiple stages of weight loss. First stage (Td_1) of

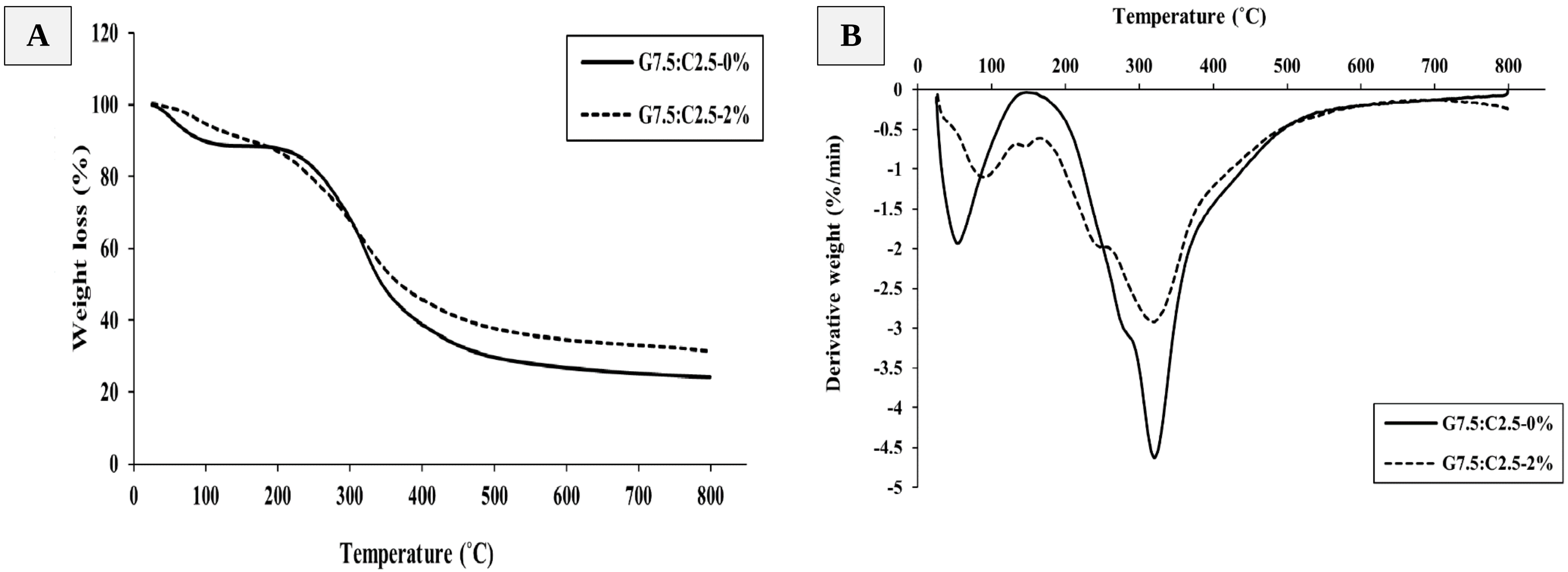

Figure 33. Thermogravimetric analysis (A) and Derivative weight loss (B) thermograms of the selected gelatin/chitosan blend films without (G7.5:C2.5-0%) and with 2% BLEE (G7.5:C2.5-2%).

weight loss (ΔW_1 = 11.4%) for G7.5:C2.5-0% sample took place at 32.64˚C, while weight loss at 49.76˚C with ΔW_1 of 8.27% was found for G7.5:C2.5-2% sample. Higher temperature and lower weight loss for G7.5:C2.5-2% sample was probably attributed to the stronger bonding in the film network, thus making the film more stable. In general, such weight loss was associated with the gradual loss of water and other components absorbed in the film matrix (Mittal *et al.*, 2021). The second stage (Td_2) took place at 231.81 and 211.77 ˚C with ΔW_2 of 16.77 and 11.8% for G7.5:C2.5-0% and G7.5:C2.5-2% samples, respectively. Degradation at this temperature range was more likely related to the loss of plasticizer (glycerol), short chain and lower interacting polymeric molecules (Wu *et al.,* 2013).

The maximum rate of degradation (ΔW_3 = 30.9 and 30.25%) happened at the temperatures (Td_3) of 304.18 and 280.12˚C for G7.5:C2.5-0% and G7.5:C2.5-2% samples, respectively, signifying the continuous degradation of highly interacted gelatin, chitosan, and other components in the films. Lower degradation temperatures (Td_2 and Td_3) noticed in G7.5:C2.5-2% film might be connected to the lower polymer-polymer interactions and lesser ordered and compact network as compared to that of film without BLEE (G7.5:C2.5-0%). This result coincided with the mechanical and morphological data. The degradation of both films continued until the end of heating (800˚C), but the rate of degradation was lower for G7.5:C2.5-2% sample than G7.5:C2.5-0% sample. The residual mass remaining after heating was 39.97 and 46.35% of G7.5:C2.5-0% and G7.5:C2.5-2% samples, respectively. This difference could be due to the incorporation of BLEE into the films, which could render higher char content.

7.6. Conclusion

Incorporation of BLEE into gelatin/chitosan blend films affected their mechanical properties and slightly changed the color of films. The heat sealing of some films was achieved, while films having high proportion of chitosan was not sealable. UV-Vis light barrier property was improved, and water vapor barrier properties were enhanced when added with BLEE. Water resistance of film was also increased. Furthermore, AO-A and AB-A of films were elevated with addition of BLEE ($p < 0.05$). Therefore, biodegradable gelatin/chitosan films with seal ability and good physicochemical properties along with augmented bioactivities could be prepared using gelatin and chitosan at a ratio of 7.5:2.5 and incorporated with 2% BLEE. Such films can be further used for preservation and shelf-life extension of food products.

7.7. References

Abelson, J. 2021. COP26: Our 4 take-aways from Glasgow and recent UN reports. Available: https://plasticodyssey.org/en/cop26-take-aways-climate-plastic-pollution/

Benjakul, S., Kittiphattanabawon, P., Sumpavapol, P. and Maqsood, S. 2014. Antioxidant activities of lead (*Leucaena leucocephala*) seed as affected by extraction solvent, prior dechlorophyllisation and drying methods. Journal of Food Science and Technology. 51: 3026 - 3037.

Bergo, P., Moraes, I. and Sobral, P. 2013. Infrared spectroscopy, mechanical analysis, dielectric properties and microwave response of pigskin gelatin films plasticized withglycerol. Food Bioscience. 1: 10 - 15.

Bitencourt, C., Fávaro-Trindade, C., Sobral, P. D. A. and Carvalho, R. D. 2014. Gelatin-based films additivated with curcuma ethanol extract: Antioxidant activity and physical properties of films. Food Hydrocolloids. 40: 145 - 152.

Bonilla, J., Fortunati, E., Atarés, L., Chiralt, A. and Kenny, J. M. 2014. Physical, structural and antimicrobial properties of poly vinyl alcohol–chitosan biodegradable films. Food Hydrocolloids. 35: 463 - 470.

Bonilla, J. and Sobral, P. J. 2016. Investigation of the physicochemical, antimicrobial and antioxidant properties of gelatin-chitosan edible film mixed with plant ethanolic extracts. Food Bioscience. 16: 17 - 25.

Burt, S. 2004. Essential oils: their antibacterial properties and potential applications in foods—a review. International Journal of Food Microbiology. 94: 223 - 253.

Cao, N., Fu, Y. and He, J. 2007. Mechanical properties of gelatin films cross-linked, respectively, by ferulic acid and tannin acid. Food Hydrocolloids. 21: 575 - 584.

Cazón, P. and Vázquez, M. 2020. Mechanical and barrier properties of chitosan combined with other components as food packaging film. Environmental Chemistry Letters. 18: 257 - 267.

Damodaran, S., Parkin, K. L. and Fennema, O. R. 2007. Fennema's food chemistry, 4th edtion. CRC press. Taylor and Francis Group. Environmental Chemistry. 28: 453 - 467.

De Campos, S. S., De Oliveira, A., Moreira, T. F. M., Da Silva, T. B. V., Da Silva, M. V., Pinto, J. A., Bilck, A. P., Gonçalves, O. H., Fernandes, I. P. and Barreiro, M.-F. 2019. TPCS/PBAT blown extruded films added with curcumin as a technological approach for active packaging materials. Food Packaging and Shelf Life. 22: 100424.

Fathima, P., Panda, S. K., Ashraf, P. M., Varghese, T. and Bindu, J. 2018. Polylactic acid/chitosan films for packaging of Indian white prawn (*Fenneropenaeus indicus*). International Journal of Biological Macromolecules. 117: 1002 - 1010.

Giménez, B., De Lacey, A. L., Pérez-Santín, E., López-Caballero, M. and Montero, P. 2013. Release of active compounds from agar and agar–gelatin films with green tea extract. Food Hydrocolloids. 30: 264 - 271.

Gómez-Estaca, J., De Lacey, A. L., López-Caballero, M., Gómez-Guillén, M. and Montero, P. 2010. Biodegradable gelatin–chitosan films incorporated with essential oils as antimicrobial agents for fish preservation. Food Microbiology. 27: 889 - 896.

Han, J. H. and Floros, J. D. 1997. Casting antimicrobial packaging films and measuring their physical properties and antimicrobial activity. Journal of Plastic Film and Sheeting. 13: 287 - 298.

Hosseini, S. F., Kaveh, F., and Schmid, M. 2022. Facile fabrication of transparent high-barrier poly (lactic acid)-based bilayer films with antioxidant/antimicrobial performances. Food Chemistry. 384: 132540.

Karim, A. and Bhat, R. 2009. Fish gelatin: properties, challenges, and prospects as an alternative to mammalian gelatins. Food Hydrocolloids. 23: 563 - 576.

Kester, J. and Fennema, O. 1989. An edible film of lipids and cellulose ethers: barrier properties to moisture vapor transmission and structural evaluation. Journal of Food Science. 54: 1383 - 1389.

Kumar, R., Ghoshal, G. and Goyal, M. 2019. Synthesis and functional properties of gelatin/CA–starch composite film: excellent food packaging material. Journal of Food Science and Technology. 56: 1954 - 1965.

Ling, X., Zu-Yu, Y., Chao, Y., Hua-Yue, Z. and Yu-Min, D. 2004. Swelling studies of chitosan-gelatin films cross-linked by sulfate. Wuhan University Journal of Natural Sciences. 9: 247 - 251.

Liu, C., Huang, J., Zheng, X., Liu, S., Lu, K., Tang, K. and Liu, J. 2020. Heat sealable soluble soybean polysaccharide/gelatin blend edible films for food packaging applications. Food Packaging and Shelf Life. 24: 100485.

Liu, Z., Ge, X., Lu, Y., Dong, S., Zhao, Y. and Zeng, M. 2012. Effects of chitosan molecular weight and degree of deacetylation on the properties of gelatine-based films. Food Hydrocolloids. 26: 311 - 317.

Madhumita, M., Guha, P. and Nag, A. 2019. Extraction of betel leaves (*Piper betle* L.) essential oil and its bio-actives identification: Process optimization, GC-MS analysis and anti-microbial activity. Industrial Crops and Products. 138: 111578.

Mai-Prochnow, A., Clauson, M., Hong, J. and Murphy, A. B. 2016. Gram-positive and Gram-negative bacteria differ in their sensitivity to cold plasma. Scientific Reports. 6: 1 - 11.

Mittal, A., Singh, A., Benjakul, S., Prodpran, T., Nilsuwan, K., Huda, N. and De La Caba, K. 2021. Composite films based on chitosan and epigallocatechin gallate grafted chitosan: characterization, antioxidant and antimicrobial activities. Food Hydrocolloids. 111: 106384.

Monsur, H. A., Jaswir, I., Salleh, H. M. and Alkahtani, H. A. 2014. Effects of pretreatment on properties of gelatin from perch (*Lates niloticus*) skin. International Journal of Food Properties. 17: 1224 - 1236.

Moradi, M., Tajik, H., Rohani, S. M. R., Oromiehie, A. R., Malekinejad, H., Aliakbarlu, J. and Hadian, M. 2012. Characterization of antioxidant chitosan film incorporated with *Zataria multiflora* Boiss essential oil and grape seed extract. LWT-Food Science and Technology. 46: 477 - 484.

Nilsuwan, K., Benjakul, S. and Prodpran, T. 2018. Physical/thermal properties and heat seal ability of bilayer films based on fish gelatin and poly (lactic acid). Food Hydrocolloids. 77: 248 - 256.

Nouri, L. and Nafchi, A. M. 2014. Antibacterial, mechanical, and barrier properties of sago starch film incorporated with betel leaves extract. International Journal of Biological Macromolecules. 66: 254 - 259.

Nowzari, F., Shábanpour, B. and Ojagh, S. M. 2013. Comparison of chitosan–gelatin composite and bilayer coating and film effect on the quality of refrigerated rainbow trout. Food Chemistry. 141: 1667 - 1672.

Nuthong, P., Benjakul, S. and Prodpran, T. 2009. Characterization of porcine plasma protein-based films as affected by pretreatment and cross-linking agents. International Journal of Biological Macromolecules. 44: 143 - 148.

Park, S. H., Lee, H. S., Choi, J. H., Jeong, C. M., Sung, M. H., and Park, H. J. 2012. Improvements in barrier properties of poly (lactic acid) films coated with chitosan or chitosan/clay nanocomposite. Journal of Applied Polymer Science. 125(S1): 675 - 680.

Pereda, M., Ponce, A., Marcovich, N., Ruseckaite, R. and Martucci, J. 2011. Chitosan-gelatin composites and bi-layer films with potential antimicrobial activity. Food Hydrocolloids. 25: 1372 - 1381.

Qiao, C., Ma, X., Zhang, J. and Yao, J. 2017. Molecular interactions in gelatin/chitosan composite films. Food Chemistry. 235: 45 - 50.

Rattaya, S., Benjakul, S. and Prodpran, T. 2009. Properties of fish skin gelatin film incorporated with seaweed extract. Journal of Food Engineering. 95: 151 - 157.

Senturk-Parreidt, T., Müller, K. and Schmid, M. 2018. Alginate-based edible films and coatings for food packaging applications. Foods. 7: 170.

Shiku, Y., Hamaguchi, P. Y., Benjakul, S., Visessanguan, W. and Tanaka, M. 2004. Effect of surimi quality on properties of edible films based on *Alaska pollack*. Food Chemistry. 86: 493 - 499.

Sobral, P. and Habitante, A. 2001. Phase transitions of pigskin gelatin. Food Hydrocolloids. 15: 377 - 382.

Sun, L., Sun, J., Chen, L., Niu, P., Yang, X. and Guo, Y. 2017. Preparation and characterization of chitosan film incorporated with thinned young apple polyphenols as an active packaging material. Carbohydrate Polymers. 163: 81 - 91.

Tagrida, M. and Benjakul, S. 2020. Ethanolic extract of Betel (*Piper betle* L.) and Chaphlu (*Piper sarmentosum* Roxb.) dechlorophyllized using sedimentation process: Production, characteristics, and antioxidant activities. Journal of Food Biochemistry. 44: e13508.

Tagrida, M. and Benjakul, S. 2021. Betel (*Piper betle* L.) leaf ethanolic extracts dechlorophyllized using different methods: antioxidant and antibacterial activities, and application for shelf-life extension of Nile tilapia (*Oreochromis niloticus*) fillets. RSC Advances. 11: 17630 - 17641.

Tagrida, M., Prodpran, T., Zhang, B., Aluko, R. E. and Benjakul, S. 2021. Liposomes loaded with betel leaf (*Piper betle* L.) ethanolic extract prepared by thin film hydration and ethanol injection methods: Characteristics and antioxidant activities. Journal of Food Biochemistry. 45(12): e14012.

Tian, B. and Liu, Y. 2020. Chitosan-based biomaterials: From discovery to food application. Polymers for Advanced Technologies. 31: 2408 - 2421.

Tongnuanchan, P., Benjakul, S., Prodpran, T. and Nilsuwan, K. 2015. Emulsion film based on fish skin gelatin and palm oil: physical, structural and thermal properties. Food Hydrocolloids. 48: 248 - 259.

UNEP. 2021. United Nations Environment Programme [Online]. Available: https://news.un.org/en/story/2021/10/1103692.

Wang, L., Dong, Y., Men, H., Tong, J. and Zhou, J. 2013. Preparation and characterization of active films based on chitosan incorporated tea polyphenols. Food Hydrocolloids. 32: 35 - 41.

Wang, L., Liu, F., Jiang, Y., Chai, Z., Li, P., Cheng, Y., Jing, H. and Leng, X. 2011. Synergistic antimicrobial activities of natural essential oils with chitosan films. Journal of Agricultural and Food Chemistry. 59: 12411 - 12419.

Wu, J., Chen, S., Ge, S., Miao, J., Li, J. and Zhang, Q. 2013. Preparation, properties and antioxidant activity of an active film from silver carp (*Hypophthalmichthys molitrix*) skin gelatin incorporated with green tea extract. Food Hydrocolloids. 32: 42 - 51.

Wu, J., Ge, S., Liu, H., Wang, S., Chen, S., Wang, J., Li, J. and Zhang, Q. 2014. Properties and antimicrobial activity of silver carp (*Hypophthalmichthys *molitrix*) skin gelatin-chitosan films incorporated with oregano essential oil for fish preservation. Food Packaging and Shelf Life. 2: 7 - 16.

Xu, D., Chen, T. and Liu, Y. 2021. The physical properties, antioxidant, and antimicrobial activity of chitosan–gelatin edible films incorporated with the extract from hop plant. Polymer Bulletin. 78: 3607 - 3624.

CHAPTER 8

PROPERTIES OF GELATIN/CHITOSAN BLEND FILMS INCORPORATED WITH BETEL LEAF ETHANOLIC EXTRACT LOADED IN LIPOSOMES AND THEIR USE AS POUCHES FOR SHRIMP OIL PACKAGING

8.1. Abstract

Properties of gelatin/chitosan blend films plasticized with different plasticizers and incorporated with liposomes loaded with betel leaf ethanolic extract (L/BLEE) at 2% or BLEE at an equivalent amount were investigated. Films plasticized with glycerol (GLY) and incorporated with BLEE showed better mechanical and barrier properties ($p < 0.05$) than other films. Type of plasticizer had no effect on antioxidant activities of films ($p > 0.05$). SEM images of the films revealed homogenous surface and cross-section in film samples devoid of active compounds, while those incorporated with BLEE had slightly rough surface and cross-section. The roughest surface and cross section were found for those incorporated with L/BLEE. During storage at room temperature, lower oxidation took place in shrimp oil packaged in pouches made from gelatin/chitosan blend plasticized with GLY and incorporated with BLEE (B-GLY) compared to that packaged in lower density polyethylene (LDPE) pouches as ascertained by less peroxide values, thiobarbituric acid reactive substances, and astaxanthin decomposition. Therefore, gelatin/chitosan blend containing BLEE plasticized with GLY (B-GLY) could be used as active packaging to retard lipid oxidation in shrimp oil.

8.2. Introduction

The emergence of environmental issues related to the excessive usage of petrochemical plastic products requires the search for alternative packaging. Biodegradable films have been proposed as novel packaging materials to replace the commonly used plastics (Nilsuwan *et al.,* 2019). Gelatin and chitosan are among the natural polymers with great potential to form films having superior barrier properties in addition to their biocompatibility and non-toxicity (Hosseini *et al.,* 2013). To overcome some drawbacks of either gelatin film such as swelling and poor water vapor barrier ability or chitosan film including poor seal ability and brittleness, blends made from both polymers can produce film with improved mechanical and physiochemical properties due to their interconnections and compatibility (Qiao *et al.,* 2017). Plasticizers are generally added to the film solutions to reduce chains interactions, thus increasing mobility of film molecules, and lowering the film brittleness. Type, concentration, and nature of the plasticizers greatly affect film network differently. Therefore, a proper plasticizer with the optimum concentration must be used to avoid undesirable problems in the produced film such as poor vapor and gas barrier abilities (Jongjareonrak *et al.,* 2006).

To improve the bioactivities of the films, plant-based extracts with antioxidant activities were incorporated in the film matrix. Consequently, biodegradable active packaging can be obtained using films with augmented preservative activities by incorporating natural additives (Bitencourt *et al.,* 2014). Betel, a leafy plant grown in Southeast Asian countries, was used in the traditional medicine and as a food. Betel leaf ethanolic extract (BLEE) dechlorophyllized via sedimentation process contained high number of phenolic compounds such as isovitexin, vitexin 4′-O-galactoside, epigallocatechin, and kaempferol derivatives known for their bioactivities (Tagrida and Benjakul, 2020). However, due to remaining color and the typical odor of BLEE in addition to its instability, its use could induce some unsought changes on the treated samples. Encapsulation of BLEE in liposomes was documented for their biocompatibility and suitability to mask undesired attributes (Tagrida and Benjakul, 2022). Therefore, either BLEE or liposomes loaded with BLEE (L/BLEE) could be incorporated to develop biodegradable active packaging.

Shrimp oil is known to exhibit health promoting effects as it contains the high amount of n-3 PUFAs and astaxanthin (Gulzar *et al.,* 2022). Shrimp oil is generally susceptible to oxidation and quality loss, thus lowering its nutritional value in addition to the formation of toxic substances linked to serious health effects (de Oliveira *et al.,* 2018). The use of active packaging has been documented to lower the deterioration (Nilsuwan *et al.,* 2019). Nevertheless, no information on the use of pouches incorporated with active compounds, especially from betel leaves, as active packaging for keeping the quality of shrimp oil exists.

The purpose of the current work was to investigate the mechanical, physical, and bioactive properties of gelatin/chitosan blend films incorporated with either BLEE or L/BLEE as affected by different plasticizers. Additionally, the quality of shrimp oil stored in pouches made from the selected film was also investigated during the extended storage at room temperature.

8.3. Objectives

To study the effects of pouches made from gelatin/chitosan blend films containing betel leaf ethanolic extract or liposomes loaded with the extract on shelf-life and quality attributes of shrimp oil during extending storage.

8.4. Materials and methods

8.4.1. Chemicals

Chitosan (MW: ~2.1×10^3 KDa; degree of deacetylation (DDA): ~82%; viscosity: 1000 – 2000 cps) was procured from Marine Bioresources Co. Ltd. (Samut-Sakhon, Thailand). Fish gelatin (bloom: 250; molecular weight (MW): ~5.1×10^4 Da) was brought from Vinh Hoan Corp. (Dong Thap, Vietnam). Glycerol was acquired from Ajax Finechem Pty. Ltd. (Taren Point, Australia). Polyethylene glycol 4000 was purchased from Fluka Chemie GmbH (Buchs, Switzerland).

8.4.2. Preparation and dechlorophyllization of BLEE and liposomes loaded with BLEE (L/BLEE)

Extraction and dechlorophyllization of BLEE was performed as tailored by Tagrida and Benjakul (2020), in which betel leaf powder was mixed with 70% ethanol (v/v) at the ratio of 1:15 (w/v). Dechlorophyllization of the resultant concentrated extract was conducted, after solvent removal using a rotary evaporator, by sedimentation technique. The extract was frozen, lyophilized, and the dried extract was placed in a capped vial and stored at -20˚C.

L/BLEE containing 2% BLEE was prepared by thin film hydration method as tailored by Tagrida *et al.* (2021a), in which soybean phosphatidylcholine (SPC) and cholesterol (CHL) at a molar ratio of 4:1 was used as the shell material encapsulating the BLEE. The resulting L/BLEE possessed polydispersity, particle size, and zeta potential of 0.22, 388 nm, and -42 mV, respectively. Encapsulation efficiency (EE) and releasing efficiency (RE) were 64% and 30%, respectively.

8.4.3. Preparation of gelatin/chitosan blend films

Casting technique was adopted for film preparation. Fish gelatin film forming solution (G-FFS) was prepared at 3.5% (Nilsuwan *et al.*, 2018). Chitosan-FFS (C-FFS) was prepared at 1% using 1% (v/v) acetic acid (Mittal *et al.*, 2021). G-FFS and C-FFS were mixed at ratio of 7.5 : 2.5 (w/w) (based on the preliminary study, in which the film showed highest mechanical properties). Glycerol (GLY) and polyethylene glycol 4000 (PEG) as plasticizers were added separately at 30% (w/w, based on total solid content). The resulting FF-S was adjusted to pH 3.0 to avoid the precipitation of chitosan. Subsequently, FF-S were further stirred for 1 h. L/BLEE at 2% and BLEE at an equivalent amount were incorporated into the FF-S and stirred until full solubilization was attained. FF-S with GLY as plasticizer incorporated with BLEE or L/BLEE were termed as B-GLY or LB-GLY, respectively, while those added with PEG as plasticizer were named as B-PEG and LB-PEG, respectively.

FF-S without the incorporation of BLEE or L/BLEE using GLY and PEG as the plasticizers were also prepared and termed as F-GLY and F-PEG, respectively, to serve as controls. The different prepared FF-S were degassed (5 min) in a sonication bath. Four grams of the FF-S were casted onto a rimmed silicone resin plates with 9 units (5×5 cm^2). The plates were air-dried overnight with the aid of an air-blower at the relative humidity (RH) of 65–70% and 25˚C. Subsequently, casted plates were equilibrated in an environmental chamber with RH of 50 ± 5% at 25 ± 0.5˚C for 48 h. After being peeled off, films were conditioned in a desiccator containing a saturated NaBr solution (58% RH) at room temperature for 24 h before analysis.

8.4.4. Characterization of films

8.4.4.1. Thickness and Mechanical properties

Thickness was determined as described by Nilsuwan *et al.* (2018) following the ASTM D6988-21 method (ASTM, 2021). Tensile strength (TS) and elongation at break (EAB) were examined according to ASTM D3759/D3759M-05 methods (ASTM, 2019).

8.4.4.2. Seal ability

Seal strength (SS) and seal efficiency (SE) were examined using the peel test (Nilsuwan *et al.*, 2018). Both SS and SE were determined using the following equations:

$$\text{SS (N/m)} = \frac{\text{Peak force}}{\text{Film width}}$$

$$\text{SE (\%)} = \left(\frac{\text{Peak force}}{\text{Tensile force}}\right) \times 100$$

where tensile force is the force (N) acquired from TS testing of each single film and peak force (N) is the maximum force obtained from the seal testing.

8.4.4.3. Color

Color attributes (Lightness (L^*), redness/greenness (a^*), yellowness/blueness (b^*) and Total color difference (ΔE) of the films were determined using a colorimeter (Hunterlab, Reston, VA, USA) against the white standard (L^* = 92.83, a^* = -1.23, b^* = 0.48).

8.4.4.4. Light transmission and transparency

Light transmission of the films in both ultraviolet (200 – 280 nm) and visible (350 – 800 nm) ranges was measured following the method of Shiku *et al*. (2004) with the aid of an UV-vis spectrophotometer (UV-1800, Shimadzu, Kyoto, Japan). Transparency value of films was evaluated (Han and Floros, 1997):

$$\text{Transparency value} = \frac{-\log T_{600}}{X}$$

where T_{600} is the fractional transmission at 600 nm and X is thickness of film (mm). Less transparent film was indicated by higher transparency value.

8.4.4.5. Water vapor permeability (WVP)

The method described by Nilsuwan *et al*. (2018) was adopted. Films were set on aluminum permeation cups containing 0% RH dried silica gel (20 g) and tightly sealed with silicon vacuum grease and a rubber gasket. The prepared cups were left in an environmental chamber (25 ± 2˚C and 50 ± 5% RH) and weighed every 1 h over a 10-h period. WVP was subsequently calculated using the equation:

$$\text{WVP } (g\ m^{-1}\ s^{-1}\ Pa^{-1}) = \left(\frac{WVTR \times L}{\Delta P \times A}\right)$$

where WVTR is water vapor transmission rate acquired from the slope of plot of cup's weight gain vs time (g/s), L is thickness of film (m), ΔP is water vapor pressure difference across the film (1583.74 Pa at 25˚C), and A is the exposed area of the film (m^2).

8.4.4.6. Scanning electron microscopy (SEM)

Morphology of the surface and cross-section of the selected film samples was visualized using Quanta 400-FEI scanning electron microscope (Eindhoven, The Netherlands). Film samples fractured in the presence of liquid nitrogen were subjected to cross-sectional visualization. Film samples were mounted on bronze stub and gold layers were sputtered (Sputter coater SPI-Module, West Chester, PA, USA) for conductivity. The acceleration voltage at 20 kV was used.

8.4.4.7. Antioxidant activities (AO-A)

Film specimens (0.1 g) cut into small pieces were mixed with 80% methanol (10 mL). The mixture was stirred overnight and centrifuged for 20 min at 8000 x g. Supernatants of films incorporated with L/BLEE were treated with triton X-100 at 10% (v/v) prior to centrifugation (10,000 xg, 20 min) at 4˚C to disrupt the liposomes. The supernatants of both films (with free BLEE and L/BLEE) were collected and used for determination of their AO-A following the method of Tagrida *et al.* (2021a). DPPH and ABTS radicals scavenging activities (DPPH-RSA and ABTS-RSA, respectively), and ferric reducing antioxidant power (FRAP) were examined and reported as μmol Trolox equivalent (TE)/g sample. Metal chelating activity (MCA) was expressed as μmol EDTA equivalent (EE)/g sample.

8.4.5. Quality changes of shrimp oil (SO) packaged in gelatin/chitosan blend pouches

8.4.5.1. Preparation of SO

Extraction of SO was performed as described by Gulzar *et al.* (2022) from Pacific white shrimp (*Litopenaeus vannamei*) cephalothorax. One hundred g of the cephalothorax were thoroughly grounded and homogenized with 500 mL of n-hexane/isopropanol (1:1) mixture. After homogenization, SO was collected by centrifugation at 9000 xg and 4˚C for 30 min. Solvents were completely evaporated using a rotary evaporator and SO was transferred into vial, capped, and stored at -40˚C.

8.4.5.2. Gelatin/chitosan blend pouches preparation and packaging of SO

Selected gelatin/chitosan blend films having the highest physical and bioactive properties were used to prepare a 3-side sealed pouches with the aid of an impulse sealer. Film samples (5 x 5 cm^2) were heat-sealed at 150 ± 0.5˚C for 1.50 s and subsequently cooled for 1.50 s with a sealed area width of 2 mm. Two mL of SO were pipetted into a pouch. Thereafter the pouch was heat-sealed and placed on a tray for storage at room temperature (25 - 28˚C). LDPE pouches with the same dimensions were also prepared. Each pouch was added with the same amount of SO, heat-sealed and used as the control. Samples were randomly taken for analysis every 5 days for a total of 30 days.

8.4.5.3. Analyses

8.4.5.3.1. Lipid oxidation

The method of Gulzar *et al.* (2022) was followed for the determination of peroxide values (PV) from standard curve prepared from cumene hydroperoxide (0.5 – 2 ppm) and reported as mg cumene hydroperoxide equivalent/kg lipid. Thiobarbituric acid reactive substances (TBARS) were determined and TBARS concentration was calculated from the standard curve of malonaldehyde (MDA) (0 – 6 ppm) and expressed as mg MDA equivalent/kg lipid.

8.4.5.3.2. Fatty acid (FA) profile

FA profiles were evaluated at day 0 and 30 of SO storage following the method of Nilsuwan *et al.* (2019). Ten mg of SO sample was trans-methylated with 2 M methanolic NaOH and 2 M methanolic HCl to obtain fatty acid methyl esters (FAMEs). FAMEs were injected into gas chromatography system (7890B, Agilent Technologies, Santa Clara, CA, USA) equipped with a flame ionization detector (FID) using a split ratio of 1:20. The retention time of standards was used to identify the generated peaks and the results were expressed as g fatty acid/ 100 g oil.

8.4.5.3.3. Astaxanthin content

Astaxanthin content in SO was quantified following the method of Gulzar *et al*. (2022) using high-performance liquid chromatography system (Waters 2475, Milford, MA, USA) equipped with Thermo-scientific column (C18, 150 × 4.6 mm, 5 μm) and a photodiode array detector (Waters 2998, Milford, MA, USA). Absorbance at 470 nm was monitored for chromatogram. Astaxanthin content was computed based on standard curve (25 – 100 ppm) and expressed as mg/100 g oil.

8.4.6. Statistical analysis

Completely randomized design (CRD) was applied for all studies. Data were reported as mean ± standard deviation (SD). One-way Analysis of Variance (ANOVA) was conducted, and Duncan's Multiple Range Test (DMRT) was done for mean comparison. SPSS package (SPSS 28.0 for Windows, SPSS Inc, Chicago, IL, USA) software was utilized for data analysis.

8.5. Results and discussion

8.5.1. Properties of the prepared films

8.5.1.1. Thickness

Control films, irrespective of plasticizer used, had the lowest thickness that ranged between 0.031 and 0.033 mm ($p > 0.05$). Incorporation of BLEE or L/BLEE augmented the thickness markedly ($p < 0.05$), in which films with BLEE had the thickness ranged from 0.045 to 0.047 mm, while highest thickness was observed for those with L/BLEE (0.073 and 0.075 mm) (Table 18). The increment in thickness might be related to the increased solid content in the films containing either BLEE or L/BLEE. The interaction of gelatin and chitosan molecules or their matrix arrangements might be impeded by BLEE or L/BLEE, resulting in the relatively protruded network. Similarly, Kumar *et al.* (2019) reported that composite films of gelatin and starch incorporated with citric acid, had an increased thickness due to reorientation of the films' matrix. Furthermore, the SPC used for L/BLEE preparation elevated the viscosity of the FF-S and augmented the protruded film network which came in line with Kong *et al.* (2022). Similar thickness was obtained between films added with GLY and PEG as plasticizer, regardless of treatment. Thus, the type of plasticizer had no profound effect on the thickness of the resulting films.

8.5.1.2. Mechanical properties

The combination of gelatin and chitosan yielded a film with better mechanical properties since gelatin yielded more flexible films due to its amorphous structure, while chitosan is semi-crystalline structure containing reactive groups, especially amino (-NH_2) groups and hydroxyl (-OH) groups, which favored intermolecular interaction via hydrogen bonds and hydrophobic interactions. In addition, ionic interactions also strengthened the films, rendering stiffer and stronger film (Hosseini *et al.,* 2013). Plasticizers generally reduce interactions between polymer chains, leading to the formation of more flexible film. Film samples plasticized with GLY had higher TS and EAB ($p < 0.05$) than those plasticized with PEG, in which F-GLY had TS of 34.45 ± 1.56 MPa and EAB of 5.9 ± 1.45%, while F-PEG showed TS of 21.59 ± 1.05 MPa and EAB of 1.29 ± 0.03% (Table 18). Films plasticized with PEG having higher molecular wight could impede cross-linkages, thus negatively affecting the film properties as reflected by the lower TS and EAB (Faradilla *et al.,* 2019).

Also, the lower TS and EAB could be owing to the exceeding of PEG to its compatibility limit in the polymer mixture, thereby causing phase separation and physical exclusion of the plasticizer (Aulton *et al.,* 1981). Such effect was evidenced by the presence of white residues or spotting on the surface of the films containing PEG (Fig. 34D), referred to as blooming or blushing (Laohakunjit and Noomhorm, 2004). When BLEE was incorporated, B-GLY had a reduced TS (7.84 ± 0.57 MPa) but an augmented EAB (45.63 ± 1.29%). This could be due to the impediment of BLEE for the interactions or entanglement between both gelatin and chitosan chains to form the ordered network. This phenomenon resulted in the films having lower TS, but the film became more flexible as seen by higher EAB. Varying cross-linking activities of different compounds in different plant extracts were postulated, in which amino acids within gelatin chains were probably the cross-linking sites induced by plant polyphenols (Cao *et al.,* 2007).

Wu *et al.* (2014) documented the decreased TS and the augmented EAB due to the disturbance of the gelatin/chitosan film network by oregano essential oil, making film matrix discontinuous. High elongation is highly regarded as an indication of the high capacity of film to wrap foods (Kong *et al.,* 2022). BLEE was able to lessen

Table 18. Thickness, mechanical properties, seal strength, seal efficiency, and color of gelatin/chitosan blend films plasticized with glycerol or polyethylene glycol and added with BLEE, or liposomes loaded with BLEE (L/BLEE).

Sample	Thickness (mm)	TS (MPa)	EAB (%)	Seal strength (N/m)	Seal efficiency (%)	*L**	*a**	*b**	Δ*E**
F-GLY	0.031 ± 0.002^{c}	34.45 ± 1.56^{a}	5.90 ± 1.45^{b}	NA*	NA	90.57 ± 0.21^{a}	-1.13 ± 0.07^{a}	2.16 ± 0.22^{d}	2.82 ± 0.24^{d}
B-GLY	0.045 ± 0.001^{b}	7.84 ± 0.57^{e}	45.63 ± 1.29^{a}	168.75 ± 7.78^{a}	43.03 ± 2.73^{a}	80.29 ± 0.87^{c}	-5.02 ± 0.49^{c}	45.71 ± 0.46^{a}	47.09 ± 0.63^{a}
LB-GLY	0.073 ± 0.005^{a}	14.16 ± 1.56^{c}	7.25 ± 0.96^{b}	51.60 ± 6.71^{b}	17.28 ± 2.20^{b}	86.49 ± 0.96^{b}	-4.6 ± 0.51^{bc}	34.54 ± 1.46^{c}	34.82 ± 1.45^{c}
F-PEG	0.033 ± 0.001^{c}	21.59 ± 1.05^{b}	1.29 ± 0.03^{c}	NA	NA	90.28 ± 0.33^{a}	-1.12 ± 0.09^{a}	1.89 ± 0.06^{d}	2.91 ± 0.29^{d}
B-PEG	0.047 ± 0.003^{b}	10.1 ± 1.38^{de}	2.96 ± 0.65^{c}	26.38 ± 0.81^{c}	5.26 ± 0.16^{c}	80.1 ± 1.25^{c}	-5.63 ± 0.4^{d}	46.65 ± 0.56^{a}	48.11 ± 0.72^{a}
LB-PEG	0.075 ± 0.006^{a}	11.9 ± 1.03^{cd}	1.37 ± 0.26^{c}	NA	NA	86.01 ± 0.43^{b}	-4.46 ± 0.56^{b}	37.21 ± 1.45^{b}	37.5 ± 1.35^{b}

Values are mean ± SD. Different lowercase superscripts in the same column denote significant difference ($p < 0.05$). TS: tensile strength; EAB: elongation at break. F-GLY, LB-GLY, and B-GLY represent gelatin/chitosan blend films plasticized with glycerol without and with L/BLEE at 2% or BLEE at equivalent amount based on the encapsulation efficiency. F-PEG, LB-PEG, and B-PEG represent gelatin/chitosan blend films plasticized with polyethylene glycol-4000 without and with L/BLEE at 2% or BLEE at equivalent amount based on the encapsulation efficiency.

the blooming of PEG plasticized films. However, it failed to enhance elasticity of the film as witnessed by very low EAB (2.96 ± 0.65%) associated with its brittleness. LB-GLY had lower TS of 14.16 ± 1.56 MPa, mainly caused by the hinderance or disturbance between polymer chains by L/BLEE within the film matrix. Nevertheless, LB-GLY had a slight increase ($p < 0.05$) in EAB (7.25 ± 0.96%) as compared to F-GLY. This might be due to the phase transitions that occur in liposomal structures during the drying process, which plausibly promoted the rupture of liposomes. This might bring about the restructuring of film matrix with less flexibility (Jiménez *et al.*, 2014). LB-PEG showed similar trend to that of B-PEG, in which TS decreased considerably ($p < 0.05$) and EAB was much lower than those containing GLY. The effect of PEG was prominent in bestowing a phase separation of LB-PEG, as reflected by the decrease in both TS and EAB.

8.5.1.3. Seal ability

Efficient sealing between two films is performed by melting the surface of two films by the applied heat. This could improve the interfacial interactions or the merging across the contacted surfaces. Preliminary trials showed that heating temperature of 150 ± 0.5˚C for 1.50 s, with subsequent cooling for 1.50 s could provide the sufficient melting and fusion for most tested specimens. Among all the prepared films, only three film samples showed heat-sealing ability (Table 18). Failure in heat-sealing, especially in F-GLY and F-PEG, was probably due to the presence of chitosan within the blend films and the inability of the plasticizers to favor the melting of these films. Chitosan has poor thermoplastic properties and can be degraded before the melting point. It also cannot be molded, or extruded. Films containing high amount of chitosan were generally not sealable as they had compact network and higher rigidity (Cazón and Vázquez, 2020).

Furthermore, seal strength of films tended to be weakened due to poor interfacial adhesion when a hydrophobic polymer became incompatible with hydrophilic polymer, even at low level (Fathima *et al.*, 2018). B-GLY had the highest seal strength and efficiency (168.75 ± 7.78 N/m and 43.03 ± 2.73%) followed by LB-GLY (51.60 ± 6.71 N/m and 17.28 ± 2.20%) and B-PEG (26.38 ± 0.81 N/m and 5.26 ± 0.16%) ($p < 0.05$), respectively. BLEE presumably lowered the interaction among polymer chains in the film matrix, thus allowing the films to be molten and sealed with ease. Nouri and Nafchi (2014) noted that betel extract provided efficient seal ability to films made from sago starch by increasing the hydrogen bonds between film components, which were easily destroyed by heat during sealing. Phase transitions took place by presence of L/BLEE might play a role in the considerably poor seal efficiency and seal strength of LB-GLY while LB-PEG was not sealable.

Electrostatic interactions between the functional groups of both gelatin and chitosan coupled with the hydrogen bonds between the gelatin molecules and the plasticizer could be disrupted by heat, thus favoring the melting during heat sealing (Qiao *et al.,* 2017). B-GLY plausibly had the most well-balanced electrostatic interactions between gelatin and chitosan molecules via weak bonds such as hydrogen bonding and between gelatin molecules and GLY together with BLEE, resulting in looser network. This could facilitate the melting of film network, leading to interdiffusion of gelatin or chitosan molecules as shown by better seal ability. For PEG plasticized films, only B-PEG could be sealed but with low seal strength and efficiency. The phase separation caused by PEG was probably responsible for the exposure of chitosan toward heat applied, especially in the presence of L/BLEE or the absence of BLEE. This led to the lack of any seal ability.

8.5.1.4. Color

F-PEG was observed to have white residues on its surface (blooming or blushing) which occurred when PEG exceeded its compatibility limit in the film matrix (Fig. 34D), rendering phase separation and physical exclusion (Aulton *et al.*, 1981). Color of the films turned to yellowish when BLEE was incorporated, but when L/BLEE was incorporated, the yellow color lessened ($p < 0.05$). L^* and a^* values of films without BLEE or L/BLEE were the highest ($p < 0.05$), while their b^* and ΔE^* values were the lowest ($p < 0.05$) (Table 18). Addition of BLEE or L/BLEE led to the decreases in both L^* and a^* values ($p < 0.05$), indicating the decrease in films' lightness and the increase in greenness. Such an effect was lesser in LB-GLY or LB-PEG which had more lightness and less greenness. The values of b^* and ΔE^* were increased ($p < 0.05$) in B-GLY and B-PEG, reflecting the increases in both yellowness and total color difference of these films containing BLEE.

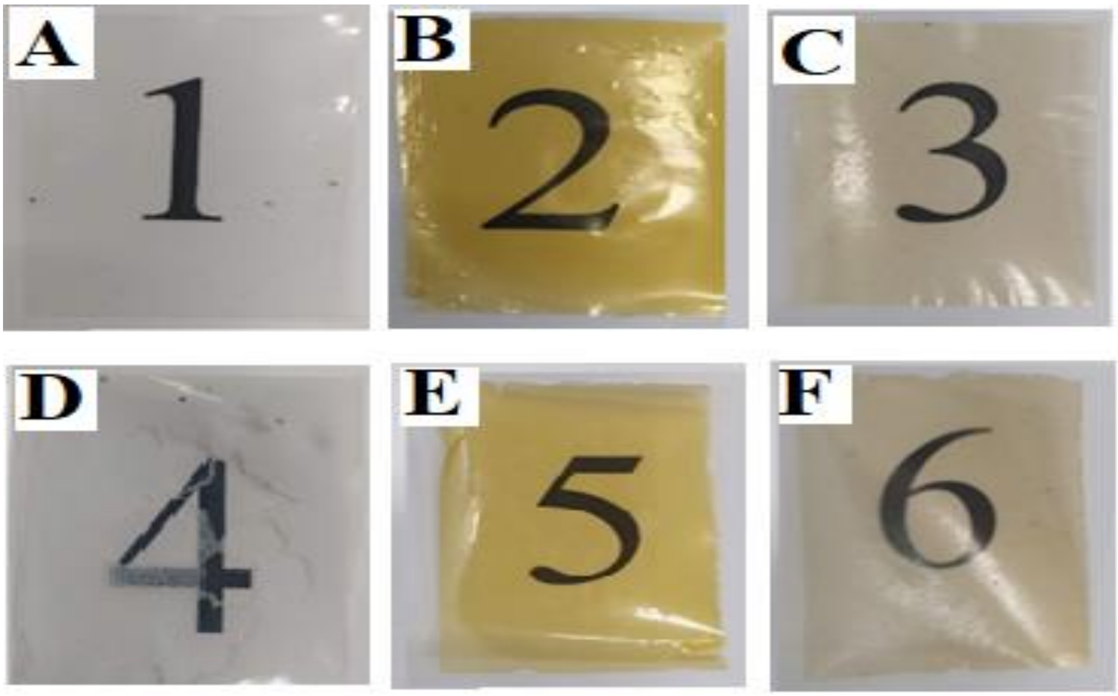

Figure 34. Photographic images of glycerol plasticized gelatin/chitosan blend films without BLEE or L/BLEE (F-GLY) (A), with BLEE (B-GLY) (B), and with L/BLEE (LB-GLY) (C) and polyethylene glycol plasticized gelatin/chitosan blend films without BLEE or L/BLEE (F-PEG) (D), with BLEE (B-PEG) (E), and with L/BLEE (LB-PEG) (F).

These values also augmented in films incorporated with L/BLEE but at lesser degree ($p < 0.05$). Such a change in color was more likely attributed to remaining pigmented compounds, especially chlorophyll, even though dechlorophyllization was applied (Bitencourt *et al.*, 2014). For films added with L/BLEE, the change in their color was attributed to BLEE that might not completely entrapped in liposomes or the rupture of liposomes could occur during the preparation of the film. In addition, lecithin with yellowish color could contribute to the color of resulting films. Apart from the blooming in F-PEG, the plasticizer used had negligible effect on the color of the films. Overall, the difference was pronounced between blend films incorporated with BLEE and L/BLEE ($p < 0.05$).

8.5.1.5. Light transmission and transparency value

Films with excellent ultraviolet and visible (UV/Vis) light barrier abilities are highly regarded for the prevention of the adverse effects of light toward food quality. Films without BLEE or L/BLEE had higher transmission at all wavelengths (Fig. 35). UV negatively impacts food systems, especially enhancement of oxidation process at initiation stage. Gelatin containing amino acid residues, especially those containing aromatic rings with double bonds, can absorb UV light thus, better UV barrier ability (Bonilla and Sobral, 2016). Irrespective of the plasticizer used, the incorporation with BLEE enhanced the UV/Vis light barrier abilities of gelatin/chitosan blend films ($p<0.05$), as compared to films without BLEE (Fig. 35). Film samples containing BLEE showed low transmission values close to zero in the wavelength range of 200 – 400 nm (UV region), indicating a remarkable barrier ability towards the UV light. This finding could be related to the diverse phenolic compounds or other components in BLEE such as vitexin and isovitexin (Tagrida and Benjakul, 2020), which contain abundant unsaturated bonds in their structures and can absorb UV light, thus preventing harmful effect to the products (Bitencourt *et al.*, 2014).

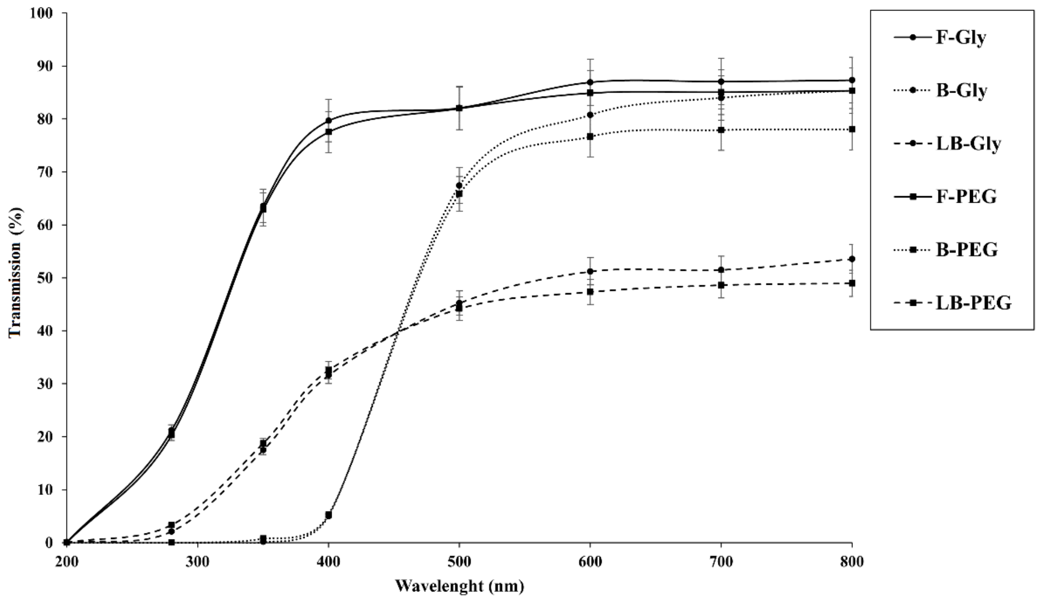

Figure 35. Light transmission (200-800 nm) of gelatin/chitosan blend films plasticized with glycerol or polyethylene glycol without and with BLEE or L/BLEE.

Addition of L/BLEE decreased transmission of the films ($p < 0.05$) in the range of 450 – 800 nm, indicating that SPC and CHL along with phenolic compounds could prevent transmission of visible light. Also, phase transitions caused by liposomes might contribute to the decrease in transmission (Jiménez *et al.*, 2014). However, both LB-GLY and LB-PEG showed higher transmission than B-GLY and B-PEG in the UV range, which could be related to the entrapment of BLEE.

Visual observation (Fig. 34) showed that all the prepared films without and with BLEE or L/BLEE were transparent, indicating their homogeneity. Films plasticized with PEG were observed to have higher transparency values ($p < 0.05$) compared to GLY plasticized films (Table 19). This indicated that films containing PEG as plasticizer were more turbid than those added with GLY. Additionally, the incorporation with either BLEE or L/BLEE led to increased transparency values, in which films added with L/BLEE had the highest transparency values. Therefore, BLEE or L/BLEE incorporation into the films along with plasticizer used affected their transparency to some degree.

Table 19. Transparency value and water vapor permeability (WVP) of gelatin/chitosan blend films plasticized with glycerol or polyethylene glycol and added BLEE or L/BLEE.

Sample	Transparency value	WVP ($\times 10^{-11}$ g m^{-1} s^{-1} Pa^{-1})
F-GLY	1.91 ± 0.55^{bc}	7.51 ± 0.49^{a}
B-GLY	2.03 ± 0.14^{bc}	3.84 ± 0.29^{e}
LB-GLY	4.01 ± 0.63^{ab}	4.89 ± 0.18^{d}
F-PEG	2.15 ± 0.72^{bc}	6.81 ± 0.12^{b}
B-PEG	2.41 ± 0.30^{c}	3.39 ± 0.29^{e}
LB-PEG	4.33 ± 0.37^{a}	5.58 ± 0.18^{c}

Values are mean ± SD. Different lowercase superscripts in the same column denote significant difference ($p < 0.05$). WVP: water vapor permeability; For captions see Table 18.

8.5.1.6. Water vapor permeability (WVP)

WVP is the function of two simultaneous processes: solubility and the diffusion of water vapor. Addition of plasticizer increases water solubility of polymers' matrix and enhanced the mobility of the chains by extending and softening the polymers (Haq *et al.*, 2014). Usually, films having low WVP are preferable as they could prevent the migration of the moisture from environment to food products (Nilsuwan *et al.*, 2018). The types of plasticizers and addition of either BLEE or

L/BLEE affected the WVP of resulting films (Table 19). Film samples devoid of BLEE or L/BLEE had the highest WVP ($p < 0.05$). The hydrophilic nature of gelatin allowed higher quantities of water vapor to migrate through the film. F-GLY had the highest WVP ($p < 0.05$) due to the presence of GLY which enhanced the hydrophilicity of film, leading to the increase in its WVP. On the other hand, PEG possessing high molecular weight created lesser diffusion pathways for water vapor because of the restriction in chain mobility (Faradilla *et al.*, 2019). In addition, the less hydrophilic nature of PEG might contribute to less WVB than GLY.

Marked decrease in WVP ($p < 0.05$) was found for film samples with BLEE. This reduction in WVP could be attributed to the enhancement of the gelatin and chitosan cross-linking, which led to the more compact matrix with decreased hydrophilic functional groups. Consequently, the decrease in permeation of water vapor through the films was attained (Nilsuwan *et al.*, 2018). BLEE also contains several hydrophobic compounds such as eugenol, estragole, chavicol, and linalool that could act as barrier for water vapor migration (Madhumita *et al.*, 2019). Lesser WVP was expected in films with L/BLEE due to the increased hydrophobicity mediated by SPC used for liposomal preparation. However, WVB was found to be higher ($p < 0.05$) than those added with BLEE. This could be mainly attributed to the pores and cracks formed because of the non-homogeneity and phase transitions of liposomes, especially during drying of the films. This eventually led to the increased accessibility of water vapor as witnessed by the increased WVP. Similarly, Imran *et al.* (2012) reported an upsurge in WVP for hydroxypropyl methylcellulose (HPMC)-lecithin-nisin composite films because of non-homogenous dispersion of lecithin in the film's matrix.

8.5.1.7. Scanning electron microscopic (SEM)

SEM micrographs (Fig. 36) showed smoother surface and cross-section for gelatin/chitosan blend film samples devoid of BLEE or L/BLEE (Fig. 36A, D, G and J). However, a high degree of phase separation was detected in films plasticized with PEG by the presence of clusters appeared as whitish staining or droplets on the surface of the film. This indicated less compatibility and deficiency in polymers' interactions. This effect was referred to as blooming or blushing (Laohakunjit and Noomhorm, 2004), which was found on F-PEG surface (Fig. 36G) but was absent in

F-GLY (Fig. 36A). Lower molecular weight plasticizers such as GLY have facilitated the accessibility to more hydroxyl groups, allowing the plasticizer to diffuse and interact efficiently with the film's components. However, PEG having higher molecular weight could not migrate to hydroxyl groups easily, leading to phase separation (Faradilla *et al.*, 2019). For B-GLY, the rougher and slightly non-uniform surface and cross section were observed (Fig. 36B and E). Nevertheless, no phase separation was noticeable, reflecting a high degree of compatibility between all the components in the film matrix.

The rougher and non-uniform surface and cross section were also observed in B-PEG however, the phase separation was lessened (Fig. 36H and K). This was probably because of the polyphenols of BLEE that provided more hydroxyl groups which formed more compatible interactions within the film matrix. Surface and cross-sectional roughness of B-GLY and B-PEG were attributed to the disturbance of the ordered alignment of both gelatin and chitosan chains caused by BLEE, leading to the increased tortuosity. Less compact and non-uniform morphology might contribute to the lower TS and higher EAB in B-GLY as compared to F-GLY (Table 18). Similarly, Bitencourt *et al.* (2014) found that gelatin-based films added with curcuma ethanolic extract had less compact and uniform surface.

When L/BLEE was incorporated in the film matrix, a much coarser structure was observed, which was mainly related to the large size of liposomes. Micrographs of LB-GLY and LB-PEG (Fig. 36C, F, I, and L) showed the presences of pores and cracks. The addition of the liposomes resulted in steric hindrance. As a result, the formation of uniform and continuous network between the film components was impeded leading to formation of these voids (Wu *et al.*, 2015). On the other hand, the cracks could be induced by the mutual collision of the liposomes during the film drying process, in which the liposomes were gathered in the film matrix during water evaporation, resulting in the formation of hydrophobic aggregation and phase transition. This eventually led to the existence of cracks (Bao *et al.*, 2009). Apart from pores and cracks, LB-PEG possessed whitish staining (blooming) at lower degree, compared to those found in F-PEG. Polyphenols of BLEE might be released from the liposomes, providing more hydroxyl groups, thus lowering the phase separation.

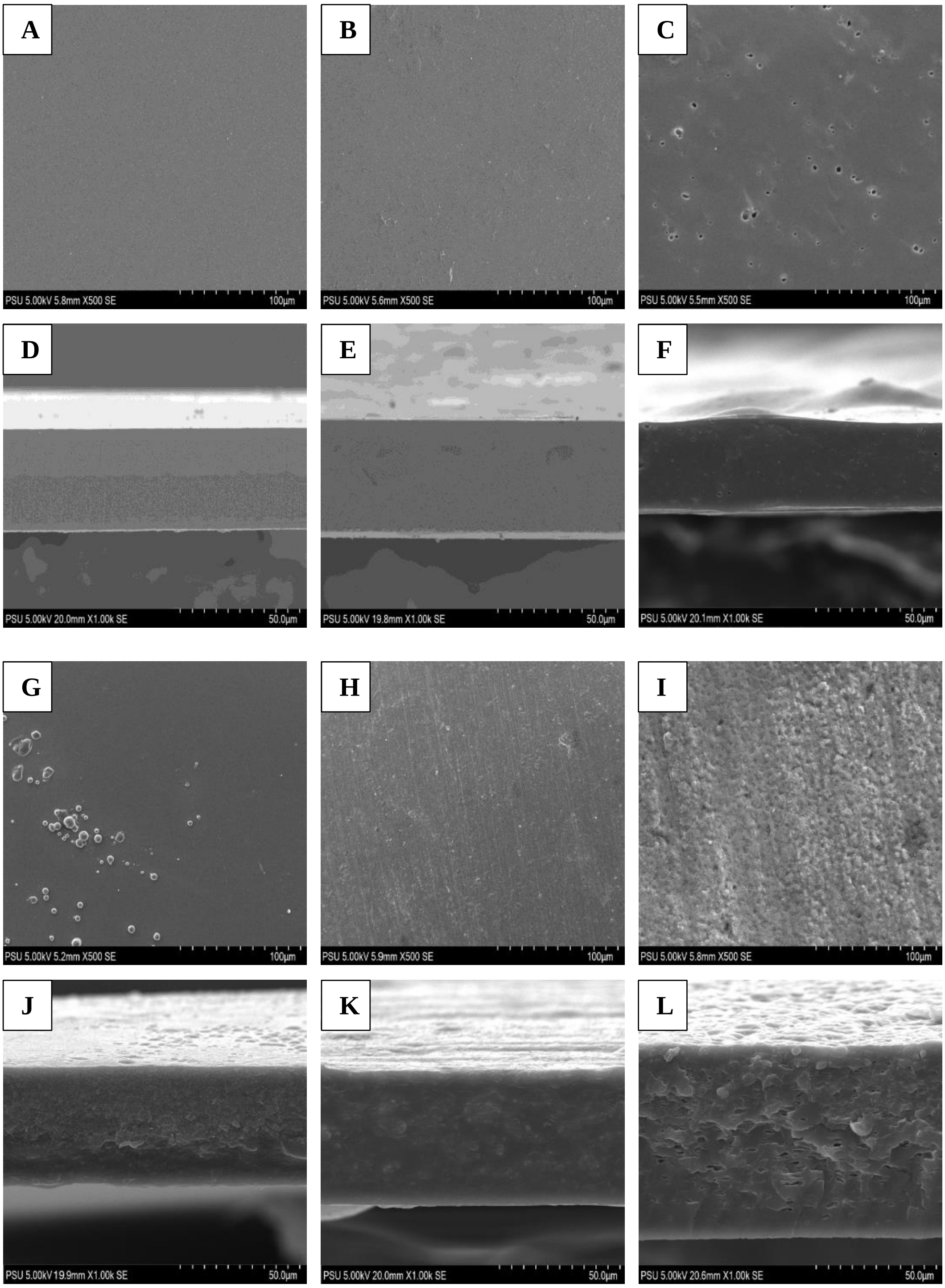

Figure 36. SEM micrographs (surfaces and cross-sections) of GLY plasticized gelatin/chitosan blend films without BLEE or L/BLEE (F-GLY) (A, and D), with BLEE (B-GLY) (B, and E), and with L/BLEE (LB-GLY) (C and F) and polyethylene glycol plasticized gelatin/chitosan blend films without BLEE or L/BLEE (F-PEG) (G and J), with BLEE (B-PEG) (H and K), and with L/BLEE (LB-PEG) (I and L).

8.5.1.8. Antioxidant activities (AO-A)

Active packaging is referred to films added with components with bioactivities such as antioxidant or antibacterial activities that contributes to better prevention of food deterioration by lowering lipid oxidation and retarding microbial growth (de Campos *et al.*, 2019). Incorporation of either BLEE or L/BLEE to the gelatin/chitosan blend films increased their AO-A (Table 20). Films without BLEE or L/BLEE had the lowest AO-A ($p < 0.05$), showing the lowest DPPH-RSA and ABTS-RSA. Radical scavenging activities could be attributed to the residual -NH_2 or -OH groups of chitosan and gelatin molecules (Mittal *et al.*, 2021). Films without BLEE showed no FRAP and MCA. The result was in line with Xu *et al.* (2021) who found that films prepared solely from either gelatin or chitosan had no reducing power or chelating activity. DPPH-RSA, ABTS-RSA, FRAP, and MCA increased markedly with addition of BLEE or L/BLEE into the film matrix ($p < 0.05$).

However, films incorporated with L/BLEE showed lower AO-A than those added with BLEE ($p < 0.05$). L/BLEE was strongly embedded in the films' matrix. Consequently, the release of BLEE was impeded as shown by lower AO-A. Similar effect was reported by Jiménez *et al.* (2014) who found poorer bioactivity of corn starch and sodium caseinate based films incorporated with nanoliposomes due to the slow release of active compounds. Additionally, the activity of BLEE could be affected during the preparation of films as BLEE was found to be sensitive towards changes in pH (Tagrida and Benjakul, 2020). AO-A of films containing BLEE or L/BLEE was strongly connected to the diverse polyphenols or reducing components in BLEE such as isovitexin, epigallocatechin, and kaempferol derivatives, in which these compounds acted as free radical scavengers, and exhibited the reduction of ferric into ferrous ion, and metal chelating (Tagrida and Benjakul, 2020). Irrespective of plasticizer used, no difference could be detected in the AO-A of films containing either BLEE or L/BLEE ($p > 0.05$).

Table 20. Antioxidant activity of gelatin/chitosan blend films plasticized with glycerol or polyethylene glycol and added with BLEE or L/BLEE.

Sample	DPPH-RSA (µmol TE/g sample)	ABTS-RSA (µmol TE/g sample)	FRAP (µmol TE/g sample)	MCA (µmol EDTA/g sample)
F-GLY	3.51 ± 0.72^{c}	25.55 ± 1.22^{c}	ND*	ND
B-GLY	126.84 ± 0.58^{a}	2273.7 ± 7.22^{a}	1570.7 ± 2.23^{a}	237.85 ± 0.54^{a}
LB-GLY	111.27 ± 1.32^{b}	2106.6 ± 10.7^{b}	1494.9 ± 7.22^{b}	219.84 ± 1.78^{b}
F-PEG	5.12 ± 0.71^{c}	28.87 ± 0.87^{c}	ND	ND
B-PEG	124.93 ± 1.02^{a}	2264.4 ± 6.93^{a}	1571.3 ± 3.13^{a}	236.07 ± 1.12^{a}
LB-PEG	108.57 ± 0.40^{b}	2096.6 ± 9.87^{b}	1493.4 ± 7.18^{b}	217.55 ± 1.43^{b}

Values mean ± SD (n=3). Different lowercase superscripts in the same column denote significant difference (p<0.05). For captions see Table 18.

ND*: not detected

8.5.2. Quality changes of shrimp oil (SO) packaged in gelatin/chitosan blend pouches

8.5.2.1. Lipid oxidation

Quality changes of SO packaged in pouches made from B-GLY film, which was selected as the film with the most satisfactory mechanical, physical, and bioactive properties, were monitored in comparison with those packaged in LDPE pouches considered as the control. PV is an indication of primary oxidation products formed, mainly hydroperoxides (Gulzar *et al.,* 2022). Changes in PV of SO packaged in B-GLY or LDPE pouches are depicted in Fig. 37A. No difference was detected at the beginning of the storage (day 0) between the two samples ($p > 0.05$). PV was increased markedly as storage time augmented ($p < 0.05$). SO packaged in B-GLY pouches reached the plateau at day 20 and constant PV was obtained up to day 30. SO consisted of PUFAs, which were highly susceptible to oxidation induced by many factors such as UV light and free radicals, etc. (Nilsuwan *et al.,* 2019). Increased formation of hydroperoxide significantly reduces PUFAs content and negatively affects overall quality of SO (Gulzar *et al.,* 2022). The packaging of SO in B-GLY pouches enhanced the oxidative stability of SO due to the improved UV/Vis light, and water vapor barrier abilities. Also, antioxidants in BLEE were able to be released and scavenge the free radicals, thus lowering oxidation considerably.

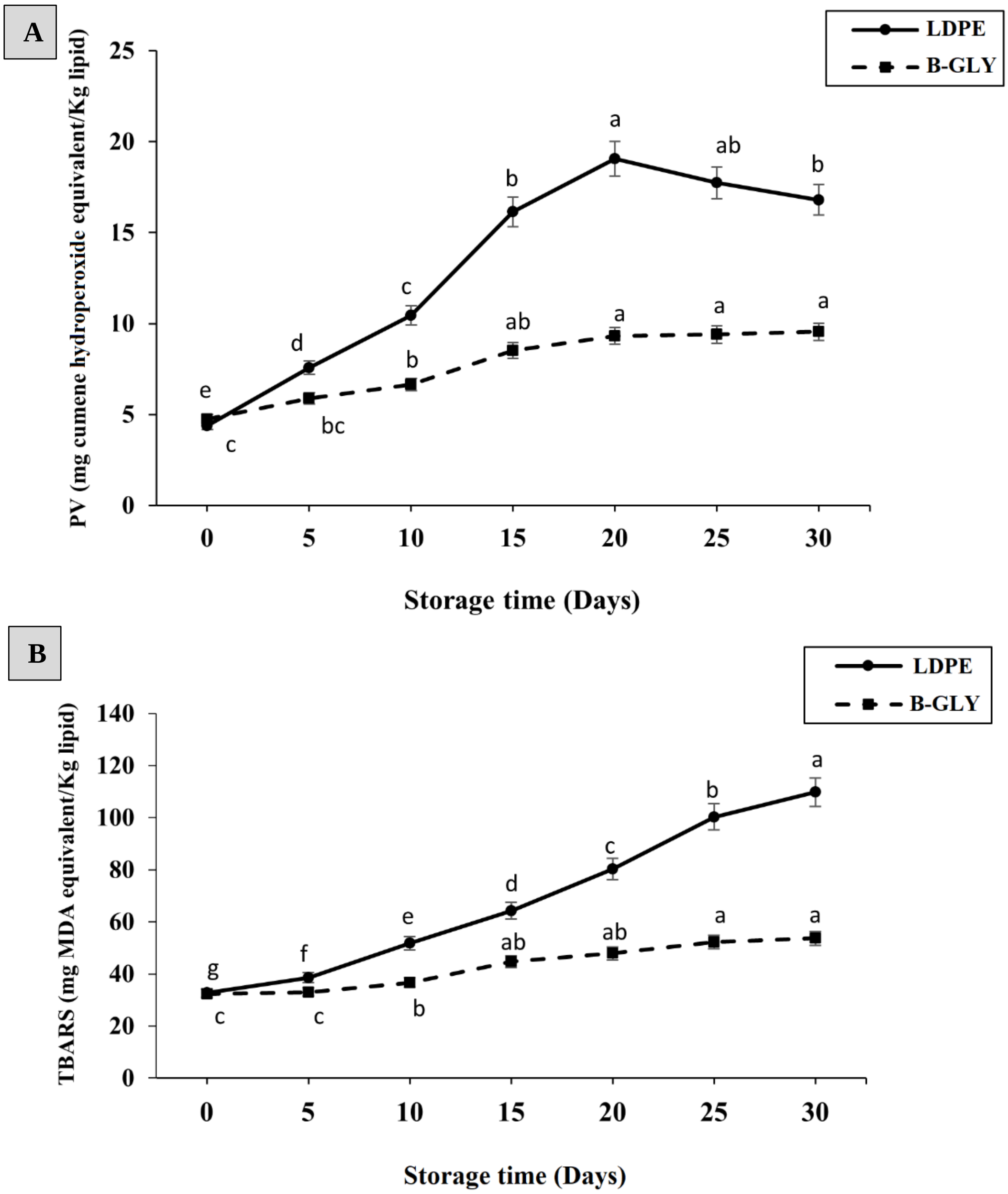

Figure 37. Peroxide value (A) and thiobarbituric acid reactive substances (B) of shrimp oil packaged in LDPE pouches and B-GLY pouches made from gelatin/chitosan blend film plasticized with glycerol and incorporated with BLEE. Different lower letters within the same packaging indicate significant differences ($p < 0.05$).

During 20-30 days of storage, PV remained stable for SO packaged in B-GLY pouch, while PV became lowered for SO packaged in LDPE pouch at day 30 ($p < 0.05$). This drop was probably attributed to the decomposition of existing hydroperoxides and simultaneous formation of volatile secondary oxidation products (Gulzar *et al.*, 2022).

TBARS of SO packaged in LDPE pouches upsurged ($P < 0.05$) (Fig. 37B) continuously up to the end of storage (day 30). However, SO packaged in B-GLY pouch had the lower values at all storage times. It was noted that TBARS values reached a plateau at day 15 and remained constant up to the end of storage. Elevated TBARS values reflected the generation of secondary oxidation products such as malonaldehyde, aldehydes, and ketones, known for their off-flavor and rancid odor (Tagrida and Benjakul, 2022). The elevated values are considered as an index of increased lipid decomposition. Lower TBARS increasing rate for SO packaged in B-GLY pouches indicated a higher oxidative stability of SO, in which active compounds could be released from the pouches. Therefore, active pouches containing BLEE with its superior barrier abilities, effectively prevent oxidation of SO stored for an extended time.

8.5.2.2. Fatty acid (FA) profile

FA profiles of SO packaged in LDPE or B-GLY pouches at day 0 and after 30 days of storage are tabulated in Table 21. The SO at the beginning of storage (day 0) contained 43.8% saturated fatty acid (SFA), 19.22% monosaturated fatty acid (MUFA), and 36.98% polyunsaturated fatty acid (PUFA). Palmitic was the most abundant SFA. This FA can be used as energy source for some body cells but can cause serious health issues if consumed excessively (Tagrida *et al.*, 2021b). Stearic and tricosanoic acids were also among the identified SFA found in SO in relatively higher amounts (3.52 ± 0.00 and 3.18 ± 0.00 g/100 g oil, respectively). Both fatty acids are known for their health and industrial benefits, however, they can have adverse effects when consumed at high amount (Kotlęga *et al.*, 2021). Between the unsaturated fatty acid found in SO, oleic (5.81 ± 0.01 g/100 g oil) and linoleic (6.12 ± 0.03 g/100 g oil) acids were the most abundant unsaturated FA. The former belongs to MUFA, while the latter is considered as PUFA, and both are reported for their valued health benefits (Khan *et al.*, 2003).

Eicosapentaenoic acid (EPA) and docosahexaenoic acid (DHA) were also observed in the SO profile at day 0 in a considerably high amounts (5.51 ± 0.02 and 3.78 ± 0.03 g/100 g oil, respectively). These FA belong to the valuable n-3 PUFA and are renowned for their importance in enhancing health promotion and preventing several diseases (Tagrida *et al.*, 2021b). At the end of storage (30 days), the SFA had a noticeable

Table 21. Fatty acid profile of shrimp oil packaged in LDPE or B-GLY pouches at day 0 and 30 of storage at 25-28˚C.

Fatty acid (g/ 100g oil)	Day 0	Day 30	
		LDPE	B-GLY
Saturated fatty acid (SFA)			
C14:0 (Myristic)	1.37 ± 0.01[a]	1.38 ± 0.00[a]	1.37 ± 0.03[a]
C15:0 (Pentadecanoic)	0.64 ± 0.00[c]	0.72 ± 0.00[a]	0.68 ± 0.01[b]
C16:0 (Palmitic)	8.81 ± 0.02[c]	9.72 ± 0.07[a]	8.98 ± 0.01[b]
C17:0 (Heptadecanoic)	0.93 ± 0.04[c]	0.99 ± 0.01[a]	0.95 ± 0.00[b]
C18:0 (Stearic)	3.52 ± 0.00[c]	3.71 ± 0.03[a]	3.54 ± 0.00[b]
C20:0 (Docosanoic)	1.06 ± 0.03[b]	1.20 ± 0.01[a]	1.19 ± 0.03[a]
C23:0 (Tricosanoic)	3.18 ± 0.00[c]	3.38 ± 0.02[a]	3.20 ± 0.01[b]
C24:0 (Lignoceric)	1.09 ± 0.00[b]	1.13 ± 0.01[a]	1.09 ± 0.00[b]
Total	**20.6 ± 0.02[c]**	**22.3 ± 0.04[a]**	**21.0 ± 0.01[b]**
Mono-unsaturated fatty acid (MUFA)			
C15:1 (cis-10-Pentadecanoic)	0.51 ± 0.00[a]	0.49 ± 0.01[a]	0.49 ± 0.00[a]
C16:1 (Palmitoleic)	1.17 ± 0.03[a]	1.16 ± 0.00[a]	1.17 ± 0.01[a]
C18:1 (Oleic)	5.81 ± 0.01[a]	5.78 ± 0.00[b]	5.80 ± 0.01[a]
C20:1 (cis-11-Eicosenoic)	0.87 ± 0.05[a]	0.81 ± 0.01[b]	0.87 ± 0.00[a]
C24:1 (Nervonic)	0.67 ± 0.00[a]	0.63 ± 0.01[b]	0.66 ± 0.01[a]
Total	**9.04 ± 0.06[a]**	**8.88 ± 0.05[c]**	**9.00 ± 0.01[ab]**
Poly-unsaturated fatty acid (PUFA)			
C18:2 (Linoleic)	6.12 ± 0.03[a]	5.70 ± 0.04[c]	5.99 ± 0.01[b]
C18:3 (alpha-Linolenic)	0.65 ± 0.02[a]	0.58 ± 0.00[c]	0.61 ± 0.00[b]
C20:2 (cis-11,14-Eicosadienoic)	1.39 ± 0.00[a]	1.19 ± 0.01[c]	1.30 ± 0.03[b]
C20:5 (cis-5,8,11,14,17-Eicosapentaenoic acid) (EPA)	5.51 ± 0.02[a]	3.58 ± 0.01[c]	4.91 ± 0.02[b]
C22:6 (cis-4,7, 10,13,16,19-Docosahexaenoic acid) (DHA)	3.78 ± 0.03[a]	2.96 ± 0.02[c]	3.14 ± 0.01[b]
Total	**17.4 ± 0.06[a]**	**14.0 ± 0.01[c]**	**15.9 ± 0.01[b]**

Values mean ± SD (n=3). Different lowercase superscripts in the same column denote significant difference ($p<0.05$). LDPE: low-density polyethylene film; B-GLY: betel extract incorporated gelatin/chitosan blend film plasticized with glycerol.

increase ($p < 0.05$), while the unsaturated fatty acids, particularly PUFAs, decreased ($p < 0.05$) for both SO packaged in LDPE and B-GLY pouches. However, such a decrease was more pronounced in SO packaged in LDPE pouches, where a 19.54% reduction in PUFAs was attained, while only 8.62% reduction took place in SO packaged in B-GLY pouches. The reduction in PUFAs was plausibly due to their high susceptibility to oxidation induced by numerous factors such as free radicals and UV light (Rupasinghe *et al.,* 2010). Superior antioxidant activities and UV barrier properties of B-GLY pouches could retard SO oxidation as indicated by lower reduction of PUFAs and lower increase in SFA content. On the other hand, LDPE pouches failed to prevent the oxidation of SO as reflected by the increment of their SFA and the marked decrease in MUFAs and PUFAs. The results of FA profiles were in accordance with the higher increase in both PV and TBARS of SO during the storage of 30 days (Fig. 37A and B).

8.5.2.3. Astaxanthin content

Astaxanthin, found prominently in many crustaceans, is a reddish-orange keto-carotenoid with various uses such as a nutritive supplement and as a food colorant. It was also considered to protect SO from oxidation, additionally it exhibits several health benefits including anticancer, anti-inflammatory activities, and can be regarded as an immunity booster (Gulzar *et al.,* 2022). At the beginning of storage, the initial astaxanthin content of SO was 136.11 mg/100 g oil but, astaxanthin content was reduced significantly after 30 days ($p < 0.05$) (Fig. 38). At the end of storage, astaxanthin content of SO packaged in LDPE pouch was 45.97 mg/100 g oil, whereas it was 115.64 mg/100 g oil in B-GLY pouch. Apart from peroxidation induced by free radicals, astaxanthin is sensitive to photodegradation which causes the destruction or oxidation of its double bonds thus reducing its content (Takeungwongtrakul and Benjakul, 2016). The result confirmed the high protective ability of B-GLY pouches against astaxanthin degradation, mainly due to antioxidant activity and UV barrier abilities of the pouches used.

8.6. Conclusion

Types of plasticizers as well as the incorporation of BLEE or L/BLEE into gelatin/chitosan blend films affected their properties. The heat sealing of some films was achieved, while other films were not sealable. UV/Vis light and WVP barrier properties were improved when added with BLEE. Furthermore, AO-A of films was

Day 0 | **Day 30**

LDPE | **B-GLY**

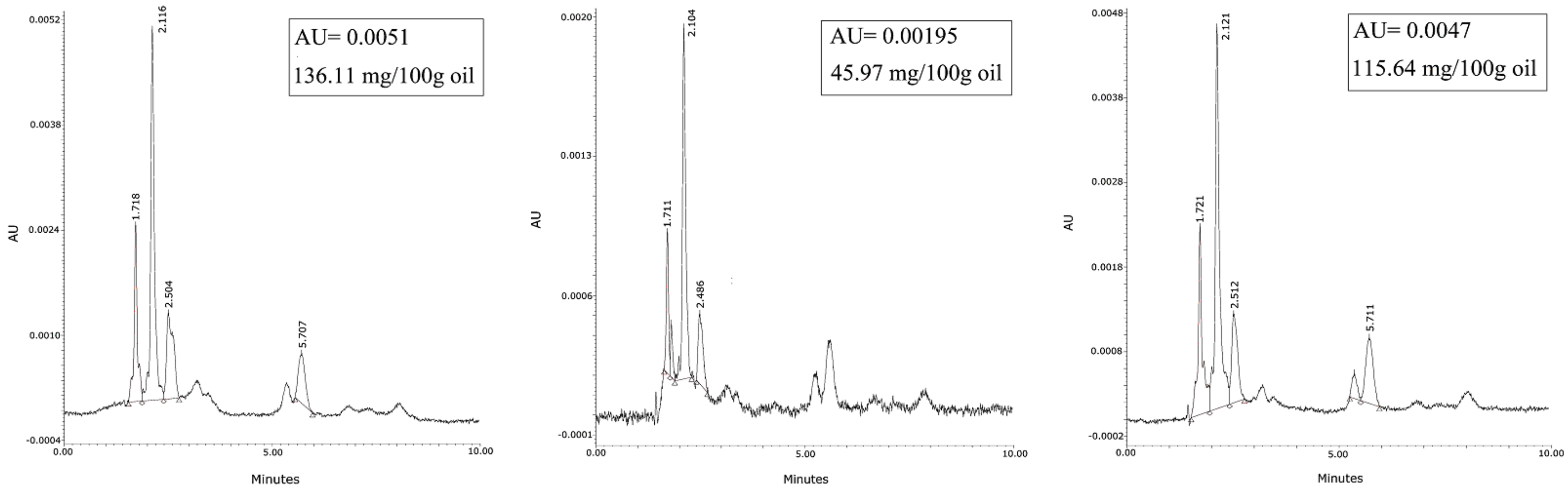

Figure 38. HPLC chromatograms of astaxanthin content in shrimp oil packaged in pouches made from LDPE or B-GLY at day 0 and after 30 days of storage at 25-28˚C.

enhanced with the addition of L/BLEE or BLEE ($p < 0.05$). Oxidative stability of SO was maintained when packaged in pouches made from gelatin/chitosan blend incorporated with BLEE and plasticized with glycerol (B-GLY) as ascertained by lower PV, TBARS, PUFA oxidation and astaxanthin degradation ($p < 0.05$) throughout 30 days of storage, compared to that packaged in LDPE pouches. Therefore, pouches based on gelatin/chitosan plasticized with glycerol and incorporated with BLEE could be used as active packaging to extend the shelf-life of non-aqueous food products, particularly oil susceptible to lipid oxidation.

8.7. References

ASTM. 2019. Standard Test Method for Breaking Strength and Elongation of Pressure-Sensitive Tape, ASTM D3759/D3759M-05(2019). doi: 10.1520/D3759_D3759M-05R19. rom https://www.astm.org/d3759_d3759m-05r19.html

ASTM. 2021. Standard Guide for Determination of Thickness of Plastic Film Test Specimens, ASTM D6988-21. doi: 10.1520/D6988-21. Retrived from https://www.astm.org/d6988-21.html

Aulton, M., Abdul-Razzak, M., and Hogan, J. 1981. The mechanical properties of hydroxypropylmethylcellulose films derived from aqueous systems Part 1: the influence of plasticisers. Drug Development and Industrial Pharmacy. 7(6): 649 - 668.

Bao, S., Xu, S., and Wang, Z. 2009. Antioxidant activity and properties of gelatin films incorporated with tea polyphenol-loaded chitosan nanoparticles. Journal of the Science of Food and Agriculture. 89(15): 2692 - 2700.

Bitencourt, C., Fávaro-Trindade, C., Sobral, P. D. A. and Carvalho, R. D. 2014. Gelatin-based films additivated with curcuma ethanol extract: Antioxidant activity and physical properties of films. Food Hydrocolloids. 40: 145 - 152.

Bonilla, J. and Sobral, P. J. 2016. Investigation of the physicochemical, antimicrobial and antioxidant properties of gelatin-chitosan edible film mixed with plant ethanolic extracts. Food Bioscience. 16: 17 - 25.

Cao, N., Fu, Y. and He, J. 2007. Mechanical properties of gelatin films cross-linked, respectively, by ferulic acid and tannin acid. Food Hydrocolloids. 21: 575 - 584.

Cazón, P. and Vázquez, M. 2020. Mechanical and barrier properties of chitosan combined with other components as food packaging film. Environmental Chemistry Letters. 18: 257 - 267.

De Campos, S. S., De Oliveira, A., Moreira, T. F. M., Da Silva, T. B. V., Da Silva, M. V., Pinto, J. A., Bilck, A. P., Gonçalves, O. H., Fernandes, I. P. and Barreiro, M.-F. 2019. TPCS/PBAT blown extruded films added with curcumin as a technological approach for active packaging materials. Food Packaging and Shelf Life. 22: 100424.

De Oliveira, V. S., Ferreira, F. S., Cople, M. C. R., Labre, T. d. S., Augusta, I. M., Gamallo, O. D., and Saldanha, T. 2018. Use of natural antioxidants in the inhibition of cholesterol oxidation: A review. Comprehensive Reviews in Food Science and Food Safety. 17(6): 1465 - 1483.

Faradilla, R. F., Lee, G., Sivakumar, P., Stenzel, M., and Arcot, J. 2019. Effect of polyethylene glycol (PEG) molecular weight and nanofillers on the properties of banana pseudostem nanocellulose films. Carbohydrate Polymers. 205: 330 - 339.

Fathima, P., Panda, S. K., Ashraf, P. M., Varghese, T. and Bindu, J. 2018. Polylactic acid/chitosan films for packaging of Indian white prawn (*Fenneropenaeus indicus*). International Journal of Biological Macromolecules. 117: 1002 - 1010.

Gulzar, S., Raju, N., Prodpran, T., and Benjakul, S. 2022. Chitosan-tripolyphosphate nanoparticles improves oxidative stability of encapsulated shrimp oil throughout the extended storage. European Journal of Lipid Science and Technology. 124(1): 2100178.

Haq, M. A., Hasnain, A., and Azam, M. 2014. Characterization of edible gum cordia film: Effects of plasticizers. LWT-Food Science and Technology. 55(1): 163 - 169.

Hosseini, S. F., Rezaei, M., Zandi, M., and Ghavi, F. F. 2013. Preparation and functional properties of fish gelatin–chitosan blend edible films. Food Chemistry. 136(3-4): 1490 - 1495.

Hosseini, S. F., Kaveh, F., and Schmid, M. 2022. Facile fabrication of transparent high-barrier poly (lactic acid)-based bilayer films with antioxidant/antimicrobial performances. Food Chemistry. 384: 132540.

Imran, M., Revol-Junelles, A.-M., René, N., Jamshidian, M., Akhtar, M. J., Arab-Tehrany, E., Jacquot, M., and Desobry, S. 2012. Microstructure and physico-chemical evaluation of nano-emulsion-based antimicrobial peptides embedded in bioactive packaging films. Food Hydrocolloids. 29(2): 407 - 419.

Jiménez, A., Sánchez-González, L., Desobry, S., Chiralt, A., and Tehrany, E. A. 2014. Influence of nanoliposomes incorporation on properties of film forming dispersions and films based on corn starch and sodium caseinate. Food Hydrocolloids. 35: 159 - 169.

Jongjareonrak, A., Benjakul, S., Visessanguan, W., and Tanaka, M. 2006. Effects of plasticizers on the properties of edible films from skin gelatin of bigeye snapper and brownstripe red snapper. European Food Research and Technology. 222(3): 229 - 235.

Khan, F., Elherik, K., Bolton-Smith, C., Barr, R., Hill, A., Murrie, I., and Belch, J. J. 2003. The effects of dietary fatty acid supplementation on endothelial function and vascular tone in healthy subjects. Cardiovascular Research. 59(4): 955 -962.

Kong, I., Degraeve, P., and Pui, L. P. 2022. Polysaccharide-Based Edible Films Incorporated with Essential Oil Nanoemulsions: Physico-Chemical, Mechanical Properties and Its Application in Food Preservation - A Review. Foods. 11(4): 555.

Kotlęga, D., Peda, B., Palma, J., Zembroń-Łacny, A., Gołąb-Janowska, M., Masztalewicz, M., Nowacki, P., and Szczuko, M. 2021. Free fatty acids are Associated with the cognitive functions in stroke survivors. International Journal of Environmental Research and Public Health. 18(12): 6500.

Kumar, R., Ghoshal, G. and Goyal, M. 2019. Synthesis and functional properties of gelatin/CA–starch composite film: excellent food packaging material. Journal of Food Science and Technology. 56: 1954 - 1965.

Laohakunjit, N., and Noomhorm, A. 2004. Effect of plasticizers on mechanical and barrier properties of rice starch film. Starch-Stärke. 56(8): 348 - 356.

Madhumita, M., Guha, P. and Nag, A. 2019. Extraction of betel leaves (*Piper betle* L.) essential oil and its bio-actives identification: Process optimization, GC-MS analysis and anti-microbial activity. Industrial Crops and Products. 138: 111578.

Mittal, A., Singh, A., Benjakul, S., Prodpran, T., Nilsuwan, K., Huda, N. and De La Caba, K. 2021. Composite films based on chitosan and epigallocatechin gallate grafted chitosan: characterization, antioxidant and antimicrobial activities. Food Hydrocolloids. 111: 106384.

Nilsuwan, K., Benjakul, S. and Prodpran, T. 2018. Physical/thermal properties and heat seal ability of bilayer films based on fish gelatin and poly (lactic acid). Food Hydrocolloids. 77: 248 - 256.

Nilsuwan, K., Benjakul, S., Prodpran, T., and de la Caba, K. 2019. Fish gelatin monolayer and bilayer films incorporated with epigallocatechin gallate: Properties and their use as pouches for storage of chicken skin oil. Food Hydrocolloids. 89: 783 - 791.

Nouri, L. and Nafchi, A. M. 2014. Antibacterial, mechanical, and barrier properties of sago starch film incorporated with betel leaves extract. International Journal of Biological Macromolecules. 66: 254 - 259.

Park, S. H., Lee, H. S., Choi, J. H., Jeong, C. M., Sung, M. H., and Park, H. J. 2012. Improvements in barrier properties of poly (lactic acid) films coated with chitosan or chitosan/clay nanocomposite. Journal of Applied Polymer Science. 125(S1): 675 - 680.

Qiao, C., Ma, X., Zhang, J. and Yao, J. 2017. Molecular interactions in gelatin/chitosan composite films. Food Chemistry. 235: 45 - 50.

Rupasinghe, H. V., Erkan, N., and Yasmin, A. 2010. Antioxidant protection of eicosapentaenoic acid and fish oil oxidation by polyphenolic-enriched apple skin extract. Journal of Agricultural and Food Chemistry. 58(2): 1233 - 1239.

Tagrida, M. and Benjakul, S. 2020. Ethanolic extract of Betel (*Piper betle* L.) and Chaphlu (*Piper sarmentosum* Roxb.) dechlorophyllized using sedimentation process: Production, characteristics, and antioxidant activities. Journal of Food Biochemistry. 44: e13508.

Tagrida, M., Prodpran, T., Zhang, B., Aluko, R. E. and Benjakul, S. 2021a. Liposomes loaded with betel leaf (*Piper betle* L.) ethanolic extract prepared by thin film hydration and ethanol injection methods: Characteristics and antioxidant activities. Journal of Food Biochemistry. 45(12): e14012.

Tagrida, M., Benjakul, S., and Zhang, B. 2021b. Use of betel leaf (*Piper betle* L.) ethanolic extract in combination with modified atmospheric packaging and nonthermal plasma for shelf-life extension of Nile tilapia (*Oreochromis niloticus*) fillets. Journal of Food Science. 86(12): 5226 - 5239.

Tagrida, M., and Benjakul, S. 2022. Liposomes loaded with betel leaf (*Piper betle* L.) extract: Antibacterial activity and preservative effect in combination with hurdle technologies on tilapia slices. Food Control. 138: 108999.

Takeungwongtrakul, S., and Benjakul, S. 2016. Astaxanthin degradation and lipid oxidation of Pacific white shrimp oil: kinetics study and stability as affected by storage conditions. International Aquatic Research. 8(1): 15 - 27.

Wu, J., Ge, S., Liu, H., Wang, S., Chen, S., Wang, J., Li, J. and Zhang, Q. 2014. Properties and antimicrobial activity of silver carp (*Hypophthalmichthys molitrix*) skin gelatin-chitosan films incorporated with oregano essential oil for fish preservation. Food Packaging and Shelf Life. 2: 7 - 16.

Wu, J., Liu, H., Ge, S., Wang, S., Qin, Z., Chen, L., Zheng, Q., Liu, Q., and Zhang, Q. 2015. The preparation, characterization, antimicrobial stability and in vitro release evaluation of fish gelatin films incorporated with cinnamon essential oil nanoliposomes. Food Hydrocolloids. 43: 427 - 435.

Xu, D., Chen, T. and Liu, Y. 2021. The physical properties, antioxidant, and antimicrobial activity of chitosan–gelatin edible films incorporated with the extract from hop plant. Polymer Bulletin. 78: 3607 - 3624.

CHAPTER 9

POLYLACTIC ACID FILM COATED WITH ELECTROSPUN GELATIN/CHITOSAN NANOFIBERS CONTAINING BETEL LEAF ETHANOLIC EXTRACT: PROPERTIES, BIOACTIVITIES, AND USE FOR SHELF-LIFE EXTENSION OF TILAPIA SLICES

9.1. Abstract

Gelatin/chitosan solutions incorporated with betel leaf ethanolic extract (BLEE) at varying concentrations were electrospun on polylactic acid (PLA) films. Nanofibers with different morphologies, as indicated by scanning electron microscopy (SEM), were formed after solutions of gelatin/chitosan with and without BLEE were electrospun on PLA films at a constant voltage (25 kV) and a feed rate of 0.4 mL/h. Beaded gelatin/chitosan nanofibers (GC/NF) were found, particularly when high concentrations of BLEE were encapsulated. PLA films coated with GC/NF, and with BLEE added, showed antioxidant and antibacterial activities, which were augmented by increasing BLEE concentrations. Lower water vapor permeability and enhanced mechanical properties were achieved for GC/NF-coated PLA film ($p < 0.05$). Microbial growth and lipid oxidation of Nile tilapia slices packaged in PLA film coated with GC/NF containing 2% BLEE were more retarded than those packaged in low-density polyethylene (LDPE) bags over refrigerated storage of 12 days. Based on microbial limits, the shelf-life was escalated to 9 days, while the control had a shelf-life of 3 days. Therefore, such a novel film/bag could be a promising active packaging for foods.

9.2. Introduction

Generally, most food packaging materials are produced from non-biodegradable petrochemical plastics, which are the major cause of environmental pollution. There is an urgent need for natural alternatives, which are environmentally friendly; these are essential for implementation in food packaging (Nilsuwan *et al.*, 2018). Recently, food packaging design is not limited to packaging and protection, but also includes “active packaging”, which is the packaging that interacts positively with foods and promotes benefits, for retarding microbial growth and preventing oxidation (Fonseca *et al.*, 2019).

Several natural polymers are used for preparation of biodegradable active packaging to reduce the usage of their non-degradable counterparts (Behera *et al.,* 2021). Polylactic acid (PLA) is one such polymer, which is the fermented product from some types of agricultural crops or waste. It is classified as being "Generally Recognized as Safe (GRAS)" (Jamshidian *et al.,* 2010). Due to its excellent mechanical and physical properties, PLA was introduced to replace common petrochemicals used in food packaging (Gu *et al.,* 2017). Nevertheless, several limitations, such as low thermal stability and gas barrier dysfunctionality, may hinder the use of PLA at a commercial scale. In an attempt to tackle such limitations, different approaches were implemented. The lamination of other biopolymers with better barrier abilities on the PLA film is a promising technique; in this technique, the barrier property was improved, thus showing better protection toward packaged items. Therefore, the physical and mechanical properties of PLA film could be enhanced by mixing with other biopolymers (Rasal *et al.,* 2010).

Gelatin and chitosan are used as biopolymers in food packaging because of their biocompatibility, biodegradability, and other eminent characteristics (Nowzari *et al.,* 2013). Laminating PLA films with gelatin and chitosan can overcome the limitations of its barrier abilities and stability. Bilayer and/or multilayer films made from such biodegradable polymers are considered an innovative approach (Hosseini *et al.,* 2022). Additionally, the production of nanofibers with a good nanostructure and mechanical property requires a mixture of polymers, such as gelatin or chitosan, because a single polymer cannot produce nanofibers of adequate quality (Liu *et al.,* 2020).

Materials at the nanometric scale, such as nanofibers, can not only increase the contacted surface area, but can also be loaded with bioactive agents, for application as active packaging (Morie *et al.,* 2016). Bioactive compounds, such as plant extracts or essential oils having antioxidant and antimicrobial activities, were widely used in active packaging (Gimenez *et al.,* 2013). Betel, grown in Southeast Asian countries, is a leafy plant used in traditional medicine and as a food, due to its bioactivities. Betel leaf ethanolic extract (BLEE), dechlorophyllized using the sedimentation process, contained numerous phenolic compounds, such as isovitexin, vitexin 4′-O-galactoside, and kaempferol derivatives, possessing immense bioactivities (Tagrida and Benjakul, 2020). BLEE could, therefore, be used to develop biodegradable active packaging, especially via embedding in nanofibers.

Electrospinning gained attention because it can produce different bioactive packaging systems, particularly by the loading and controlled release of natural compounds (He *et al.*, 2019). Electrospinning can generate a mat of polymer nanofibers that can be loaded with bioactive compounds (Radusin *et al.*, 2019). Additionally, some techniques, such as nozzleless electrospinning, are capable of producing nanofibers on a large or commercial scale (Ebrahimi *et al.*, 2019). The high surface area-to-volume ratio of nanofibers with elevated porosity guarantees the sustained release of the bioactive compounds (Wen *et al.*, 2016). This technology is based on high electric fields applied to viscoelastic polymer-based solutions containing bioactive compounds. The resultant nonwoven nanofibers containing bioactive compounds can be applied as coatings on films to form a novel active packaging system (Torres-Giner *et al.*, 2018).

The purpose of the current work was to produce PLA films coated with electrospun gelatin/chitosan nanofibers loaded with BLEE. The mechanical, physical, and bioactive properties of the resulting films were examined. Additionally, the quality changes of tilapia slices stored in bags made from the selected PLA film coated with gelatin/chitosan electrospun fiber (GC/NF) containing BLEE was also monitored during refrigerated storage.

9.3. Objectives

To evaluate the characteristics and bioactivities of polylactic acid films electrospun by gelatin/chitosan nanofibers containing betel leaf ethanolic extract and the effectiveness of bags made from such films in extending the shelf-life of Nile tilapia slices.

9.4. Materials and methods

9.4.1. Chemicals

Fish gelatin powder (bloom: 250; molecular weight (MW): ~5.1×10^4 Da) was acquired from Lapi Gelatine S.P.A (Empoli, Italy). Chitosan (MW: ~2.1×10^3 KDa; degree of deacetylation (DDA): ~82%) was purchased from Sigma-Aldrich (St. Louis, MO, USA). Acetic acid and ethanol were procured from RCI Labscan Limited

(Bangkok, Thailand). Polylactic acid pellets were obtained from Nature Work Co. Ltd. (Blair, NE, USA).

9.4.2. Preparation and dechlorophyllization of BLEE

Extraction and dechlorophyllization of BLEE were performed as described by Tagrida and Benjakul (2020). Betel leaf powder was mixed with ethanol (70%, v/v) at 1:15 (w/v) and the mixture was stirred for 60 min. After filtration using filter paper, the solvent was removed from the filtrate with the aid of a rotary evaporator. The sedimentation method was applied to the concentrated extract for dechlorophyllization, in which the extract was mixed with distilled water at a 1:1 ratio and left at 4˚C for 24 h. Thereafter, the dechlorophyllized extract was freeze dried, and the powder was stored in a capped vial at -20˚C until use.

9.4.3. Preparation of polylactic acid (PLA) Film

A casting technique was adopted for the PLA film preparation. PLA pellets were mixed with chloroform to obtain a final concentration of 5% (w/v). Glycerol (1%, w/v based on solid content) was added as a plasticizer. The mixture was stirred using a magnetic stirrer at room temperature until complete solubilization was achieved. The PLA solution (200 mL) was degassed for 10 min in a sonication bath. Subsequently, the solution was poured into a stainless-steel tray (35 × 25 cm^2) and placed for 3 days at room temperature in an aerated chamber for solvent evaporation. PLA films were peeled from the trays and conditioned in an environmental chamber (Binder GmbH, Tuttlingen, Germany) with a relative humidity (RH) of 50 ± 5% and a temperature of 25 ± 0.5˚C for 48 h before analyses.

9.4.4. Preparation of electrospun gelatin/chitosan nanofiber (GC/NF) incorporated with BLEE

Fish gelatin was added to 90% (v/v) acetic acid to obtain 20% concentration (w/v) and then stirred at 250 rpm using a magnetic stirrer for 2 h at 45˚C until complete dissolution. Thereafter, chitosan was mixed with gelatin solution at 3% (w/v) and stirred constantly until the chitosan was totally solubilized. BLEE was added into a 10 mL gelatin/chitosan (GC) mixture to obtain several concentrations (0.5, 1, and 2% (w/v)). The solutions, namely GC-0.5%BLEE, GC-1%BLEE, and GC-

2%BLEE, were further used as electrospinning solutions. GC mixture devoid of BLEE was used as the electrospinning solution and served as the control.

The electrospinning process was conducted at a temperature of 25 ± 2 ˚C and 45 ± 2% RH as specified by Gulzar *et al.* (2022); the process was performed by injecting the solutions into a plastic syringe equipped with a stainless-steel needle (23-guage). The syringe was then loaded to the pump of the electrospinning machine (NanoSpinner, Inovenso Technology Inc., Woborn, MA, USA). The needle was positioned 12 cm away from the stainless-steel drum collector (10 cm diameter and 20 cm length) which was adjusted at a rotation rate of 200 rpm and oscillation of 10 mm/s. A previously prepared PLA film (12 x 30 cm^2) was wrapped around the drum collector and the electrospinning solution was pumped at a feed rate of 0.4 mL/h with 25 kV applied voltage. A collection time of 24 ± 1 h was used. The obtained films were then removed from the drum collector and further conditioned in an environmental chamber for 24 h at a temperature of 25 ± 0.5˚C and 50 ± 5% RH until analysis. Films were named GC/NF-0%BLEE, GC/NF-0.5%BLEE, GC/NF-1%BLEE, and GC/NF-2%BLEE for PLA film samples coated with GC/NF and loaded without BLEE (0%), and with BLEE at 0.5, 1, and 2%, respectively.

9.4.5. Characterization of PLA films coated with electrospun GC/NF without and with BLEE at various concentrations

9.4.5.1. Morphology

The microstructure of nanofibers was analyzed by a scanning electron microscope (SEM) (Quanta 400, FEI, Eindhoven, the Netherlands). A gold layer was sputter-coated on the film samples using a sputter coater (SPI-Module, West Chester, PA, USA). Thereafter, films were visualized at an acceleration voltage of 20 kV.

9.4.5.2. Thickness

The thickness of films was determined using a digital micrometer (Mitutoyo, Model ID-C112PM, Mitutoyo Corp., Kawasaki shi, Japan). Nine random positions on the film samples were measured for thickness and the average thickness was calculated.

9.4.5.3. Mechanical properties

Tensile strength (TS) and elongation at break (EAB) were determined as specified by Nilsuwan *et al.* (2018). TS (MPa) was computed by dividing the maximum force (N) required to break down film with a designated cross-section area (m^2). EAB was computed by dividing the elongation of the film with the initial grip length of the film samples (30 mm). The crosshead speed was fixed at 30 mm/min and the EAB was reported as a percentage.

9.4.5.4. Water vapor permeability (WVP)

The method described by Nilsuwan *et al*. (2018) was followed. Film samples were placed on the aluminum permeation cups containing 0% RH dried silica gel (20 g), in which the film coated with nanofibers was facing the silica gel. Thereafter, the films were tightly sealed on the cups using silicon vacuum grease and a rubber gasket. The cups were kept in an environmental chamber (25 ± 2 °C and 50 ± 5% RH) and were weighed every 1 h over a 10 h period. WVP was subsequently computed as follows:

$$\text{WVP } (g\ m^{-1}\ s^{-1}\ Pa^{-1}) = \left(\frac{WVTR \times L}{\Delta P \times A}\right)$$

where WVTR is the water vapor transmission rate obtained from the slope of plot between cup weight gain vs time (g/s), L is thickness of the film (m), ΔP is the water vapor pressure difference across the film (1588.69 Pa at 25˚C), and A is the exposed area of the film (m^2).

9.4.5.5. Oxygen permeability (OP)

The OP of the prepared films was determined as specified by Nilsuwan *et al.* (2018). The oxygen transmission rate (OTR) through each film was measured using an oxygen permeation analyzer (model 8000, Illinois Instruments Inc., Johnsburg, IL, USA). Films were clamped in the diffusion chamber and pure oxygen (99.8% purity) was then introduced into the upper half of the sample chamber, while nitrogen was injected into the lower half of the chamber where there was an oxygen sensor. The OTR was determined at 25˚C and 50% RH. Measurements were performed in triplicate. OP was calculated using the following equation:

$$\text{OP } (mol\ m^{-1}\ s^{-1}\ Pa^{-1}) = \frac{OTR \times L}{\Delta P}$$

where *OTR* is the oxygen transmission rate (mol m^{-2} s^{-1}), *L* is thickness of the film (m), and ΔP is the partial pressure of oxygen (1.015×10^5 Pa at 25˚C).

9.4.5.6. Color, light transmission, and transparency

The colors of the films were determined as reported by Mittal *et al.* (2021) using a colorimeter (Hunterlab, Reston, VA, USA). L^* (lightness), a^* (redness/greenness), b^* (yellowness/blueness), and ΔE (total color difference) were recorded.

The method of Shiku *et al.* (2004) was adopted for the determination of light transmission of the films in both ultraviolet (200 – 280 nm) and visible (350 – 800 nm) ranges with the aid of an UV-vis spectrophotometer (UV-1800, Shimadzu, Kyoto, Japan). The transparency value was computed (Gulzar *et al.*, 2022):

$$\text{Transparency value} = \frac{-\log T_{600}}{X}$$

where T_{600} is the fractional transmission at 600 nm and *X* is film thickness (mm). A lower film transparency is indicated by a higher transparency value.

9.4.5.7. Bioactivities of PLA films coated with electrospun GC/NF without and with BLEE at various concentrations

9.4.5.7.1. Antioxidant activities (AO-A)

Small pieces of film (0.1 g) were mixed with distilled water (10 mL) and stirred overnight. The mixture was centrifuged for 20 min at 8000 xg, and the supernatants were collected and used for determination of AO-A following the method of Tagrida *et al.* (2021a). DPPH and ABTS radical-scavenging activities (DPPH-RSA and ABTS-RSA, respectively), and ferric-reducing antioxidant power (FRAP) were examined and reported as μmol Trolox equivalent (TE)/g sample. Metal chelating activity (MCA) was expressed as μmol EDTA equivalent (EE)/g sample.

9.4.5.7.2. Antibacterial activities (AB-A)

AB-A of different films was assessed by the agar diffusion method described by Giménez *et al.* (2013). *Staphylococcus aureus*, *Escherichia coli*, *Listeria monocytogenes*, and *Pseudomonas aeruginosa* gifted from the Food Safety Laboratory, Prince of Songkla University, Hat Yai, Thailand, were the tested microorganisms. One hundred μL of bacterial suspension (10^6 CFU/mL) was spread on tryptic soy agar (TSA) plates under aseptic conditions. Subsequently, film samples cut into discs (diameter: 5 mm) were placed on the surface of the inoculated TSA plates. All the plates were incubated for 24 h at 37˚C. The inhibition zone diameter including the film sample was then determined in millimeters.

9.4.5.8. Thermogravimetric analysis (TGA)

The thermostability of the selected film was evaluated with the aid of a simultaneous thermal analyzer (STA-8000, PerkinElmer, Norwalk, CT, USA) using a heating flow rate of 10˚C/min from 30 to 800˚C. The thermal degradation temperature and weight loss of the film samples were recorded. Nitrogen was used as a purge gas at a flow rate of 20 mL/min.

9.4.6. Quality changes in Nile tilapia slices packaged in bags prepared from the selected PLA films coated with GC/NF containing BLEE during refrigerated storage

9.4.6.1. Preparation of Nile tilapia slices

Freshly deceased Nile tilapia (3 kg; 1 ± 0.1 kg per fish) were bought from the local market and the fish were placed in ice (1:2 ratio). Thereafter, the fish were transported to the laboratory within 30 min where fish slices were prepared as per the method of Tagrida *et al.* (2021b): the fish were washed with tap water and decapitated, skinned, filleted, and sliced (4 × 2 cm^2) using a sanitized stainless-steel knife. Slices were kept in ice during preparation.

9.4.6.2. Preparation of bags

Selected film samples (28 × 7 cm^2) were folded in half, in which the GC/NF coated side was the inner side of the bags and then thermally sealed on 2 sides (150 ± 0.5˚C for 5 s, followed by cooling for 1.50 s) with the aid of an impulse sealer (magnet model ME-300HIM, S.N. Mark Ltd., Park, Nonthaburi, Thailand). The width of the seal area was 2 mm, and the final dimensions of the bags were 14 × 7 cm^2. Fish slices (10 g) were aseptically placed in the prepared bags, which were subsequently closed via sealing. Fish slices were placed in LDPE bags with the same dimensions and sealed to serve as the control. All bags were stored at 4˚C and quality assessments were conducted on randomly taken samples every 3 days up to 12 days.

9.4.6.3. Microbiological analyses

The spread plate method detailed by Tagrida and Benjakul (2021) was adopted for monitoring the changes in the microbiological load of fish slices during storage. A volume of 45 mL of 0.85% sterilized saline solution was added to slices (5 g) in a stomacher bag. The mixture was mixed well using a stomacher blender (M400, Seward Ltd., West Sussex, England) for 1 min at 220 rpm. The required serial dilutions were performed using 0.85% sterilized saline solution and 0.1 mL of the appropriate dilutions were spread on the surface of the corresponding media for enumeration. Plate count agar was used for the enumeration of total viable count (TVC) and psychrophilic bacterial count (PBC) after incubation at 37˚C for 3 days and 4˚C for 10 days, respectively. Triple sugar iron agar and Pseudomonas isolation agar were used for the H_2S-producing bacterial count (H_2S-BC) and the *Pseudomonas* sp. count (PC), respectively. The counts were recorded after incubation for 3 days at 25˚C. The *Enterobacteriaceae* count (EC) was evaluated after inoculation on eosin methylene blue agar and incubation at 37˚C for 24 h.

9.4.6.4. Chemical analyses

Lipid oxidation of slices was evaluated by determination of the peroxide value (PV) as specified by Richards and Hultin (2002) and was expressed as an mg cumene hydroperoxide equivalent/kg flesh. Thiobarbituric acid reactive substances (TBARS) values were examined as described by Buege and Aust (1978) and expressed as an mg malonaldehyde (MDA) equivalent/kg flesh. Total volatile base (TVB) content was measured following the method of Olatunde *et al*. (2019) and reported as an mg N/100 g sample. The pH of the sample homogenate (slices: distilled water = 1:10, w/v, 13,000 rpm, for 1 min) was measured using a pH-meter (Sartorious North America, Edge-wood, NY, USA).

9.4.7. Statistical analysis

Completely randomized design (CRD) was applied for all studies. Data were re-ported as mean ± standard deviation (SD). For mean comparison, One-way Analysis of Variance (ANOVA) was conducted, and Duncan’s Multiple Range Test (DMRT) was performed. SPSS package (SPSS 24.0 for Windows, SPSS Inc, Chicago, IL, USA) software was used for data analysis.

9.5. Results and discussion

9.5.1. Properties of PLA films coated with electrospun GC/NF with, and without, BLEE at different concentrations

9.5.1.1. Morphology

SEM images of all the films are depicted in Fig. 39A. Smooth homogenous and bead-free nanofibers, with diameters ranging from 35 to 116 nm, were coated on PLA films, specifically, those without or with 0.5% BLEE (Fig. 39A and B). However, when the BLEE concentration was augmented, nanofibers with diameters ranging from 56 to 183 nm were observed and beads were also found (Fig. 39C and D). Bead formation could be attributed to the decreased viscosity in the nanofiber-forming solutions, plausibly caused by several compounds in BLEE, which impeded the entanglement of nanofibers (Tagrida and Benjakul, 2020). Viscosity is a crucial factor determining the structure and diameter of the electrospun nanofibers. Solutions with elevated viscosity have higher viscoelastic forces which can resist axial stretching, resulting in diameter increment and less bead formation (Gulzar *et al.*, 2022). On the other hand, solutions with lower viscosity exhibited a higher surface tension in the charged jet, thus overpowering the viscoelastic forces. This led to the phenomenon termed Rayleigh–Taylor instability, which occurs when solutions with different fluidities become unstable at their interface due to the penetration of the heavy fluids into the lighter fluids (Nezarati *et al.*, 2013). The aforementioned phenomenon resulted in beaded nanofibers of higher diameter. The viscosity of the electrospinning solutions was 48.44 ± 0.91, 47.13 ± 1.04, 44.86 ± 1.12, and 43.01 ± 1.32 cP for GC/NF-0%BLEE, GC/NF-0.5%BLEE, GC/NF-1%BLEE, and GC/NF-2%BLEE, respectively. Additionally, the conductivity of the GC/NF-forming solutions determined the morphology of the resulting nanofiber mat. The solutions with higher BLEE concentrations had lower conductivity, leading to the formation of nanofiber mats of increased diameters. This was in line with Vafania *et al.* (2010) who documented that electrospinning solutions with lower conductivity, due to augmented thyme essential oil concentration, had a higher nanofiber diameter. In the current study, the conductivity of the electrospinning solutions was 553.17 ± 3.22, 542.77 ± 4.62, 519.76 ± 4.36, and 509.41 ± 2.19 µS/cm for GC/NF-0%BLEE, GC/NF-0.5%BLEE, GC/NF-1%BLEE, and GC/NF-2%BLEE, respectively. Some hydrophobic compounds in the extract might lower conductivity of the GC/NF forming solutions. These results indicate that BLEE concentration affected the nanofiber diameter size and morphology by impacting the viscosity and conductivity of the electrospinning solutions.

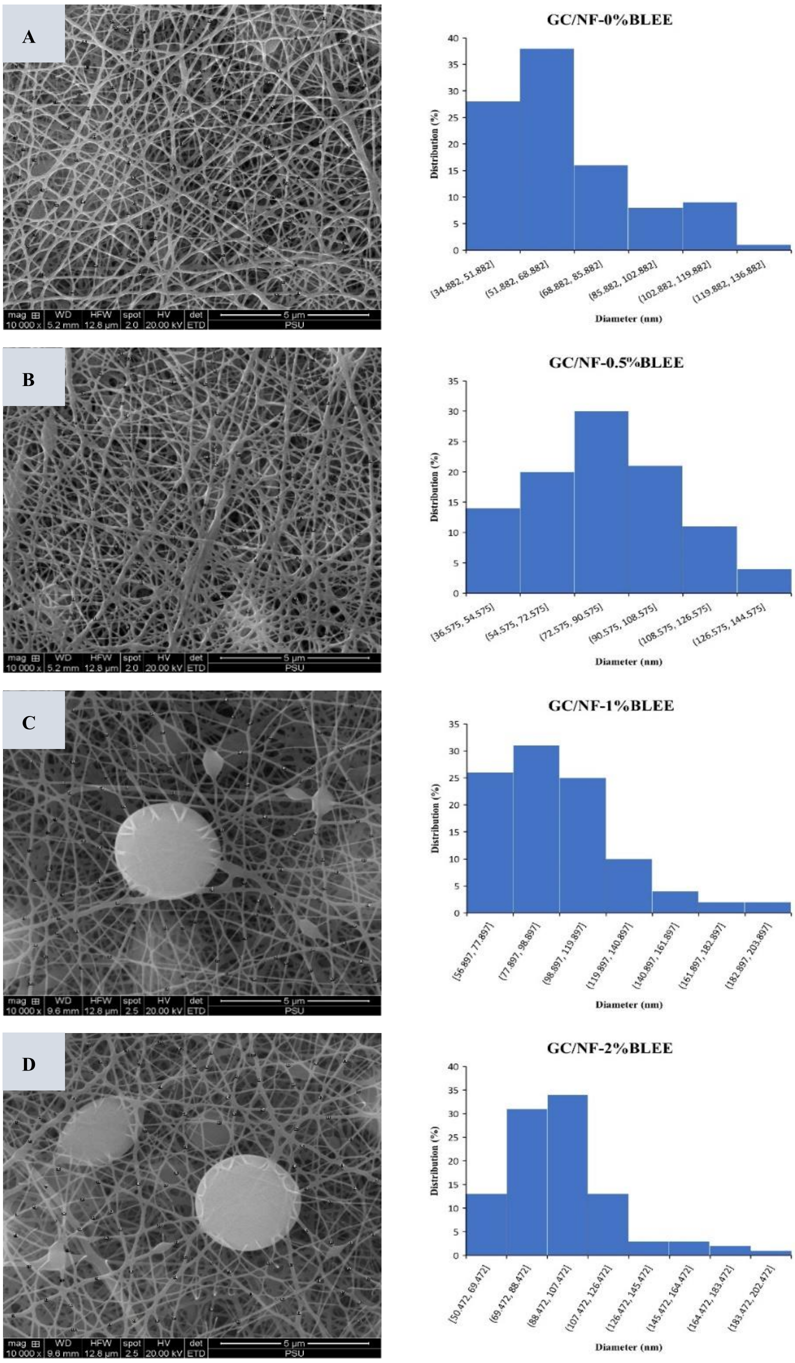

Figure 39. Scanning electron microscopic (SEM) images and histograms representing nanofiber diameter dis-tributions coated on the PLA films containing betel leaf ethanolic extract (BLEE) at 0% (A), 0.5% (B), 1% (C), and 2% (D).

9.5.1.2. Thickness

Thickness is another factor influencing the mechanical and barrier properties of the produced films. PLA films coated with GC/NF with and without BLEE had an average thickness ranging between 0.115 and 0.121 mm (Table 22), which was generally greater than the control PLA film (0.106 mm) ($p < 0.05$). Films containing BLEE at elevated concentrations (1 and 2%) were thicker than those with 0.5%, or without any BLEE ($p < 0.05$). However, no differences in thickness were detected among the films containing BLEE at different levels ($p > 0.05$). The fibrous network could augment the thickness of resulting films. The results indicate that embedding of BLEE and its concentration, especially at 1 and 2%, increased the thickness of the resulting films. Similarly, increased thickness was attributed to the embedding of pomegranate peel extract and sodium dehydro-acetate, which contain both soluble and insoluble matter (He *et al.*, 2019).

9.5.1.3. Mechanical properties

Mechanical strength is vital to maintain the integrity of a film when it is used as food packaging, and during transportation and storage. Mechanical properties are expressed as TS and EAB (Table 22). Overall, the TS and EAB of PLA films coated with GC/NF containing BLEE were higher than those without the coating ($p < 0.05$), indicating a significant improvement in mechanical properties. However, no difference in TS was found between PLA films and that coated with GC/NF containing no BLEE ($p > 0.05$). GC/NF coating on PLA surface plausibly augmented TS, in which nanofiber entanglement could strengthen the resulting film. Ebrahimi *et al.* (2015) found that nanofibers made from chitosan/gelatin and coated on a gelatin film surface improved the TS of the film by acting like scaffolds in the film structure. The stretch ability of GC/NF coated PLA films was enhanced when BLEE concentrations above 0.5% were added into the GC/NF, compared with the uncoated PLA films, as ascertained by an increased EAB ($p < 0.05$). Coating with GC/NF probably enhanced the elasticity of the PLA film by rearranging the nanofiber network, leading to the increased stretching (Wang *et al.*, 2017). Additionally, the presence of hydrogen bonding mediated by chitosan might enhance the mechanical properties of the PLA films, in which chitosan could act as an H-donor, thus strengthening the nanofiber network (Liu *et al.*, 2019).

Table 22. Thickness, mechanical properties, color, water vapor permeability, and oxygen permeability of PLA film and PLA films coated with GC/NF loaded with, or without betel leaf ethanolic extract (BLEE) at different levels.

Sample	Thickness (mm)	TS (MPa)	EAB (%)	*L**	*a**	*b**	Δ*E**	WVP ($\times 10^{-11}$ g m^{-1} s^{-1} Pa^{-1})	OP ($\times 10^{-18}$ mol m^{-1} s^{-1} Pa^{-1})
PLA	0.106 ± 0.004^{a}	29.55 ± 0.54^{a}	4.85 ± 1.00^{a}	91.79 ± 0.01^{d}	-0.01 ± 0.01^{d}	0.07 ± 0.01^{a}	-	4.10 ± 0.18^{c}	216.6 ± 11.07^{e}
GC/NF-0%BLEE	0.115 ± 0.001^{b}	32.88 ± 1.50^{b}	5.00 ± 0.97^{a}	89.45 ± 1.05^{cd}	-1.28 ± 0.06^{c}	1.50 ± 0.20^{a}	3.08 ± 0.84^{a}	3.86 ± 0.20^{bc}	25.88 ± 0.28^{d}
GC/NF-0.5%BLEE	0.118 ± 0.001^{bc}	34.03 ± 1.47^{b}	5.45 ± 1.02^{ab}	87.79 ± 1.19^{bc}	-4.63 ± 0.51^{b}	5.71 ± 0.46^{a}	8.37 ± 0.82^{b}	3.39 ± 0.20^{b}	22.59 ± 2.07^{c}
GC/NF-1%BLEE	0.121 ± 0.001^{c}	34.40 ± 1.58^{b}	6.80 ± 0.18^{b}	85.60 ± 1.71^{b}	-7.03 ± 0.51^{a}	17.65 ± 1.04^{b}	20.48 ± 1.95^{c}	3.15 ± 0.21^{ab}	10.54 ± 1.78^{b}
GC/NF-2%BLEE	0.121 ± 0.002^{c}	34.45 ± 2.65^{b}	7.04 ± 2.26^{b}	81.99 ± 3.02^{a}	-7.43 ± 0.74^{a}	20.20 ± 0.89^{b}	23.78 ± 0.61^{c}	3.00 ± 0.01^{a}	6.23 ± 0.59^{a}

Values are mean ± SD. Different lowercase superscripts in the same column denote significant difference ($p < 0.05$). TS: tensile strength; EAB: elongation at break; L*: lightness; a*: red-ness/greenness; b*: blueness/yellowness; WVP: water vapor permeability; OP: oxygen permeability. PLA: polylactic acid film without electrospinning. GC/NF-0%BLEE, GC/NF-0.5%BLEE, GC/NF-1%BLEE, and GC/NF-2%BLEE represent PLA films coated with GC/NF without BLEE (0%) and loaded with BLEE at 0.5, 1, and 2% BLEE, respectively.

The addition of BLEE enhanced the EAB, probably via increasing hydrogen bonding due to the presence of several -OH groups in the BLEE. Overall, the enhancement of the mechanical properties of the PLA films coated with GC/NF containing BLEE was observed when compared with the uncoated PLA films, signifying the valuable effect of electrospinning as a promising means of producing food packaging with improved mechanical properties.

9.5.1.4. Water vapor permeability (WVP)

WVP is the measure for the water vapor migration rate through the surface of a film. Usually, in food packaging, films with a low WVP are favored as they prevent the migration of water vapor such as moisture from the environment, to packaged food products (Kester and Fennema, 1989). The WVP of uncoated PLA films, and those with the GC/NF coating with and without BLEE, is shown in Table 22. WVP was observed to be reduced when coated with GC/NF and when the BLEE concentration was increased, especially at 1 and 2% BLEE ($p < 0.05$), suggesting that coating nanofibers with high levels of BLEE augmented the resistance of the film to the migration of water vapor. Types of polymers and additives generally affect the barrier properties of the films. PLA is a hydrophobic polymer with moderate WVP, and it can suppress the easy migration of water molecules (Wang *et al.*, 2016). Cross-linking between gelatin and chitosan created a dense nanofiber mat that was able to prevent water vapor permeability (Gulzar *et al.*, 2022).

BLEE also increased the cross-linking between the gelatin and chitosan molecules, leading to the decrease in the hydrophilic functional groups and lower water migration (Rattaya *et al.*, 2009). In addition, BLEE contains many hydrophobic compounds, such as eugenol, estragole, chavicol, linalool, etc., that might repel the water molecules (Madhumita *et al.*, 2019). The presence of the GC/NF layer on the surface of the PLA film reduced the WVP. This reduction was more prominent when the BLEE concentration was above 0.5% ($p < 0.05$). Fabra *et al.* (2016) documented that coating a zein/gluten bilayer film with electrospun nanofibers reduced the WVP effectively. Therefore, PLA film coated with GC/NF containing BLEE could improve the water vapor barrier property of the resulting films.

9.5.1.5. Oxygen permeability (OP)

A crucial property in food packaging materials is their oxygen barrier ability, which dictates the applicability of the proposed packaging to enhance the quality of the packaged foods by retarding microbial growth and lowering lipid oxidation, thus extending their shelf-life (Burgos *et al.*, 2013; Liu *et al.*, 2020; Hosseini *et al.*, 2022). The OP of the PLA film and films with a GC/NF coating, with and without BLEE, is presented in Table 22. The uncoated PLA film displayed the highest OP ($p < 0.05$), indicating its poor oxygen barrier ability. This might be related to the non-polar nature of the PLA, thereby allowing the diffusion of oxygen, which is known as a non-polar molecule (Nilsuwan *et al.*, 2018; Hosseini *et al.*, 2022). However, when GC/NF was laminated on the PLA film by electrospinning, the OP decreased considerably ($p < 0.05$) and this reduction was augmented, when the concentration of BLEE increased ($p < 0.05$). A similar reduction in the OP was observed in film coated with nanospun fibers (Liu *et al.*, 2020; Hosseini *et al.*, 2022; Park et al., 2012). The reduction in OP could be related to the high polarity of the electrospun PLA films, induced by the addition of the GC/NF layer and further increased with the loading of BLEE that contains many polar compounds, thus posing very low oxygen permeation (Hosseini *et al.*, 2022). Additionally, Liu *et al.* (2020) attributed a lowered OP to the high cross-linking reactions of the different polymers with PLA film, minimizing the free area available for oxygen molecules to diffuse through the film, and increasing the distance that the oxygen molecules must cross in the film due to the increased tortuosity.

9.5.1.6. Color, light transmission, and transparency

The color attributes of different films are tabulated in Table 22. Coating with GC/NF augmented the film cloudiness, which was in tandem with the lower L^* values as compared with uncoated PLA films. The L^* value continued to decrease, particularly with increasing BLEE concentrations ($p < 0.05$). Apart from the reduction in L^*, the GC/NF coated PLA films had an increased yellowish color when BLEE was encapsulated, particularly when BLEE at 1 and 2% was loaded into the GC/NF ($p < 0.05$). The films with the high BLEE concentration (1 and 2%) had the lowest a^* value, representing more greenness. This might be caused by an amount of chlorophyll being retained in the BLEE. ΔE^* value also increased with augmenting levels of BLEE in the

GC/NF ($p < 0.05$), indicating the elevated change in color and the increases in both greenness and yellowness. The color of the PLA films was more likely attributed to some remaining pigmented compounds in the BLEE embedded in the GC/NF.

Light transmission in ultraviolet (UV) and visible (Vis) domains (200 – 800 nm) decreased significantly in all the GC/NF coated PLA films, irrespective of BLEE loading (Table 23). An elevated UV/Vis light barrier ability was ascribed to the amino acid residues, especially those containing aromatic rings with double bonds in GC/NF, that can absorb UV light (Sobral and Habitante, 2001). Furthermore, the loading of BLEE into GC/NF lowered the transmission due to the diverse phenolic compounds or other components in BLEE, such as vitexin and iso-vitexin (Tagrida and Benjakul, 2020). These compounds contain abundant aromatic rings and unsaturated bonds in their structures, which have the ability to absorb UV/Vis light (Damodaran *et al.*, 2007). Films with excellent UV/Vis light barrier abilities are highly regarded for the prevention of the adverse effects of light toward quality changes, especially lipid oxidation.

The transparency values of the different films (Table 23) showed that only the uncoated PLA film was transparent, while the coated counterparts were opaque. GC/NF-coated films, particularly those with GC/NF loaded with BLEE, had the highest transparency values, indicating a lower transparency in these films. These high transparency values coincided with the lower L^* values and decreased transmission. Overall, the electrospinning of GC/NF containing BLEE on the surface of PLA films considerably reduced their transparency, thus serving as a UV/Vis light barrier and preventing its damaging effect on packaged foods.

9.5.1.7. Bioactivities of PLA films coated with electrospun GC/NF without and with BLEE at different concentrations

9.5.1.7.1. Antioxidant activities (AO-A)

The term ‘active packaging’ describes films with bioactivities, such as antioxidant or antibacterial activities, which are able to prevent food deterioration by retarding lipid oxidation and inhibiting microbial growth (de Campos *et al.*, 2019).

Table 23. Light transmission and transparency values of PLA film and PLA films coated with GC/NF loaded with, and without, BLEE at different levels.

Sample	Light transmission (%) at different wavenumbers (nm)								Transparency value
	200	280	350	400	500	600	700	800	
PLA	0.06	49.75	69.33	78.79	83.80	88.21	88.48	88.60	0.51 ± 0.14[a]
GC/NF-0%BLEE	0.07	0.09	3.82	5.55	6.42	7.02	7.50	7.91	10.0 ± 0.33[b]
GC/NF-0.5%BLEE	0.06	0.06	2.05	3.03	3.93	4.87	5.05	5.28	11.05 ± 0.35[c]
GC/NF-1%BLEE	0.07	0.07	2.07	2.80	3.70	4.47	4.77	4.87	11.15 ± 0.23[c]
GC/NF-2%BLEE	0.07	0.09	1.91	2.61	3.67	4.38	4.63	4.71	11.21 ± 0.25[c]

Values are mean ± SD. Different lowercase superscripts in the same column denote significant difference ($p < 0.05$). For captions, see Table 22.

GC/NF loaded with BLEE and coated on PLA films increased the film AO-A ($p < 0.05$) (Table 24). This increase was in a BLEE concentration dependent manner. GC/NF-0%BLEE was noted to have very low DPPH and ABTS radical scavenging activity. In addition, it had no ferric reducing or metal chelating abilities. This might be attributed to the absence of BLEE. Nevertheless, the AO-A of this particular sample was more likely linked to the presence of residual amino groups of chitosan and -NH_2 or -OH groups in the side chains of gelatin that might contribute to radical scavenging activities (Moradi *et al.*, 2012). AO-A increased markedly with the augmenting concentration of BLEE added into GC/NF ($p < 0.05$). The highest AO-A tested by all assays was highest in GC/NF-2%BLEE, which possessed the highest level of BLEE ($p < 0.05$). This increase was strongly connected to the numerous polyphenols in the BLEE, such as isovitexin, epigallocatechin, and kaempferol derivatives, possessing high AO-A (Tagrida and Benjakul, 2020). These compounds acted as electron donors or free radical scavengers and exhibited the reduction of ferric ions into ferrous ions, and a metal chelating ability (Tagrida *et al.*, 2021a). Active packaging with such abilities, particularly those with reducing power and radical scavenging activities, are highly regarded for their ability to lower lipid oxidation of foods and re-strain the oxidative stress (Avelelas *et al.*, 2019).

9.5.1.7.2. Antibacterial activities (AB-A)

Various antibacterial activities of different films were observed against the tested bacteria (Table 24). Only the PLA films coated with GC/NF loaded with BLEE showed AB-A against all tested bacteria and the activity increased with augmenting concentration of BLEE ($p < 0.05$). Previous reports documented that the AB-A of the chitosan were related to its amino groups that could interact with microbial cell membranes, resulting in the leakage of intracellular proteinaceous constituents and the death of cells (Bonilla and Sobral, 2016; Mittal *et al.*, 2021). Lack of AB-A of the chitosan in the current study was probably caused by the strong fixation of chitosan in the coating layer and complexation with gelatin. This resulted in the weak diffusion of chitosan into the agar surface, so no AB-A was obtained. Wang *et al.* (2011) also found no noticeable AB-A by pure chitosan films due to the firm fixation of chitosan and its poor diffusion into the media. Therefore, it could be presumed that most AB-A was related to the added BLEE, which could diffuse into the agar surface and inhibit bacterial growth.

Table 24. Antioxidant and antibacterial activities of PLA film and PLA films coated with GC/NF loaded with and without BLEE at different levels.

Sample	**Antioxidant activities**				**Antibacterial activity (mm)**			
	DPPH-RSA (µmol TE/g sample)	**ABTS-RSA (µmol TE/g sample)**	**FRAP (µmol TE/g sample)**	**MCA (µmol EDTA/g sample)**	***S. aureus***	***E. coli***	***L. monocytogenes***	***P. aeruginosa***
PLA	ND*	ND	ND	ND	ND	ND	ND	ND
GC/NF-0%BLEE	3.50 ± 1.72 ^{a}	25.55 ± 2.22 ^{a}	ND	ND	ND	ND	ND	ND
GC/NF-0.5%BLEE	23.21 ± 0.69 ^{b}	792.5 ± 8.41^{b}	336.66 ± 5.50 ^{a}	76.52 ± 3.91 ^{a}	5.58 ± 0.50 ^{a}	6.83 ± 0.57 ^{a}	5.91 ± 0.68 ^{a}	7.16 ± 0.88 ^{a}
GC/NF-1%BLEE	75.89 ± 1.20 ^{c}	1829.2 ± 7.22 ^{c}	928.69 ± 8.72 ^{b}	170.61 ± 1.13 ^{b}	7.75 ± 0.63 ^{b}	9.08 ± 0.31 ^{b}	7.66 ± 0.72 ^{b}	8.91 ± 0.87 ^{b}
GC/NF-2%BLEE	93.49 ± 1.01^{d}	2817.03 ± 7.39 ^{d}	1484.3 ± 3.13 ^{c}	277.37 ± 0.92 ^{c}	9.08 ± 0.68 ^{c}	11.25 ± 0.31 ^{c}	9.33 ± 0.89 ^{c}	10.66 ± 0.90 ^{c}

Values are the mean ± SD (n = 3). Different lowercase superscripts in the same column denote significant difference ($p < 0.05$). DPPH-RSA: 2,2-diphenyl-1-picrylhydrazyl radical-scavenging activity; ABTS-RSA: 2, 2'-azino-Bis-3-ethylbenzothiazoline-6-sulfonic acid radical-scavenging activity; FRAP: ferric-reducing antioxidant power; MCA: metal-chelating activity. For captions see Table 22.

* ND: not detected.

The AB-A of BLEE was associated with the copious amounts of polyphenols and other components, such as essential oil, etc., within BLEE that had the profound ability to inhibit bacterial growth (Nouri and Nafchi, 2014; Tagrida *et al.,* 2021a). Gram-positive bacteria (*S. aureus* and *L. monocytogenes*) were observed to show more resistance towards PLA films coated with GC/NF containing BLEE than Gram-negative bacteria (*E. coli* and *P. aeruginosa*). This could be owed to the presence of a thick layer of peptidoglycan in the Gram-positive bacteria, which showed more resistance against the actions of antibacterial agents (Mai-Prochnow *et al.*, 2016). Hydroxyl groups of polyphenols in BLEE plausibly acted as proton exchangers and destabilized the cytoplasmic membrane of the bacterial cells. This could further reduce the pH gradient and disturb the membrane ion permeability, thereby leading to the disruption of the electron flow and the proton motive forces. Those changes result in the discharge of ATPs and other constituents required for the metabolism of bacterial cells and, finally, cause bacterial death (Nouri and Nafchi, 2014; Burt, 2004).

9.5.1.8. Thermal stability

The thermal degradation behavior of GC/NF-2%BLEE showing the most satisfactory mechanical, barrier, and bioactive properties in comparison with uncoated PLA film was evaluated by TGA (Fig. 40A and B). Similar thermal degradation behavior was observed at the first stages of the analysis. The first significant weight loss (ΔW) took place at an approximate thermal degradation temperature (Td) of 100˚C, where weight losses of 6.5 and 7.062% were observed for PLA and GC/NF-2%BLEE films, respectively. Such losses can be ascribed to the evaporation of moisture and residual solvent in the PLA film, and to the loss of volatile compounds in BLEE in the case of GC/NF-2%BLEE film, which showed a slight increase in its ΔW (Radusin *et al.,* 2019). The maximum rate of degradation (ΔW = 91.054 and 76.052%) occurred at 340.16 and 315.05˚C for PLA and GC/NF-2%BLEE films, respectively. PLA usually decomposes at temperatures ranging between 285 and 368˚C, in which cyclic oligomers, lactide molecules, CO, and CO_2 are released (Laaziz *et al.*, 2017). The lower Td of GC/NF-2%BLEE was probably due to the lower PLA polymerization and high degradation of the gelatin/chitosan nanofibers, causing the film to thermally degrade at a slightly higher rate.

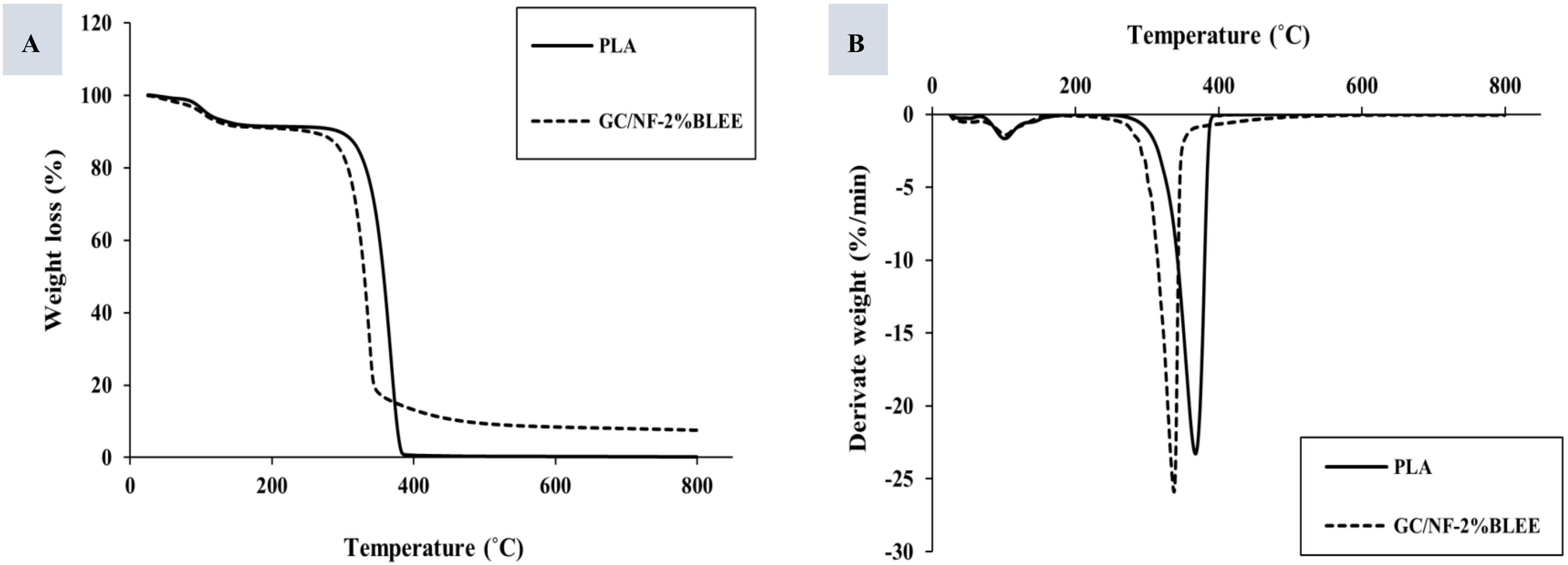

Figure 40. Thermogravimetric analysis (A) and derivative weight loss (B) thermograms of GC/NF-2%BLEE film and PLA film.

A similar degradation trend was reported by Boudjema *et al.* (2020) who observed that PLA films coated with *Atriplex halimus* fibers had a lower *T*d than that of the PLA film, this resulted from the irregularity of the fiber distribution on the PLA film with the presence of some agglomerations. Both film samples continued to de-grade until the end of heating (800˚C). Nevertheless, the rate of degradation was much lower for GC/NF-2%BLEE film, as ascertained by the higher residue. This could be attributed to the thermal stability of several components in the nanofiber coating, indicating better thermal stability. The residual mass remaining after completion of analysis was 0.132 and 6.972% for the PLA and GC/NF-2%BLEE films, respectively. In addition, the low degradation could be related to the affinity between the GC/NF-2%BLEE film components (Boudjema *et al.*, 2020). The derivative weight-loss curves of the films (Fig. 40B) show another step process overlapping PLA decomposition, which might be linked to the GC/NF-2%BLEE coating. A similar behavior was observed by Arrieta *et al.* (2013) when PLA films were loaded with limonene.

9.5.2. Quality changes of Nile tilapia slices during refrigerated storage

9.5.2.1. Changes in microbiological load

Bags made from GC/NF-2%BLEE, which showed the most satisfactory physical and bioactive properties, were used for packaging of tilapia slices. Changes in the microbiological load of tilapia slices packaged in these bags were compared to those packaged in normal LDPE bags (control). Bacterial counts were monitored during 12 days of refrigerated storage (Fig. 41). On day 0, the total viable count (TVC) of slices packaged in either LDPE or GC/NF-2%BLEE bags (Fig. 41A) ranged from 4.30 to 4.37 log CFU/g, indicating a slight contamination that probably took place during handling or preparation. A rapid increase in TVC was observed for both samples at day 3 ($p < 0.05$); however, the increase was much lower for the slices stored in the GC/NF-2%BLEE bags (5.53 log CFU/g) than for those packaged in the LDPE bags (6.55 log CFU/g). Since the accepted TVC marginal limit for most fresh water and marine fish species is 6.0 log CFU/g (Olatunde *et al.*, 2019), it can be deduced that the LDPE bags could maintain the eating quality for only 3 days, while the GC/NF-2%BLEE bags showed a better preservative effect, more likely due to the BLEE diffusing from the GC/NF and acting as an antibacterial agent towards any spoilage bacteria. The TVC continued to increase markedly for the control ($p < 0.05$) until the end of the storage period, confirming the unsuitability of LDPE bags for tilapia slice preservation. On the other hand, the GC/NF-2%BLEE bags were able to maintain a TVC below the accepted limit after 6 days of storage (5.72 log CFU/g). At day 9, the TVC of the slices packaged in the GC/NF-2%BLEE bags was still below the limit (5.97 log CFU/g); however, the TVC surpassed the limit at day 12 (6.67 log CFU/g), denoting the ability of the GC/NF-2%BLEE bags to maintain a TVC within the acceptable limit for 9 days under refrigerated conditions.

The psychrophilic bacteria count (PBC) for tilapia slices packaged in the LDPE and GC/NF-2%BLEE bags was slightly increased within 3 days of storage ($p < 0.05$) (Fig. 41B), with the counts of 3.65 and 3.38 log CFU/g, respectively. At day 6, the PBC for the slices packed in the GC/NF-2%BLEE bag was 5.54 log CFU/g, but the PBC of the slices packaged in the LDPE bag upsurged and reached 6.14 log CFU/g. During 9 – 12 days, the PBC kept increasing for both samples. Nevertheless, the rate of increase was much lower in the slices packaged in the GC/NF-2%BLEE bags, which had a PBC of 5.98 log CFU/g on day 9. Psychrophilic bacteria are known for their ability to flourish at low temperatures, thus causing spoilage of fish samples under refrigerated storage (Arfat *et al.*, 2015). Therefore, retardation of psychrophilic bacteria growth was crucial to prevent or re-tard the undesired spoilage.

The majority of food spoilage, especially in fish and its products, was linked to the presence of a high load of *Pseudomonas* sp., known for their endurance and high survival rate, particularly at refrigerated temperatures (Olatunde *et al.*, 2019). The PC for both samples showed a marked increase after day 0 (Fig. 41C), but the increase rate was greater in slices packaged in the LDPE bags, which had a PC higher than 6.0 log CFU/g after 9 days of storage, while the PC was lower for the slices packaged in the GC/NF-2%BLEE bags at the same time of storage. A lower PC rate of increase was observed for the slices kept in the GC/NF-2%BLEE bags throughout the storage period. The GC/NF-2%BLEE bags, therefore, had a superior ability in retarding the growth of *Pseudomonas* sp. in tilapia slices compared with the LDPE bags.

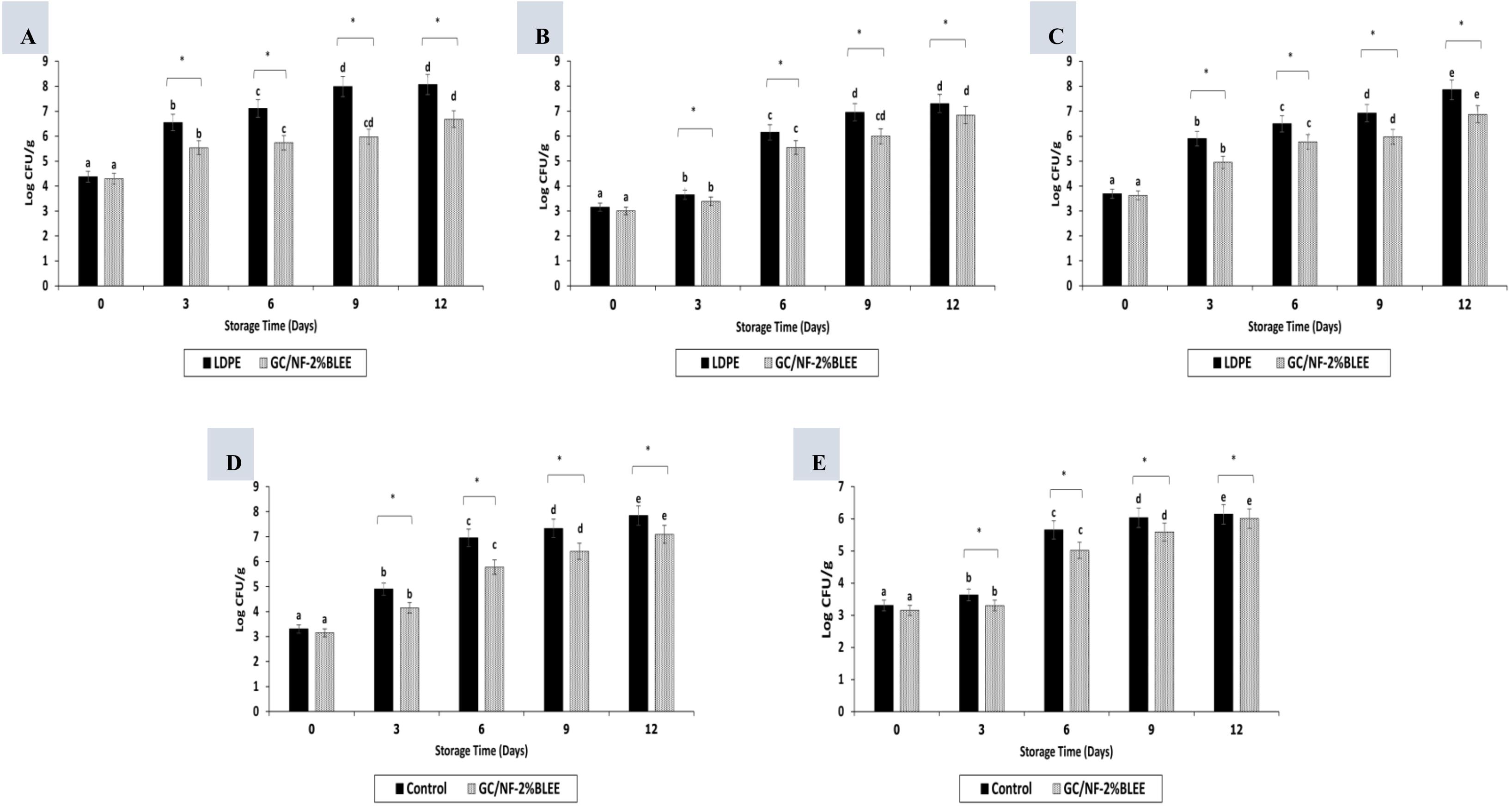

Figure 41. Total viable count (A), psychrophilic bacteria count (B), *Pseudomonas* sp. count (C), hydrogen sulfide-producing bacteria count (D), and *Enterobacteriaceae* count (E) of tilapia slices packaged in different bags, during 12 days of refrigerated storage. Bars represent standard deviation (n = 3). Single asterisk (*) indicates significant difference ($p < 0.05$). Different lowercase letters of samples packaged in the same bag indicate significant difference ($p < 0.05$).

A similar trend was noticed for H_2S-BC (Fig. 41D), for which growth was accelerated in the slices packaged in LDPE, compared with slices kept in the GC/NF-2%BLEE bags throughout the storage period. The results signify the higher ability of GC/NF-2%BLEE bags in lowering the growth of H_2S-producing bacteria, well known for their capability in utilizing amino acids, such as methionine and L-cysteine, besides other amino acids in proteins present in fish meat. This was associated with the generation of the unpleasant odor of H_2S (Szabo, 2018).

The presence of *Enterobacteriaceae* is related to highly unhygienic or improper conditions for the preparation of fish (Gullian-Klanian *et al.,* 2018). Under suitable growth conditions, *Enterobacteriaceae* counts can augment rapidly even if the initial count is very low (Tagrida *et al.,* 2021b). Although EC was generally lower than the other bacterial counts (Fig. 41E), it followed the same trend. Slices packaged in the GC/NF-2%BLEE bags generally showed a lower rate of increase compared with those kept in LDPE bags during the 12 days of storage. The result confirmed the appropriateness of the GC/NF-2%BLEE bags against the growth of a broad spectra of food spoilage bacteria mainly due to the highly diffusible BLEE from GC/NF coated on PLA film, thus acting as an antibacterial agent.

9.5.2.2. Changes in chemical indices

Tilapia slices containing polyunsaturated fatty acids (PUFA) and other unsaturated fatty acids underwent lipid oxidation induced by free radicals and active oxygen species. This led to hydroperoxide formation along with other lipid oxidation products, which are responsible for the rancidity and the nutritional loss of fish (Masniyom *et al.,* 2002). Additionally, the contaminated bacteria can cause lipolysis, initiating the release of free fatty acids that could be further utilized by these bacteria as an energy source and in other biochemical processes (Tagrida and Benjakul, 2022). These FFAs are highly prone to oxidation associated with the formation of hydroperoxides and other secondary lipid oxidation products, such as malonaldehyde and aldehydes (Tagrida and Benjakul, 2022).

At day 0, no difference in peroxide values (PV) could be detected between the slices packaged in the LDPE and GC/NF-2%BLEE bags ($p > 0.05$) (Fig. 42A). An increase ($p < 0.05$) was observed at day 3 in both samples; however, the increase was lower in the slices packaged in the GC/NF-2%BLEE bags. The PV increment continued for both samples, but a lower rate was noticeable in the samples packaged in the GC/NF-2%BLEE bags. By day 9, the PV of the slices packaged in LDPE bags reached 9.23 mg cumene hydroperoxide equivalent/kg flesh, which exceeded the accepted PV limit of 9 mg cumene hydroperoxide equivalent /kg flesh (Feiner, 2006). The PV of the slices packaged in the GC/NF-2%BLEE bags was 7.01 mg cumene hydroperoxide equivalent /kg flesh after the same period, denoting better preservative effects towards lipid oxidation. The result was in line with that of microbial growth retardation at the same period. After 9 days, the PV remained constant for the slices packaged in LDPE bags, signifying the slow formation of new hydroperoxides and the existing decomposition. Nevertheless, the PV of slices in GC/NF-2%BLEE bags continued to increase. By the end of storage (12 days), both samples surpassed the accepted limit and no differences in PV were detected ($p > 0.05$). Therefore, GC/NF-2%BLEE bags could prevent lipid oxidation of slices for 9 days under refrigerated conditions.

The TBARS value indicates the extent of lipid oxidation by the determination of any formed secondary oxidation products, such as ketones, aldehydes, etc., (Chen *et al.*, 2017). No difference in TBARS was observed up to day 3 (Fig. 42B) ($p < 0.05$). On day 3, the slices packaged in the GC/NF-2%BLEE bags showed a slightly lower TBARS value (0.94 mg MDA equivalent/kg flesh) than those packaged in the LDPE bags (1.22 mg MDA equivalent/kg flesh). The TBARS values for both samples surged with increasing storage time but, in general, the increase was lower for slices packaged in the GC/NF-2%BLEE bags. Ozogul *et al.* (2010) reported that TBARS values higher than 4 mg MDA equivalent/kg flesh were considered as an indication of unacceptable quality. On day 9, the slices packaged in the LDPE bags had a TBARS value of 4.26 mg MDA equivalent/kg flesh, while those kept in the GC/NF-2%BLEE bags had a value of 3.07 mg MDA equivalent/kg flesh. The results indicate the capability of the latter to lower TBARS formation for 9 days. In addition to the antioxidant compounds from the BLEE embedded in GC/NF that were able to scavenge the free radicals causing the oxidation, gelatin and chitosan in the nanofiber matrix could act as an oxygen barrier, thus lowering the oxidation of lipid in the slices (Antoniewski *et al.*, 2007).

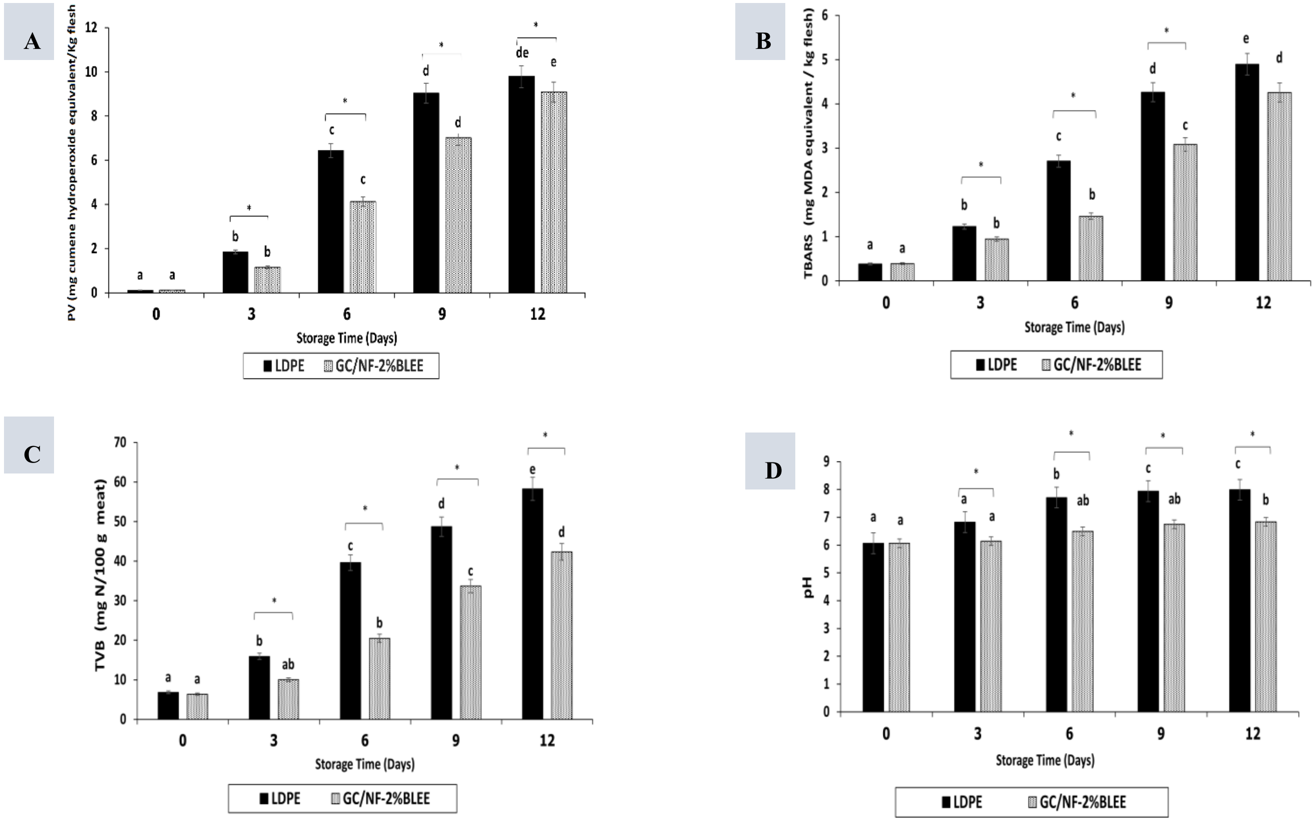

Figure 42. Peroxide value (PV) (A), thiobarbituric acid reactive substances (TBARS) (B), total volatile base (TVB) content (C), and pH (D) of tilapia slices packaged in different bags during 12 days of refrigerated storage. Bars represent standard deviation (n = 3). Single asterisk (*) indicates significant difference ($p < 0.05$). Different lowercase letters of samples packaged in the same bag indicate significant difference ($p < 0.05$).

TVB content can reflect fish quality by quantifying the total nitrogenous compounds, such as ammonia (NH_3), dimethylamine (DMA), and trimethylamine (TMA), formed due to the uncontrollable growth of contaminated microorganisms (Tacon, 2020). Usually, high TVB contents are connected to the poor quality of the fish and augmented levels are connected with an increase in the pH of tested samples, since most compounds generated are basic in pH, which could favor the growth of many spoilage bacteria (Tagrida and Benjakul, 2022). No differences in TVB contents (6.82 and 6.37 mg N/100 g) or pH (6.06 and 6.07) for the slices packaged in the LDPE and GC/NF-2%BLEE bags were found at day 0 ($p > 0.05$) (Fig. 42C and D). Both indices showed a marked increase ($p < 0.05$) for both samples with augmenting storage time, but the rate of increase was much higher ($p < 0.05$) for the slices packaged in LDPE bags. At day 6, the TVB content of the slices packaged in the LDPE bags was 39.60 mg N/100 g. TVB content higher than 35 mg N/100 g is regarded by the European Union (EU) Commission (2008) as an indication of poor-quality fish.

It can be inferred that the LDPE bags can maintain the slice quality for no longer than 6 days. On the other hand, the slices packaged in the GC/NF-2%BLEE bags had a TVB content of 33.69 mg N/100 g after 9 days of storage, signifying its acceptable quality. However, the TVB content after 12 days surpassed the accepted limit of freshness. Thus, the preservative ability of the GC/NF-2%BLEE bags in maintaining the quality of tilapia slices for 9 days was mainly due to the presence of BLEE which was able to retard microbial growth. The increase in the TVB contents of both samples was accompanied with a coincidental increase in pH. Nevertheless, after 12 days of storage, the pH of the slices packaged in the GC/NF-2%BLEE bags was 6.83, while that of the slices packaged in the LDPE bags was 7.98. The result confirmed the improved keeping quality of the tilapia slices by the GC/NF-2%BLEE bags.

9.6. Conclusion

Electrospun gelatin/chitosan nanofibers (GC/NF) with and without betel leaf ethanolic extract (BLEE) were coated on PLA films. The nanofibers appeared to be bead-free, with a fibrous network structure particularly at low concentrations of BLEE. Mechanical and barrier properties were improved by the nanofiber coating. The WVP was lowered with an increasing BLEE concentration, while the tensile strength and stretch ability of PLA film coated with GC/NF were considerably enhanced, particularly when BLEE at 1 and 2% was added in GC/NF. BLEE loaded into GC/NF, especially at higher concentrations, provided antioxidant and antibacterial activities to PLA films. Bags prepared from GC/NF-coated PLA films and loaded with 2% BLEE (GC/NF-2%BLEE) could impede microbial growth in tilapia slices as compared with LDPE bags under refrigerated storage. Additionally, GC/NF-2%BLEE bags prevented lipid oxidation and other chemical changes associated with microbial spoilage in slices during storage. Therefore, PLA films coated with GC/NF containing BLEE could serve as a promising active packaging for food preservation.

9.7. References

Antoniewski, M. N., Barringer, S., Knipe, C., and Zerby, H. 2007. Effect of a gelatin coating on the shelf life of fresh meat. Journal of Food Science. 72(6): 382 - 387.

Arfat, Y. A., Benjakul, S., Vongkamjan, K., Sumpavapol, P., and Yarnpakdee, S. 2015. Shelf-life extension of refrigerated sea bass slices wrapped with fish protein isolate/fish skin gelatin-ZnO nanocomposite film incorporated with basil leaf essential oil. Journal of Food Science and Technology. 52(10): 6182 - 6193.

Arrieta, M. P., López, J., Ferrándiz, S., and Peltzer, M. A. 2013. Characterization of PLA-limonene blends for food packaging applications. Polymer Testing 32(4): 760 - 768.

Behera, K., Chang, Y.-H., and Chiu, F.-C. 2021. Manufacturing poly (butylene adipate-co-terephthalate)/high density polyethylene blend-based nanocomposites with enhanced burning anti-dripping and physical properties - Effects of carbon nanofillers addition. Composites Part B: Engineering. 217: 108878.

Bonilla, J., and Sobral, P. J. 2016. Investigation of the physicochemical, antimicrobial and antioxidant properties of gelatin-chitosan edible film mixed with plant ethanolic extracts. Food Bioscience. 16: 17 - 25.

Boudjema, H. L., Bendaikha, H., and Maschke, U. 2020. Green composites based on Atriplex halimus fibers and PLA matrix. Journal of Polymer Engineering. 40(8): 693 - 702.

Buege, J. A., and Aust, S. D. 1978. [30] Microsomal lipid peroxidation Methods in Enzymology. (52): 302 - 310.

Burgos, N., Martino, V. P., and Jiménez, A. 2013. Characterization and ageing study of poly (lactic acid) films plasticized with oligomeric lactic acid. Polymer Degradation and Stability. 98(2): 651 - 658.

Burt, S. 2004. Essential oils: their antibacterial properties and potential applications in foods—a review. International Journal of Food Microbiology. 94(3): 223 - 253.

Chen, Q., Kong, B., Han, Q., Xia, X., and Xu, L. 2017. The role of bacterial fermentation in lipolysis and lipid oxidation in Harbin dry sausages and its flavour development. LWT-Food Science and Technology. 77: 389 - 396.

Damodaran, S., Parkin, K. L., and Fennema, O. R. 2007. Fennema's food chemistry: CRC press. ISBN: 34333-F33-4566.

de Campos, S. S., de Oliveira, A., Moreira, T. F. M., da Silva, T. B. V., da Silva, M. V., Pinto, J. A., and Barreiro, M.-F. 2019. TPCS/PBAT blown extruded films added with curcumin as a technological approach for active packaging materials. Food Packaging and Shelf Life. 22: 100424.

Ebrahimi, S., Fathi, M., and Kadivar, M. 2019. Production and characterization of chitosan-gelatin nanofibers by nozzle-less electrospinning and their application to enhance edible film’s properties. Food Packaging and Shelf Life. 22: 100387.

EC. 2008. European Commission Regulation (EC) No 1022/2008 of 17 October 2008 amending Regulation (EC) No 2074/2005 as regards the total volatile basic nitrogen (TVB-N) limits. L277/18 EN Official Journal the European Union.

Fabra, M. J., López-Rubio, A., and Lagaron, J. M. 2016. Use of the electrohydrodynamic process to develop active/bioactive bilayer films for food packaging applications. Food Hydrocolloids. 55: 11 - 18.

Feiner, G. 2006. Meat products handbook: Practical science and technology: Boca Raton: Woodhead Publishing Limited. Elsevier. ISBN: 978-1-84569-050-2.

Fonseca, L. M., dos Santos Cruxen, C. E., Bruni, G. P., Fiorentini, Â. M., da Rosa Zavareze, E., Lim, L.-T., and Dias, A. R. G. 2019. Development of antimicrobial and antioxidant electrospun soluble potato starch nanofibers loaded with carvacrol. International Journal of Biological Macromolecules. 139: 1182 - 1190.

Giménez, B., De Lacey, A. L., Pérez-Santín, E., López-Caballero, M., and Montero, P. 2013. Release of active compounds from agar and agar–gelatin films with green tea extract. Food Hydrocolloids. 30(1): 264 - 271.

Gu, J., Xiao, P., Chen, P., Zhang, L., Wang, H., Dai, L., and Chen, T. 2017. Functionalization of biodegradable PLA nonwoven fabric as superoleophilic and superhydrophobic material for efficient oil absorption and oil/water separation. ACS Applied Materials and Interfaces. 9(7): 5968 - 5973.

Gullian Klanian, M., Delgadillo Díaz, M., and Sánchez Solís, M. J. 2018. Molecular characterization of histamine-producing psychrotrophic bacteria isolated from red octopus (*Octopus maya*) in refrigerated storage. High-Throughput. 7(3): 25.

Gulzar, S., Tagrida, M., Nilsuwan, K., Prodpran, T., and Benjakul, S. 2022. Electrospinning of gelatin/chitosan nanofibers incorporated with tannic acid and chitooligosaccharides on polylactic acid film: Characteristics and bioactivities. Food Hydrocolloids. 133: 107916.

He, L., Lan, W., Ahmed, S., Qin, W., and Liu, Y. 2019. Electrospun polyvinyl alcohol film containing pomegranate peel extract and sodium dehydroacetate for use as food packaging. Food Packaging and Shelf Life 22: 100390.

Hosseini, S. F., Kaveh, F., and Schmid, M. 2022. Facile fabrication of transparent high-barrier poly (lactic acid)-based bilayer films with antioxidant/antimicrobial performances. Food Chemistry. 384: 132540.

Jamshidian, M., Tehrany, E. A., Imran, M., Jacquot, M., and Desobry, S. 2010. Poly-Lactic Acid: production, applications, nanocomposites, and release studies. Comprehensive Reviews in Food Science and Food Safety. 9(5): 552 - 571.

Kester, J., and Fennema, O. 1989. An edible film of lipids and cellulose ethers: barrier properties to moisture vapor transmission and structural evaluation. Journal of Food Science. 54(6): 1383 - 1389.

Laaziz, S. A., Raji, M., Hilali, E., Essabir, H., Rodrigue, D., and Bouhfid, R. 2017. Bio-composites based on polylactic acid and argan nut shell: Production and properties. International Journal of Biological Macromolecules. 104: 30 - 42.

Liu, F., Liu, Y., Sun, Z., Wang, D., Wu, H., Du, L., and Wang, D. 2020. Preparation and antibacterial properties of ε-polylysine-containing gelatin/chitosan nanofiber films. International Journal of Biological Macromolecules. 164: 3376 - 3387.

Liu, Y., Wang, S., Lan, W., and Qin, W. 2019. Fabrication of polylactic acid/carbon nanotubes/chitosan composite fibers by electrospinning for strawberry preservation. International Journal of Biological Macromolecules. 121: 1329 - 1336.

Madhumita, M., Guha, P., and Nag, A. 2019. Extraction of betel leaves (*Piper betle* L.) essential oil and its bio-actives identification: Process optimization, GC-MS analysis and anti-microbial activity. Industrial Crops and Products. 138: 111578.

Mai-Prochnow, A., Clauson, M., Hong, J., and Murphy, A. B. 2016. Gram positive and Gram negative bacteria differ in their sensitivity to cold plasma. Scientific Reports. 6(1): 1 - 11.

Masniyom, P., Benjakul, S., and Visessanguan, W. 2002. Shelf-life extension of refrigerated seabass slices under modified atmosphere packaging. Journal of the Science of Food and Agriculture. 82(8): 873 - 880.

Mittal, A., Singh, A., Benjakul, S., Prodpran, T., Nilsuwan, K., Huda, N., and de la Caba, K. 2021. Composite films based on chitosan and epigallocatechin gallate grafted chitosan: characterization, antioxidant and antimicrobial activities. Food Hydrocolloids. 111: 106384.

Moradi, M., Tajik, H., Rohani, S. M. R., Oromiehie, A. R., Malekinejad, H., Aliakbarlu, J., and Hadian, M. 2012. Characterization of antioxidant chitosan film incorporated with Zataria multiflora Boiss essential oil and grape seed extract. LWT-Food Science and Technology. 46(2): 477 - 484.

Morie, A., Garg, T., Goyal, A. K., and Rath, G. 2016. Nanofibers as novel drug carrier– an overview. Artificial Cells, Nanomedicine, and Biotechnology. 44(1): 135 - 143.

Nezarati, R. M., Eifert, M. B., and Cosgriff-Hernandez, E. 2013. Effects of humidity and solution viscosity on electrospun fiber morphology. Tissue Engineering Part C: Methods. 19(10): 810 - 819.

Nilsuwan, K., Benjakul, S., and Prodpran, T. 2018. Physical/thermal properties and heat seal ability of bilayer films based on fish gelatin and poly (lactic acid). Food Hydrocolloids. 77: 248 - 256.

Nouri, L., and Nafchi, A. M. 2014. Antibacterial, mechanical, and barrier properties of sago starch film incorporated with betel leaves extract. International Journal of Biological Macromolecules. 66: 254 - 259.

Nowzari, F., Shábanpour, B., and Ojagh, S. M. 2013. Comparison of chitosan–gelatin composite and bilayer coating and film effect on the quality of refrigerated rainbow trout. Food Chemistry. 141(3): 1667 - 1672.

Olatunde, O. O., Benjakul, S., and Vongkamjan, K. 2019. Combined Effect of ethanolic coconut husk extract and modified atmospheric packaging (MAP) in extending the shelf life of Asian sea bass slices. Journal of Aquatic Food Product Technology. 28(6): 689 - 702.

Ozogul, Y., Ayas, D., Yazgan, H., Ozogul, F., Boga, E. K., and Ozyurt, G. 2010. The capability of rosemary extract in preventing oxidation of fish lipid. International Journal of Food Science and Technology. 45(8): 1717 - 1723.

Park, S. H., Lee, H. S., Choi, J. H., Jeong, C. M., Sung, M. H., and Park, H. J. 2012. Improvements in barrier properties of poly (lactic acid) films coated with chitosan or chitosan/clay nanocomposite. Journal of Applied Polymer Science. 125(S1): 675 - 680.

Radusin, T., Torres-Giner, S., Stupar, A., Ristic, I., Miletic, A., Novakovic, A., and Lagaron, J. M. 2019. Preparation, characterization and antimicrobial properties of electrospun polylactide films containing *Allium ursinum* L. extract. Food Packaging and Shelf Life. 21: 100357.

Rasal, R. M., Janorkar, A. V., and Hirt, D. E. 2010. Poly (lactic acid) modifications. Progress in Polymer Science. 35(3): 338 - 356.

Rattaya, S., Benjakul, S., and Prodpran, T. 2009. Properties of fish skin gelatin film incorporated with seaweed extract. Journal of Food Engineering. 95(1): 151-157.

Richards, M. P., and Hultin, H. O. 2002. Contributions of blood and blood components to lipid oxidation in fish muscle. Journal of Agricultural and Food Chemistry. 50(3): 555 - 564.

Shiku, Y., Hamaguchi, P. Y., Benjakul, S., Visessanguan, W., and Tanaka, M. 2004. Effect of surimi quality on properties of edible films based on *Alaska pollack*. Food Chemistry. 86(4): 493 - 499.

Sobral, P., and Habitante, A. 2001. Phase transitions of pigskin gelatin. Food Hydrocolloids. 15(4-6): 377 - 382.

Szabo, C. 2018. A timeline of hydrogen sulfide (H_2S) research: from environmental toxin to biological mediator. Biochemical Pharmacology. 149: 5 - 19.

Tacon, A. G. 2020. Trends in global aquaculture and aquafeed production: 2000–2017. Reviews in Fisheries Science and Aquaculture. 28(1): 43 - 56.

Tagrida, M., and Benjakul, S. 2020. Ethanolic extract of Betel (*Piper betle* L.) and Chaphlu (*Piper sarmentosum* Roxb.) dechlorophyllized using sedimentation process: Production, characteristics, and antioxidant activities. Journal of Food Biochemistry. 44(12): e13508.

Tagrida, M., and Benjakul, S. 2021. Betel (*Piper betle* L.) leaf ethanolic extracts dechlorophyllized using different methods: antioxidant and antibacterial activities, and application for shelf-life extension of Nile tilapia (*Oreochromis niloticus*) fillets. RSC Advances. 11(29): 17630 - 17641.

Tagrida, M., and Benjakul, S. 2022. Liposomes loaded with betel leaf (*Piper betle* L.) extract: Antibacterial activity and preservative effect in combination with hurdle technologies on tilapia slices. Food Control. 138: 108999.

Tagrida, M., Benjakul, S., and Zhang, B. 2021a. Use of betel leaf (*Piper betle* L.) ethanolic extract in combination with modified atmospheric packaging and nonthermal plasma for shelf-life extension of Nile tilapia (*Oreochromis niloticus*) fillets. Journal of Food Science. 138(17): 630 - 641

Tagrida, M., Prodpran, T., Zhang, B., Aluko, R. E., and Benjakul, S. 2021b. Liposomes loaded with betel leaf (*Piper betle* L.) ethanolic extract prepared by thin film hydration and ethanol injection methods: Characteristics and antioxidant activities. Journal of Food Biochemistry. 45(12): e14012.

Torres-Giner, S., Busolo, M., Cherpinski, A., and Lagaron, J. 2018. Electrospinning in the packaging industry. Electrospinning. ISBN: 978-1-78801-294-2. 238 - 260.

Vafania, B., Fathi, M., and Soleimanian-Zad, S. 2019. Nanoencapsulation of thyme essential oil in chitosan-gelatin nanofibers by nozzle-less electrospinning and their application to reduce nitrite in sausages. Food and Bioproducts Processing. 116: 240 - 248.

Wang, L.-F., and Rhim, J.-W. 2016. Grapefruit seed extract incorporated antimicrobial LDPE and PLA films: Effect of type of polymer matrix. LWT-Food Science and Technology. 74: 338 - 345.

Wang, L., Liu, F., Jiang, Y., Chai, Z., Li, P., Cheng, Y., and Leng, X. 2011. Synergistic antimicrobial activities of natural essential oils with chitosan films. Journal of Agricultural and Food Chemistry. 59(23): 12411 - 12419.

Wang, N., Xu, Z., Zhan, P., Dai, K., Zheng, G., Liu, C., and Shen, C. 2017. A tunable strain sensor based on a carbon nanotubes/electrospun polyamide 6 conductive nanofibrous network embedded into poly (vinyl alcohol) with self-diagnosis capabilities. Journal of Materials Chemistry C. 5(18): 4408 - 4418.

Wen, P., Zhu, D.-H., Wu, H., Zong, M.-H., Jing, Y.-R., and Han, S.-Y. 2016. Encapsulation of cinnamon essential oil in electrospun nanofibrous film for active food packaging. Food Control. 59: 366 - 376.

CHAPTER 10

SUMMARY AND SUGGESTIONS

10.1. Summary

The sedimentation process was successful in reducing the green color of betel leaf ethanolic extract associated with high chlorophyll content. Extract/water ratios showed insignificant impact on chlorophyll removal efficacy. Dechlorophyllized BLEE has more total phenolic content than the extract without dechlorophyllization. The BLEE also showed superior antioxidant activities.

Organic solvents were not as efficient in reducing the distinct color of BLEE as the sedimentation process. The BLEE dechlorophyllized by sedimentation (BLEE-SED) had the lower chlorophyll content, paler color, and higher antioxidant and antibacterial activities. Nile tilapia slices treated with BLEE-SED, especially at 400 and 600 ppm, effectively lowered the chemical changes as well as retarded microbial growth for up to 9 days of storage at 4˚C.

Encapsulation of BLEE into liposomes was optimally done by using thin film hydration method. The liposomes produced by this method had the smallest particle size and were more stable. Additionally, loading into liposomes reduced the remaining color of BLEE. Encapsulation of BLEE in liposomes had no adverse effect on antioxidant activities, but in the contrary, it delayed the diffusion or release of the extract. Liposomes loaded with 1% BLEE and prepared by thin film method showed higher ability in maintaining antioxidant activities when subjected to a gastro-intestinal tract (GIT) digestion system.

The antibacterial activity of BLEE was enhanced when encapsulated in liposomes. Treatments with L/BLEE at 400 ppm combined with MAP (CO_2: Ar: O_2 = 60: 30: 10) and NTP (80 KV-RMS for 5 min) had the profound preservative efficiency on tilapia slices for up to 12 days of storage at 4˚C against all bacteria inoculated.

When nonthermal plasma was applied on Nile tilapia slices packaged under modified atmosphere and pretreated with liposomes loaded with BLEE or the equivalent amount of unencapsulated BLEE at 400 ppm, the shelf-life of tilapia slices could be extended to 12 days under refrigerated storage. Such a treatment yielded lower lipid oxidation and provided better keeping qualities.

Incorporation of BLEE into gelatin/chitosan blend films improved their mechanical properties but slightly changed the color of films. The heat sealing of some films was achieved, while films having high proportion of chitosan was not sealable. UV-Vis light barrier property was improved, and water vapor barrier properties were enhanced when added with BLEE. Water resistance of film was also increased. Furthermore, antioxidant and antibacterial activities of films were elevated with addition of BLEE.

The types of plasticizers as well as the incorporation of BLEE or liposomes loaded with BLEE (L/BLEE) into gelatin/chitosan blend films affected their properties. Films added with L/BLEE had paler color but poor mechanical properties and incompetent barrier abilities. Oxidative stability and astaxanthin of shrimp oil were more maintained when packaged in pouches made from gelatin/chitosan blend incorporated with BLEE and plasticized with glycerol (B-GLY) throughout 30 days of storage, compared to that packaged in LDPE pouches.

Electrospun gelatin/chitosan nanofibers (GC/NF) with and without betel leaf ethanolic extract (BLEE) were coated on PLA films. Nanofibers with lower BLEE concentration were bead-free nanofibers. The WVP was lowered with an increasing BLEE concentration, while the tensile strength and stretch ability of PLA film coated with GC/NF were considerably enhanced. BLEE loaded into GC/NF, especially at higher concentrations, provided antioxidant and antibacterial activities to PLA films. Bags prepared from GC/NF-coated PLA films and loaded with 2% BLEE (GC/NF-2%BLEE) could impede microbial growth and lower lipid oxidation in tilapia slices as compared with LDPE bags under refrigerated storage.

10.2. Suggestions

Further in-depth research is needed to better understand the mode of actions of the betel leaf extract as antioxidant and antibacterial agent.

The stability and the controlled release of the liposomes loaded with betel leaf extract should be further studied in different systems.

Studies on the synergistic effect of using active packaging in combination with non-thermal process on the keeping qualities of different packaged foods should be investigated.

Further improvements on active packaging films to enhance their effectiveness in preservation of seafoods or other foods should be carried out.

VITAE

Name Mr. Mohamed Abdelmonem Tagrida

Student ID 6211030008

Education Attainment

Degree	Name of Institution	Year of Graduation
Bachelor of Science (Chemistry and Microbiology)	Menoufia University, Menoufia governorate (Egypt)	2010
Master of Science (Microbiology)	Cairo University, Giza governorate (Egypt)	2017

Scholarship awards during enrolment

- Prachayacharn grant program (Grant no. AGR6402088N) provided by the Prince of Songkla University (PSU), Hat Yai campus.
- Research Grant for Thesis (Fiscal year 2022). Graduate School, Prince of Songkla university.

List of Publication and Proceeding

Publication

Mohamed, M. S., Khalil, M. S., Tagrida, M. A., and Mawgoud, Y. A. 2017. Purification of gelatinase from the bacteria contaminating gelatin production process. Research Journal of Pharmaceutical Biological and Chemical Sciences, *8*(4), 914-931.

Tagrida, M., and Benjakul, S. 2020. Ethanolic extract of Betel (*Piper betle* L.) and Chaphlu (*Piper sarmentosum* Roxb.) dechlorophyllized using sedimentation process: Production, characteristics, and antioxidant activities. Journal of Food Biochemistry, *44*(12), e13508.

Tagrida, M., and Benjakul, S. 2021. Betel (*Piper betle* L.) leaf ethanolic extracts dechlorophyllized using different methods: antioxidant and antibacterial activities, and application for shelf-life extension of Nile tilapia (*Oreochromis niloticus*) fillets. RSC Advances, *11*(29), 17630-17641.

Tagrida, M., Prodpran, T., Zhang, B., Aluko, R. E., and Benjakul, S. 2021. Liposomes loaded with betel leaf (*Piper betle* L.) ethanolic extract prepared by thin film hydration and ethanol injection methods: Characteristics and antioxidant activities. Journal of Food Biochemistry, e14012.

Tagrida, M., Benjakul, S., and Zhang, B. 2021. Use of betel leaf (*Piper betle* L.) ethanolic extract in combination with modified atmospheric packaging and nonthermal plasma for shelf-life extension of Nile tilapia (*Oreochromis niloticus*) fillets. Journal of Food Science.*86*(12), 5226 – 5239.

Tagrida, M., and Benjakul, S. 2022. Liposomes loaded with betel leaf *(Piper betle* L.) extract: Antibacterial activity and preservative effect in combination with hurdle technologies on tilapia slices. Food Control, 108999.

Tagrida, M., Gulzar, S., Nilsuwan, K., Prodpran, T., Zhang, B., and Benjakul, S. 2022. Polylactic acid film coated with electrospun gelatin/chitosan nanofibers containing betel leaf ethanolic extract: Properties, bioactivities, and use for shelf-life extension of tilapia slices. Molecules, 27, 5877.

Chantakun, K., Nilsuwan, K., Tagrida, M., Sumpavapol, P., and Benjakul, S. 2022. Tender coconut water fortified with edible bird's nest protein hydrolysate subjected to sterilization and high hydrolytic pressure processes: Qualities, acceptability and changes during refrigerated storage. Food Control, 109116.

Gulzar, S., Tagrida, M., Nilsuwan, K., Prodpran, T., and Benjakul, S. 2022. Electrospinning of gelatin/chitosan nanofibers incorporated with tannic acid and chitooligosaccharides on polylactic acid film: Characteristics and bioactivities. Food Hydrocolloids, 107916.

Gulzar, S., Tagrida, M., Prodpran, T., and Benjakul, S. 2022. Antimicrobial film based on polylactic acid coated with gelatin/chitosan nanofibers containing nisin extends the shelf life of Asian seabass slices. Food Packaging and Shelf Life, 100941.

<u>Proceeding</u>

Tagrida, M., and Benjakul, S. Shelf-life extension of Nile tilapia fillets using betel leaf ethanolic extract dechlorophyllized using sedimentation process. Food Innovation Asia Conference 2021. Bio-Circular Green Economy. June 17-18,

2021. organized by the Food Science and Technology Association of Thailand. Poster presentation.

Tagrida, M., and Benjakul, S. Liposomes loaded with betel leaf extract: antibacterial activity and its use for shelf-life extension of tilapia slices. International Symposium on Science and Technology UKM-PSU 2022 (ISSTUP2022). hosted jointly by the University of Kebangsaan Malaysia and Prince of Songkla University. 16-17 March 2022. Oral presentation